Oxidative Medicine and Cellular Longevity

Vascular Oxidative Stress: Pharmacological and Nonpharmacological Approaches

Lead Guest Editor: Albino Carrizzo
Guest Editors: Maurizio Forte and Valeria Conti

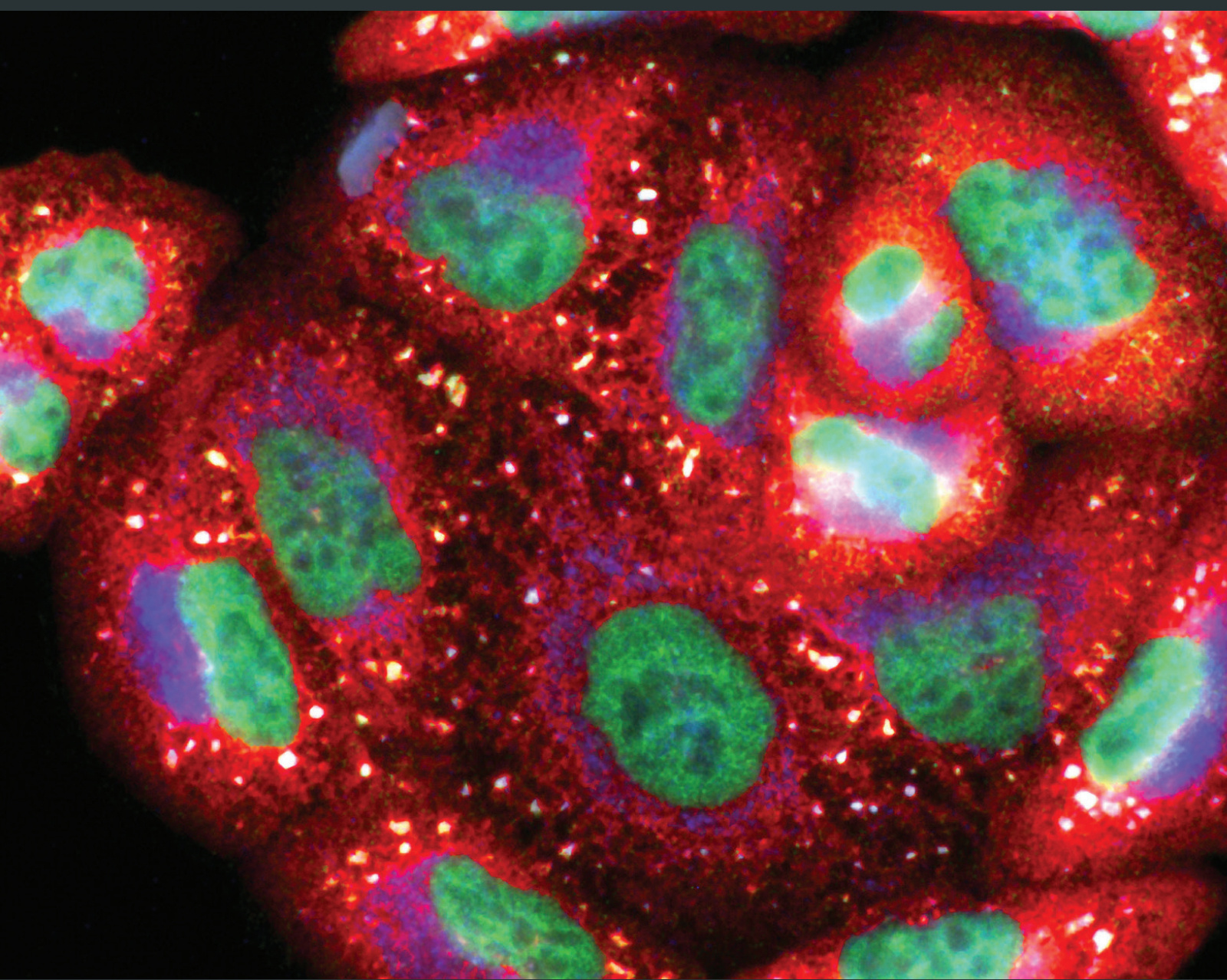

Vascular Oxidative Stress: Pharmacological and Nonpharmacological Approaches

Oxidative Medicine and Cellular Longevity

Vascular Oxidative Stress: Pharmacological and Nonpharmacological Approaches

Lead Guest Editor: Albino Carrizzo
Guest Editors: Maurizio Forte and Valeria Conti

Editorial Board

Contents

Hindawi
Oxidative Medicine and Cellular Longevity
Volume 2018, Article ID 8539350, 2 pages
https://doi.org/10.1155/2018/8539350

Editorial

Vascular Oxidative Stress: Pharmacological and Nonpharmacological Approaches

Valeria Conti,[1] **Maurizio Forte**,[2] **and Albino Carrizzo**[2]

[1]*Department of Medicine, Surgery and Dentistry "Scuola Medica Salernitana", University of Salerno, Baronissi, 84081 Salerno, Italy*
[2]*Department of AngioCardioNeurology, IRCCS Neuromed, Pozzilli, 86077 Isernia, Italy*

Correspondence should be addressed to Albino Carrizzo; albino.carrizzo@gmail.com

Received 20 May 2018; Accepted 20 May 2018; Published 22 July 2018

Cerebral and cardiovascular diseases represent a big public health problem and a leading cause of mortality in the world. In more than 40% of cases, they occur before 75 years of age. The most common forms of CVDs are ischemic heart disease, stroke, and arterial hypertension.

The cardiovascular risk is continuous during the life, and all people have to reckon cardiovascular risk, which depends on the combination of different factors (age, sex, smoking and diet habits, high blood pressure, and cholesterolemia).

The modifiable risk factors should be tackled with interventions promoting correct lifestyles and appropriate pharmacological therapy. Right lifestyles must be encouraged in the population starting from young age in order to maintain a favourable cardiovascular risk profile as long as possible.

Oxidative stress results from an imbalance between oxidizing compounds and antioxidant resources provided by the endogenous defense system. The generation of oxidizing compounds occurs physiologically in response to insults and tissue repair processes. On the other hand, an improper activation of oxidative processes can be chronically present in pathological conditions, such as arterial hypertension and diabetes mellitus, contributing to the oxidative damage. Vasorelaxant molecules, such as nitric oxide (NO), hydrogen sulfide (H_2S), and prostaglandin I2 (PGI_2), play a fundamental role in the regulation of vascular tone and are especially damaged by excessive oxidative stress production.

The present special issue includes papers that explore the effects of the oxidative stress on the onset and progression of the cerebral and cardiovascular diseases and the mechanisms helpful to slow down their occurrence.

It has been shown that radical oxygen species, including hydrogen peroxide hydroxyl radical, peroxynitrite, and superoxide anion, act as molecule signal that modulate multiple cellular responses. The main sources of $O2^{\bullet-}$ generated in the organism are NOx. These oxidases produce $O2^{\bullet-}$ from oxygen using NADPH as an electron donor. The NOX family is the only family of enzymes known with the function of producing ROS that can be activated by different stimuli. NADPH oxidase-derived ROS act as intracellular second messengers by activating several redox signalling cascades implicated in VEGFR2 autophosphorylation, EC migration, angiogenesis, and proliferation, but molecular mechanisms responsible for NADPH oxidase activation and the function of ROS in redox signalling linked to angiogenesis remain unclear.

F. Cattaneo and colleagues in an experimental model of human endothelial cell line reported that the activation of formyl-peptide receptors (FPRs) induces superoxide generation as a consequence of MEK- and PKC-dependent phosphorylation of the regulatory subunit $p47^{phox}$, demonstrating that ROS generation is regulated by the binding of N-formyl-methionyl-leucyl-phenylalanine (N-fMLP) to FPR1 and that produced ROS mediate Flk-1/KDR transactivation, playing a crucial role in VEGFR2 signalling related to angiogenesis, provides new insights in NADPH oxidase and/or FPR1 as possible targets for therapies against angiogenesis-dependent diseases. The discovery of crosstalk between FPR1 and Flk-1/KDR provides further opportunities for drug discovery strategies for angiogenesis driven by an increase of VEGFR2 activity.

S. Franceschelli et al. examined the effects of phenethyl isothiocyanate (PEITC), one of the best-studied members of the organic isothiocyanates (ITC) family in the regulation of the cytoskeleton and morphology of endothelial cells (ECs). They demonstrated that PEITC induces PI3K/Akt promoting significant morphological changes in ECs that come back to the normal size and morphology after 16 hours from treatment. This effect was related to the activation of an important small GTPase protein Rac1. The activation of this latter led to JNK activation that promoted cytoskeleton remodelling influencing endothelial cell survival and growth. The authors showed that JNK promoted BAG3 overexpression. The expression of BAG3 corresponds to a recovery of cellular morphology after an initial damage by PEITC treatment; in fact, downregulation of Bag3 protein resulted in the loss of morphology recovery. In conclusion, they identified an important mechanism that led to actin refolding and the recovery of cell morphology which is driven by BAG3 that could represent an important target to recovery endothelial cells damage during cardiovascular diseases.

A. Fedorowicz et al. showed that in diabetic condition, increased ROS production may promote an increased permeability of pulmonary microcirculation related to NO impairment and increase compensatory levels of PGI2 and CD141 while the endothelial alteration detected in the aorta was associated with NO, PGI2, and CD141 impairment. This study highlighted various changes in pulmonary and peripheral endothelial function leading to endothelial dysfunction during diabetes.

The endothelial dysfunction is also a characteristic of patients affected by inflammatory bowel disease (IBD) such as Crohn's disease. In fact, IBD even in the absence of classic cardiovascular risk factors have a higher risk for endothelial dysfunction and atherosclerosis. In this context, A. G. Gravina et al. analysed the relationship between inflammation, oxidative stress, and endothelial dysfunction in IBD in order to predict the possible role of such inflammation in cardiovascular disease development. The authors focused their attention on pharmacological and nonpharmacological therapeutic targets, both of them aiming at attenuating chronic inflammation and oxidative stress.

Y. Shen and colleagues demonstrated that transplantation of bone marrow mesenchymal stem cells can be used to treat radiation-induced artery injury once again by suppressing oxidative stress and inflammation. Actually, the authors showed that this approach was able to upregulate antioxidant enzymes including HO-1 and catalase and downregulate inflammatory factors such as TNF-α, ICAM-1, and TGF-β.

C. R. Balistreri and colleagues found in patients with bicuspid valve disease a significant reduction of T and B lymphocyte cell subsets, compared to tricuspid aortic valve patients. This reduction, like those observed in old people, makes the individuals more vulnerable to chronic stress, inflammation, and oxidative stress, leading to cardiovascular diseases.

Interestingly, in a review article, G. Amodio et al. extensively highlighted the involvement of the unfolded protein response (UPR) pathways in the oxidative stress-induced endothelial dysfunction. In particular, authors underlined the importance of the endoplasmic reticulum (ER) source of ROS in the pathogenesis of cardiovascular diseases and the dual role of UPR, both prooxidant and antioxidant. They also reported the recent literature suggesting how the modulation of ER stress and UPR signalling may be a new therapeutic strategy to counteract the endothelial dysfunction. However, since some aspects on this field remain unclear, more investigations on animal models are encouraged. Identification of new molecular pathways aimed to develop therapeutic procedure based on pharmacological and nonpharmacological approaches, at different cellular levels, could represent an important milestone to reduce the onset of cerebral and cardiovascular diseases.

Valeria Conti
Maurizio Forte
Albino Carrizzo

Hindawi
Oxidative Medicine and Cellular Longevity
Volume 2018, Article ID 4036709, 15 pages
https://doi.org/10.1155/2018/4036709

Research Article

Comparison of Pulmonary and Systemic NO- and PGI_2-Dependent Endothelial Function in Diabetic Mice

Andrzej Fedorowicz,[1,2] **Elżbieta Buczek**,[1] **Łukasz Mateuszuk**,[1] **Elzbieta Czarnowska**,[3] **Barbara Sitek**,[1] **Agnieszka Jasztal**,[1] **Antonina Chmura-Skirlińska**,[1] **Mobin Dib**,[4] **Sebastian Steven**,[4] **Andreas Daiber**,[4] **and Stefan Chlopicki**[1,2]

[1]*Jagiellonian Centre for Experimental Pharmacology (JCET), Jagiellonian University, Bobrzyńskiego 14, 30-348 Kraków, Poland*
[2]*Chair of Pharmacology, Jagiellonian University Medical College, Grzegórzecka 16, 31-531 Kraków, Poland*
[3]*Department of Pathology, The Children's Memorial Health Institute, Al. Dzieci Polskich 20, 04-730 Warsaw, Poland*
[4]*Center for Cardiology 1, Laboratory of Molecular Cardiology, University Medical Center of the Johannes Gutenberg University, Mainz 55131, Germany*

Correspondence should be addressed to Stefan Chlopicki; stefan.chlopicki@jcet.eu

Received 17 January 2018; Revised 3 April 2018; Accepted 16 April 2018; Published 4 June 2018

Academic Editor: Valeria Conti

Diabetes increases the risk of pulmonary hypertension and is associated with alterations in pulmonary vascular function. Still, it is not clear whether alterations in the phenotype of pulmonary endothelium induced by diabetes are distinct, as compared to peripheral endothelium. In the present work, we characterized differences between diabetic complications in the lung and aorta in db/db mice with advanced diabetes. Male, 20-week-old db/db mice displayed increased HbA1c and glucose concentration compatible with advanced diabetes. Diabetic lungs had signs of mild fibrosis, and pulmonary endothelium displayed significantly ultrastructural changes. In the isolated, perfused lung from db/db mice, filtration coefficient ($K_{f,c}$) and contractile response to TXA_2 analogue were enhanced, while endothelial NO-dependent modulation of pulmonary response to hypoxic ventilation and cumulative production of NO_2^- were impaired, with no changes in immunostaining for eNOS expression. In turn, 6-keto-$PGF_{1\alpha}$ release from the isolated lung from db/db mice was increased, as well as immunostaining of thrombomodulin (CD141). In contrast to the lung, NO-dependent, acetylcholine-induced vasodilation, ionophore-stimulated NO_2^- generation, and production of 6-keto-$PGF_{1\alpha}$ were all impaired in aortic rings from db/db mice. Although eNOS immunostaining was not changed, that of CD141 was clearly lowered. Interestingly, diabetes-induced nitration of proteins in aorta was higher than that in the lungs. In summary, diabetes induced marked ultrastructural changes in pulmonary endothelium that were associated with the increased permeability of pulmonary microcirculation, impaired NO-dependent vascular function, with compensatory increase in PGI_2 production, and increased CD141 expression. In contrast, endothelial dysfunction in the aorta was featured by impaired NO-, PGI_2-dependent function and diminished CD141 expression.

1. Introduction

Diabetes induces profound alterations in systemic circulation and is the leading cause of macro- and microangiopathies such as diabetic retinopathy, nephropathy, and myocardial infarct, as well as peripheral artery disease [1–3]. The detrimental effects of diabetes in the lungs are less clinically apparent. However, epidemiological and experimental data suggested that insulin resistance and diabetes affect the lung. In diabetic subjects, the risk of pulmonary hypertension and pulmonary embolism was increased [4]. Interestingly, several studies have suggested that diabetes results in the impairment of respiratory function [5–7] and increased susceptibility to allergic response/inflammation induced with LPS or airway bacterial infection [8–10]. Structural changes in blood-alveolar barrier and diffusion impairment *in vivo* have also been reported [11, 12]. Despite these reports, the possible detrimental effects of insulin resistance and diabetes

on the pulmonary circulation have received little attention, and therefore research on this aspect of the pathophysiology of diabetes has largely been neglected. To the best of our knowledge, there are only few reports directly comparing systemic and pulmonary circulation response to diabetes in the same experimental model. Such an approach could give a better understanding of similarities and differences between diabetes-induced changes in pulmonary and peripheral circulation [13, 14].

Furthermore, although peripheral endothelial dysfunction represents a well-recognized hallmark of peripheral diabetic macro- and microangiopathies [2, 7, 15], the evidence on the development of pulmonary endothelial dysfunction in diabetes is rather conflicting. Both the presence and lack of impairment of NO-dependent pulmonary endothelial function have been reported [13, 16, 17]. In turn, an increase in pulmonary microvascular permeability without changes in eNOS or with increased iNOS expression has also been demonstrated [13, 16–18].

Similarly, reports on diabetes-induced changes in PGI_2 production in the pulmonary circulation are also not consistent. In streptozotocin-treated rats, basal PGI_2 production and stimulated PGI_2 production in pulmonary circulation were reported to increase or to remain unchanged [14, 19, 20]. Interestingly, PGI_2 is a major regulator of the expression of thrombomodulin (CD141) [21, 22], which complexes with thrombin (IIa) and activates protein C to act as an anticoagulant and endothelial protective mediator [23]. Thus, the changes in the activity of PGI_2 may result in the alteration in the activity of thrombomodulin, despite the fact that previous studies reported no changes [24–26].

Given the nonconsistent literature, the aim of the present work was to characterize changes in pulmonary endothelial function in comparison with changes in peripheral endothelial function in the aorta, with special focus on NO- and PGI_2-dependent pathways. For this purpose, male db/db mice at the age of 20 weeks with features of advanced diabetes were used, and pulmonary and peripheral endothelial functions and NO and PGI_2 activities were analyzed in the isolated, perfused diabetic lung, or in the aortic rings, respectively.

2. Material and Methods

2.1. Animals. 20-week-old db/db (BKS.Cg-Dock7m +/+LeprdbJ) and C57BL/6J mice, purchased from Charles River Laboratories, were housed in specific pathogen-free conditions (SPF) and fed with a standard laboratory diet and water *ad libitum*.

All experimental procedures used in the present study were conducted according to the Guidelines for Animal Care and Treatment of the European Communities and the Guide for the Care and Use of Laboratory Animals published by the US National Institutes of Health (NIH Publication number 85-23, revised 1996). All procedures were approved by the local Jagiellonian University Ethical Committee on Animal Experiments (number 53/2009).

2.2. Blood Count, HbA1c, and Basal Biochemistry in Plasma. Blood was collected from anaesthetized animals (pentobarbital, 140 mg/kg, i.p.) via the right ventricle to a syringe with nadroparine (end concentration: 10 U/ml) for analysis of blood count and HbA1c, and the rest of the sample were centrifuged to obtain plasma (1000g, 5 min, 4°C). Complete blood count was analyzed within 15 minutes after collection (by automatic blood counter ABC Vet, HORIBA). HbA1c and total hemoglobin concentrations were measured using a biochemical analyser (ABX Pentra 400, HORIBA), and the ratio was given as a percentage of HbA1c. Glucose, aspartate aminotransferase, alanine aminotransferase, creatinine, albumin, and total protein were measured using colorimetric methods (ABX Pentra 400, HORIBA).

2.3. Histological Analysis of the Lungs. The lungs were removed under anaesthesia and fixed in 4% buffered formalin (24 h) and were then dehydrated, embedded in paraffin, cut into 5 μm sections on Accu-Cut® SRM™ 200 Rotary Microtome, and stained with either hematoxylin and eosin (H&E), Masson Trichrome, Orcein and Methyl Scarlet Blue (OMSB [27]), or Picro Sirius Red. Light microscopic examination and photographic documentation were performed using an Olympus BX53F microscope equipped with a digital camera.

2.4. Assessment of Changes in Lung Ultrastructure. The chest of anaesthetized rats was opened, and samples of lung tissue were cut and fixed immediately using a mixture of 2.5% glutaraldehyde and 2% freshly prepared paraformaldehyde in 0.1 mol/L cacodylate buffer at pH 7.4. The lung tissue was fixed for 12 h at 4°C. Then, the lungs were postfixed in buffered 2% osmium tetroxide, dehydrated in a graded ethanol series and propylene oxide, and embedded in Epon 812. The ultrathin sections were stained according to routine protocol with uranyl acetate and lead citrate and were examined and documented by transmission electron microscopy (Jem 1011, JEOL, Japan).

2.5. Immunohistochemistry of Lung Tissue. After excision, lung tissues were fixed with 4% formalin solution (10 min) and placed in 50% OCT for cryopreservation (24 h), then snap frozen at −80°C. Blocks were cut into 10 μm-thick cross-sectional slides. 5% normal goat serum (Jackson Immuno) or 2.5% horse serum (Vector Labs) and 2% filtered dry milk were applied to minimalize nonspecific binding of antibodies. For indirect immunohistochemical detection of von Willebrand factor (vWF), thrombomodulin (CD141), endothelial nitric oxide synthase (eNOS), vascular cell adhesion molecule 1 (VCAM-1), and macrophage content (MAC3), sections were incubated with rabbit anti-vWF polyclonal Ig (Abcam), rat polyclonal anti-CD141 Ig (BD Bioscience), mouse monoclonal anti-eNOS Ig (BD Bioscience), rat anti-VCAM-1 monoclonal Ig (Millipore), or rat anti-MAC3 monoclonal Ig (Thermo), respectively (1 h). Antibodies were applied at concentrations of 5 μg/ml or 10 μg/ml (dilution 1 : 100–1 : 300 of stock solution). After rinsing in PBS, secondary biotinylated horse anti-rabbit (Vector Labs), goat anti-mouse, goat anti-rat, or goat anti-rabbit (Jackson Immuno) antibodies were applied for 30 min. At a third step of staining, Cy3-conjugated

streptavidin (Jackson Immuno) and Hoechst 33258 solution were used.

2.6. Assessment of Endothelial Function in the Isolated Lung Preparation. Trachea in anesthetized mice were cannulated, and the lungs were ventilated with positive pressures at a rate of 90 breaths/min (VCM module from Hugo Sachs Electronic (HSE)). After laparotomy, the diaphragm was cut and nadroparine at a dose of 600 I.U. was injected into the right ventricle to prevent microthrombi formation during the surgical procedure. Then, the animals were exsanguinated by incision of the left renal artery. The lungs were exposed via a median sternotomy. The pulmonary artery and left atrium were cannulated via the right and left atrium, respectively.

Immediately after cannulation, the lung/heart block was dissected from the thorax. Using tracheal cannula, the isolated lung was mounted in a water-jacketed (38°C), air-tight glass chamber (HSE) and ventilated with negative pressures. The lungs were perfused with low-glucose DMEM with 4% albumin and 0.3% HEPES; the pH of perfusate was maintained at 7.35 throughout the whole experiment by continuous addition of 5% CO_2 to the inspiratory air, using a peristaltic pump (ISM 834, HSE) at a constant flow (CF) of about 1.50 ml/min. The venous pressure was set between 2 and 5 cmH_2O. The end-expiratory pressure in the chamber was set to be $-3\,cmH_2O$, and inspiratory pressure was adjusted between −6 and $-10\,cmH_2O$ to yield the initial tidal volume (TV) of about 0.2 ml. Breathing frequency was set to be 90 breaths/min, and a duration of inspiration versus expiration was 1 : 1 in each breath. Every 5 min throughout the experiments, a deep breath of end-inspiratory pressure of $-21\,cmH_2O$ was automatically initiated by VCM module (HSE) to avoid atelectasis. Airflow velocity was measured with a pneumotachometer tube connected to a differential pressure transducer (HSE), from which the value of respiratory tidal volume was determined. In experiments with constant pressure perfusion (CP), CP mode was turned on just after placing the lungs in the artificial thorax. The PAP was set to be around $3\,cmH_2O$. The venous pressure was set between 2 and $5\,cmH_2O$.

Both arterial and venous pulmonary pressures (PAP, PVP) were continuously monitored by ISOTEC pressure transducers (HSE) connected to a perfusion line on arterial and venous sides, respectively. The weight of the lungs was monitored by a weight transducer (HSE). TC, PAP, PVP, and lung weight data were acquired by the PC transducer card and subsequently analyzed by Pulmodynpulmo software (HSE).

All lung preparations were allowed to equilibrate for the first 15 min of perfusion with fresh buffer until baseline PAP, PVP, TV, and weight were stable. At this time point, weight of the lung (the value of which varied considerably between experiments) was set to zero.

2.6.1. Hypoxic Pulmonary Vasoconstriction (HPV). HPV was evoked by 10-minute intervals of hypoxic ventilation with a mixture of 95% N_2 and 5% CO_2. HPV, measured as changes in PAP, was stabilized after 5 minutes. After cessation of acute hypoxia, PAP returned to a basal level. There was a 10-minute interval of normal ventilation between HPV procedures. HPV was repeated twice, then L-NAME (300 μM) was added to the perfusate and recirculated through the lung for 10 minutes, and HPV response was repeated twice again. Although TV, PAP, PVP, and weight were continuously monitored throughout the experiment, for data analysis, only maximum increase in PAP (ΔPAP) elicited by HPV was taken. TV, PVP, and weight did not change significantly during HPV.

2.6.2. Vasoreactivity. After equilibration, U46619 (1 μM) was added to the perfusate, which resulted in an increase of PAP, but other parameters of isolated lungs did not change. For data analysis, only maximum increase of PAP (ΔPAP) was taken.

2.6.3. Pulmonary Microcirculation Permeability. In equilibrated isolated lung, perfused with constant pressure, the pulmonary venous pressure was increased to obtain PVP 1.5 cmH_2O above PAP and was maintained at this level through 15 minutes. This resulted in an increase in weight of the lungs; other parameters were stable. After 15 minutes, PVP was set to basal value, and the process was repeated. The filtration coefficient ($K_{f,c}$) was calculated based on recordings for 5 minutes after PVP increase [28].

2.6.4. Biochemical Measurements. 6-keto-$PGF_{1\alpha}$ and NO_2^-/NO_3^- concentrations were measured in samples of effluents collected after 15 minutes of equilibration of isolated lungs perfused with constant flow, and then 5 and 45 minutes after recirculation of the perfusate was started. To assess the enzymatic source of 6-keto-$PGF_{1\alpha}$, a sample was taken before and after administration of COX-2 selective inhibitor (DuP-697, 1 μM) or nonselective COX-1/COX-2 inhibitor (indomethacin, 1 μM).

2.7. Assessment of Endothelial Function in the Isolated Aortic Rings. The thoracic aorta was quickly dissected out of the chest of anaesthetized mice, and the surrounding fat/connective tissue was removed in Krebs-Henseleit (KH) solution (mM: NaCl 118.0, $CaCl_2$ 2.52, $MgSO_4$ 1.16, $NaHCO_3$ 24.88, K_2PO_4 1.18, KCl 4.7, glucose 10.0, pyruvic acid 2.0, and EDTA 0.5). Then, the aorta was cut into 2-3 mm rings, which were mounted between two pins filled with 5 ml of KH solution chambers (37°C, pH 7.4, gassed with carbogen: 95% O_2, 5% CO_2) of wire myograph (620 M, Danish Myo Technology, Denmark). The unstretched aortic rings were allowed to equilibrate for 30 minutes. Then, the resting tension of the rings was increased stepwise to reach 10 mN, and the rings were washed with fresh KH solution and incubated to equilibrate for the next 30 mins.

After equilibration, the viability of the tissue was examined by contractile responses to potassium chloride (KCl 30 mM, 60 mM), and then the aortic rings were contracted with phenylephrine (Phe 0.01–3.0 μM) to obtain maximal possible constriction of the rings. All tissue responses were recorded, using a data acquisition system and recording software (PowerLab, LabChart, and ADInstruments, Australia). The aortic rings were next contracted with phenylephrine

to obtain 80–90% of maximal contraction, and the endothelial-dependent response was assessed using cumulative concentrations of acetylcholine (ACh 0.01–10 μM). After washout, the vessels were again contracted with phenylephrine, and endothelial-independent vasodilation to cumulative concentrations of sodium nitroprusside (SNP 0.001–1 μM) was assessed. The relaxation response was expressed as a percentage of the precontraction induced by phenylephrine.

2.8. Assessment of Prostacyclin (PGI_2) Production in the Isolated Aortic Rings. The concentration of PGI_2, produced by aortic rings, was quantified on the basis of the formation of 6-keto-$PGF_{1\alpha}$, a stable metabolite of PGI_2. The aorta rings were preincubated for 15 minutes on the thermoblock (Liebisch Labortechnik) at a temperature of 37°C, in 250 μl KH buffer, gassed with carbogen in the absence or in the presence of COX-2 selective inhibitor (DuP-697, 1 μM) or nonselective COX-1/COX-2 inhibitor (indomethacin, 5 μM). All inhibitors were dissolved in DMSO, and then control rings were incubated with addition of the same amount of DMSO (1 μl/ml).

Aortic rings were then incubated for 60 minutes, and samples of effluents were collected after 3 and 60 minutes. After the experiment, aortic rings were dried (1 h, 50°C) and weighed. 6-keto-$PGF_{1\alpha}$ concentration in the effluents was measured using an EIA kit (Enzo, Life Technologies). Results were expressed as the change in 6-keto-$PGF_{1\alpha}$ concentration between 60 and 3 minutes of ring incubation and normalized to dry weight of aortic rings (pg/ml/mg).

2.9. Assessment of Nitrite Production in the Isolated Aortic Rings. Basal NO production by the aorta was estimated by measurements of nitrite, a primary stable product of nitric oxide oxidation, and thus considered relevant for estimation of NO synthesis by the aortic endothelium. Segments from the aortic arch were longitudinally opened, placed in 96-well plates facing up with endothelium, and incubated for one hour in 120 μl KH buffer at 37°C, using a specially designed closed chamber (BIO-V(Noxygen)) that was equilibrated with carbogen gas mixture (95% O_2, 5% CO_2). The nitrite concentration after back reduction to NO was measured using the gas-phase chemiluminescent reaction between NO and ozone using a Sievers* Nitric Oxide Analyzer NOA 280i. The reduction of nitrites was performed in a closed glass chamber containing a reducing agent (1% wt/vol of KI in acetic acid) to convert nitrite to NO. The independent calibration on fresh $NaNO_2$ standard solution was prepared for every experiment before measurements of series of samples after each refilling of glass reaction chamber, according to the manufacturer's instructions (Sievers* Nitric Oxide Analyzer NOA 280i). The limit of detection was around 10 nM of nitrite. Multiple blank samples (without aortic rings) were used to monitor nitrite contamination in the buffer and/or by laboratory atmosphere in every set of experiments. The averaged blank signal from a blank sample in a given experiment was subtracted as a background signal. Samples were kept on ice and measured directly after experiments. Nitrite concentration was expressed as ng/ml/mg of dry weight of aortic rings.

2.10. Immunohistochemistry in Aorta. Dissected thoracic aorta, cleared of the surrounding fat/connective tissue in Krebs-Henseleit (KH) solution, was fixed with 4% formalin solution (10 min), embedded in 50% OCT for cryopreservation (24 h), snap frozen at −80°C, and cut in 10 μm-thick cross-sectional slides for immunohistochemistry. 2.5% horse serum (Vector Labs) and 2% dry milk were applied to minimalize nonspecific binding of antibodies. For von Willebrand factor (vWF) staining, rabbit anti-mouse vWF polyclonal Ig (Abcam) was used, followed by biotinylated horse anti-rabbit Ig (Vector Labs) and Cy3-streptavidin (Jackson Immuno), as described above. Nuclei were counterstained with Hoechst 33258 (Sigma-Aldrich). Images were acquired using an Axio Observer D2 fluorescent microscope, and fluorescence parameters were analyzed automatically by Columbus software (PerkinElmer).

2.11. Dot Blot Analysis in Aorta and Lungs. Protein expression and modification were assessed by standard dot blot analysis using established protocols [29]. 3-Nitrotyrosine-(3NT-) positive proteins were assessed by dot blot analysis of protein homogenates in aorta and lungs, which were transferred to a Protran BA85 (0.45 μm) nitrocellulose membrane (Schleicher & Schuell, Dassel, Germany) by a Minifold I vacuum dot-blot system (Schleicher & Schuell, Dassel, Germany) [30]. A mouse monoclonal 3NT antibody (1 : 1000, Upstate Biotechnology, MA, USA) was used for dot blot analysis. Detection and quantification of all blots were performed by ECL with peroxidase anti-mouse (1 : 10,000, Vector Lab., Burlingame, CA). Densitometric quantification of antibody-specific bands was performed with a ChemiLux Imager (CsX-1400 M, Intas, Göttingen, Germany) and Gel-Pro Analyzer software (Media Cybernetics, Bethesda, MD).

3. Statistical Analysis

Results are presented as the mean ± SEM. The normality of the results was analysed using the D'Agostino & Pearson omnibus normality test and the Shapiro-Wilk test. To calculate statistical significance, a paired Student's *t*-test, Mann-Whitney test, or unpaired Student *t*-test was used. Post hoc analysis was calculated using Dunn's multiple comparisons test.

4. Results

4.1. Basal Characteristics of db/db Mice. 20-week-old db/db mice were obese (body weight: 53.77 ± 0.18 *versus* 29.5 ± 0.12 g, db/db and control, resp.; $P < 0.05$) and had increased HbA1c (15.38 ± 1.7 *versus* 4.12 ± 1.36%, db/db and control, resp.; $P < 0.05$) and fasting glucose concentration in plasma (40.64 ± 5.41 *versus* 8.66 ± 1.24 mmol/l, db/db and control, resp.; $P < 0.05$) as compared to control mice. In addition to hyperglycaemic profile, db/db mice displayed signs of liver injury (increased plasma AST, ALT, e.g., for ALT: 141.90 ± 19.68 *versus* 38.02 ± 2.80, db/db and control, resp.; $P < 0.001$) and kidney injury (increased plasma

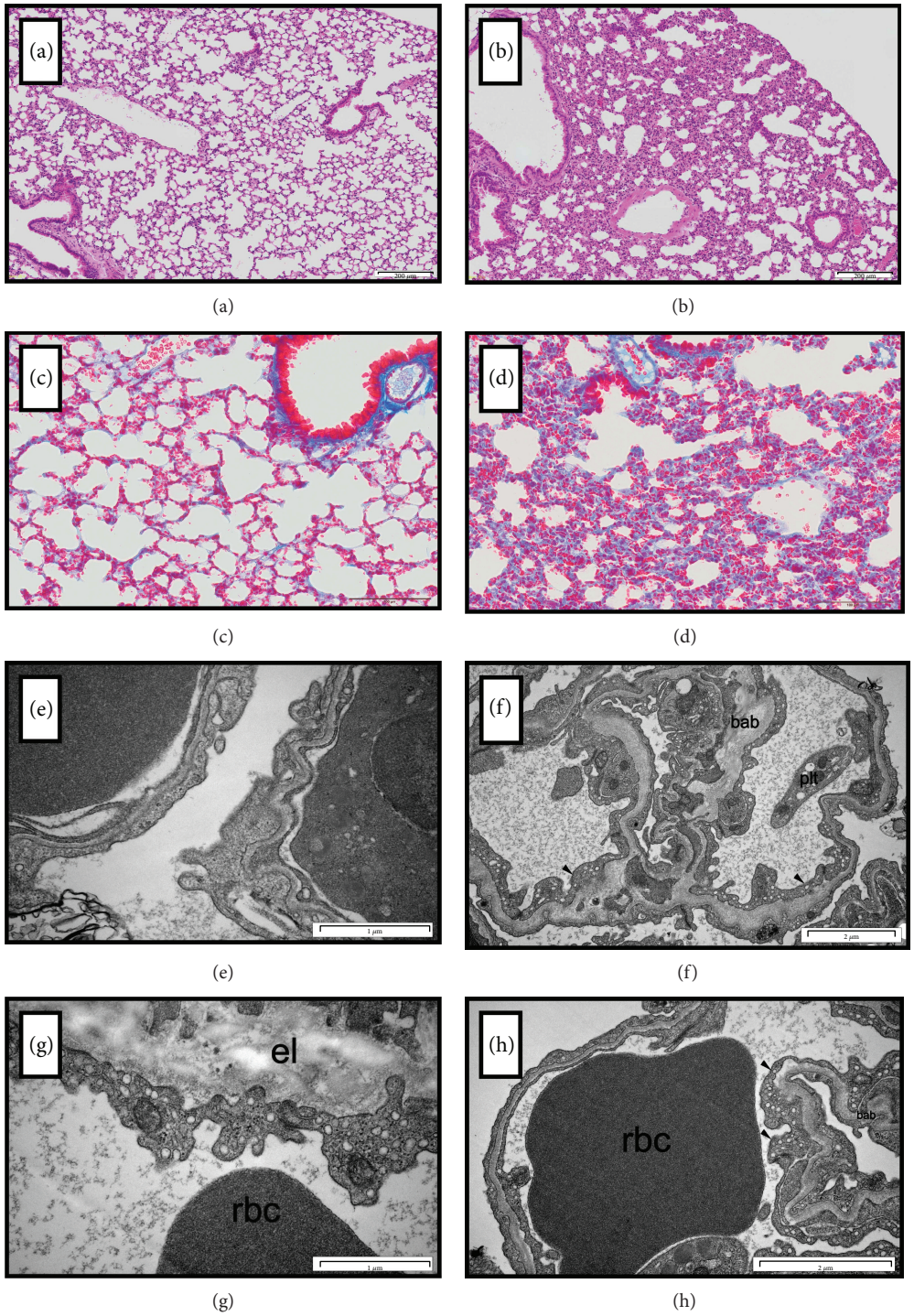

Figure 1: Histology of the lungs and ultrastructure of pulmonary endothelial cells from the control (a, c, e, g) and diabetic (b, d, f, h) lungs (db/db mice). (a) Histological structure of the control lungs. (b) Inflammation in the lung tissue: increased amount of cells (including granulocytes and macrophages) and (d) collagen in parenchyma of the diabetic lung tissue as compared to control; visible decreased aerial space in diabetic lungs as compared to the control (c). (e) Microphotographs of ultrastructure of the control lungs—blood-air barrier (alveolar–capillary barrier) with normal endothelial layer. (f, g, h) Microphotographs of ultrastructure of the lungs from the db/db mice. (f) Capillary endothelial cells (arrows) with numerous plasmalemmal vesicles (caveolae) on thickened blood-air barrier (bab). In the center: collapsed pulmonary alveoulus, on the right: blood platelet (plt) inside the vessel. (g) A presence of convoluted apical region in endothelial cells with cytoplasmic extensions on hyperplastic basal laminae enriched with elastine (el); on the bottom: red blood cell (rbc). (h) Endothelial cells of various heights (arrows) separated by thickened blood-air barrier (bab) from pulmonary alveolus; neighbouring red blood cell (rbc). Representative images of at least 3 independent experiments.

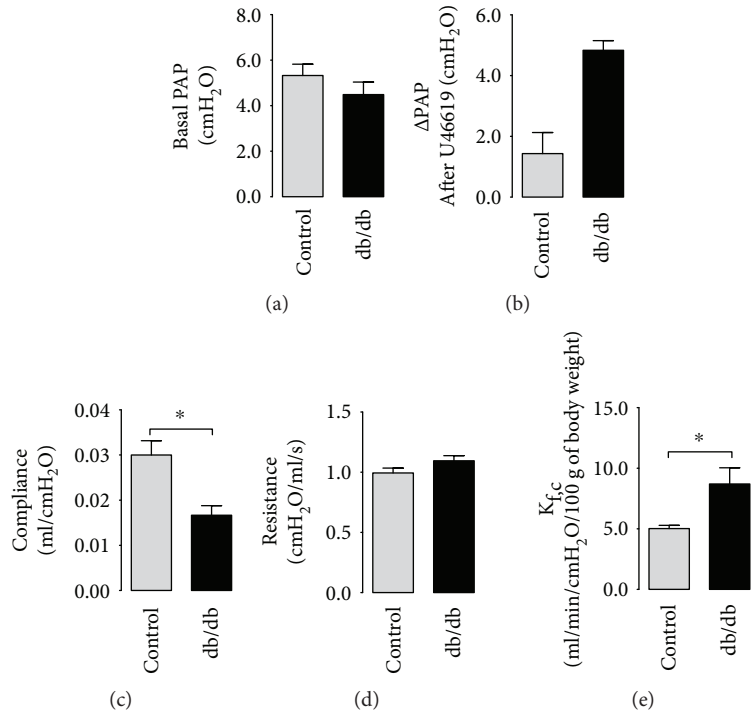

Figure 2: Comparison of basal parameters of the isolated, perfused lungs amongst diabetic and control animals. (a) No change in basal pulmonary pressure, although (b) enhanced reactivity to thromboxane analogue in the lungs of the diabetic mice (U-44619, 1 μM, control $n = 5$, diabetes $n = 5$). (c) Decreased compliance without changes in (d) resistance of the lungs (control $n = 5$, diabetes $n = 6$). (e) Increased filtration coefficient in the diabetic pulmonary circulation (control $n = 5$, diabetes $n = 5$). Data are presented as the means ± SEM. $^*P < 0.05$.

creatinine 62.90 ± 63.61 *versus* $46.74 \pm 7.02\,\mu$mol/(L*cm^2), db/db and control, resp.; $P < 0.05$).

4.2. Histology and Ultrastructure of Lungs in db/db Mice. Lungs from db/db mice displayed inflammation, as evidenced by multicellular (including granulocytes, macrophages) infiltrations in the interstitial space (HE staining, Figure 1(b)) as compared to the control group (Figure 1(a)); mild fibrosis (increased amount of collagen), as evidenced by Trichrome staining (Figure 1(d)) as compared to the control group (Figure 1(c)); and endothelial inflammation, as evidenced by increased VCAM-1 expression in pulmonary endothelium ($480{,}937 \pm 70{,}112$ *versus* $247{,}193 \pm 64{,}821$ AU, db/db and control, resp.; $P = 0.07$). Interestingly, ultrastructural investigations confirmed the presence of numerous macrophages (often lying next to each other) in the lungs from db/db mice, as compared to control mice, and they were also detected as adhering to endothelium (data not shown). Moreover, semithin sections of lung tissue revealed diminished area of alveoli (34.13 ± 4.25 *versus* 50.75 ± 3.83, db/db and control, resp.). Capillary endothelial cells displayed protruded apical regions into the capillary lumen, increased area of sarcoplasmic reticulum, plasmalemmal vesicles (caveolae), and sometimes presence of multivesicular bodies or lysosomes.

One of the typical features of db/db pulmonary microcirculation was the hyperplasia of basal lamina in db/db (Figures 1(f) and 1(h)) that was not evident in control samples (Figures 1(e) and 1(g)). Thickness of capillaries' basal lamina ranges from 0.1 μm to 0.35 μm, compared to 0.05 μm in controls. Additionally, septa separating lung alveoli in db/db were thicker, with abundant collagen fibrils and probably contained also elastin fibrils marked by an uncontrasted area in the thin sections routinely stained with uranyl acetate and lead citrate (Figures 1(f) and 1(h)), which was also not seen in control samples (Figures 1(e) and 1(g)).

4.3. Alterations in Pulmonary Vascular Function and Inflammation in the Isolated, Perfused Lung from db/db Mice

4.3.1. Changes in Basal Pulmonary Parameters and Vasoreactivity. The basal pulmonary artery pressures in the isolated, perfused lungs (bPAP) were comparable in db/db and control mice (PAP: 4.70 ± 0.62 *versus* 5.20 ± 0.30 cmH$_2$O, db/db and control, resp., Figure 2(a)). Vasoreactivity to thromboxane A$_2$ analogue U46619 was increased threefold in the isolated lungs from db/db mice (ΔPAP: 4.83 ± 0.32 *versus* 1.43 ± 0.69 cmH$_2$O, db/db and control, resp.; $P = 0.073$) (Figure 2(b)). Compliance but not resistance was decreased in db/db mice (compliance: 0.016 ± 0.002 *versus* 0.030 ± 0.003 ml/cmH$_2$O, db/db and control, resp.; $P < 0.05$; resistance: 1.09 ± 0.04 *versus* 0.99 ± 0.04 cmH$_2$O/ml/s, db/db and control, resp.; Figures 2(c) and 2(d)).

4.3.2. Changes in Permeability Coefficient ($K_{f,c}$). In the isolated, perfused lung, an increase in pulmonary venous pressure resulted in slow, reversible weight gain of the lungs, both in control and db/db mice. Calculation of $K_{f,c}$ revealed a higher filtration coefficient in the diabetic lungs as compared with the control lungs (8.70 ± 1.33 *versus* 5.02 ± 0.27 ml/

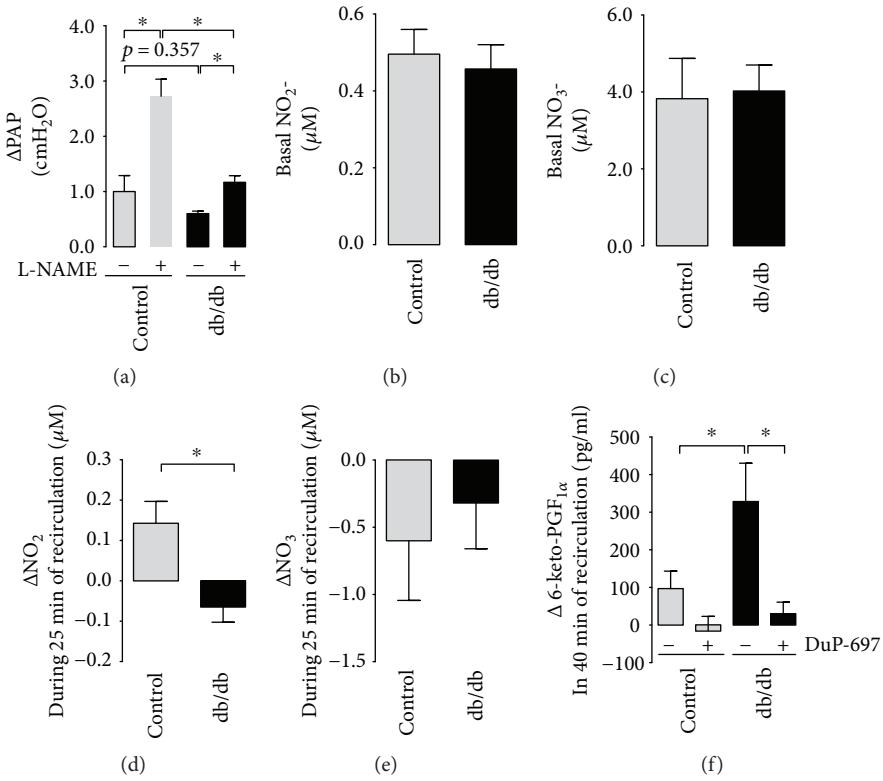

FIGURE 3: NO- and PGI_2-dependent function in the diabetic isolated lungs. (a) Impaired NO-dependent hypoxic pulmonary vasoconstriction response after L-NAME in the lungs of the diabetic mice (control $n = 5$, diabetes $n = 5$). (b, c) Lack of change in basal production of nitrite and nitrate and (d, e) impaired capacity to cumulative production of nitrite but not nitrate in effluents from the isolated, perfused lungs of the diabetic mice (control $n = 6$, diabetes $n = 7$). (f) Increased COX-2-dependent prostacyclin production in effluents from the isolated, perfused lungs and effects of a COX-2 inhibitor (DuP-697, 1 μM, control $n = 6$, diabetes $n = 7$). Data are presented as the means ± SEM. $^*P < 0.05$.

min/cmH_2O/100 g of body weight, db/db and control, resp.; $P < 0.05$, Figure 2(e)).

4.3.3. Impairment of NO-Dependent Regulation of Hypoxic Pulmonary Vasoconstriction (HPV). In the isolated, perfused lung from control mice, episodes of hypoxic ventilation resulted in an increase of pulmonary arterial pressure (PAP) without significant changes in other parameters of isolated lung preparation (Figure 3(a)). In control lungs, the nonselective inhibitor of nitric oxide synthases, L-NAME, augmented HPV response (ΔPAP: 0.87 ± 0.32 *versus* 2.73 ± 0.44 cmH_2O, before and after L-NAME, resp.; $P < 0.05$). However, in the isolated, perfused lung from db/db mice, the effect of L-NAME on HPV was substantially lost (ΔPAP: 0.60 ± 0.04 *versus* 1.17 ± 0.12 cmH_2O, before and after L-NAME, resp.; $P < 0.05$) suggesting impaired NO-dependent function. L-NAME did not modify basal PAP (Δ basal PAP after L-NAME: 0.17 ± 0.03 *versus* 0.19 ± 0.06 cmH_2O, in control and db/db mice, resp.).

4.3.4. Nitrite/Nitrate (NO_2^-/NO_3^-) and Prostacyclin (PGI_2) Production. In effluents from the isolated, perfused lungs, basal NO_2^-/NO_3^- concentrations were comparable in both groups (e.g., NO_2^- 0.40 ± 0.04 *versus* 0.56 ± 0.19 μM, db/db and control, resp., Figures 3(b) and 3(c)). The cumulative concentrations of NO_2^- from the diabetic lungs (see Methods for details) were significantly lower (ΔNO_2^-: -0.04 ± 0.04 *versus* 0.11 ± 0.05 μM, db/db and control, resp.), but there were no changes in NO_3^- concentrations (Figures 3(d) and 3(e)). The cumulative concentration of stable PGI_2 metabolite, 6-keto-$PGF_{1\alpha}$, in the effluents from the isolated diabetic lungs was higher than that in the control (Δ6-keto-$PGF_{1\alpha}$: 223.5 ± 57.91 versus 95.06 ± 24.00 pg/ml, db/db and control, resp.) and was blunted after COX-2 inhibitor, DuP-697 (Figure 3(f)).

4.3.5. Markers of Vascular Inflammation. In diabetic lungs, immunohistochemical staining intensity of vascular adhesion molecule-1 (VCAM-1) was increased by a trend as compared to the control samples (Figure 4(a)). Von Willebrand factor (vWF) and thrombomodulin (CD141) (but not eNOS) were higher in the diabetic lungs than in the control lungs (Figures 4(b)–4(d)). All together these results support an increased inflammatory state in the pulmonary system of diabetic mice.

4.4. Impairment of Endothelial Function and Inflammatory Markers in the Aorta of db/db Mice. Vasoreactivity to phenylephrine (30 μM) in the aortic rings from db/db mice was increased (not shown). Acetylcholine- (ACh-) induced endothelium-dependent vasodilation was decreased for all concentrations in db/db mice, while sodium nitroprusside-

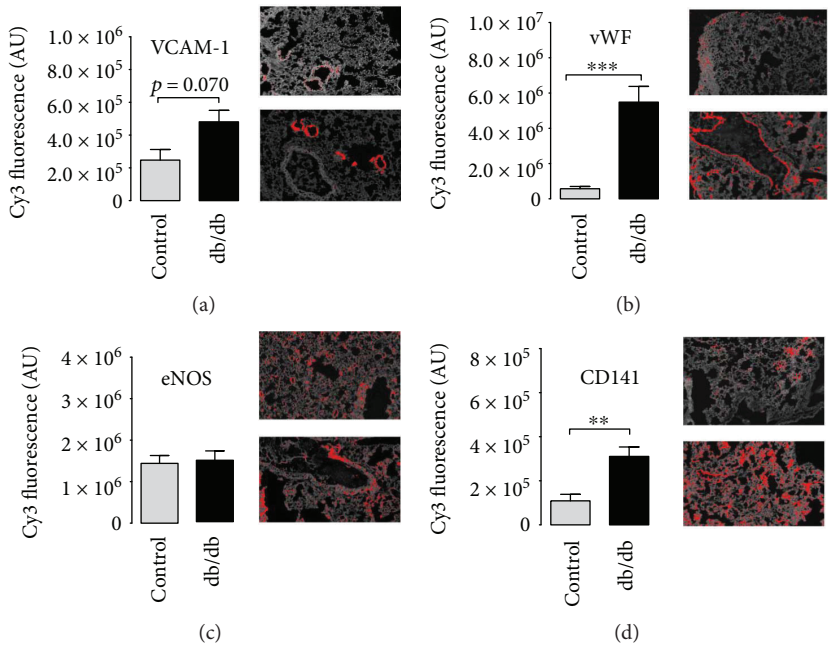

Figure 4: Immunohistochemical profile of the diabetic lungs. (a) Inflammation in vascular wall related to increased immunostaining of vascular cell adhesion molecule 1 (VCAM-1) and (b) von Willebrand factor in the lungs of the diabetic mice (both for VCAM-1 and vWF: control $n = 4$, diabetes $n = 4$). (c) No change in eNOS immunostaining in the diabetic lungs as compared to the control (control $n = 4$, diabetes $n = 4$). (d) Increased thrombomodulin (CD141) immunostaining in the diabetic lungs as compared to the control (control $n = 4$, diabetes $n = 4$). Data are presented as the means ± SEM. $^{**}P < 0.01$, $^{***}P < 0.001$.

(SNP-) induced response was preserved as compared to the control group (Figures 5(a) and 5(b)). Impairment of functional response was supported by a decline in ionophore-stimulated NO_2^- production in the aortic rings from the db/db mice (33.88 ± 10.01 *versus* 173.30 ± 77.79 nM, db/db and control, resp.; $P < 0.05$). Basal NO_2^- concentrations in buffer from the incubated aortic rings were comparable in both groups (27.17 ± 13.43 *versus* 32.75 ± 11.68 nM, db/db and control, resp.), whereas the effect of the NOS inhibitor, L-NIO, was striking in the aorta of the control mice and absent in the diabetic group (Figure 5(c)). COX-2-dependent production of PGI_2 (measured as 6-keto-$PGF_{1\alpha}$ concentration in effluent) was decreased in the aortic rings from the db/db mice as compared to the control (148.80 ± 27.20 *versus* 329.30 ± 68.18 pg/ml, db/db and control, resp.; $P < 0.05$), and COX inhibitors decreased PGI_2 production in the aorta of the control but not the diabetic mice (Figure 5(d)). Furthermore, endothelium in the aorta displayed increased VCAM-1 expression compatible with endothelial dysfunction (Figure 6(a)), although there were no changes in the eNOS immunostaining intensity (Figure 6(c)). In turn, in contrast to the pulmonary endothelium, thrombomodulin (CD141) immunostaining intensity was decreased (Figure 6(b)).

4.5. Nonenzymatic Nitration in the Lungs and Aorta. Dot-blot-assessed general protein nitration was increased in the aorta but not in the lungs from the db/db mice, as compared with the control; in the lung, only a trend of increased nitration was observed (Figure 7(a) and 7(b)). Immunohistochemical staining showed only a slight increase in the signal of nitrated proteins in the lungs. A slight increase in PGIS immunostaining in diabetic lungs was also found (Figure 7(c)).

5. Discussion

In the present work, we characterized the phenotype of endothelial dysfunction in pulmonary endothelium, as compared with peripheral endothelium in the diabetic mice (db/db mice). We demonstrated that diabetes induced marked ultrastructural changes in pulmonary endothelium that were associated with the increased permeability of pulmonary microcirculation and impaired NO-dependent function, as well as compensatory increase in PGI_2 production with increased thrombomodulin expression. In contrast, endothelial dysfunction in the aorta was featured by impaired NO- and PGI_2-dependent function and diminished thrombomodulin (CD141) expression. These results suggest a differential response of pulmonary vasculature to diabetic insult in terms of PGI_2-dependent function that might be associated with a lesser nonenzymatic protein nitration in the lung, as compared with peripheral endothelium and preserved PGI_2 synthase activity.

Endothelial dysfunction induced by diabetes in peripheral circulation in db/db mice has been well documented [31–33] and involves (1) increased reactive oxygen species production, scavenging of endothelial NO, and increased

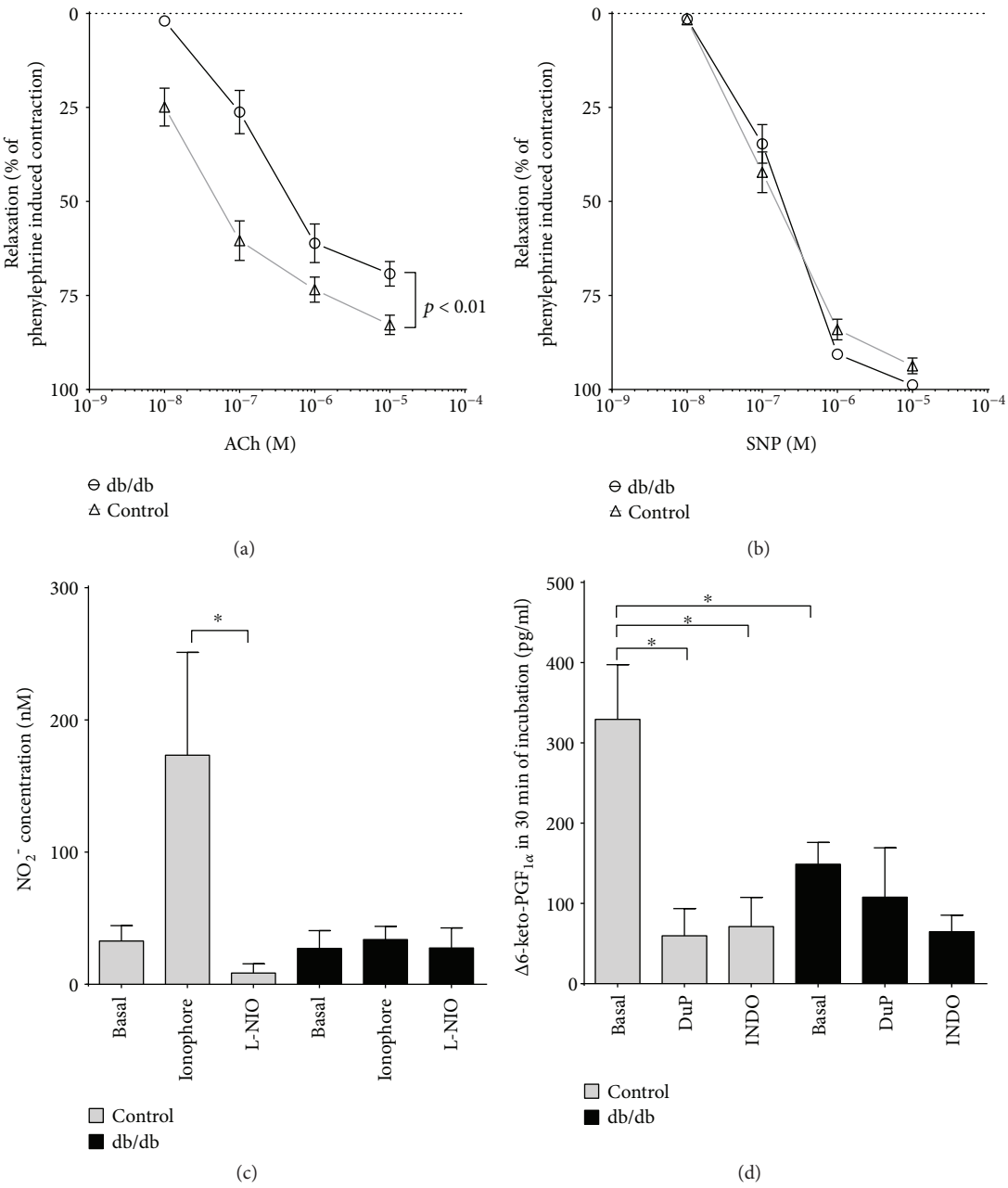

Figure 5: Endothelial dysfunction in systemic conduit vessel (aorta). (a, b) Impaired endothelium-dependent response to acetylcholine (ACh) with preserved endothelium-independent vasodilation in response to sodium nitroprusside (SNP) (control $n = 6$, diabetes $n = 7$). (c) Preserved basal but impaired ionophore-stimulated production of nitrite in the aortic rings of diabetic mice (control $n = 6$, diabetes $n = 7$). (d) Impaired basal production of prostacyclin as assessed by concentrations of its stable 6-keto-$PGF_{1\alpha}$ product (control $n = 6$, diabetes $n = 6$). Data are presented as the means ± SEM. $^*P < 0.05$.

nonenzymatic protein nitration [31, 32]; (2) decreased production of PGI_2 and CD141 expression and impaired endothelial-dependent functional responses [31, 34–36]. Our results are in line with the previous studies as regards phenotype of endothelial dysfunction in the aorta. Importantly, we evaluated the peripheral endothelial phenotype for comparison with the analysis of the phenotype of endothelial dysfunction in pulmonary circulation that has been significantly less studied, including only few reports in the db/db mice [13, 17, 18] and studies in models of diabetes in rats [16, 37].

In the present work, we demonstrated that diabetic lungs from db/db mice displayed mild inflammatory cell infiltration and ultrastructural alterations featured by profound thickening of the basal membrane, compatible with the previous reports on diabetic lungs in humans [11, 38, 39]. Indeed, thickening of the basal membrane and an impairment of permeability of the alveolar basement membrane coexist in diabetes type II in the human lungs, and these changes are followed by a decrease in respiratory function [6, 40]. Ultrastructural changes of pulmonary endothelium

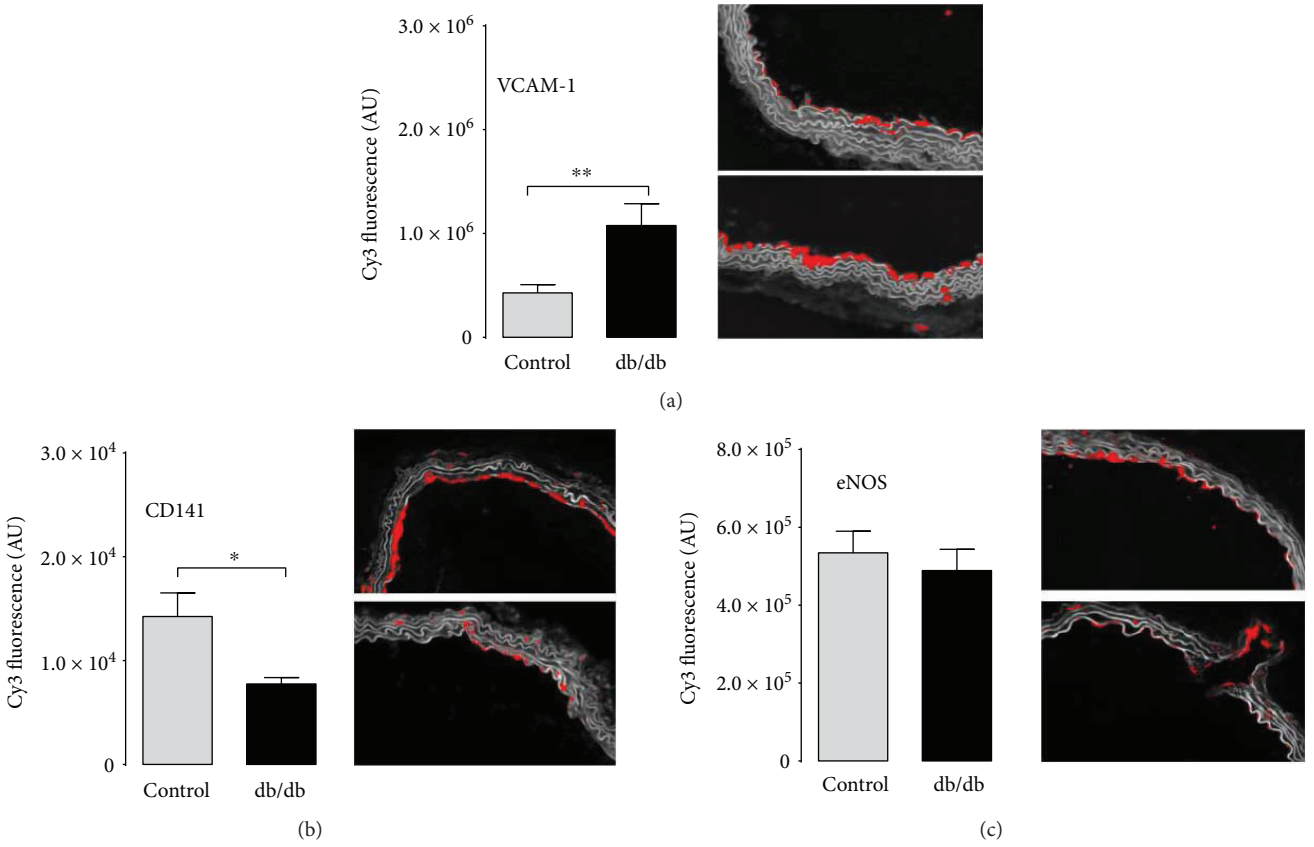

Figure 6: Immunohistochemical profile of systemic conduit vessel (aorta). (a) Increased VCAM-1 immunostaining intensity suggesting aortic wall inflammation in the diabetic mice (control $n = 3$, diabetes $n = 4$). (c) Comparable eNOS immunostaining intensity in the diabetic and control aortic rings (control $n = 3$, diabetes $n = 4$). (b) Decreased immunostaining intensity of thrombomodulin (CD141) in the aortic wall from the diabetic mice (control $n = 3$, diabetes $n = 4$). Data are presented as the means ± SEM. $^{*}P < 0.05$, $^{**}P < 0.01$.

reported here were also featured by activated endothelial cells that were, however, less pronounced as high-convoluted apical plasmalemma and numerous plasmalemmal vesicles reported in transgenic mice model of diabetes type I [41], suggesting milder pulmonary endothelial activation in the db/db mice. Nevertheless, we found a significant increase in endothelial permeability of diabetic pulmonary circulation, as evidenced by increase $K_{f,c}$ measurements [28] that seem also compatible with increased permeability of the human lungs from diabetic patients [42].

The important finding of this work was the demonstration of the impairment of NO-dependent function in the lungs from the db/db mice. We took advantage of the dominant role of endogenous NO in blunting HPV [43] to study functional NO-dependent response in the whole isolated lung, instead of choosing isolated pulmonary arteries that may reflect NO-dependent function only in the selected part of the pulmonary circulation. Our original approach to detect impaired NO-dependent function was based on diminished modulatory effects of NOS inhibition on HPV response in the isolated, perfused lungs [43, 44] supported also by lowered cumulative concentrations of NO_2^- in effluents from diabetic lungs. On the other hand, eNOS expression in the lungs from the control and db/db mice was not different, suggesting that alteration of the NO bioavailability was responsible for functionally impaired NO-dependent response in pulmonary circulation from the db/db mice.

Endothelium-derived PGI_2 is often released in a coupled manner with NO [45, 46]. NO deficiency is sometimes linked with a decrease in PGI_2 production, but in many vascular pathologies, PGI_2 production may increase in response to nitric oxide deficiency [44, 47]. Here, PGI_2 production in the aorta was reduced, but in the isolated lungs from the db/db mice, PGI_2 production was augmented. The major enzymatic source of PGI_2 in the aorta and lung was COX-2, as evidenced by the pronounced effect of COX-2 inhibition, and this is in line with the notion of COX-2 as the major source of systemic PGI_2 [48] and important contributor to pulmonary endothelial dysfunction [49, 50]. PGI_2 amplifies CD141 expression [21–23]. As shown here, CD141 immunointensity in the lungs was increased, while it was diminished in the aorta, which supports the link between PGI_2 production and CD141. PGI_2 via CD141 activates protein C, thus enhancing the anticoagulant mechanism of the vascular wall. Reciprocally, activated protein C boosts PGI_2 production in endothelial cells [51].

Thus, pulmonary PGI_2 affords potent antiplatelet and vasoprotective activity, activating also CD141-dependent

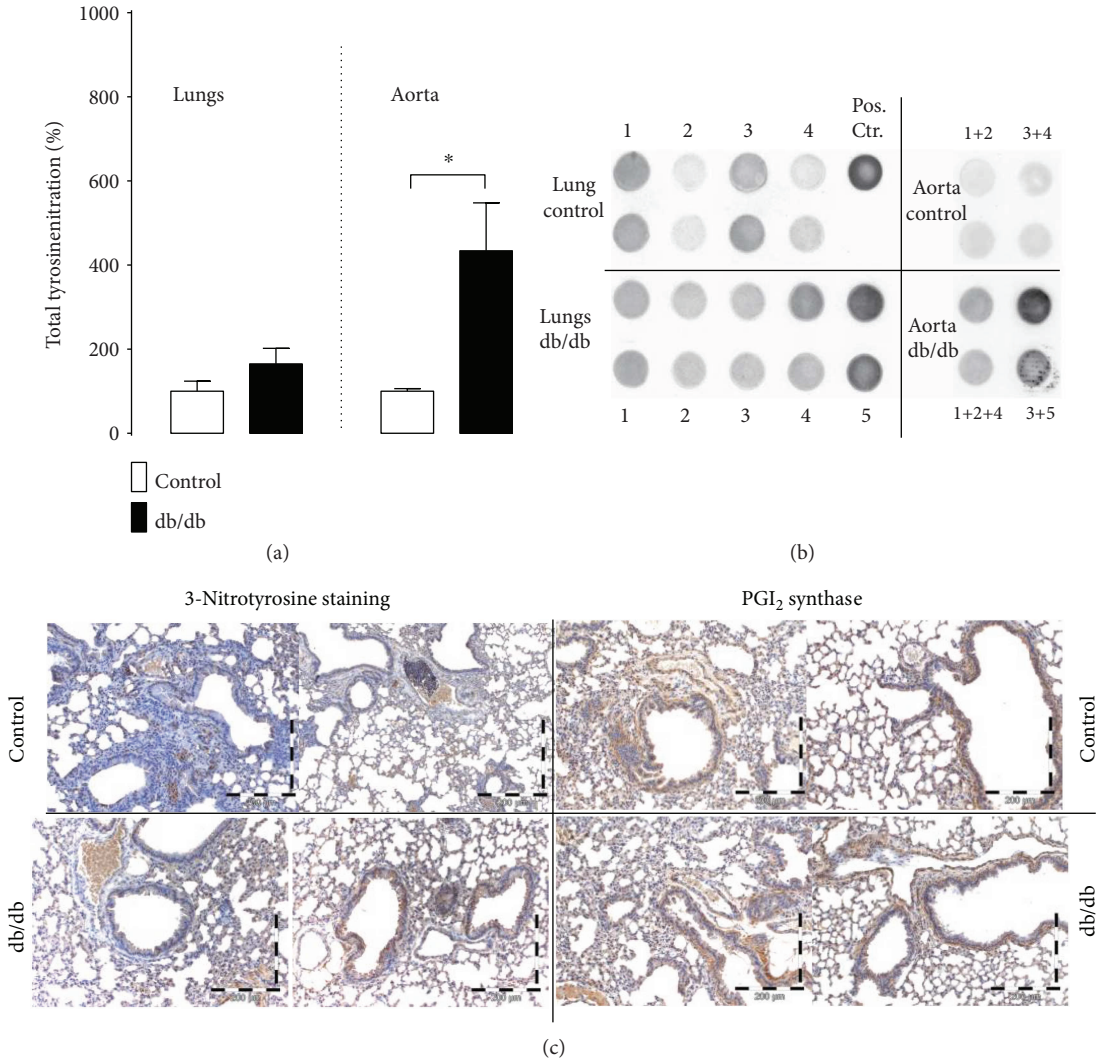

FIGURE 7: Protein nitration in the lungs and aorta. (a, b) Increased general protein nitration in the aorta but not in the lungs of diabetic mice as revealed by dot blot analysis (control $n = 5$, diabetes $n = 5$). Representative original blot images are also shown. (c) Immunohistochemical determination of 3-nitrotyrosine (3-NT) and PGIS with the slight increase in 3-NT immunostaining in the diabetic lungs—the comparison of similar regions of tissues. Data are presented as the means ± SEM. $^*P < 0.05$. Representative images of at least 2 independent experiments.

anticoagulant mechanisms which might constitute an important compensatory mechanism in diabetes offsetting inflammatory and thrombotic processes in diabetes involving also detrimental COX-2-derived metabolites contributing to endothelial dysfunction in diabetes [49, 50, 52] .

Interestingly, 1-MNA exerts antithrombotic [53] and anti-inflammatory [54] properties mediated by the activation of COX-2 and PGI_2 pathways. It could well be that the therapeutic efficacy of 1-MNA reported previously [53–62] is linked with the capacity of 1-MNA to stimulate compensatory mechanisms linked to pulmonary PGI_2 [44]. Obviously, this hypothesis needs to be verified in further studies.

It is well known that diabetes is associated with increased local ROS production in intrapulmonary arteries, as well as in systemic circulation [16, 63, 64]. Superoxide anions and NO by forming peroxynitrite may lead to nonenzymatic nitration of proteins [63, 65] including PGIS; the nitration-mediated inactivation of which plays an important role in the development of endothelial dysfunction [66–69]. In systemic circulation in diabetes patients, protein nitration affects a number of enzymes, including PGIS [64, 70]. Here, we present significantly increased general nitration of protein in the aorta, and a milder effect (nonstatistically significant) was noticed in the lungs. Nonenzymatic nitration may have less significance in the diabetic lungs as compared to systemic circulation. Therefore, despite locally increased ROS generation in pulmonary vessels [16, 37, 71], in the whole lungs, ROS may not play such an important role in pulmonary circulation of the db/db mice as compared to systemic endothelium.

6. Conclusions

In conclusion, our results demonstrate that diabetes induced profound changes in the lung in the db/db mice involving

endothelial ultrastructural changes, increased endothelial permeability, and increased vasoreactivity, as well as lung inflammation and fibrosis. Impaired NO-dependent pulmonary vascular function was associated with upregulated PGI_2 and CD141 that might constitute an important compensatory mechanism in pulmonary circulation in diabetes that does not operate in endothelium in the aorta, whereby endothelial dysfunction is featured by impaired NO, PGI_2, and CD141.

Abbreviations

6-keto-$PGF_{1\alpha}$:	Stable prostacyclin metabolite
Ang:	Angiotensin
AST/ALT:	Aspartate transaminase/alanine transaminase
CD141:	Thrombomodulin
CF:	Constant flow
CP:	Constant pressure
COX:	Cyclooxygenase
DuP-697:	Selective COX-2 inhibitor
eNOS:	Endothelial nitric oxide synthase
H&E:	Hematoxylin and eosin
HPV:	Hypoxic pulmonary vasoconstriction
iNOS:	Inducible nitric oxide synthase
1-MNA:	1-Methylnicotinamide
NO:	Nitric oxide
NO_2^-/NO_3^-:	Nitrite/nitrate
OMSB:	Orcein and methyl scarlet blue staining
PAP:	Pulmonary arterial pressure
ΔPAP:	The change in pulmonary arterial pressure
PGI_2:	Prostacyclin
PVP:	Pulmonary venous pressure
RVW/BW:	Right ventricular to body weight ratio
SNP:	Sodium nitroprusside
TV:	Tidal volume
U46619:	Thromboxane A_2 analogue
vWF:	von Willebrand factor.

Data Availability

The datasets generated during and/or analysed during the current study are available from the corresponding author on reasonable request.

Conflicts of Interest

The authors declared that no conflict of interest exists.

Authors' Contributions

Andrzej Fedorowicz and Stefan Chlopicki conceived and designed the research; Andrzej Fedorowicz, Elżbieta Buczek, Barbara Sitek, Łukasz Mateuszuk, Agnieszka Jasztal, Antonina Chmura-Skirlińska, Mobin Dib, and Sebastian Steven carried out the experiments; Elzbieta Czarnowska, Agnieszka Jasztal, and Andreas Daiber contributed with the analytic tools; Andrzej Fedorowicz, Elzbieta Czarnowska, Agnieszka Jasztal, Antonina Chmura-Skirlińska, Mobin Dib, Andreas Daiber, and Sebastian Steven performed the data analysis; Andrzej Fedorowicz and Stefan Chlopicki drafted the manuscript; Elżbieta Buczek, Łukasz Mateuszuk, Elzbieta Czarnowska, Mobin Dib, Sebastian Steven, and Andreas Daiber revised the manuscript; Andrzej Fedorowicz and Stefan Chlopicki wrote the final version of the manuscript. All authors read and approved the final manuscript.

Acknowledgments

The work was supported by a grant from the resources of the European Regional Development Fund under the Innovative Economy Programme (grant coordinated by JCET-UJ, no. POIG.01.01.02-00-069/09) and partially by National Science Centre Grant Symfonia no. DEC-2015/16/W/NZ4/00070.

References

[1] D. Jay, H. Hitomi, and K. K. Griendling, "Oxidative stress and diabetic cardiovascular complications," *Free Radical Biology & Medicine*, vol. 40, no. 2, pp. 183–192, 2006.

[2] S. B. Williams, J. A. Cusco, M. A. Roddy, M. T. Johnstone, and M. A. Creager, "Impaired nitric oxide-mediated vasodilation in patients with non-insulin-dependent diabetes mellitus," *Journal of the American College of Cardiology*, vol. 27, no. 3, pp. 567–574, 1996.

[3] T. Yamamoto, N. Horikawa, Y. Komuro, and Y. Hara, "Effect of topical application of a stable prostacyclin analogue, SM-10902 on wound healing in diabetic mice," *European Journal of Pharmacology*, vol. 302, no. 1-3, pp. 53–60, 1996.

[4] M.-R. Movahed, M. Hashemzadeh, and M. M. Jamal, "The prevalence of pulmonary embolism and pulmonary hypertension in patients with type II diabetes mellitus," *Chest Journal*, vol. 128, no. 5, pp. 3568–3571, 2005.

[5] O. L. Klein, J. A. Krishnan, S. Glick, and L. J. Smith, "Systematic review of the association between lung function and type 2 diabetes mellitus," *Diabetic Medicine*, vol. 27, no. 9, pp. 977–987, 2010.

[6] K. Ozşahin, A. Tuğrul, S. Mert, M. Yüksel, and G. Tuğrul, "Evaluation of pulmonary alveolo-capillary permeability in type 2 diabetes mellitus: using technetium ^{99m}Tc-DTPA aerosol scintigraphy and carbon monoxide diffusion capacity," *Journal of Diabetes and its Complications*, vol. 20, no. 4, pp. 205–209, 2006.

[7] N. Toda, T. Imamura, and T. Okamura, "Alteration of nitric oxide-mediated blood flow regulation in diabetes mellitus," *Pharmacology & Therapeutics*, vol. 127, no. 3, pp. 189–209, 2010.

[8] R. A. Johnston, M. Zhu, Y. M. Rivera-Sanchez et al., "Allergic airway responses in obese mice," *American Journal of Respiratory and Critical Care Medicine*, vol. 176, no. 7, pp. 650–658, 2007.

[9] X. Meng, S. Tancharoen, K.-I. Kawahara et al., "1,5-Anhydroglucitol attenuates cytokine release and protects mice with type 2 diabetes from inflammatory reactions," *International Journal of Immunopathology and Pharmacology*, vol. 23, no. 1, pp. 105–119, 2010.

[10] A. A. Pezzulo, J. Gutiérrez, K. S. Duschner et al., "Glucose depletion in the airway surface liquid is essential for sterility of the airways," *PLoS One*, vol. 6, no. 1, article e16166, 2011.

[11] D. Popov and M. Simionescu, "Alterations of lung structure in experimental diabetes, and diabetes associated with hyperlipidaemia in hamsters," *The European Respiratory Journal*, vol. 10, no. 8, pp. 1850–1858, 1997.

[12] C. Yilmaz, P. Ravikumar, D. J. Bellotto, R. H. Unger, and C. C. W. Hsia, "Fatty diabetic lung: functional impairment in a model of metabolic syndrome," *Journal of Applied Physiology*, vol. 109, no. 6, pp. 1913–1919, 2010.

[13] P. Sridulyakul, D. Chakraphan, P. Bhattarakosol, and S. Patumraj, "Endothelial nitric oxide synthase expression in systemic and pulmonary circulation of streptozotocin induced diabetic rats: comparison using image analysis," *Clinical Hemorheology and Microcirculation*, vol. 29, no. 3-4, pp. 423–428, 2003.

[14] M. Dewhurst, E. J. Stevens, and D. R. Tomlinson, "Effects of aminoguanidine and N^G-nitro-L-arginine methyl ester on vascular responses of aortae and lungs from streptozotocin-diabetic rats," *Prostaglandins, Leukotrienes, and Essential Fatty Acids*, vol. 56, no. 4, pp. 317–324, 1997.

[15] C. Maric-Bilkan, "Sex differences in micro- and macrovascular complications of diabetes mellitus," *Clinical Science*, vol. 131, no. 9, pp. 833–846, 2017.

[16] J. G. Lopez-Lopez, J. Moral-Sanz, G. Frazziano et al., "Diabetes induces pulmonary artery endothelial dysfunction by NADPH oxidase induction," *American Journal of Physiology. Lung Cellular and Molecular Physiology*, vol. 295, no. 5, pp. L727–L732, 2008.

[17] A. M. Gurney and F. C. Howarth, "Effects of streptozotocin-induced diabetes on the pharmacology of rat conduit and resistance intrapulmonary arteries," *Cardiovascular Diabetology*, vol. 8, no. 1, p. 4, 2009.

[18] S. Lu, L. Xiang, J. S. Clemmer, P. N. Mittwede, and R. L. Hester, "Oxidative stress increases pulmonary vascular permeability in diabetic rats through activation of transient receptor potential melastatin 2 channels," *Microcirculation*, vol. 21, no. 8, pp. 754–760, 2014.

[19] I. S. Watts, J. T. Zakrzewski, and Y. S. Bakhle, "Altered prostaglandin synthesis in isolated lungs of rats with streptozotocin-induced diabetes," *Thrombosis Research*, vol. 28, no. 3, pp. 333–342, 1982.

[20] E. J. Stevens, G. B. Willars, P. Lidbury, F. House, and D. R. Tomlinson, "Vasoreactivity and prostacyclin release in streptozotocin-diabetic rats: effects of insulin or aldose reductase inhibition," *British Journal of Pharmacology*, vol. 109, no. 4, pp. 980–986, 1993.

[21] K. Rabausch, E. Bretschneider, M. Sarbia et al., "Regulation of thrombomodulin expression in human vascular smooth muscle cells by COX-2-derived prostaglandins," *Circulation Research*, vol. 96, no. 1, pp. e1–e6, 2005.

[22] M. Usui, H. Kato, N. Kuriyama et al., "Effect of a prostaglandin I_2 analog on the expression of thrombomodulin in liver and spleen endothelial cells after an extensive hepatectomy," *Surgery Today*, vol. 41, no. 2, pp. 230–236, 2011.

[23] K. Okajima, "Prevention of endothelial cell injury by activated protein C: the molecular mechanism(s) and therapeutic implications," *Current Vascular Pharmacology*, vol. 2, no. 2, pp. 125–133, 2004.

[24] M. Nakano, M. Furutani, H. Shinno, T. Ikeda, K. Oida, and H. Ishii, "Elevation of soluble thrombomodulin antigen levels in the serum and urine of streptozotocin-induced diabetes model rats," *Thrombosis Research*, vol. 99, no. 1, pp. 83–91, 2000.

[25] M. Konieczynska, K. Fil, M. Bazanek, and A. Undas, "Prolonged duration of type 2 diabetes is associated with increased thrombin generation, prothrombotic fibrin clot phenotype and impaired fibrinolysis," *Thrombosis and Haemostasis*, vol. 111, no. 4, pp. 685–693, 2017.

[26] L. Rodella, L. Vanella, S. Peterson et al., "Heme oxygenase-derived carbon monoxide restores vascular function in type 1 diabetes," *Drug Metabolism Letters*, vol. 2, no. 4, pp. 290–300, 2008.

[27] M. Gajda, A. Jasztal, T. Banasik, E. Jasek-Gajda, and S. Chlopicki, "Combined orcein and martius scarlet blue (OMSB) staining for qualitative and quantitative analyses of atherosclerotic plaques in brachiocephalic arteries in apoE/$LDLR^{-/-}$ mice," *Histochemistry and Cell Biology*, vol. 147, no. 6, pp. 671–681, 2017.

[28] S. Uhlig and A. N. von Bethmann, "Determination of vascular compliance, interstitial compliance, and capillary filtration coefficient in rat isolated perfused lungs," *Journal of Pharmacological and Toxicological Methods*, vol. 37, no. 3, pp. 119–127, 1997.

[29] M. Oelze, S. Kröller-Schön, P. Welschof et al., "The sodium-glucose co-transporter 2 inhibitor empagliflozin improves diabetes-induced vascular dysfunction in the streptozotocin diabetes rat model by interfering with oxidative stress and glucotoxicity," *PLoS One*, vol. 9, no. 11, article e112394, 2014.

[30] M. Oelze, S. Kröller-Schön, S. Steven et al., "Glutathione peroxidase-1 deficiency potentiates dysregulatory modifications of endothelial nitric oxide synthase and vascular dysfunction in aging," *Hypertension*, vol. 63, no. 2, pp. 390–396, 2014.

[31] S. Lee, H. Zhang, J. Chen, K. C. Dellsperger, M. A. Hill, and C. Zhang, "Adiponectin abates diabetes-induced endothelial dysfunction by suppressing oxidative stress, adhesion molecules, and inflammation in type 2 diabetic mice," *American Journal of Physiology - Heart and Circulatory Physiology*, vol. 303, no. 1, pp. H106–H115, 2012.

[32] Y. Liu, D. Li, Y. Zhang, R. Sun, and M. Xia, "Anthocyanin increases adiponectin secretion and protects against diabetes-related endothelial dysfunction," *American Journal of Physiology - Endocrinology and Metabolism*, vol. 306, no. 8, pp. E975–E988, 2014.

[33] X. Tian, W. Wong, A. Xu et al., "Rosuvastatin improves endothelial function in *db*/*db* mice: role of angiotensin II type 1 receptors and oxidative stress," *British Journal of Pharmacology*, vol. 164, no. 2b, pp. 598–606, 2011.

[34] S. J. Peterson, D. Husney, A. L. Kruger et al., "Long-term treatment with the apolipoprotein A1 mimetic peptide increases antioxidants and vascular repair in type I diabetic rats," *Journal of Pharmacology and Experimental Therapeutics*, vol. 322, no. 2, pp. 514–520, 2007.

[35] Y. Takahashi and I. Wakabayashi, "Depression of cyclooxygenase-2 induction in aortas of rats with type 1 and type 2 diabetes mellitus," *European Journal of Pharmacology*, vol. 595, no. 1-3, pp. 114–118, 2008.

[36] T. Y. Lam, S. W. Seto, Y. M. Lau et al., "Impairment of the vascular relaxation and differential expression of caveolin-1 of the aorta of diabetic +*db*/+*db* mice," *European Journal of Pharmacology*, vol. 546, no. 1-3, pp. 134–141, 2006.

[37] J. Moral-Sanz, C. Menendez, L. Moreno, E. Moreno, A. Cogolludo, and F. Perez-Vizcaino, "Pulmonary arterial dysfunction in insulin resistant obese Zucker rats," *Respiratory Research*, vol. 12, no. 1, p. 51, 2011.

[38] E. C. Carlson, J. L. Audette, N. J. Veitenheimer, J. A. Risan, D. I. Laturnus, and P. N. Epstein, "Ultrastructural morphometry of capillary basement membrane thickness in normal and transgenic diabetic mice," *The Anatomical Record*, vol. 271A, no. 2, pp. 332–341, 2003.

[39] X. Xiong, W. Wang, L. Wang, L. Jin, and L. Lin, "Diabetes increases inflammation and lung injury associated with protective ventilation strategy in mice," *International Immunopharmacology*, vol. 13, no. 3, pp. 280–283, 2012.

[40] B. Weynand, A. Jonckheere, A. Frans, and J. Rahier, "Diabetes mellitus induces a thickening of the pulmonary basal lamina," *Respiration*, vol. 66, no. 1, pp. 14–19, 1999.

[41] E. Uyy, F. Antohe, L. Ivan, R. Haraba, D. L. Radu, and M. Simionescu, "Upregulation of caveolin-1 expression is associated with structural modifications of endothelial cells in diabetic lung," *Microvascular Research*, vol. 79, no. 2, pp. 154–159, 2010.

[42] K. Kuziemski, J. Pieńkowska, W. Słomiński et al., "Role of quantitative chest perfusion computed tomography in detecting diabetic pulmonary microangiopathy," *Diabetes Research and Clinical Practice*, vol. 91, no. 1, pp. 80–86, 2011.

[43] S. Chlopicki, J. B. Bartus, and R. J. Gryglewski, "Hypoxic pulmonary vasoconstriction in isolated blood-perfused rat lung; modulation by thromboxane A_2, platelet-activating factor, cysteinyl leukotrienes and endothelin-1," *Polish Journal of Pharmacology*, vol. 54, no. 5, pp. 433–441, 2002.

[44] A. Fedorowicz, Ł. Mateuszuk, G. Kopec et al., "Activation of the nicotinamide N-methyltransferase (NNMT)-1-methylnicotinamide (MNA) pathway in pulmonary hypertension," *Respiratory Research*, vol. 17, no. 1, p. 108, 2016.

[45] T. He, T. Lu, L. V. d'Uscio, C. F. Lam, H. C. Lee, and Z. S. Katusic, "Angiogenic function of prostacyclin biosynthesis in human endothelial progenitor cells," *Circulation Research*, vol. 103, no. 1, pp. 80–88, 2008.

[46] M.-C. Tsai, L. Chen, J. Zhou et al., "Shear stress induces synthetic-to-contractile phenotypic modulation in smooth muscle cells via peroxisome proliferator-activated receptor α/δ activations by prostacyclin released by sheared endothelial cells," *Circulation Research*, vol. 105, no. 5, pp. 471–480, 2009.

[47] A. Kij, L. Mateuszuk, B. Sitek et al., "Simultaneous quantification of PGI_2 and TXA_2 metabolites in plasma and urine in NO-deficient mice by a novel UHPLC/MS/MS method," *Journal of Pharmaceutical and Biomedical Analysis*, vol. 129, pp. 148–154, 2016.

[48] C. D. Funk and G. A. Fitzgerald, "Cox-2 inhibitors and cardiovascular risk," *Journal of Cardiovascular Pharmacology*, vol. 50, no. 5, pp. 470–479, 2007.

[49] H. Zhang, J. Liu, D. Qu et al., "Inhibition of miR-200c restores endothelial function in diabetic mice through suppression of COX-2," *Diabetes*, vol. 65, no. 5, pp. 1196–1207, 2016.

[50] Y. Shi and P. M. Vanhoutte, "Oxidative stress and COX cause hyper-responsiveness in vascular smooth muscle of the femoral artery from diabetic rats," *British Journal of Pharmacology*, vol. 154, no. 3, pp. 639–651, 2008.

[51] M. Brueckmann, S. Horn, S. Lang et al., "Recombinant human activated protein C upregulates cyclooxygenase-2 expression in endothelial cells via binding to endothelial cell protein C receptor and activation of protease-activated receptor-1," *Thrombosis and Haemostasis*, vol. 93, no. 4, pp. 743–750, 2005.

[52] J. G. Lopez-Lopez, J. Moral-Sanz, G. Frazziano et al., "Type 1 diabetes-induced hyper-responsiveness to 5-hydroxytryptamine in rat pulmonary arteries via oxidative stress and induction of cyclooxygenase-2," *Journal of Pharmacology and Experimental Therapeutics*, vol. 338, no. 1, pp. 400–407, 2011.

[53] S. Chlopicki, J. Swies, A. Mogielnicki et al., "1-Methylnicotinamide (MNA), a primary metabolite of nicotinamide, exerts anti-thrombotic activity mediated by a cyclooxygenase-2/prostacyclin pathway," *British Journal of Pharmacology*, vol. 152, no. 2, pp. 230–239, 2007.

[54] K. Bryniarski, R. Biedron, A. Jakubowski, S. Chlopicki, and J. Marcinkiewicz, "Anti-inflammatory effect of 1-methylnicotinamide in contact hypersensitivity to oxazolone in mice; involvement of prostacyclin," *European Journal of Pharmacology*, vol. 578, no. 2-3, pp. 332–338, 2008.

[55] T. Brzozowski, P. C. Konturek, S. Chlopicki et al., "Therapeutic potential of 1-methylnicotinamide against acute gastric lesions induced by stress: role of endogenous prostacyclin and sensory nerves," *Journal of Pharmacology and Experimental Therapeutics*, vol. 326, no. 1, pp. 105–116, 2008.

[56] C. Watała, P. Kaźmierczak, M. Dobaczewski et al., "Anti-diabetic effects of 1-methylnicotinamide (MNA) in streptozocin-induced diabetes in rats," *Pharmacological Reports*, vol. 61, no. 1, pp. 86–98, 2009.

[57] M. Sternak, T. I. Khomich, A. Jakubowski et al., "Nicotinamide N-methyltransferase (NNMT) and 1-methylnicotinamide (MNA) in experimental hepatitis induced by concanavalin A in the mouse," *Pharmacological Reports*, vol. 62, no. 3, pp. 483–493, 2010.

[58] Ł. Mateuszuk, T. I. Khomich, E. Słomińska et al., "Activation of nicotinamide N-methyltrasferase and increased formation of 1-methylnicotinamide (MNA) in atherosclerosis," *Pharmacological Reports*, vol. 61, no. 1, pp. 76–85, 2009.

[59] K. Przyborowski, M. Wojewoda, B. Sitek et al., "Effects of 1-methylnicotinamide (MNA) on exercise capacity and endothelial response in diabetic mice," *PLoS One*, vol. 10, no. 6, article e0130908, 2015.

[60] A. Blazejczyk, M. Switalska, S. Chlopicki et al., "1-Methylnicotinamide and its structural analog 1,4-dimethylpyridine for the prevention of cancer metastasis," *Journal of Experimental & Clinical Cancer Research*, vol. 35, no. 1, p. 110, 2016.

[61] A. Bar, M. Olkowicz, U. Tyrankiewicz et al., "Functional and biochemical endothelial profiling *in vivo* in a murine model of endothelial dysfunction; comparison of effects of 1-methylnicotinamide and angiotensin-converting enzyme inhibitor," *Frontiers in Pharmacology*, vol. 8, p. 183, 2017.

[62] A. Jakubowski, M. Sternak, K. Jablonski, M. Ciszek-Lenda, J. Marcinkiewicz, and S. Chlopicki, "1-Methylnicotinamide protects against liver injury induced by concanavalin A via a prostacyclin-dependent mechanism: a possible involvement of IL-4 and TNF-α," *International Immunopharmacology*, vol. 31, pp. 98–104, 2016.

[63] X. Gao, S. Belmadani, A. Picchi et al., "Tumor necrosis factor-α induces endothelial dysfunction in $Lepr^{db}$ mice," *Circulation*, vol. 115, no. 2, pp. 245–254, 2007.

[64] Y. Wang, F. Peng, W. Tong, H. Sun, N. Xu, and S. Liu, "The nitrated proteome in heart mitochondria of the db/db mouse model: characterization of nitrated tyrosine residues in SCOT," *Journal of Proteome Research*, vol. 9, no. 8, pp. 4254–4263, 2010.

[65] U. Hink, M. Oelze, P. Kolb et al., "Role for peroxynitrite in the inhibition of prostacyclin synthase in nitrate tolerance," *Journal of the American College of Cardiology*, vol. 42, no. 10, pp. 1826–1834, 2003.

[66] B. Zingarelli, L. Virág, A. Szabó, S. Cuzzocrea, A. L. Salzman, and C. Szabó, "Oxidation, tyrosine nitration and cytostasis induction in the absence of inducible nitric oxide synthase," *International Journal of Molecular Medicine*, vol. 1, no. 5, pp. 787–795, 1998.

[67] M. K. Mirza, J. Yuan, X.-P. Gao et al., "Caveolin-1 deficiency dampens toll-like receptor 4 signaling through eNOS activation," *The American Journal of Pathology*, vol. 176, no. 5, pp. 2344–2351, 2010.

[68] M. Redondo-Horcajo, N. Romero, P. Martínez-Acedo et al., "Cyclosporine A-induced nitration of tyrosine 34 MnSOD in endothelial cells: role of mitochondrial superoxide," *Cardiovascular Research*, vol. 87, no. 2, pp. 356–365, 2010.

[69] H. Iijima, A. Duguet, S.-Y. Eum, Q. Hamid, and D. H. Eidelman, "Nitric oxide and protein nitration are eosinophil dependent in allergen-challenged mice," *American Journal of Respiratory and Critical Care Medicine*, vol. 163, no. 5, pp. 1233–1240, 2001.

[70] C. López-Vicario, J. Alcaraz-Quiles, V. García-Alonso et al., "Inhibition of soluble epoxide hydrolase modulates inflammation and autophagy in obese adipose tissue and liver: role for omega-3 epoxides," *Proceedings of the National Academy of Sciences of the United States of America*, vol. 112, no. 2, pp. 536–541, 2015.

[71] M. Pan, Y. Han, R. Si, R. Guo, A. Desai, and A. Makino, "Hypoxia-induced pulmonary hypertension in type 2 diabetic mice," *Pulmonary Circulation*, vol. 7, no. 1, pp. 175–185, 2017.

Hindawi
Oxidative Medicine and Cellular Longevity
Volume 2018, Article ID 5967890, 12 pages
https://doi.org/10.1155/2018/5967890

Research Article

BAG3 Protein Is Involved in Endothelial Cell Response to Phenethyl Isothiocyanate

Silvia Franceschelli,[1] Anna Paola Bruno,[1] Michela Festa,[1] Antonia Falco,[1] Elisa Gionti,[2] Morena d'Avenia,[1] Margot De Marco,[3] Anna Basile,[3] Vittoria Iorio,[3] Liberato Marzullo,[3] Alessandra Rosati,[3] and Maria Pascale[1]

[1]*Department of Pharmacy (DIFARMA), University of Salerno, Via Giovanni Paolo II 132, 84084 Fisciano, Italy*
[2]*Department of Molecular Medicine and Medical Biotechnology, University of Naples Federico II, Via Pansini 5, 80131 Naples, Italy*
[3]*Department of Medicine, Surgery and Dentistry "Scuola Medica Salernitana", University of Salerno, Via S. Allende, 84081 Baronissi, Italy*

Correspondence should be addressed to Alessandra Rosati; arosati@unisa.it

Received 22 December 2017; Revised 15 March 2018; Accepted 17 April 2018; Published 31 May 2018

Academic Editor: Silvana Hrelia

Phenethyl isothiocyanate (PEITC), a cruciferous vegetable-derived compound, is a versatile cancer chemopreventive agent that displays the ability to inhibit tumor growth during initiation, promotion, and progression phases in several animal models of carcinogenesis. In this report, we dissect the cellular events induced by noncytotoxic concentrations of PEITC in human umbilical vein endothelial cells (HUVECs). In the early phase, PEITC treatment elicited cells' morphological changes that comprise reduction in cell volume and modification of actin organization concomitantly with a rapid activation of the PI3K/Akt pathway. Downstream to PI3K, PEITC also induces the activity of Rac1 and activation of c-Jun N-terminal kinase (JNK), well-known regulators of actin cytoskeleton dynamics. Interestingly, PEITC modifications of the actin cytoskeleton were abrogated by pretreatment with JNK inhibitor, SP600125. JNK signaling led also to the activation of the c-Jun transcription factor, which is involved in the upregulation of several genes; among them is the BAG3 protein. This protein, a member of the BAG family of heat shock protein (Hsp) 70 cochaperones, is able to sustain survival in different tumor cell lines and neoangiogenesis by directly regulating the endothelial cell cycle. Furthermore, BAG3 is involved in maintaining actin folding. Our findings indicate that BAG3 protein expression is induced in endothelial cells upon exposure to a noncytotoxic concentration of PEITC and its expression is requested for the recovery of normal cell size and morphology after the stressful stimuli. This assigns an additional role for BAG3 protein in the endothelial cells after a stress event.

1. Introduction

Several epidemiologic studies support the hypothesis that dietary intake of cruciferous vegetables may have protective effects against the risk of different types of cancers [1–4]. Chemopreventive and anticarcinogenic effects of cruciferous vegetables are attributed to organic isothiocyanates (ITCs), which naturally occur in a variety of edible cruciferous vegetables such as broccoli, watercress, and cabbage in which they are stored as glucosinolate precursors [5]. ITCs are effective in blocking carcinogenesis in a variety of tissues and are known to inhibit angiogenesis in vitro and in vivo [6–8].

Phenethyl isothiocyanate (PEITC) is one of the best-studied members of the ITC family, due to its anticarcinogenic and antiangiogenic activities reported in myelomas [7] and lung [9] and prostate cancer [10, 11].

In particular, the antiangiogenic properties of PEITC may be largely related to suppression of vascular endothelial growth factor (VEGF) secretion, downregulation of vascular endothelial growth factor receptor-2 protein (VEGF-R2), and Akt inactivation [12, 13].

Furthermore, several studies indicate that ITCs can modulate the expression level of hypoxia-inducible factors (HIF) in tumors [14] and endothelial cells [15]; in fact,

PEITC inhibits HIF transcription [16]. Induction of HIF in hypoxic conditions increases the level of proangiogenic factors, including interleukin 8 (IL8), angiopoietin 2 (Ang2), and VEGF. Moreover, the decreased translational efficiency of the HIF1α subunit may contribute to the antiangiogenetic effect of PEITC [7]. PEITC can also induce cellular oxidative stress by rapidly conjugating glutathione (GSH). Depletion of GSH followed by rapid accumulation of ROS may be related to PEITC-mediated apoptotic cell death [9, 17]. An additional more interesting property of PEITC and sulforaphane (SFN) regards the ability to determine disruption of microtubule polymerization *in vitro* and *in vivo*. In fact, PEITC can form covalent binding with microtubular tubulin, leading to the collapse of the microtubule cytoskeleton in A549 cells. This property may explain the ITC-induced mitotic cell cycle arrest and apoptosis observed in cancer and noncancer cells [13, 18]. It is of interest that BAG3, the only stress-inducible member of the BAG family of cochaperones, has been reported to sensitize HPV18+ HeLa cells to PEITC-induced apoptosis restoring p53 levels [19]. Indeed, BAG3 has also been described for its ability to sustain neoangiogenesis acting on the endothelial cell cycle [20] and to regulate actin folding through its interaction with the cytosolic chaperonin CCT (containing TCP-1) [21].

In this study, we report for the first time that the F-actin cytoskeleton undergoes remodeling during the early phase of PEITC treatment of HUVECs. Our data indicate that this effect is associated with an immediate activation of the PI3K/Akt and PI3K/Rac1/JNK pathways. Pretreatment with the JNK inhibitor SP600125 reverses PEITC-induced actin filament remodeling, thus providing direct evidence of JNK-mediated actin cytoskeleton modifications occurring immediately after PEITC administration. The stress-induced BAG3 protein was found increased in its levels upon PEITC induction. We also found a marked colocalization of BAG3 with F-actin, thus sustaining its role in actin localization and cellular morphology changes upon PEITC treatment.

2. Results

2.1. PEITC Induces Actin Cytoskeleton Alterations and Activation of the PI3K/Akt Pathway in HUVECs. Human endothelial vein umbilical cells are a well-known model used to study many aspects of endothelial function and disease, such as normal, abnormal, and tumor-associated angiogenesis, oxidative stress, and hypoxia-related pathways in endothelia under normal and pathological conditions. We have observed a cytotoxic effect of PEITC at 20 and 40 μM concentrations as revealed by an MTT assay performed on two different HUVEC donors. In particular, we observed a decrease of more than 75% of the viable cells in respect to controls at a concentration of 20 μM after 24 and 48 h (Figure 1(a)), in contrast with evidences published by Xiao and Singh [22] which demonstrate a concentration of 2 μM as cytotoxic. Indeed, in our hands, the treatment of HUVECs at 10 μM PEITC was not cytotoxic, but we observed an effect on the cell cycle as shown in Figure 1(b); in HUVECs from two different donors, we observed, at 24 hours, cells accumulating in S and G2/M phases. However, this effect on the cell cycle does not significantly affect the cell number after 48 hours of treatment in respect to 24 hours (Figure 1(a)), thus suggesting that cells have activated survival pathways to overcome the PEITC insult. Phase-contrast observations of HUVECs revealed that PEITC induced a dramatic change in cellular morphology after 15 and 120 min of treatment (Figure 1(c), A–C). Furthermore, control HUVECs show a highly developed actin cytoskeleton with clearly visible, numerous stress fibers (Figure 1(c), D). After 120 min treatment with PEITC, we observed distinct changes in cell morphology and reorganization of actin filaments (Figure 1(c), E). Cells reduce their volume, which resulted in a decrease in the area of intercellular contacts (Figure 1(c), B–E). Phalloidin staining shows the disappearance of actin stress fibers and short fibril or small aggregate formations. Focal adhesion kinase (FAK) has been widely reported to be involved in the control of focal adhesion organization and stress fiber formation, through phosphorylation and dephosphorylation of its tyrosine residues [23]. Therefore, we further investigated whether PEITC treatment modulates FAK phosphorylation; Figure 1(d) shows a decrease in FAK phosphorylation after treatment with 10 μM of PEITC for 120 min.

In cancer cells, PEITC is known to downregulate the PI3K/Akt prosurvival pathway through a marked decrease in Akt Ser473 phosphorylation and subsequent apoptosis [13] and the involvement of the PI3K/Akt pathway in actin filament remodeling and cell migration is well known [24–26]. In order to verify, in the endothelial primary cell model, a possible connection between Akt activity and the effect on actin remodeling upon PEITC treatment, we first focused on PI3K and Akt phosphorylation/activation kinetics. As shown in Figure 1(e), cell exposure to 10 μM PEITC for 15, 30, 60, and 120 min revealed that levels of phospho-Akt and phospho-PI3K started to increase as early as 15 min, the highest levels being obtained 2 h after PEITC administration. No significant changes occurred in the expression of total PI3K and Akt. These results indicated that high activation of the PI3K/Akt prosurvival pathway can be observed concomitantly with cell morphology and actin redistribution changes.

2.2. PEITC Induces Rac1 Activity via PI3K, and Rac1 in turn Activates JNK. PI3K and Rac1 are key molecules in the activation of cell migration brought about by dynamic changes in the actin cytoskeleton [27, 28]. PI3K is an important activator of Rac1 [28, 29]. Notably, in HUVECs, Rac1 is a downstream effector for PI3K but does not act upstream of Akt [30]. In addition, Rac1 activity is known to be dramatically reduced in HUVECs depleted of p110α (a class I PI 3-kinase catalytic subunit) [31]. A Rac1 activity assay was performed to investigate whether the protein is induced after PEITC treatment. As observed in Figure 2(a), an increase in Rac1 activity was present in 10 μM PEITC-treated cells for 2 h compared to control cells. Unexpectedly, we also observed that PEITC induced an increase in total Rac1 protein, thus suggesting a novel mechanism for Rac1 upregulation. These results indicate that Rac1 probably acts as a downstream PI3K effector.

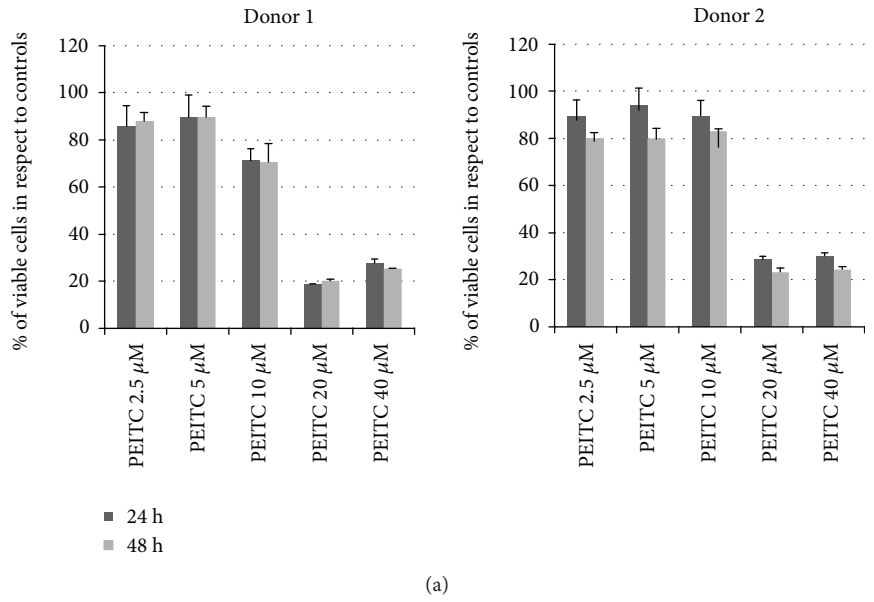

(a)

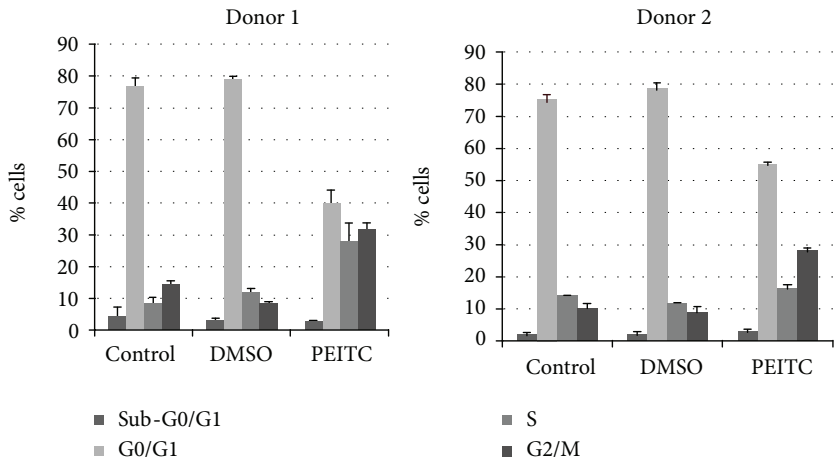

(b)

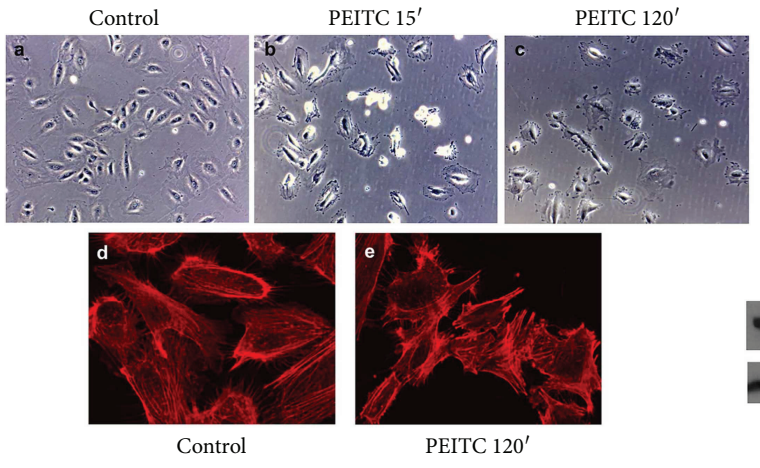

(c)

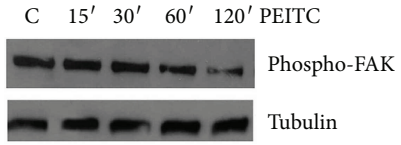

(d)

Figure 1: Continued.

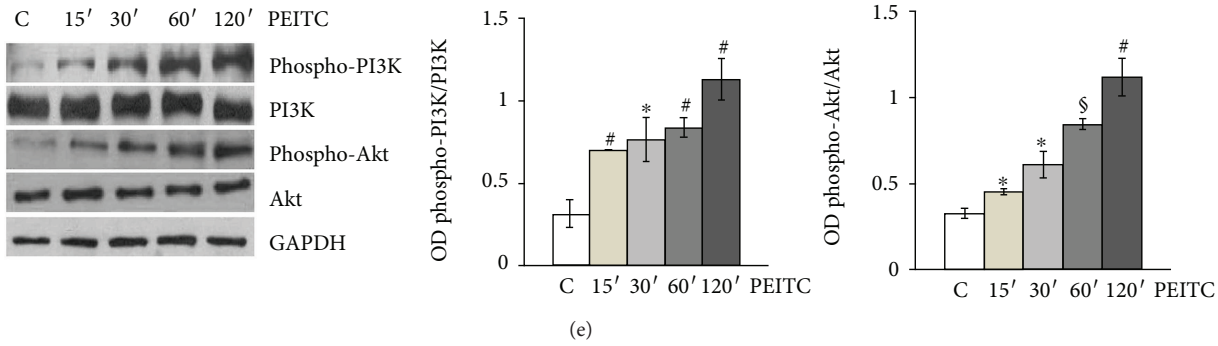

Figure 1: PEITC induces actin cytoskeleton alterations and activation of the PI3K/Akt pathway in HUVECs. (a) HUVECs from 2 different donors were plated at $5 \times 10^3/cm^2$ and then treated with PEITC at indicated concentrations for 24 and 48 h. Then, cells were subjected to the MTT assay, and results are shown in a bar graph as % of viable cells in respect to controls (untreated or 0.01% DMSO-treated cells). (b) HUVECs from 2 different donors were treated as described above. After 24 h, a cell cycle assay was performed by using PI on permeabilized cells. Results are expressed as % of cells in each cell cycle phase. (c) Phase-contrast images and confocal analysis of HUVECs treated with (A, D) DMSO (control) at a final concentration (0.01%), with (B) PEITC (10 μM) for 15 min, and with (C, E) PEITC (10 μM) for 120 min. (B, C, E) Images of PEITC-treated cells showing blebbing formation in the outer cytoskeletal domain. (d) HUVECs were seeded as described above and treated with PEITC; at the indicated time points, cells were harvested and subjected to cell lysis. Protein contents were analyzed by Western blot to analyze the levels of phospho-FAK protein. Tubulin was used as a loading control. (e) HUVECs were treated with 0.01% DMSO (C) and with 10 μM PEITC for 15, 30, 60, and 120 min. Total protein extracts were analyzed by Western blot using anti-phospho-Akt (Ser473), anti-Akt, anti-phospho-PI3K, and anti-PI3K to test PI3K/Akt activation levels. The anti-GAPDH antibody was used as an internal loading control. Each lane was loaded with 20 μg protein. The bar graph depicts densitometric analysis of the data (expressed as phospho-PI3K/PI3K and phospho-Akt/Akt ratios) corresponding to the left panel. Results were obtained from at least two independent experiments and are expressed as the mean ± SEM. $^*P < 0.05$, $^\#P < 0.01$, and $^\S P < 0.001$, statistically significant differences, compared to DMSO-treated cells (C), were calculated by Student's *t*-test for unpaired data.

c-Jun N-terminal kinase (JNK, also known as stress-activated protein kinase-1 (SAPK1)) is strongly activated by cell stress inducers. UV irradiation, hyperosmolarity, and inflammatory cytokines stimulate the activity of JNK [32]. PEITC induces JNK activation in a dose-dependent manner [33]. To establish whether 10 μM PEITC induced activation of JNK in our settings, Western blot analysis was performed and, as shown in Figure 2(b), PEITC elicited a significant increase in phospho-JNK activation after 2 h drug exposure. No effects on expression levels of total JNK were observed. These results suggest the involvement of JNK phosphorylation in PEITC-mediated remodeling of the actin filament cytoskeleton (Figure 3(a)).

To assess whether Rac1 is a downstream effector of PI3K in PEITC-treated HUVECs, we performed a pull-down assay in which GTP-bound Rac1 was isolated from control cells or cells pretreated for 1 h with 10 μM LY294002, a PI3K inhibitor (p110α catalytic subunit inhibitor), in control or PEITC-treated cells. PI3K inhibition resulted in the concomitant downregulation of Rac1 activity and JNK phosphorylation levels as shown in Figure 2(c). Conversely, the PI3K inhibitor had no effect on a PEITC-mediated increase in total Rac1 protein levels. To investigate whether Rac1 acted upstream of JNK, HUVECs were cultured in the absence/presence of a specific Rac1-GEF inhibitor (NSC23766, 100 μM) for 4 h and subsequently treated with PEITC for additional 2 h. As shown in Figure 2(d), inhibition of Rac1 downregulated JNK activation. In contrast, Rac1 did not seem to act upstream of Akt, since Rac1 inhibition by NSC23766 did not affect Akt phosphorylation in PEITC-treated cells. Taken together, these results suggest that the PI3K/Rac1/JNK pathway is activated in PEITC-treated endothelial cells exhibiting cytoskeleton modifications.

2.3. JNK Activity Is Involved in Actin Remodeling Processes during PEITC Treatment. To assess whether JNK activation is involved in actin cytoskeleton modifications, 1 h before PEITC administration, HUVECs were pretreated with non-toxic concentration (10 μM) of the specific JNK inhibitor SP600125 [34]. Phase-contrast observations revealed that the JNK inhibitor significantly reduced PEITC-induced morphological changes (Figure 3(a), A–D). Confocal analysis of actin staining indicated that pretreatment with the JNK inhibitor reverts cytoskeletal modifications induced by PEITC (Figure 4(a), E–H). The levels of phospho-JNK and phospho-c-Jun, a nuclear substrate of activated JNK, were detected by Western blot analysis to confirm the effectiveness of JNK inhibition. Activation of Rac1 in cells treated with PEITC in the presence of SP600125 confirmed that Rac1 acted upstream of JNK (Figure 3(b)). Taken together, these data strongly suggest the involvement of phospho-JNK in PEITC-mediated actin cytoskeleton remodeling.

2.4. PEITC Treatment Induces BAG3 Expression and Its Delocalization in HUVECs. BAG3 is the only member of the BAG family induced by stressful stimuli, mainly through the binding of the heat shock factor 1 to the *bag3* gene promoter [35] and also by JNK pathway activation [36]. BAG3 protein is also highly expressed in different tumor types [37–42] and regulates neoangiogenesis by interacting with and regulating ERK activity [20]. In addition, it has been demonstrated that BAG3 plays an important role in cell

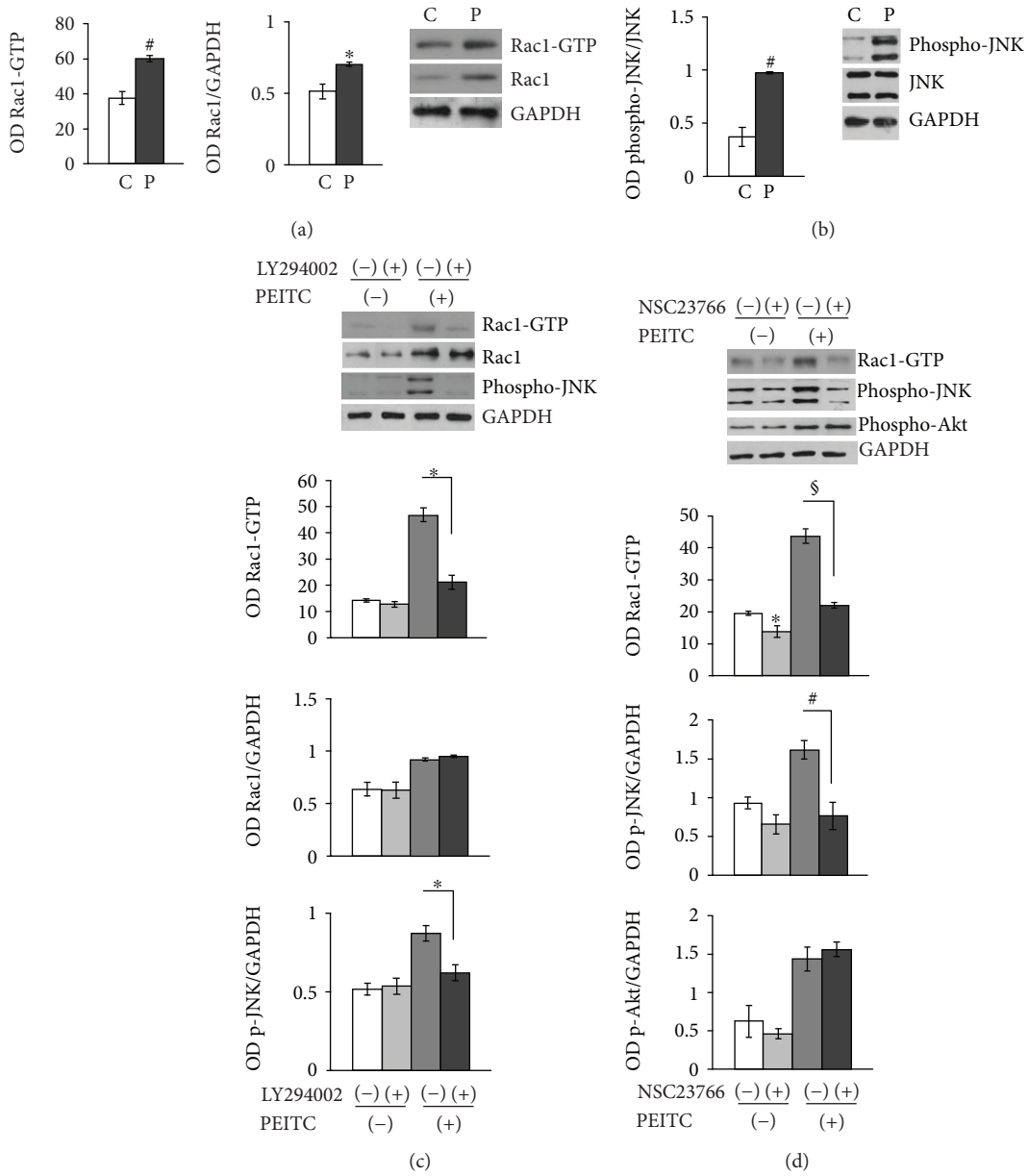

Figure 2: PEITC induces Rac1 activity via PI3K, and Rac1 in turn activates JNK. (a) HUVECs were treated with 0.01% DMSO (C) or treated with 10 μM of PEITC (P) for 2 h and subjected to Western blot analysis of total proteins to measure the effect of PEITC on Rac1-GTPase activity and Rac1 total protein levels and on JNK activation. The left and middle panels display columns representing densitometric analysis of Rac1 activity and of Rac1 total protein levels (expressed as Rac1/GAPDH ratios). Representative blot analysis for Rac1 after a pull-down assay and for total Rac1 protein. (b) HUVECs were treated as described above. Total cell protein content was subjected to Western blot analysis to measure phospho-JNK levels. The left panel displays columns representing densitometric analysis of the data (expressed as phospho-JNK/JNK ratios) corresponding to the right panel. The anti-GAPDH antibody was used as an internal loading control. (c) The levels of GTP-bound Rac1, total Rac1, and phospho-JNK in lysates of pretreated or not with 10 μM of LY2940021 (1 h) were analyzed in HUVECs in the presence or absence of 10 μM PEITC stimulation for 2 h. The lower bar graphs depict densitometric analysis of Rac1 activity, Rac1 protein levels, and phospho-JNK levels. (d) The levels of GTP-bound Rac1, phospho-Akt, and phospho-JNK were analyzed in lysates of pretreated or not with 100 μM of NSC23766 HUVECs for 4 h, in the presence/absence of 10 μM PEITC stimulation for 2 h. The lower bar graphs depict densitometric analysis of Rac1 activity, phospho-JNK, and phospho-Akt levels. Results were obtained from at least two independent experiments and are expressed as the mean ± SEM. $^{*}P < 0.05$, $^{\#}P < 0.01$, and $^{\S}P < 0.001$, statistically significant differences, compared to DMSO-treated cells (C), were calculated by Student's t-test for unpaired data.

adhesion and cell migration [43] and is directly involved in maintaining actin folding [21]. Indirect immunofluorescence experiments were performed to investigate the cellular localization of BAG3 after PEITC treatment (Figure 4(a)). Analysis by confocal microscopy demonstrated that BAG3 in HUVECs, under physiological growth condition, appears to have a predominantly cytoplasmic localization; 2 h of PEITC treatment moved the protein in the protruding ends

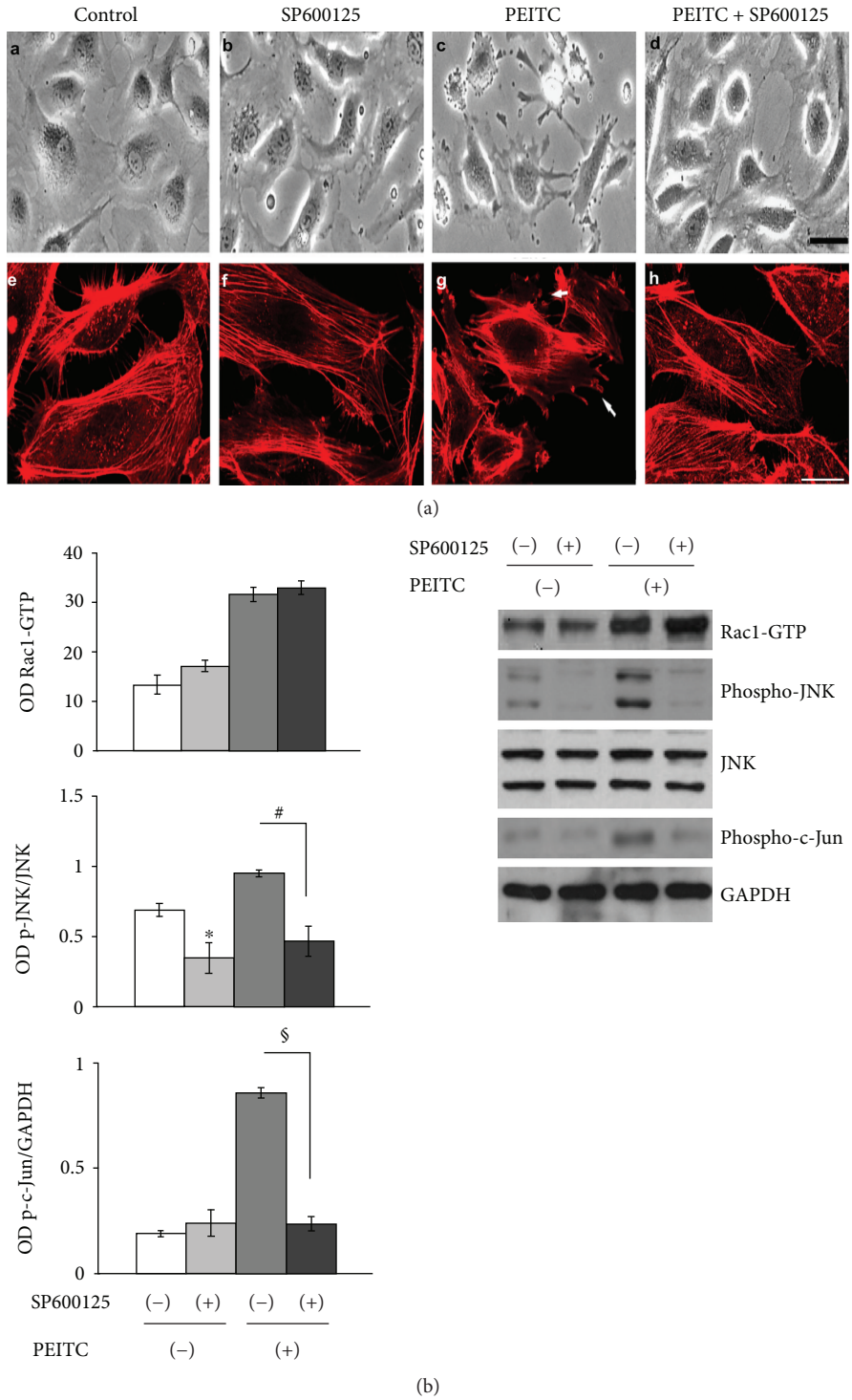

Figure 3: JNK activity is involved in actin remodeling processes during PEITC treatment. (a) The upper panel displays phase-contrast images and confocal analysis of HUVECs treated with (A, E) 0.01% DMSO (control), (B, F) 10 μM of SP600125 (JNK inhibitor) for 1 h (C, G), and 10 μM of PEITC for 2 h and (D, H) pretreated with 10 μM of SP600125 1 h before PEITC administration. Scale bars: $d = 15$ μm and $h = 5$ μm. (b) The levels of GTP-bound Rac1, phospho-JNK, and phospho-c-Jun in lysates of HUVECs, pretreated or not with 10 μM of SP600125 for 1 h, were analyzed in the presence/absence of 10 μM PEITC stimulation for 2 h. The left bar graphs depict densitometric analysis of Rac1 activity, phospho-JNK, and phospho-c-JUN levels. Results were obtained from at least two independent experiments and are expressed as the mean ± SEM. $^{*}P < 0.05$, $^{\#}P < 0.01$, $^{\S}P < 0.001$, statistically significant differences, compared to DMSO-treated cells (C), were calculated by Student's t-test for unpaired data.

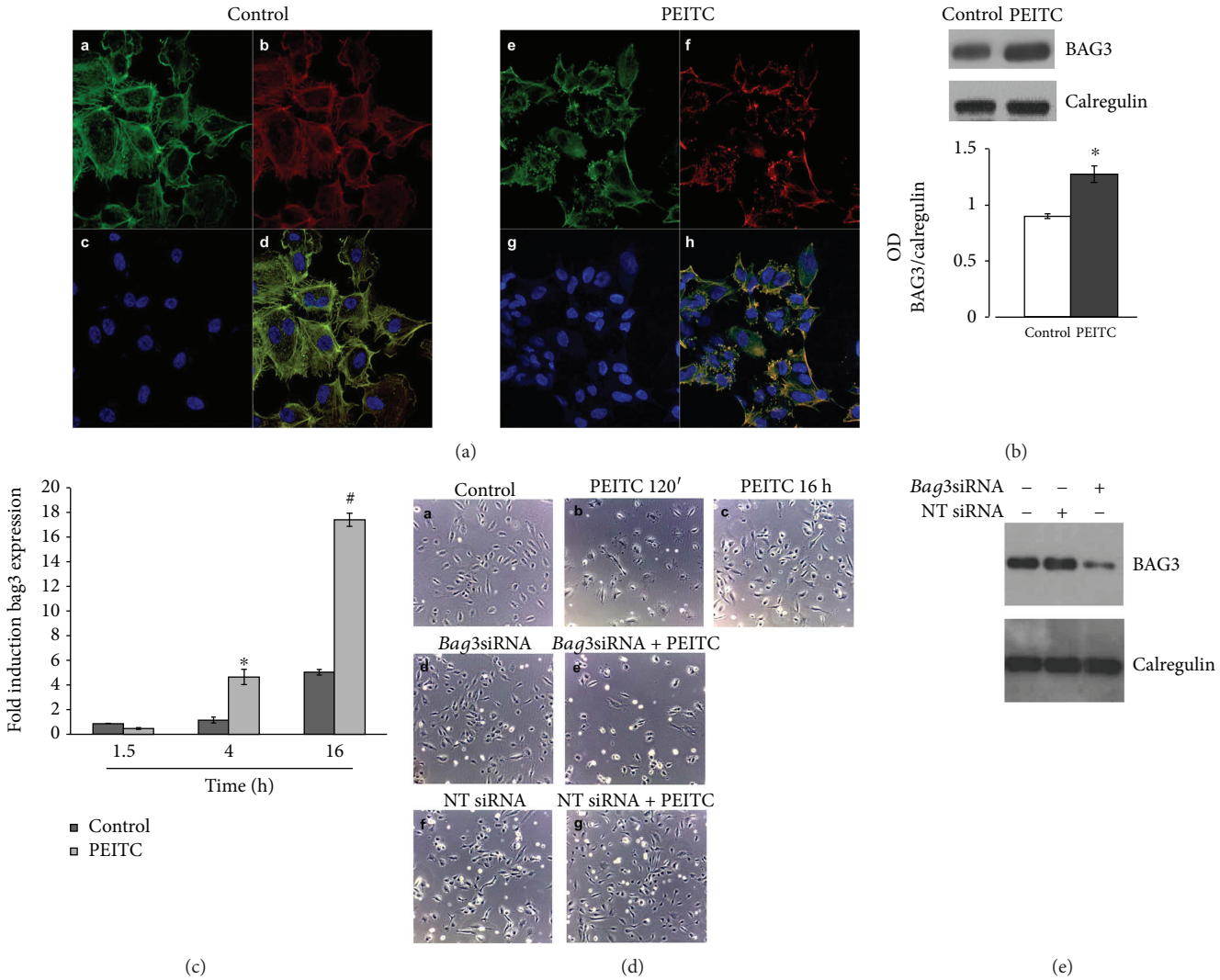

FIGURE 4: PEITC treatment induces BAG3 expression and its delocalization in HUVECs. (a) Immunofluorescence analysis of HUVECs in control conditions and after PEITC treatment. Cells were stained with the BAG3 antibody (A–E), phalloidin (B–F) that allows for the visualization of F-actin, and Hoechst (C–G), and D–H are merged images. The merged image shows overlapping localization of BAG3 and F-actin. (b) HUVECs were treated with 0.01% DMSO (control) and with 10 μM PEITC for 16 h. Total protein extracts were analyzed by Western blot using the anti-BAG3 antibody and anti-calregulin antibody, as an internal loading control. The lower panel displays columns representing densitometric analysis of the data (expressed as the BAG3/calregulin ratio) corresponding to the upper panel ($n = 2$). $^{*}P < 0.05$, statistically significant differences, were calculated by Student's t-test for unpaired data. (c) Analysis of *bag3* mRNA levels by qRT-PCR. Fold induction of *bag3* mRNA levels (y-axis) in HUVEC controls and PEITC-treated cells is expressed relative to β-actin mRNA levels. Data are the mean values ± SD from two independent experiments performed in triplicate. $^{*}P < 0.05$ and $^{\#}P < 0.01$, statistically significant differences, compared to DMSO-treated cells (C), were calculated by one-way ANOVA with Dunnett's post hoc test using SigmaPlot12.0 software. (d) Phase-contrast images of HUVECs treated with (A) DMSO (control) at a final concentration (0.01%), with (B) PEITC (10 μM) for 120 min, and with (C) PEITC (10 μM) for 16 h. (D, E, F, G) HUVECs were transfected for 48 h with *bag3* siRNA (100 nM) or with a NT siRNA (100 nM) and treated with (D, F) DMSO (control) at a final concentration (0.01%) and with (E, G) PEITC (10 μM) for 16 h. (e) HUVECs were transfected as described above. Total cell protein content was subjected to Western blot analysis to measure BAG3 levels and anti-calregulin antibody, as an internal loading control.

where it colocalized with F-actin at the cell membrane, as can be observed in the merged image (Figure 4(a), H). Taken together, these data demonstrated that BAG3 protein is subjected to changes in its expression and localization during PEITC treatment. Its delocalization to F-actin in proximity to cell membranes suggests a role of the BAG3 protein in cell morphology changes that have been observed.

To assess whether PEITC is able to induce changes in BAG3 protein levels, a protein expression analysis was performed. As shown in Figure 4(b), the BAG3 expression level increases after 16 h treatment. This result showed that PEITC also modulates BAG3 expression levels and its upregulation could be a direct consequence of JNK activation [36]. Furthermore, real-time PCR experiments have shown that the

increase in the level of BAG3 protein correlates with the increase in the *bag3* mRNA (Figure 4(c)). Phase-contrast observations of HUVECs revealed that PEITC induced a dramatic change in cellular morphology after 120 min of treatment (Figure 4(d), A and B); however, prolonged exposure to PEITC (16 h) seems to show a recovery of cellular morphology similar to the control (Figure 4(d), A–C). This condition coincides with the increase in the expression of the protein observed in Figures 4(b) and 4(c). In order to demonstrate that BAG3 protein is directly involved in the recovery of cell morphology, we performed protein silencing experiments using specific siRNAs. As can be seen in Figure 4(d), E, when the BAG3 protein is silenced, the cells, after 16 h of treatment, do not show a recovery, whereas a nontargeted (NT) siRNA, used as a control, had no effect. Western blotting analysis in Figure 4(e) confirms silencing of the protein BAG3. These data show that BAG3 expression is essential for the recovery of cell morphology.

3. Materials and Methods

3.1. Reagents and Antibodies. Endothelial growth medium (EGM-2 BulletKit) was purchased from Clonetics (Walkersville, MD), and Vascular Cell Basal Medium (EGM Kit-VEGF) was purchased from ATCC. Phenethyl isothiocyanate (PEITC), SP600125, Hoechst 33342, protease inhibitor cocktail, and phalloidin-tetramethylrhodamine B isothiocyanate were purchased from Sigma (St. Louis, MO) and NSC-23766 from Merck Chemicals Ltd. (Darmstadt, Germany). Chemiluminescent detection reagents (ECL Plus Western Blotting) were purchased from Amersham Biosciences (Piscataway, NJ). LY294002 and antibodies to phospho-Akt (Ser473), Akt, SAPK/JNK, phospho-SAPK/JNK (Thr183/Tyr185), and phospho-FAK (Tyr397) were from Cell Signaling Technology (Danvers, MA); antibodies to BAG3 were from BIOUNIVERSA s.r.l (Montoro, AV, Italy), antibodies to PI3K, phospho-PI3K, and GAPDH from Santa Cruz Biotechnology Inc. (Santa Cruz, CA, USA), and anti-Rac1 antibodies from Millipore (Bedford, MA) and Pierce (Rockford, IL). Normal goat serum, horseradish peroxidase-(HRP-) conjugated secondary antibody, enhanced chemiluminescence reagents, anti-mouse IgG, and the Dylight 488-conjugated anti-mouse IgG were purchased from Jackson ImmunoResearch Laboratories (Suffolk, UK).

3.2. Cell Culture Conditions. Human umbilical vein endothelial cells (HUVECs) were purchased from the National Institute for Cancer Research (Genova, Italy). All experiments were performed on low-passage cell cultures. Cells were grown in EGM-2 or EGM Kit-VEGF at 37°C in a 5% CO_2 atmosphere. Experiments were performed in the absence/presence of PEITC (10 μM) and in the absence/presence of LY294002 (10 μM), NSC23766 (100 μM), and SP600125 (10 μM) pretreatments, using 0.01% DMSO as a control.

3.3. Cell Viability Assay. The MTT (3-[4,5-dimetiltiazol-2,5-diphenyl-2H-tetrazolium bromide]) assay was used in order to assess the cell viability to compare the effect of the potential cytotoxicity of PEITC with a control condition. Such molecule is reduced by a mitochondrial enzyme succinate dehydrogenase to a formazan salt, which precipitates as blue/purple crystals. This is a colorimetric assay, in which the amount of formazan produced is measured spectrophotometrically and is proportional to the number of viable cells.

To perform the assay, the cells, from two different donors, were grown in 96-well plates, in numbers of $5 \times 10^3/cm^2$, and after 24 h were treated with increasing concentrations of PEITC from 2.5 μM to 40 μM in triplicate for 24 and 48 h. At the end of treatment, the plates were centrifuged at 1200 rpm for 5 min, the medium was removed, 100 μl of 1 mg/ml MTT was added to each well, and the plates were kept at 37°C for the time necessary for the formation of salt formazan. The solution was then removed from each well, and the formazan crystals within the cells were dissolved with 100 μl of DMSO. Absorption at 490 nm for each well was assessed by a Multiskan Spectrum Thermo Electron Corporation Reader. The data thus obtained were normalized with respect to the control and used to construct the dose-response histograms [44].

3.4. Flow Cytometry Analysis. Apoptosis was analyzed by propidium iodide incorporation in permeabilized cells and flow cytometry. Cells ($5 \times 10^3/cm^2$) were cultured in 12-well plates. After 24 h, PEITC was added at the concentration of 10 μM and cells were recultured for different times (24 h). For apoptosis analysis, permeabilized cells were labelled with propidium iodide (PI) by incubation at 4°C for 30 min with a solution containing 0.1% sodium citrate, 0.1% Triton X-100, and 50 mg/ml PI (Sigma-Aldrich, St. Louis, MO). The cells were subsequently analyzed by flow cytometry by a FACSCalibur flow cytometer (Becton Dickinson, North Ryde, NSW, Australia).

To evaluate cell cycle distribution, control and treated cells were harvested and nuclei were labeled with PI as described for apoptosis detection and analyzed by flow cytometry. Data from 2000 events per sample were collected, and the relative percentage of the cells in G0/G1, S, G2/M, and sub-G0/G1 phases of the cell cycle was determined using the ModFit software (Becton Dickinson, San Jose, CA, USA). Each determination was repeated three times [45].

3.5. Densitometry. Scanning densitometry of bands was performed with Image Scan (SnapScan 1212; Agfa-Gevaert NV). The area related to each band was determined using ImageJ software. Background was subtracted from calculated values. Results are expressed as mean of at least two separate experiments. Significance was determined by unpaired Student's *t*-test.

3.6. Western Blotting. Cells were harvested and immediately lysed with RIPA buffer (50 mM HEPES, 10 mM EDTA, 150 mM NaCl, 1% NP-40, 0.5% sodium deoxycholate, and 0.1% SDS (pH 7.4)) supplemented with protease inhibitor cocktail. For Western blot analysis, 20 μg of the sample extract was resolved on 10–12% SDS-polyacrylamide gels using a minigel apparatus (Bio-Rad Laboratories, Richmond, CA). Nitrocellulose blots were blocked with 10% nonfat dried milk in Tris buffered saline with Tween 20 (TBS-T) (20 mM

Tris-HCl (pH 7.4), 500 mM NaCl, and 0.01% Tween 20) and incubated overnight at 4°C with appropriate dilutions of primary antibodies with 10% (weight/vol) milk in TBS-T buffer or 5% bovine serum albumin. Immunoreactivity was detected by sequential incubation with an HRP-conjugated secondary antibody and enhanced chemiluminescence reagents according to routine protocols.

3.7. Rac1 Activity Assay. Rac1 activation assays were performed using a commercially available EZ-Detect Rac1 Activation Kit (Pierce, Rockford, IL). The assay uses a GST-fusion protein containing the p21-binding domain of p21-activated protein kinase 1 (PAK1) to selectively bind active Rac1 in the whole cell lysates. Lysates (500 μg total protein) were incubated with glutathione Sepharose beads. Active Rac1 was collected on glutathione agarose beads and quantified by immunoblot analysis using an anti-Rac1 monoclonal antibody. On a separate immunoblot, total Rac1 from cell lysates was normalized and expressed as a ratio of total Rac1 to GAPDH.

3.8. Immunofluorescence. HUVECs were seeded onto 12 mm glass coverslips and grown for 24–48 h until 60–70% confluence. After treatment, cells were washed in PBS and fixed in 3.7% formaldehyde-PBS (30 min at room temperature). After washing, coverslips were treated for 10 min with 0.1 M glycine-PBS and permeabilized with 0.1% Triton X-100 for 10 min. After permeabilization, coverslips were washed again and incubated with a blocking solution (10% normal goat serum in PBS) for 1 h at room temperature. Staining of the actin cytoskeleton in fixed cells was performed with phalloidin-tetramethylrhodamine B isothiocyanate (0.05 μg/ml) for 40 min at room temperature, followed by three rinses in PBS. Cells were labeled with an anti-BAG3 (3 μg/ml) mouse monoclonal antibody AC-1 for 2 h at room temperature and Hoechst 33342 (2 μg/ml) nuclear staining for 15 min. Coverslips were then washed 3 times in PBS, rinsed in distilled water, and glycerol-mounted on slides. A Zeiss LSM 510 Laser Scanning Microscope (Carl Zeiss MicroImaging GmbH) was used for data acquisition. To detect the nucleus, samples were excited with a 409 nm Ar laser. A 488 nm Ar or a 555 nm He-Ne laser was used to detect emission signals from target stains. A 63x (1.40 NA) Plan-Apochromat oil immersion objective was used. Images and scale bars were generated with Zeiss ZEN Confocal Software (Carl Zeiss, MicroImaging GmbH) and presented as a single stack. Images were processed using ImageJ software (NIH) and Adobe Photoshop CS version 5.0, and figures assembled using Microsoft PowerPoint (Microsoft Corporation).

3.9. mRNA Isolation and Real-Time RT-PCR. Total RNA isolation (mRNA) was performed by using the QIAzol Lysis Reagent (Qiagen). RNA (1 μg) was reverse-transcribed by using the QuantiTect Reverse Transcription Kit (Qiagen). Real-time PCR was performed on LightCycler 480 (Roche) by using LightCycler 480 SYBR Green Master Mix, 2 μl of cDNA (~50 ng), and the following primer pairs at the final concentration of 0.3 μM: BAG3-human FW: 5′-CCTGTT AGCTGTGGTTG-3′ and BAG3-human RW: 5′-AACATA CAGATATTCCTATGGC-3′ for the target gene and β-actin FW: 5′-AAAGACCTGTACGCCAACAC-3′ and β-actin RW: 5′-GTCATACTCCTGCTTGCTGAT-3′ for the housekeeping detection. Transcript quantities were compared using the relative Ct method, where the amount of the target normalized to the amount of the endogenous control (β-actin) and relative to the control sample is given by $2^{(-\Delta\Delta Ct)}$. The results are presented as mean ± SD of the mean of experimental triplicates. Significance was determined by one-way analysis of variance (ANOVA) with Dunnett's post hoc test using SigmaPlot12.0 software.

3.10. Transfections. HUVECs were transfected with a specific siRNA targeting *bag3* mRNA (50-AAGGUUCAGACCAU CUUGGAA-30) or a NT-siRNA (50-CAGUCGCGUUUGC GACUGG-30). For cell transfection, 5×10^3 cells/cm^2 were plated, in endothelial growth medium-2 media containing 2% fetal bovine serum and growth factors, to give 30–40% confluence. Cells were transfected with a final siRNA concentration of 100 nM using TransFectin (Bio-Rad Laboratories Inc., Hercules, CA, USA). Transfection efficiency was evaluated in each experiment by Western blot analysis.

4. Discussion

Cell proliferation is a tightly regulated process, organized by pro- and antiproliferative signals. Generally, the proproliferative signals are activated when new cells are required to replace damaged cells. Sustained proliferative signaling is a major characteristic of cancer cells, and PI3K/Akt activation is crucial for cell proliferation, while their PEITC-mediated inhibition is known to suppress cancer growth. PEITC inhibits Akt, a component of Ras signaling to inhibit tumor growth in several cancer types [13, 46]. PEITC is also known to inhibit EGFR and HER2, which are important growth factors and regulators of Akt in different cancer models [47, 48]. The inhibition of Akt may also be due to the suppression of EGFR or HER2 [47].

Overall, it is evident from these examples that PEITC can support the suppression of tumor cell growth through alternative pathways.

Unfortunately, so far, little is known about the activity of PEITC on normal cells, although in a contrasting manner our data are the first ones that try to clarify this activity in detail.

In order to study the activity of PEITC on the endothelial cells, we analyzed the PI3K/Akt pathway as described for tumor cells. However, surprisingly, the first results obtained conflicted with the initial hypothesis and with the literature. In fact, at the PEITC concentrations we used on HUVECs, we did not observe cell death but activation of the PI3K/Akt survival pathway. Moreover, the observation under a phase-contrast microscope showed significant morphological changes, such as volume reduction of cells at the very first minutes, while after 16 hours, cells appear again in their normal sizes without a significant loss in cell viability, even after 48 hours of treatment.

These observations have suggested to investigate the activity of Rac1, in the first minutes of PEITC treatment,

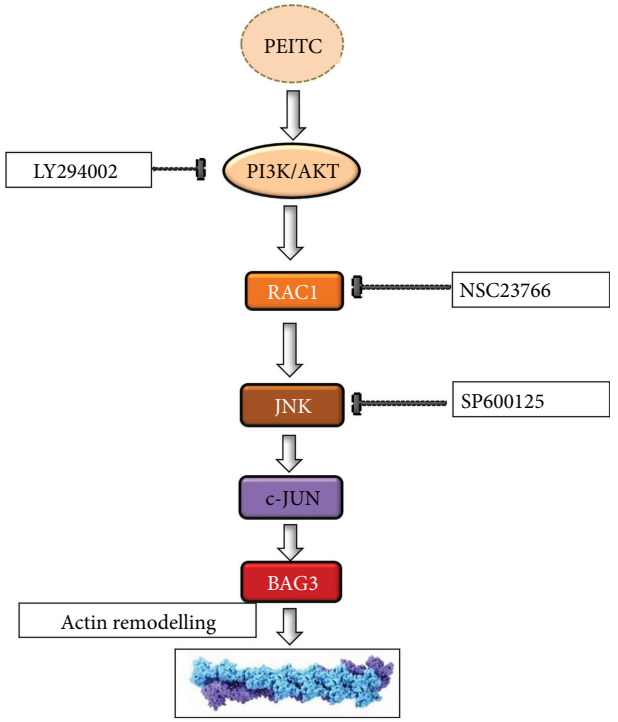

Figure 5: Schematic representation of the proposed model for PI3K/Rac1/JNK/c-Jun pathway activation and involvement of BAG3 as a target of the PEITC effect.

which is known to be required to regulate actin polymerization and membrane protrusion [49], and we observed an increase in Rac1 activity and unexpectedly we also observed that PEITC induced an increase in total Rac1 protein.

Since JNK pathways are activated in response to a wide range of stimuli but most notably following cell exposure to a variety of biotic or abiotic stress events, such as infection, inflammation, oxidative stress, DNA damage, osmotic stress, or cytoskeletal changes [32], our studies show a significant increase in JNK activity.

Several studies showed that Rac1 activation was dependent on PI3K activity and that inhibitors of PI3K/Akt blocked Rac1 activation [23, 32]. Moreover, inhibition of the activity of Rac1 reduced JNK activity [50, 51]. In our study, the activity of Rac1 was abolished by the PI3K/Akt inhibitor LY294002, and the activity of JNK was abolished by the Rac1inhibitor NSC23766 suggesting that PI3K/Akt-Rac1 contributes to JNK activation.

Our results indicate that a key target of PEITC activity in HUVECs is represented by JNK. Indeed, inhibition of this kinase results in the abrogation of PEITC effects on the cytoskeleton. This finding is in line with the reported involvement of JNK in cytoskeleton remodeling [52].

JNK signaling led also to the activation of the c-Jun transcription factor, which is involved in the upregulation of several genes, among them, the BAG3 protein [36] that exerts an important role in endothelial cell survival and growth and in tumor neoangiogenesis [20]. Indeed, PEITC induces an increase in BAG3 levels in HUVECs. This hypothesis is supported by the fact that the increase in the expression of BAG3 corresponds to a recovery of cellular morphology after initial damage by PEITC treatment.

Downmodulation of the BAG3 protein levels by a specific siRNA resulted, after 16 hours of treatment, in the loss of recovery of the normal cellular morphology in respect to controls. These data suggest a role for BAG3 in the described events induced by PEITC.

BAG3 also utilizes its WW domain to engage in YAP/TAZ signaling. Via this pathway, BAG3 stimulates filamin transcription to maintain actin anchoring and crosslinking under mechanical tension and, by integrating tension sensing, ensures tissue homeostasis and regulates fundamental cellular processes such as adhesion, migration, and proliferation [53].

In conclusion, our results suggest that treatment with PEITC causes HUVEC damage to the cytoskeleton and induces activation of the PI3K/Akt-Rac1-JNK prosurvival pathway. c-Jun, a substrate of JNK, activates the transcription of *bag3* with a consequent increase in the BAG3 protein, which allows the refolding of actin and therefore the recovery of cell morphology (Figure 5).

Conflicts of Interest

The authors declare that there is no conflict of interest regarding the publication of this paper.

Authors' Contributions

Silvia Franceschelli and Anna Paola Bruno contributed equally to this work.

References

[1] S. Chikara, L. D. Nagaprashantha, J. Singhal, D. Horne, S. Awasthi, and S. S. Singhal, "Oxidative stress and dietary phytochemicals: role in cancer chemoprevention and treatment," *Cancer Letters*, vol. 413, pp. 122–134, 2018.

[2] J. E. Park, Y. Sun, S. K. Lim et al., "Dietary phytochemical PEITC restricts tumor development via modulation of epigenetic writers and erasers," *Scientific Reports*, vol. 7, article 40569, 2017.

[3] N. M. Fofaria, A. Ranjan, S.-H. Kim, and S. K. Srivastava, "Mechanisms of the anticancer effects of isothiocyanates," *The Enzymes*, vol. 37, pp. 111–137, 2015.

[4] M. d'Avenia, A. Rosati, M. A. Belisario et al., "The expression of the pro-apoptotic gene air is inducible in human pancreatic adenocarcinoma cells," *Journal of Cellular Physiology*, vol. 226, no. 9, pp. 2207–2212, 2011.

[5] Y. J. Jeong, H. J. Cho, F. L. Chung et al., "Isothiocyanates suppress the invasion and metastasis of tumors by targeting FAK/MMP-9 activity," *Oncotarget*, vol. 8, no. 38, pp. 63949–63962, 2017.

[6] L. Mi, A. J. Di Pasqua, and F. L. Chung, "Proteins as binding targets of isothiocyanates in cancer prevention," *Carcinogenesis*, vol. 32, no. 10, pp. 1405–1413, 2011.

[7] L. Mi, N. Gan, and F. L. Chung, "Isothiocyanates inhibit proteasome activity and proliferation of multiple myeloma cells," *Carcinogenesis*, vol. 32, no. 2, pp. 216–223, 2011.

[8] B. E. Cavell, S. S. Syed Alwi, A. Donlevy, and G. Packham, "Anti-angiogenic effects of dietary isothiocyanates: mechanisms of action and implications for human health," *Biochemical Pharmacology*, vol. 81, no. 3, pp. 327–336, 2011.

[9] Q. C. Zhang, Z. H. Pan, B. N. Liu et al., "Benzyl isothiocyanate induces protective autophagy in human lung cancer cells through an endoplasmic reticulum stress-mediated mechanism," *Acta Pharmacologica Sinica*, vol. 38, no. 4, pp. 539–550, 2017.

[10] L. G. Wang and J. W. Chiao, "Prostate cancer chemopreventive activity of phenethyl isothiocyanate through epigenetic regulation (review)," *International Journal of Oncology*, vol. 37, no. 3, 2010.

[11] S. S. S. Boyanapalli, W. Li, F. Fuentes et al., "Epigenetic reactivation of RASSF1A by phenethyl isothiocyanate (PEITC) and promotion of apoptosis in LNCaP cells," *Pharmacological Research*, vol. 114, pp. 175–184, 2016.

[12] I. Dimova, G. Popivanov, and V. Djonov, "Angiogenesis in cancer - general pathways and their therapeutic implications," *Journal of B.U.ON.*, vol. 19, no. 1, pp. 15–21, 2014.

[13] N. Gao, A. Budhraja, S. Cheng et al., "Phenethyl isothiocyanate exhibits antileukemic activity in vitro and in vivo by inactivation of Akt and activation of JNK pathways," *Cell Death & Disease*, vol. 2, no. 4, article e140, 2011.

[14] R. Sarkar, S. Mukherjee, J. Biswas, and M. Roy, "Phenethyl isothiocyanate, by virtue of its antioxidant activity, inhibits invasiveness and metastatic potential of breast cancer cells: HIF-1α as a putative target," *Free Radical Research*, vol. 50, no. 1, pp. 84–100, 2015.

[15] E. Bertl, H. Bartsch, and C. Gerhäuser, "Inhibition of angiogenesis and endothelial cell functions are novel sulforaphane-mediated mechanisms in chemoprevention," *Molecular Cancer Therapeutics*, vol. 5, no. 3, pp. 575–585, 2006.

[16] X. H. Wang, B. E. Cavell, S. S. Syed Alwi, and G. Packham, "Inhibition of hypoxia inducible factor by phenethyl isothiocyanate," *Biochemical Pharmacology*, vol. 78, no. 3, pp. 261–272, 2009.

[17] Y. T. Yeh, H. Yeh, S. H. Su et al., "Phenethyl isothiocyanate induces DNA damage-associated G2/M arrest and subsequent apoptosis in oral cancer cells with varying p53 mutations," *Free Radical Biology and Medicine*, vol. 74, pp. 1–13, 2014.

[18] Z. Xiao, L. Mi, F. L. Chung, and T. D. Veenstra, "Proteomic analysis of covalent modifications of tubulins by isothiocyanates," *The Journal of Nutrition*, vol. 142, no. 7, pp. 1377S–1381S, 2012.

[19] R. Cotugno, A. Basile, E. Romano, D. Gallotta, and M. A. Belisario, "BAG3 down-modulation sensitizes HPV18+ HeLa cells to PEITC-induced apoptosis and restores p53," *Cancer Letters*, vol. 354, no. 2, pp. 263–271, 2014.

[20] A. Falco, M. Festa, A. Basile et al., "BAG3 controls angiogenesis through regulation of ERK phosphorylation," *Oncogene*, vol. 31, no. 50, pp. 5153–5161, 2012.

[21] B. Fontanella, L. Birolo, G. Infusini et al., "The co-chaperone BAG3 interacts with the cytosolic chaperonin CCT: new hints for actin folding," *The International Journal of Biochemistry & Cell Biology*, vol. 42, no. 5, pp. 641–650, 2010.

[22] D. Xiao and S. V. Singh, "Phenethyl isothiocyanate inhibits angiogenesis in vitro and ex vivo," *Cancer Research*, vol. 67, no. 5, pp. 2239–2246, 2007.

[23] K. Katoh, "Activation of Rho-kinase and focal adhesion kinase regulates the organization of stress fibers and focal adhesions in the central part of fibroblasts," *PeerJ*, vol. 5, article e4063, 2017.

[24] P. Rodriguez-Viciana, P. H. Warne, A. Khwaja et al., "Role of phosphoinositide 3-OH kinase in cell transformation and control of the actin cytoskeleton by Ras," *Cell*, vol. 89, no. 3, pp. 457–467, 1997.

[25] Z. Fan, C. Li, C. Qin et al., "Role of the PI3K/AKT pathway in modulating cytoskeleton rearrangements and phenotype switching in rat pulmonary arterial vascular smooth muscle cells," *DNA and Cell Biology*, vol. 33, no. 1, pp. 12–19, 2014.

[26] T. Hou, L. Zhou, L. Wang, G. Kazobinka, X. Zhang, and Z. Chen, "CLCA4 inhibits bladder cancer cell proliferation, migration, and invasion by suppressing the PI3K/AKT pathway," *Oncotarget*, vol. 8, no. 54, pp. 93001–93013, 2017.

[27] P. T. Hawkins, A. Eguinoa, R. G. Qiu et al., "PDGF stimulates an increase in GTP–Rac via activation of phosphoinositide 3-kinase," *Current Biology*, vol. 5, no. 4, pp. 393–403, 1995.

[28] C. Jiménez, R. A. Portela, M. Mellado et al., "Role of the PI3K regulatory subunit in the control of actin organization and cell migration," *The Journal of Cell Biology*, vol. 151, no. 2, pp. 249–262, 2000.

[29] H. C. E. Welch, W. J. Coadwell, L. R. Stephens, and P. T. Hawkins, "Phosphoinositide 3-kinase-dependent activation of Rac," *FEBS Letters*, vol. 546, no. 1, pp. 93–97, 2003.

[30] R. Heller, Q. Chang, G. Ehrlich et al., "Overlapping and distinct roles for PI3Kβ and γ isoforms in S1P-induced migration of human and mouse endothelial cells," *Cardiovascular Research*, vol. 80, no. 1, pp. 96–105, 2008.

[31] R. J. Cain, B. Vanhaesebroeck, and A. J. Ridley, "The PI3K p110α isoform regulates endothelial adherens junctions via Pyk2 and Rac1," *The Journal of Cell Biology*, vol. 188, no. 6, pp. 863–876, 2010.

[32] A. Zeke, M. Misheva, A. Reményi, and M. A. Bogoyevitch, "JNK signaling: regulation and functions based on complex protein-protein partnerships," *Microbiology and Molecular Biology Reviews*, vol. 80, no. 3, pp. 793–835, 2016.

[33] C. Xu, G. Shen, X. Yuan et al., "ERK and JNK signaling pathways are involved in the regulation of activator protein 1 and cell death elicited by three isothiocyanates in human prostate cancer PC-3 cells," *Carcinogenesis*, vol. 27, no. 3, pp. 437–445, 2006.

[34] B. L. Bennett, D. T. Sasaki, B. W. Murray et al., "SP600125, an anthrapyrazolone inhibitor of Jun N-terminal kinase," *Proceedings of the National Academy of Sciences*, vol. 98, no. 24, pp. 13681–13686, 2001.

[35] S. Franceschelli, A. Rosati, R. Lerose, S. De Nicola, M. C. Turco, and M. Pascale, "Bag3 gene expression is regulated by heat shock factor 1," *Journal of Cellular Physiology*, vol. 215, no. 3, pp. 575–577, 2008.

[36] C. Li, S. Li, D. H. Kong et al., "BAG3 is upregulated by c-Jun and stabilizes JunD," *Biochimica et Biophysica Acta (BBA) - Molecular Cell Research*, vol. 1833, no. 12, pp. 3346–3354, 2013.

[37] V. Esposito, C. Baldi, P. Zeppa et al., "BAG3 protein is overexpressed in endometrioid endometrial adenocarcinomas," *Journal of Cellular Physiology*, vol. 232, no. 2, pp. 309–311, 2017.

[38] G. Chiappetta, A. Basile, A. Barbieri et al., "The anti-apoptotic BAG3 protein is expressed in lung carcinomas and regulates small cell lung carcinoma (SCLC) tumor growth," *Oncotarget*, vol. 5, no. 16, pp. 6846–6853, 2014.

[39] L. Guerriero, K. Chong, R. Franco et al., "BAG3 protein expression in melanoma metastatic lymph nodes correlates with patients' survival," *Cell Death & Disease*, vol. 5, no. 4, article e1173, 2014.

[40] A. Rosati, S. Bersani, F. Tavano et al., "Expression of the antiapoptotic protein BAG3 is a feature of pancreatic adenocarcinoma and its overexpression is associated with poorer survival," *The American Journal of Pathology*, vol. 181, no. 5, pp. 1524–1529, 2012.

[41] R. Franco, G. Scognamiglio, V. Salerno et al., "Expression of the anti-apoptotic protein BAG3 in human melanomas," *Journal of Investigative Dermatology*, vol. 132, no. 1, pp. 252–254, 2012.

[42] M. Festa, L. Del Valle, K. Khalili et al., "BAG3 protein is overexpressed in human glioblastoma and is a potential target for therapy," *The American Journal of Pathology*, vol. 178, no. 6, pp. 2504–2512, 2011.

[43] J. N. Kassis, E. A. Guancial, H. Doong, V. Virador, and E. C. Kohn, "CAIR-1/BAG-3 modulates cell adhesion and migration by downregulating activity of focal adhesion proteins," *Experimental Cell Research*, vol. 312, no. 15, pp. 2962–2971, 2006.

[44] T. Esposito, F. Sansone, S. Franceschelli et al., "Hazelnut (Corylus avellana L.) shells extract: phenolic composition, antioxidant effect and cytotoxic activity on human cancer cell lines," *International Journal of Molecular Sciences*, vol. 18, no. 2, 2017.

[45] M. Persico, A. Ramunno, V. Maglio et al., "New anticancer agents mimicking protein recognition motifs," *Journal of Medicinal Chemistry*, vol. 56, no. 17, pp. 6666–6680, 2013.

[46] T. Okubo, K. Washida, and A. Murakami, "Phenethyl isothiocyanate suppresses nitric oxide production via inhibition of phosphoinositide 3-kinase/Akt-induced IFN-γ secretion in LPS-activated peritoneal macrophages," *Molecular Nutrition & Food Research*, vol. 54, no. 9, pp. 1351–1360, 2010.

[47] S. Loganathan, P. K. Kandala, P. Gupta, and S. K. Srivastava, "Inhibition of EGFR-AKT axis results in the suppression of ovarian tumors in vitro and in preclinical mouse model," *PLoS One*, vol. 7, no. 8, article e43577, 2012.

[48] P. Gupta, C. Adkins, P. Lockman, and S. K. Srivastava, "Metastasis of breast tumor cells to brain is suppressed by phenethyl isothiocyanate in a novel in vivo metastasis model," *PLoS One*, vol. 8, no. 6, article e67278, 2013.

[49] S. Magi, Y. Takemoto, H. Kobayashi et al., "5-Lipoxygenase and cysteinyl leukotriene receptor 1 regulate epidermal growth factor-induced cell migration through Tiam1 upregulation and Rac1 activation," *Cancer Science*, vol. 105, no. 3, pp. 290–296, 2014.

[50] J. Yamauchi, Y. Miyamoto, H. Kokubu et al., "Endothelin suppresses cell migration via the JNK signaling pathway in a manner dependent upon Src kinase, Rac1, and Cdc42," *FEBS Letters*, vol. 527, no. 1-3, pp. 284–288, 2002.

[51] J. C. Chen, B. B. Lin, H. W. Hu et al., "NGF accelerates cutaneous wound healing by promoting the migration of dermal fibroblasts via the PI3K/Akt-Rac1-JNK and ERK pathways," *BioMed Research International*, vol. 2014, Article ID 547187, 13 pages, 2014.

[52] M. Gelderblom, S. Eminel, T. Herdegen, and V. Waetzig, "c-Jun N-terminal kinases (JNKs) and the cytoskeleton functions beyond neurodegeneration," *International Journal of Developmental Neuroscience*, vol. 22, no. 7, pp. 559–564, 2004.

[53] A. Ulbricht, F. J. Eppler, V. E. Tapia et al., "Cellular mechanotransduction relies on tension-induced and chaperone-assisted autophagy," *Current Biology*, vol. 23, no. 5, pp. 430–435, 2013.

Hindawi
Oxidative Medicine and Cellular Longevity
Volume 2018, Article ID 2568569, 12 pages
https://doi.org/10.1155/2018/2568569

Review Article

Vascular Endothelial Dysfunction in Inflammatory Bowel Diseases: Pharmacological and Nonpharmacological Targets

Antonietta Gerarda Gravina,[1] Marcello Dallio,[1] Mario Masarone,[2] Valerio Rosato,[2] Andrea Aglitti,[2] Marcello Persico,[2] Carmelina Loguercio,[1] and Alessandro Federico[1]

[1]*Department of Precision Medicine, University of Campania "Luigi Vanvitelli", Via Pansini 5, 80131 Naples, Italy*
[2]*Department of Medicine and Surgery, University of Salerno, Via Salvador Allende, 84081 Baronissi, Salerno, Italy*

Correspondence should be addressed to Alessandro Federico; alessandro.federico@unicampania.it

Received 22 December 2017; Accepted 14 March 2018; Published 12 April 2018

Academic Editor: Saeid Golbidi

Inflammatory bowel diseases, including Crohn's disease and ulcerative colitis, are chronic inflammatory conditions involving primarily the gastrointestinal tract. However, they may be also associated with systemic manifestations and comorbidities. The relationship between chronic inflammation and endothelial dysfunction has been extensively demonstrated. Mucosal immunity and gastrointestinal physiology are modified in inflammatory bowel diseases, and these modifications are mainly sustained by alterations of endothelial function. The key elements involved in this process are cytokines, inflammatory cells, growth factors, nitric oxide, endothelial adhesion molecules, and coagulation cascade factors. In this review, we discuss available data in literature concerning endothelial dysfunction in patients affected by inflammatory bowel disease and we focus our attention on both pharmacological and nonpharmacological therapeutic targets.

1. Introduction

Inflammatory bowel diseases (IBD) are chronic inflammatory pathologies that primarily involve the gastrointestinal tract associated with a combination of environmental, genetic, and immunological pathogenetic factors. The consequence of this "worsening cooperation" is an uncontrolled immune response against self-antigen of the intestine, which acts as a trigger in genetically predisposed individuals to disease development [1]. Crohn's disease (CD) may occur in any region of the gastrointestinal tract involving, in most of the cases, the ileum and colon with a discontinuous, transmural, and granulomatous inflammation pattern, whereas ulcerative colitis (UC) only affects the colon and rectum and is restricted to the mucosal layer of the intestine which appears with a continuous and exudative inflammation pattern [2, 3]. Several studies have reported that the prevalence of cardiovascular risk factors such as obesity, dyslipidemia, diabetes, and hypertension is lower among subjects affected by IBD in comparison to the general population [1, 4, 5]. In accordance with this observation, we would expect a lower cardiovascular mortality and morbidity in IBD patients. However, on the contrary, cardiovascular disease incidence in patients with IBD seems to be increased [6]. It can therefore be hypothesized that there are other factors that play an important role in cardiovascular disease development in these subjects, such as chronic inflammation [1].

In chronic systemic inflammation diseases, the inflammation affects the arterial properties and causes both endothelial dysfunction and an increase of arterial stiffness. A relationship between increased arterial stiffness and inflammatory disorders has been described in a lot of inflammatory diseases including systemic vasculitis [7], rheumatoid arthritis [8], and systemic lupus erythematosus [9]. In this review, we analyze the relationship between inflammatory bowel disease inflammation and endothelial dysfunction in order to predict the possible role of this inflammation in cardiovascular disease development. Moreover, we focus our attention on

Table 1: Main studies on PWV for evaluation of arterial stiffness.

Authors (year)	Type of article	Studied people	Ref.
Laurent et al. (2006)	Consensus document	Healthy people and people with inflammatory diseases	[11]
Pietri et al. (2006)	Prospective study	Uncomplicated, never-treated Essential hypertension people	[12]
Yasmin et al. (2004)	Prospective study	Healthy people	[13]
Mäki-Petäjä et al. (2006)	Prospective study	Rheumatoid arthritis people and healthy people	[8]
Zanoli et al. (2012)	Prospective study	Inflammatory bowel disease people and healthy people	[15]
Akdoğan et al. (2013)	Prospective study	Ulcerative colitis people and healthy people	[16]
Korkmaz et al. (2014)	Prospective study	Inflammatory bowel disease people and healthy people	[17]
Aytac et al. (2015)	Prospective study	Inflammatory bowel disease people and healthy people	[18]
Zanoli et al. (2014)	Prospective study	Inflammatory bowel disease people and healthy people	[19]

the possible pharmacological and nonpharmacological therapeutic targets oriented to interrupt this dangerous link in order to reduce the cardiovascular morbidity and mortality in this category of patients.

2. Main Text

2.1. Arterial Stiffness in Chronic Inflammatory Diseases. Several studies reported that arterial stiffness and endothelial function could be considered as markers of subclinical inflammation-associated organ damage [1, 10]. However, a small number of studies evaluated both endothelial function and arterial stiffness in subjects with IBD. Laurent et al. [11] in an expert consensus document described the gold standard procedure in order to assess regional arterial stiffness in daily practice and highlighted the direct relationship between arterial stiffness and the pulse wave velocity (PWV) measurement. PWV is measured by pressure waveforms obtained transcutaneously in correspondence to the right common carotid artery and the right femoral artery (carotid-femoral PWV). PWV is calculated by dividing the distance between two detection points for the time necessary to cover it. An increased carotid-femoral PWV is considered both a marker of target organ damage and a cardiovascular risk factor [1]. The relationship between arterial stiffness, PWV, and inflammation has been reported in patients with chronic inflammatory diseases, such as systemic vasculitis, and rheumatoid arthritis, and patients with increased concentrations of high-sensitivity C-reactive protein (hsRCP). Pietri et al. [12] reported a positive correlation between PWV, direct marker of arterial stiffness, and hsRCP, independently from blood pressure, in patients with untreated primary hypertension, as well as in normotensive individuals. Yasmin et al. [13] also reported the same data about healthy individuals. Endothelial dysfunction could be considered a possible mechanism linking inflammation and arterial stiffness. Inflammation may induce structural changes in the arterial wall, by altering the balance between elastin breakdown and synthesis. Indeed, several elastolytic enzymes, including matrix metalloproteinase-9, are known to be upregulated by inflammatory cytokines [13, 14]. Increased arterial stiffness in patients with inflammatory diseases could be reversible, since in patients with rheumatoid arthritis treated with drugs against tumor necrosis factor- (TNF-) α, some authors observed a reduced PWV comparable to that obtained by healthy individuals [8]. PWV has increased in patients with IBD without differences between CD and UC patients [15–19]. An increased functional and structural arterial stiffening was described in inflammatory diseases. These structural or functional changes are supported by endothelial dysfunction (Table 1).

2.2. Endothelial Dysfunction and IBD. Endothelial dysfunction is "an imbalance between vasodilating and vasoconstricting substances produced by (or acting on) endothelial cells" [20, 21]. Endothelial dysfunction is characterized by upregulation of cellular adhesion molecules, compromised barrier function, increased leukocyte diapedesis, and increased vascular smooth muscle tone. These phenomena are related to an impaired production of vasodilator substances such as nitric oxide (NO) as well as an increase of vasoconstrictor substances including endothelin that determine the appearance of a prothrombotic state [22].

Several authors demonstrated that sex and age could influence the endothelial function. Ciccone et al. showed in 2013 that endothelial dysfunction has worsened with advancing age and that it occurs earlier in males in comparison with women. In healthy men under 40 years, endothelial function seems to be preserved and after this phase of life, it seems to be worse; in healthy women, it seems to be preserved up to 50 years and decline thereafter [23].

Endothelial dysfunction has been widely demonstrated to be the first step in the development of atherosclerosis. The consequent alteration of the vasodilation due to endothelial dysfunction is considered as a cumulative result of the dangerous actions sustained by all the atherogenic factors. Indeed, some studies have shown that endothelial dysfunction is an independent risk factor for cardiovascular disease development [24, 25]. Endothelial function seems to be compromised in patients with IBD. Garolla et al. [26] demonstrated that the number of circulating endothelial precursor cells (EPCs), which are considered markers of both endothelial reparation and vascular healing, was significantly reduced in patients with IBD compared with healthy controls. Moreover, they also demonstrated that apoptotic endothelial precursor cells were higher in patients with IBD than in healthy controls.

Finally, they hypothesized that in IBD patients, apoptosis contributes to the reduction of circulating EPC number and also influencing their ability to proliferate. This condition may represent a risk factor for cardiovascular disease and endothelial dysfunction in these patients [1].

Endothelial function is ensured thanks to the maintenance of a balance among different elements such as NO, endothelin 1, von Willebrand factor (vWF), and cellular adhesion molecule (CAM) superfamily [20, 27]. Inflammation leads to structural and functional changes in the vascular endothelium and its activation. These changes initially include increased leukocyte adhesiveness, leukocyte diapedesis, vascular smooth muscle tone, and procoagulant activity [20, 22, 28]. The interactions between integrins and chemokine receptors with endothelial and mucosal ligands promote activation of endothelial cells [20, 29, 30]. The recruitment of leukocytes happens thanks to the endothelial expression of CAMs and chemokines [20, 31, 32]. The recruitment of leukocytes is mainly mediated by a link between leukocyte CD11a/CD18 and ICAM-1 in the gut or by a link between α4-β1 or α4-b7, VCAM-1, and mucosal addressin cell adhesion molecule-1 (MAdCAM-1) [20, 29]. Microvascular expression of ICAM-1, VCAM-1, and MAdCAM-1 is upregulated in patients with IBD [20, 31, 33]. MAdCAM-1 interacts with $\alpha 4\beta 7$ integrins on the surface of a subset of naive CD4+ T-cells; therefore, an increase of MAdCAM-1 expression intensifies the recruitment of α4 integrin-expressing leukocytes [34–36]. Several inflammatory mediators, such RCP, are known to influence vascular functions. Wang et al. [37] demonstrated that RCP acts on vascular smooth muscle cells upregulating the angiotensin type I receptor and stimulating the migration and proliferation of smooth muscle cells, inducing, moreover, an increase in the production of reactive oxygen species (ROS). Pasceri et al. [38] demonstrated that RCP induces the secretion of some chemokines, adhesion molecules, and E-selectin from the endothelial cells, whereas Venugopal et al. [39] demonstrated that RCP decreases NOS expression. In contrast to these authors, Clapp et al. [40] in 2005 showed that RCP increases NO in a blood vessel cell model in vitro. However, further investigations are needed to establish if RCP is able to alter endothelial function, either favorably or unfavorably. Other inflammatory mediators implicated in vascular dynamics are IL-1, TNF-α, NO, vascular endothelial growth factor (VEGF), CD40-CD40 ligand, and IL-6, which are upregulated in IBD [41–45]. Increased levels of proinflammatory cytokines, such as IL-1 and TNF-α, and oxidative stress products are responsible for some structural changes in the muscle cells of the vascular walls because they induce an increase of the expression of matrix metalloproteinases and serine proteinases with subsequent degradation of elastin and collagen. Muscle cells of the vascular wall express osteoblast markers and are able to take up phosphate and produce bioapatite. This process produces wall calcifications and reduces vessel elasticity [1, 46]. Inflammatory cells, such as macrophages, lymphocytes, mast cells, and fibroblasts, produce angiogenic factors and promote pathological angiogenesis in inflammatory tissues [20, 33, 47]. VEGF, fibroblast growth factor, and TNF-α upregulation are stimulated by hypoxia in the inflamed area, with the successive production of vessels [20, 47]. A significant increase in endothelial CD40 expression is also reported in patients with active IBD and it results in increased recruitment of leukocytes expressing CD40L and also of platelets [20, 34]. CD40 has been found in atherosclerotic plaques and is overexpressed in both intestinal mucosa and circulating platelets of IBD patients. The CD40-CD40L pathway stimulates mucosal inflammation and causes increased production of proinflammatory cytokines, such as IL-8, chemokines, and cell adhesion molecules, and causes angiogenesis-stimulating intestinal fibroblasts to release angiogenic cytokines [20, 42] (Figure 1). CD40 binding stimulates the production of TNF-α, which increases CD40 expression [20, 43]. These mechanisms are the basis of structural changes in the vessel wall, including capillary and venule remodeling and proliferation of endothelial cells.

NO is a mediator that plays a critical role in vascular homeostasis. It is generated from conversion of L-arginine to citrulline by NOS isoforms. Mammals have three isoforms of NOS, two of them are constitutive: endothelial NOS (eNOS) and neuronal NOS (nNOS); the other one is produced in response to inflammatory stimuli (inflammatory cytokines): inducible NOS (iNOS) [48]. NO increases the concentration of cyclic guanosine monophosphate, which has a vasodilation effect, inhibits the expression of cytokines, chemokines, and leukocyte adhesion substances, inhibits blood platelet adhesion and aggregation, and limits the proliferation of smooth muscle cells in the vascular wall. Arginase is an enzyme that acts in the opposite way to NOS and its expression is increased in IBD patients. For this reason, there is a decreased NO production in patients with IBD [20, 33, 49, 50]. eNOS-derived NO is a radical scavenger able to absorb O_2 and generate the potent oxidant peroxynitrite (NO_3^-). TNF-α expression is increased in patients with IBD, binds TNF receptor and leads to diminished eNOS protein expression, and suppresses eNOS activity. Therefore, there is a low NO availability [20, 22] that consequently a vasoconstriction occurs, because of smooth muscle cell relaxation reduction. This mechanism is responsible for functional increase of arterial stiffness observed among subjects affected by chronic inflammation [1]. The levels of asymmetric dimethylarginine (ADMA) plasma, an endogenous eNOS inhibitor, are inversely correlated with NO plasma levels, and it is elevated in numerous diseases associated with cardiovascular risk; indeed, high ADMA levels are also associated with an increased cardiovascular risk [22, 51, 52]. Chronic inflammatory diseases are generally associated with increased oxidative stress. Proinflammatory cytokines, including TNF-α, are mainly responsible for the increase of ROS production in inflammatory diseases. TNF-α increases activity of NADPH oxidases (NOX), which catalyze the transfer of electrons to molecular oxygen in order to generate superoxide by neutrophils and endothelial cells [22, 53, 54]. Superoxide reacts with NO to produce peroxynitrite, thereby decreasing NO bioavailability. In addition to its production by NOS and metabolism by ADMA, NO bioavailability is also modulated by ROS [55]. Superoxide and other ROS are capable to increase the activity of nuclear factor- (NF-) κB, a critical step in the

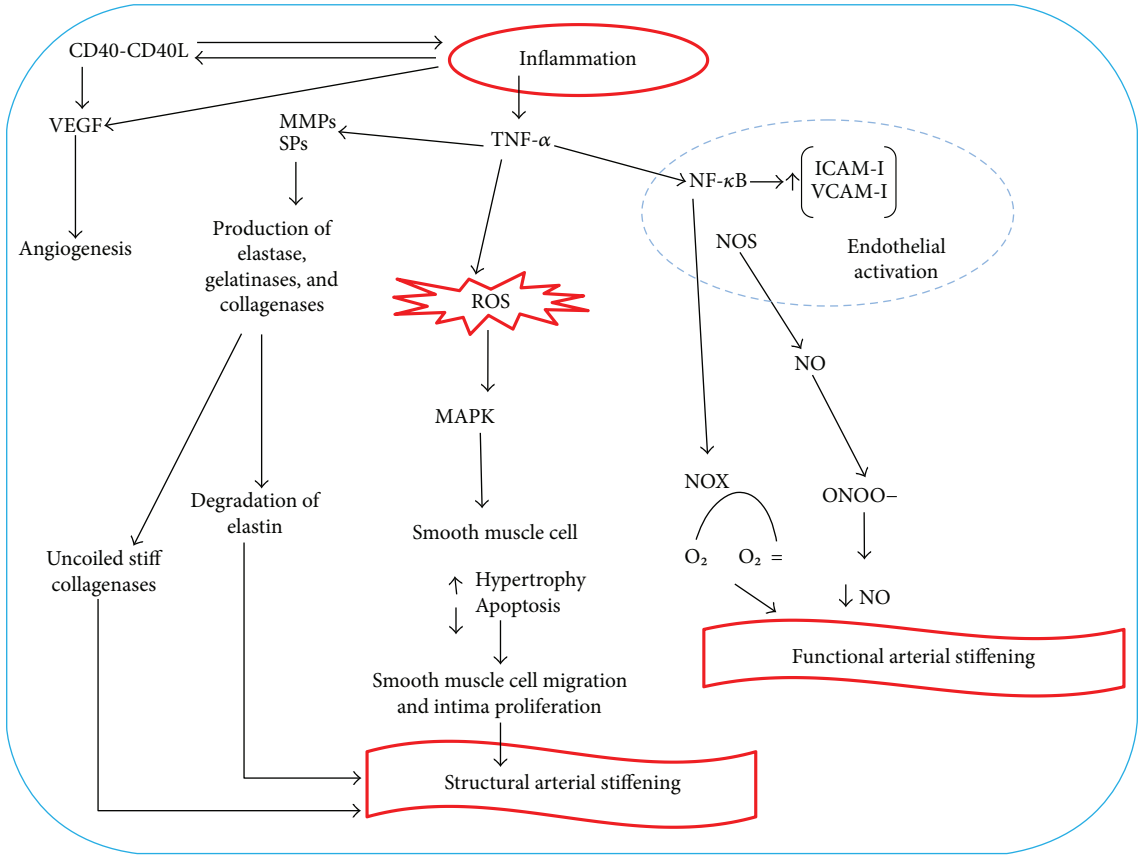

Figure 1: Mechanisms of inflammation-derived endothelial dysfunction. The CD40-CD40L pathway stimulates mucosal inflammation and causes increased production of proinflammatory cytokines, such as interleukin- (IL-) 8, chemokines, and cell adhesion molecules, and causes angiogenesis-stimulating intestinal fibroblasts to release angiogenic cytokines.

transformation of endothelial cells in "activated cells" characterized, in part, by an increase of surface expression of CAMs [22, 56, 57]. NF-κB activation may also stimulate NOX expression, further enhancing ROS production in the endothelium and regenerating the destructive loop of inflammation and oxidative stress [22, 58]. ROS produced in the inflamed area inhibit cleavage of vWF molecules and it may cause microvascular thrombosis in patients with IBD [27, 30, 59]. An increase of plasminogen activator inhibitor type 1 (PAI-1) and reduction of tissue-type plasminogen activator (t-PA) and urokinase-type plasminogen activator (u-PA) have been found in mesenteric vascular walls of patients with IBD [60, 61]. It means that the coagulation process is deeply altered in IBD. ROS production induces smooth muscle cell hypertrophy and intima proliferation through the activation of protein kinases activated by the mitogen (MAPk) pathway (Table 2). The endothelial dysfunction could be diagnosed through two main methods: physical and biochemical method. The first one is based on assessing vasodilation in large arteries in response to increased flow and receptor stimulation, mainly acetylcholine [20]. The most sensitive and widely used is the flow-mediated vasodilatation (FMD), but it is less sensitive in detecting early changes of the endothelium function, similarly to each physical method. Several studies demonstrated a decrease of FMD in IBD patients with active diseases but no changes in the carotid intima-media thickness compared to healthy control (c-IMT) [20, 62]. Roifman et al. [41] demonstrated lower pulse arterial tonometry (PAT) values in patients with IBD compared to healthy control. Theocharidou et al. [63] reported an increase of c-IMT in patients with IBD; however, they did not find any correlation with the activity of the diseases. c-IMT is the main early vascular wall morphological change preceding plaque formation [64–66]. Although some studies [62, 67, 68] did not find any difference in c-IMT values between patients with IBD and controls, other studies [63–65] identified a higher c-IMT in the IBD group than in the control group, even if patients and controls did not show higher cardiovascular risk factors [66] (Table 3).

Biochemical methods are based on the assessment of the synthesis of compounds produced by both normal and damaged endothelium. Different studies evaluated these markers; however, the outcomes are difficult to interpret. Some studies reported an increase of the levels of VEGF, ICAM-1, and E-selectin in the serum of patients with IBD [69, 70]. Magro et al. [71] demonstrated lower levels of angiogenetic factors (P-selectin, E-selectin, VCAM, ICAM, and VEGF) in serum of patients with inactive CD than of controls, thus suggesting a dysfunction of angiogenic process and wound repair. Other reliable biochemical methods have been described in the diagnosis of endothelial dysfunction by using biochemical parameters (Table 3).

Table 2: Mediators involved in endothelium dysfunction.

Author(s) (year)	Studied factors	Ref.
Garolla et al. (2009)	EPCs	[26]
Scaldaferri et al. (2011)	NO, endothelin 1, vWF, and CAM superfamily	[27]
Charo et al. (2006)	Integrins and chemokine receptors	[29]
Hatoum et al. (2003)	CAM superfamily and chemokines	[31]
Danese et al. (2011)	ICAM-1 and VCAM-1	[36]
Briskin et al. (1997)	MAdCAM-1, CD4, and $\alpha 4\beta 7$ integrins	[34]
Burgio et al. (1995)		[35]
Cromer et al. (2011)		[36]
Wang et al. (2003)	RCP	[37]
Pasceri et al. (2000)		[38]
Venugopal et al. (2005)		[39]
Clapp et al. (2005)		[40]
Roifman et al. (2008)	IL-1, TNF-α, NO, VEGF, CD40-CD40-ligand, and IL-6	[41]
Danese et al. (2007)		[42]
Danese et al. (2006)		[43]
Kullo et al. (2005)		[44]
Vita et al. (2004)		[45]
Floege et al. (2004)	IL-1, TNF-α, ROS, matrix metalloproteinases, serine proteinases	[46]
Koutroubakis et al. (2006)	Inflammatory cells (macrophages, lymphocytes, mast cells, and fibroblasts),VEGF, and TNF-α	[47]
Horowitz et al. (2007)	NO	[49]
Steyers et al. (2014)	TNF-α and NO	[22]
Sibal et al. (2010)	ADMA	[51]
Boger et al. (2009)		[52]
Kleinbongard et al. (2010)	TNF-α	[53]
Picchi et al. (2006)		[54]
Kalinowski et al. (2004)	NADH/NADPH	[55]
Kundu et al. (2012)	ROS, NF-κB, and CAM superfamily	[56]
Wolin (2000)		[57]
Biniecka et al. (2011)	NF-κB, NOX, and ROS	[58]
Lancellotti et al. (2010)	vWF	[59]
Ciccone et al. (2015)	PAI-1, t-PA, and u-PA	[60]
Desreumaux et al. 1(999)		[61]

EPCs: endothelial precursor cells; NO: nitric oxide; vWF: von Willebrand factor; CAM: cell adhesion molecule; ICAM-1: intercellular adhesion molecule; VCAM-1: vascular adhesion molecule; MAdCAM-1: mucosal addressin cell adhesion molecule-1; RCP: reactive C protein; IL: interleukin; TNF: tumor necrosis factor; VEGF: vascular endothelial growth factor; ROS: reactive oxygen species; ADMA: asymmetric dimethylarginine; NAD: nicotinamide adenine dinucleotide; NADP: nicotinamide adenine dinucleotide phosphate; NF-κB: nuclear factor kB; PAI: plasminogen activator inhibitor; t-PA: tissue-type plasminogen activator; u-PA: urokinase-type plasminogen activator.

2.3. Cardiovascular Risk and IBD. Chronic inflammatory diseases are associated with accelerated atherosclerosis and increased risk of cardiovascular diseases (CVD) with increased cardiovascular morbidity and mortality compared to the general population [5, 22, 72, 73]. The risk for CVD is controversial in patients with IBD, since different studies highlighted an increased risk for CVD [5, 20, 74, 75], whereas others demonstrated lack of evidence for an increased risk of mortality due to CVD (Table 4) [6, 20, 76, 77]. Ozturk et al. [78] suggested that patients with IBD without classic cardiovascular risk factors have a higher risk for endothelial dysfunction and atherosclerosis. Ciccone et al. demonstrated a strong correlation among body mass index (BMI), inflammation indices, RCP, erythrocyte sedimentation rate (ESR), and physical parameters of endothelial dysfunction, c-IMT, and FMD, in obese children. Because the presence of these factors is strongly related to endothelial function and to the development of atherosclerosis, the authors themselves stated that atherosclerosis could begin very early in life, during childhood, and the same author showed that the worsening of endothelial function was related to age [79]. IBD in active phase was related to enhanced risks of worse CVD outcome; on the other hand, no risk increase was found in remission compared to the control group in a large number of studies [5, 80]. Inflammatory mediators, such as RCP, TNF-α, IL-6, IL-18, and CD40L, are involved in the pathogenesis of inflammation and atherosclerosis [81, 82]. Endothelial dysfunction represents a very important pathogenetic key step in the initiation and maintenance of atherosclerosis in the general population and may be a marker for a future risk of cardiovascular events [74]. Inflammatory process underlies endothelial dysfunction and atherosclerosis pathogenesis; therefore, mechanisms linking systemic inflammatory

Table 3: Most popular parameters for diagnosis of endothelium dysfunction.

Biochemical parameters
Intercellular adhesion molecule-1 (CAM-1)
Selectins P and E
Vascular adhesion molecule-1 (VCAM-1)
Vascular endothelial growth factor (VEGF)
von Willebrand factor (vWF)
Tissue plasminogen activator (t-PA)
Thrombomodulin
Plasminogen activator inhibitor (PAI-1)
Asymmetric dimethylarginine (ADMA)
Disintegrin and metalloproteinase with thrombospondin motif-13 (ADAMTS13)
Angiopoietin-1
Angiopoietin-2
Physical parameters
Flow-mediated dilatation (FMD)
Carotid intima-media thickness (c-IMT)
Pulse wave velocity (PWV)
Pulse arterial tonometry (PAT)

Table 4: Association between cardiovascular diseases and inflammatory bowel diseases.

Authors (year)	Association	Ref.
Yarur et al. (2011)	Yes	[5]
Ciccone et al. (2015)		[60]
Rungoe et al. (2013)		[75]
Fumery et al. (2014)		[88]
Singh et al. (2014)		[89]
Dorn et al. (2007)	No	[6]
Jess et al. (2007)		[76]
Bewtra et al. (2013)		[77]
Ruisi et al. (2015)		[122]

diseases and atherosclerosis may be better understood with the analysis of the endothelium. Multiple factors, including circulating inflammatory cytokines, TNF-α, ROS, oxidized low-density lipoprotein (LDL), and traditional risk factors, activate, directly and indirectly, endothelial cells leading to impaired vascular relaxation, increased leukocyte adhesion, increased endothelial permeability, and generation of a prothrombotic state. The presence of endothelial dysfunction has been further considered in active phases of the diseases. However, this observation has been reached by comparing the active phase of the diseases to the control group. There is no certain data about a direct comparison of active and remission phases of the diseases [80], though IBD implies an increased cardiovascular risk [60, 83, 84] and the entity of the risk directly correlates with disease activity in a lot of studies. In these studies, the induction of the remission is able to reverse endothelial dysfunction in IBD, achieving a level similar to non-IBD subjects. This evidence allows to hypothesize that an adequate medical management of IBD may be able to reverse the increased cardiovascular risk characterizing active disease [85, 86, 87]. Adequate disease management would therefore be important already in childhood; as shown by Ciccone et al., atherosclerosis is a process that can begin in childhood; we should always try to manage patients with IBD well to keep the level of these atherosclerotic factors as always low, because several studies demonstrated presence of a lot of atherosclerotic markers in children affected by IBD [79].

Several studies have demonstrated an increased risk of cardiovascular disease in patients with IBD; however, regarding mortality risk, the evidences are less clear. Kristensen et al. [85] did not find an increased risk for CVD in patients with IBD without classic CVD risk factors after a 2-year follow-up. Singh et al. [88], in a meta-analysis of about 33 observational studies, showed a higher risk for ischemic heart disease and arterial thromboembolism in patients with IBD, but the increased risk for cardiovascular mortality was not observed. Fumery et al. [89], in a meta-analysis of 9 studies, demonstrated that patients with IBD had a significant increase in the risk of cardiovascular morbidity, particularly in women; however, in this paper, the mortality was not addressed. Kristensen et al. [85], in a cohort study, demonstrated an increased risk of myocardial infarction in patients with IBD during the active phase, whereas no risk was observed in remission. Dorn et al. [6], in a 2007 meta-analysis of 11 studies, failed to demonstrate an increased risk of cardiovascular mortality in patients with IBD. Consequently, they concluded that IBD was not associated with a higher incidence of cardiovascular disease. This last cited meta-analysis had numerous drawbacks [6, 41]. It is important to emphasize that some patients with CD are tobacco smokers; indeed, tobacco may also contribute to worsen endothelial damage [90]. These findings indicate that prospective studies are needed to determine the actual risks for CVD in patients with IBD.

2.4. Therapy: Pharmacological and Nonpharmacological Targets. IBD development consists of active and remission periods, and the aim of the therapy is to suppress the active phases. The endothelial dysfunction that underlies the increased cardiovascular risk in these patients is sustained by inflammation and oxidative stress. Therefore, the reduction of these two factors is associated with a reduction of endothelial dysfunction. In chronic inflammatory diseases, there are two types of treatments that can reduce the mediators of inflammation and oxidative stress. The first one is the classical drug therapy that is used to reduce the inflammation associated with the disease. Another therapy, widely used in clinical practice in patients with IBD, is anti TNF-α therapy, infliximab, or biosimilars. TNF-α is a very important cytokine in IBD, whose overexpression appears to be a common element in IBD pathogenesis. TNF-α is a cytokine involved in the pathogenesis and progression of atherosclerosis [91]. This cytokine seems to have a key role, as previously described, in endothelial dysfunction; indeed, intravascular administration of recombinant TNF-α, in both humans and experimental animals, leads to a reduction in endothelium-

dependent relaxation in vitro and in vivo [25, 92]. Some authors showed that treatment with infliximab, in rheumatoid arthritis, improves endothelial dysfunction since it improves FMD, even if all the treatments used for rheumatoid arthritis tend to improve FMD. Therefore, further studies are needed to better understand the best therapy to be used in order to reduce endothelial dysfunction among these patients [93]. Mäki-Petäjä et al. [8] demonstrated that anti-TNF-α therapy ameliorated aortic stiffness, evaluated by PWV, compared to healthy subjects in patients with rheumatoid arthritis. With respect to IBD, there is a lack of data in literature about the effects of anti-TNF-α and CVD in IBD patients and about endothelial dysfunction and the role of anti-TNF-α regarding this field. Schinzari et al. [25] demonstrated that endothelial dysfunction is beneficially affected by intravascular TNF-α neutralization in patients with CD. Danese et al. [94] reported that anti-TNF-α can reduce thrombus formation and adhesion to the endothelium by interfering with the CD40/CD40L pathway.

The second treatment is a nonpharmacological therapeutic approach, because it is based on substances with antioxidant properties among which there are natural and synthetic antioxidants. Several authors have reported the involvement of oxidative stress in the pathogenesis of IBD and consequently the presence of ROS, such as anion peroxide and hydrogen peroxide, into the mucosa of patients with IBD and in experimental colitis models. Oxidative stress also underlies endothelial dysfunction, as previously mentioned; for this reason, it can be deduced that by reducing endothelial dysfunction through the use of antioxidants, it should also improve.

Natural antioxidants contain a wide variety of compounds, mainly phenol and polyphenols, flavonoids, carotenoids, steroids, and thiol. They can prevent cell vascular damage, thus reducing the risk of chronic diseases [48, 95]. Among the natural antioxidant compounds studied in the prevention of vascular damage are vitamin E, vitamin C, goji berries, thymus extracts, rosemary, green tea, and garlic, as reported in Table 5. Vitamin E prevents ROS overproduction, improving the release of prostacyclin, a powerful vasodilator and inhibitor of platelet aggregation. Vitamin E supplementation has been proposed in the diet in order to reduce cardiovascular risk [48, 96, 97]. Vitamin C prevents damage from lipid peroxidation by free oxygen radicals [48, 98–100]. Goji berries increase endogenous antioxidant power; they are able to increase the activity of antioxidant enzymes such as superoxide dismutase (SOD), catalase (CAT), and glutathione peroxidase (GSH-Px) [48, 101, 102]. Some authors have reported that the treatment with SOD, an enzyme that converts the superoxide anion into hydrogen peroxide, has a healthy effect in both the prevention of experimental colitis and its treatment [103, 104]. Seguí et al. [105, 106] demonstrated that treatment with SOD, in a model of experimental colitis, improved the severity of intestinal damage from both a macroscopic and a microscopic point of view. Seguí et al. demonstrated that SOD induced a reduction in the expression of adhesion molecules, such as VCAM-1, ICAM-1, and MAdCAM-1, and therefore as a consequence, the recruitment of leukocytes at the site of inflammation. Thymus extracts have a free radical scavenging activity [107, 108]. Green tea has an anti-inflammatory activity, reducing both the expression of both cyclooxygenases, the constituent one (COX-1) and the inducible one (COX-2), and the quantity of ROS thanks to the action of flavonoids such as epigallocatechin gallate and gallic acid contained in green tea [109, 110]. Garlic increases NO, SOD, and GSH-Px activity and has an anti-inflammatory activity by reducing TNF-α expression [48, 111]. Synthetic antioxidants are N-acetyl-cysteine and propionyl-L-carnitine. N-Acetyl-cysteine is the intracellular precursor of glutathione, a substance with an excellent antioxidant activity furthermore minimizing oxidative stress in both endothelial cells and smooth muscle cells [112]. Sasaki et al. [113] showed that treatment with N-acetyl-L-cysteine or with pyrrolidine dithiocarbamate reduced TNF-α-induced MADCAM-1 expression. Propionyl-L-carnitine is an L-carnitine ester required in the transport of fatty acids for the production of β oxidation and adenosine triphosphate [114]. It has been proven to be a scavenger of superoxide, thus reducing oxidation stress in endothelial cells; indeed, Stasi et al. [115] demonstrated that propionyl-L-carnitine counteracted the increase of oxidative stress in the intestinal microvasculature of patients with UC. It also prevents NO decrease and therefore favors vasodilation, counteracting endothelial dysfunction, and it reduces NOX and ICAM-1 expression in experimental ischemia in rabbit limbs [115].

In literature, there are a large number of studies concerning the use of natural antioxidants in IBD, especially in animal models, which show how these substances with antioxidant properties can improve bowel damage both macroscopically and microscopically. In this regard, D'Argenio et al. [116] demonstrated the healthy effect of apple polyphenol extract in trinitrobenzensulphonic acid-induced colitis, an efficacy mediated by its effects on COX-2 and TNF-α. Binion et al. [117] demonstrated that curcumin reduced VCAM-1 expression. Zhang et al. demonstrated that α-lipoic

Table 5: Natural antioxidant compounds for prevention of vascular damage.

Author (year)	Compound	Ref
Bielli et al. (2015)	Vitamin E	[48]
Tran et al. (1990)		[96]
Brigelius-Flohé et al. (2013)		[97]
Bielli et al. (2015)	Vitamin C	[48]
Armour et al. (2001)		[98]
May et al. (2013)		[99]
Heitzer et al. (1996)		[100]
Bielli et al. (2015)	Goji berries	[48]
Amagase et al. (2009)		[101]
Li et al. (2007)		[102]
Martins et al. (2015)	Thymus extracts	[107]
Nickavar et al. (2012)		[108]
Bielli et al. (2015)	Rosemary	[48]
Murase et al. (2006)	Green tea	[109]
Lu et al. (2012)		[110]
Bielli et al. (2015)	Garlic	[48]
Kim et al. (2001)		[111]

acid, sulfhydryl compound, found in all plant and animal species, inhibits VCAM-1 expression by suppressing NF-κB in human aortic endothelial cells. Sakthivel et al. [118] demonstrated the healthy effect of amentoflavone, which is a bioflavonoid active ingredient of the plant *Biophytum sensitivum* and of other plants, in an experimental colitis model since it inhibits iNOS and COX-2 expression [119].

3. Conclusions

A higher prevalence of classic cardiovascular risk factors is usually associated with a higher risk of cardiovascular events. However, this consideration cannot be applied to patients with IBD. Although patients with IBD have a lower prevalence of classic cardiovascular risk factors than in the general population, they have an increased risk of CVD. In patients with IBD, body mass index, lipid levels, diabetes, obesity, and hypertension are lower than in the general population [1, 4, 5, 120, 121]. In patients with IBD, there is an endothelial dysfunction that causes an increased arterial stiffness. There are no standardized therapies, and many studies in the literature evaluate how, reducing the endothelial dysfunction in patients with IBD, cardiovascular risk can be reduced. Endothelial dysfunction has inflammation and oxidative stress as its genesis. The effects of different therapies aimed at reducing these endothelial dysfunction mediators are not well known. Anti-TNF-α therapy appears to be associated with improvements in both endothelial function and arterial stiffness; however, further studies are needed to determine whether the improvements in arterial stiffness and endothelial function are associated with a decreased risk of cardiovascular events in subjects with IBD. With respect to natural or synthetic antioxidant substances, a large number of studies evaluate the effect on cardiovascular health. Furthermore, these studies demonstrate that vitamin E, vitamin C, goji berries, thymus extracts, rosemary, green tea, and garlic have a healthy effect on oxidative stress and inflammation, reducing them. Other substances, similar to antioxidants, were described, especially in models of experimental colitis, to be very effective in reducing macroscopic and microscopic damage, oxidative stress, and the most important mediators of inflammation. Consequently, we can suppose that in patients with IBD, these substances could be used as an adjunct to the traditional therapy, not only to improve the outcome of IBD but also to reduce cardiovascular risk. Further studies are needed to demonstrate the role of these substances.

Conflicts of Interest

All authors declare no conflicts of interest for this publication.

References

[1] L. Zanoli, S. Rastelli, G. Inserra, and P. Castellino, "Arterial structure and function in inflammatory bowel disease," *World Journal of Gastroenterology*, vol. 21, no. 40, pp. 11304–11311, 2015.

[2] T. Tian, Z. Wang, and J. Zhang, "Pathomechanisms of oxidative stress in inflammatory bowel disease and potential antioxidant therapies," *Oxidative Medicine and Cellular Longevity*, vol. 2017, 18 pages, 2017.

[3] D. Corridoni, K. O. Arseneau, and F. Cominelli, "Inflammatory bowel disease," *Immunology Letters*, vol. 161, no. 2, pp. 231–235, 2014.

[4] E. Levy, Y. Rizwan, L. Thibault et al., "Altered lipid profile, lipoprotein composition, and oxidant and antioxidant status in pediatric Crohn disease," *The American Journal of Clinical Nutrition*, vol. 71, no. 3, pp. 807–815, 2000.

[5] A. J. Yarur, A. R. Deshpande, D. M. Pechman, L. Tamariz, M. T. Abreu, and D. A. Sussman, "Inflammatory bowel disease is associated with an increased incidence of cardiovascular events," *The American Journal of Gastroenterology*, vol. 106, no. 4, pp. 741–747, 2011.

[6] S. D. Dorn and R. S. Sandler, "Inflammatory bowel disease is not a risk factor for cardiovascular disease mortality: results from a systematic review and meta-analysis," *The American Journal of Gastroenterology*, vol. 102, no. 3, pp. 662–667, 2007.

[7] A. D. Booth, S. Wallace, C. M. McEniery et al., "Inflammation and arterial stiffness in systemic vasculitis: a model of vascular inflammation," *Arthritis and Rheumatism*, vol. 50, no. 2, pp. 581–588, 2004.

[8] K. M. Mäki-Petäjä, F. C. Hall, A. D. Booth et al., "Rheumatoid arthritis is associated with increased aortic pulsewave velocity, which is reduced by anti-tumor necrosis factor-alpha therapy," *Circulation*, vol. 114, no. 11, pp. 1185–1192, 2006.

[9] M. J. Roman, R. B. Devereux, J. E. Schwartz et al., "Arterial stiffness in chronic inflammatory diseases," *Hypertension*, vol. 46, no. 1, pp. 194–199, 2005.

[10] G. Mancia, R. Fagard, K. Narkiewicz et al., "2013 Practice guidelines for the management of arterial hypertension of the European Society of Hypertension (ESH) and the European Society of Cardiology (ESC)," *Journal of Hypertension*, vol. 31, no. 10, pp. 1925–1938, 2013.

[11] S. Laurent, J. Cockcroft, L. Van Bortel et al., "Expert consensus document on arterial stiffness: methodological issues and clinical applications," *European Heart Journal*, vol. 27, no. 21, pp. 2588–2605, 2006.

[12] P. Pietri, G. Vyssoulis, C. Vlachopoulos et al., "Relationship between low-grade inflammation and arterial stiffness in patients with essential hypertension," *Journal of Hypertension*, vol. 24, no. 11, pp. 2231–2238, 2006.

[13] Y. Yasmin, C. McEniery, S. Wallace, I. Mackenzie, J. Cockcroft, and I. Wilkinson, "C-reactive protein is associated with arterial stiffness in apparently healthy individuals," *Arteriosclerosis, Thrombosis, and Vascular Biology*, vol. 24, no. 5, pp. 969–974, 2004.

[14] S. McDonnell, M. Morgan, and C. Lynch, "Role of matrix metalloproteinases in normal and disease processes," *Biochemical Society Transactions*, vol. 27, no. 4, pp. 734–740, 1999.

[15] L. Zanoli, M. Cannavò, S. Rastelli et al., "Arterial stiffness is increased in patients with inflammatory bowel disease," *Journal of Hypertension*, vol. 30, no. 9, pp. 1775–1781, 2012.

[16] R. A. Akdoğan, M. E. Durakoğlugil, S. A. Kocaman et al., "Increased pulse wave velocity and carotid intima-media thickness in patients with ulcerative colitis," *Digestive Diseases and Sciences*, vol. 58, no. 8, pp. 2293–2300, 2013.

[17] H. Korkmaz, F. Sahin, S. H. Ipekci, T. Temel, and L. Kebapcilar, "Increased pulse wave velocity and relationship with inflammation, insulin, and insulin resistance in inflammatory bowel disease," *European Journal of Gastroenterology & Hepatology*, vol. 26, no. 7, pp. 725–732, 2014.

[18] E. Aytac, D. Buyuktas, B. Baysal et al., "Visual evoked potentials and pulse wave velocity in inflammatory bowel disease," *The Turkish Journal of Gastroenterology*, vol. 26, no. 1, pp. 15–19, 2015.

[19] L. Zanoli, S. Rastelli, G. Inserra et al., "Increased arterial stiffness in inflammatory bowel diseases is dependent upon inflammation and reduced by immunomodulatory drugs," *Atherosclerosis*, vol. 234, no. 2, pp. 346–351, 2014.

[20] D. Cibor, R. Domagala-Rodacka, T. Rodacki, A. Jurczyszyn, T. Mach, and D. Owczarek, "Endothelial dysfunction in inflammatory bowel diseases: pathogenesis, assessment and implications," *World Journal of Gastroenterology*, vol. 22, no. 3, pp. 1067–1077, 2016.

[21] J. Deanfield, A. Donald, C. Ferri et al., "Endothelial function and dysfunction. Part I: methodological issues for assessment in the different vascular beds," *Journal of Hypertension*, vol. 23, no. 1, pp. 7–17, 2005.

[22] C. Steyers III and F. Miller Jr, "Endothelial dysfunction in chronic inflammatory diseases," *International Journal of Molecular Sciences*, vol. 15, no. 7, pp. 11324–11349, 2014.

[23] M. M. Ciccone, E. Bilianou, A. Balbarini et al., "Task force on," *Journal of Cardiovascular Medicine*, vol. 14, no. 10, pp. 757–766, 2013.

[24] A. Lerman and A. M. Zeiher, "Endothelial function: cardiac events," *Circulation*, vol. 111, no. 3, pp. 363–368, 2005.

[25] F. Schinzari, A. Armuzzi, B. De Pascalis et al., "Tumor necrosis factor-α antagonism improves endothelial dysfunction in patients with Crohn's disease," *Clinical Pharmacology & Therapeutics*, vol. 83, no. 1, pp. 70–76, 2007.

[26] A. Garolla, R. D'Incà, D. Checchin et al., "Reduced endothelial progenitor cell number and function in inflammatory bowel disease: a possible link to the pathogenesis," *The American Journal of Gastroenterology*, vol. 104, no. 10, pp. 2500–2507, 2009.

[27] F. Scaldaferri, S. Lancellotti, M. Pizzoferrato, and R. De Cristofaro, "Haemostatic system in inflammatory bowel diseases: new players in gut inflammation," *World Journal of Gastroenterology*, vol. 17, no. 5, pp. 594–608, 2011.

[28] L. Deban, C. Correale, S. Vetrano, A. Malesci, and S. Danese, "Multiple pathogenic roles of microvasculature in inflammatory bowel disease: a jack of all trades," *The American Journal of Pathology*, vol. 172, no. 6, pp. 1457–1466, 2008.

[29] I. F. Charo and R. M. Ransohoff, "The many roles of chemokines and chemokine receptors in inflammation," *The New England Journal of Medicine*, vol. 354, no. 6, pp. 610–621, 2006.

[30] S. D'Alessio, C. Tacconi, C. Fiocchi, and S. Danese, "Advances in therapeutic interventions targeting the vascular and lymphatic endothelium in inflammatory bowel disease," *Current Opinion in Gastroenterology*, vol. 29, no. 6, pp. 608–613, 2013.

[31] O. A. Hatoum, H. Miura, and D. G. Binion, "The vascular contribution in the pathogenesis of inflammatory bowel disease," *American Journal of Physiology. Heart and Circulatory Physiology*, vol. 285, no. 5, pp. H1791–H1796, 2003.

[32] S. Danese, S. Semeraro, M. Marini et al., "Adhesion molecules in inflammatory bowel disease: therapeutic implications for gut inflammation," *Digestive and Liver Disease*, vol. 37, no. 11, pp. 811–818, 2005.

[33] S. Danese, "Role of the vascular and lymphatic endothelium in the pathogenesis of inflammatory bowel disease: 'brothers in arms'," *Gut*, vol. 60, no. 7, pp. 998–1008, 2011.

[34] M. Briskin, D. Winsor-Hines, A. Shyjan et al., "Human mucosal addressin cell adhesion molecule-1 is preferentially expressed in intestinal tract and associated lymphoid tissue," *The American Journal of Pathology*, vol. 151, no. 1, pp. 97–110, 1997.

[35] V. Lelio Burgio, S. Fais, M. Boirivant, A. Perrone, and F. Pallone, "Peripheral monocyte and naive T-cell recruitment and activation in Crohn's disease," *Gastroenterology*, vol. 109, no. 4, pp. 1029–1038, 1995.

[36] W. E. Cromer, J. M. Mathis, D. N. Granger, G. V. Chaitanya, and J. S. Alexander, "Role of the endothelium in inflammatory bowel diseases," *World Journal of Gastroenterology*, vol. 17, no. 5, pp. 578–593, 2011.

[37] C. H. Wang, S. H. Li, R. D. Weisel et al., "C-reactive protein upregulates angiotensin type 1 receptors in vascular smooth muscle," *Circulation*, vol. 107, no. 13, pp. 1783–1790, 2003.

[38] V. Pasceri, J. T. Willerson, and E. T. H. Yeh, "Direct proinflammatory effect of C-reactive protein on human endothelial cells," *Circulation*, vol. 102, no. 18, pp. 2165–2168, 2000.

[39] S. K. Venugopal, S. Devaraj, and I. Jialal, "Macrophage conditioned medium induces the expression of C-reactive protein in human aortic endothelial cells," *The American Journal of Pathology*, vol. 166, no. 4, pp. 1265–1271, 2005.

[40] B. R. Clapp, G. M. Hirschfield, C. Storry et al., "Inflammation and endothelial function: direct vascular effects of human C-reactive protein on nitric oxide bioavailability," *Circulation*, vol. 111, no. 12, pp. 1530–1536, 2005.

[41] I. Roifman, Y. C. Sun, J. P. Fedwick et al., "Evidence of endothelial dysfunction in patients with inflammatory bowel disease," *Clinical Gastroenterology and Hepatology*, vol. 7, no. 2, pp. 175–182, 2009.

[42] S. Danese, F. Scaldaferri, S. Vetrano et al., "Critical role of the CD40 CD40-ligand pathway in regulating mucosal inflammation-driven angiogenesis in inflammatory bowel disease," *Gut*, vol. 56, no. 9, pp. 1248–1256, 2007.

[43] Y. H. Liu, Y. Ding, C. C. Gao, L. S. Li, Y. X. Wang, and J. D. Xu, "Functional macrophages and gastrointestinal disorders," *World Journal of Gastroenterology*, vol. 24, no. 11, pp. 1181–1195, 2018.

[44] I. Kullo, J. Seward, K. Bailey et al., "C-reactive protein is related to arterial wave reflection and stiffness in asymptomatic subjects from the community," *American Journal of Hypertension*, vol. 18, no. 8, pp. 1123–1129, 2005.

[45] J. A. Vita, J. F. Keaney Jr, M. G. Larson et al., "Brachial artery vasodilator function and systemic inflammation in the Framingham Offspring Study," *Circulation*, vol. 110, no. 23, pp. 3604–3609, 2004.

[46] J. Floege and M. Ketteler, "Vascular calcification in patients with endstage renal disease," *Nephrology, Dialysis, Transplantation*, vol. 19, Supplement_5, pp. V59–v66, 2004.

[47] I. E. Koutroubakis, G. Tsiolakidou, K. Karmiris, and E. A. Kouroumalis, "Role of angiogenesis in inflammatory bowel

disease," *Inflammatory Bowel Diseases*, vol. 12, no. 6, pp. 515–523, 2006.

[48] A. Bielli, M. G. Scioli, D. Mazzaglia, E. Doldo, and A. Orlandi, "Antioxidants and vascular health," *Life Sciences*, vol. 143, pp. 209–216, 2015.

[49] S. Horowitz, D. G. Binion, V. M. Nelson et al., "Increased arginase activity and endothelial dysfunction in human inflammatory bowel disease," *American Journal of Physiology-Gastrointestinal and Liver Physiology*, vol. 292, no. 5, pp. G1323–G1336, 2007.

[50] F. Magro, J. B. Soares, and D. Fernandes, "Venous thrombosis and prothrombotic factors in inflammatory bowel disease," *World Journal of Gastroenterology*, vol. 20, no. 17, pp. 4857–4872, 2014.

[51] L. Sibal, S. C Agarwal, P. D Home, and R. H Boger, "The role of asymmetric dimethylarginine [ADMA] in endothelial dysfunction and cardiovascular disease," *Current Cardiology Reviews*, vol. 6, no. 2, pp. 82–90, 2010.

[52] R. H. Boger, R. Maas, F. Schulze, and E. Schwedhelm, "Asymmetric dimethylarginine [ADMA] as a prospective marker of cardiovascular disease and mortality–an update on patient populations with a wide range of cardiovascular risk," *Pharmacological Research*, vol. 60, no. 6, pp. 481–487, 2009.

[53] P. Kleinbongard, G. Heusch, and R. Schulz, "TNFalpha in atherosclerosis, myocardial ischemia/reperfusion and heart failure," *Pharmacology & Therapeutics*, vol. 127, no. 3, pp. 295–314, 2010.

[54] A. Picchi, X. Gao, S. Belmadani et al., "Tumor necrosis factor-alpha induces endothelial dysfunction in the prediabetic metabolic syndrome," *Circulation Research*, vol. 99, no. 1, pp. 69–77, 2006.

[55] L. Kalinowski and T. Malinski, "Endothelial NADH/NADPH-dependent enzymatic sources of superoxide production: relationship to endothelial dysfunction," *Acta Biochimica Polonica*, vol. 51, no. 2, pp. 459–469, 2004.

[56] S. Kundu, P. Ghosh, S. Datta, A. Ghosh, S. Chattopadhyay, and M. Chatterjee, "Oxidative stress as a potential biomarker for determining disease activity in patients with rheumatoid arthritis," *Free Radical Research*, vol. 46, no. 12, pp. 1482–1489, 2012.

[57] M. S. Wolin, "Interactions of oxidants with vascular signaling systems," *Arteriosclerosis, Thrombosis, and Vascular Biology*, vol. 20, no. 6, pp. 1430–1442, 2000.

[58] M. Biniecka, A. Kennedy, C. T. Ng et al., "Successful tumour necrosis factor [TNF] blocking therapy suppresses oxidative stress and hypoxia-induced mitochondrial mutagenesis in inflammatory arthritis," *Arthritis Research & Therapy*, vol. 13, no. 4, p. R121, 2011.

[59] S. Lancellotti, V. De Filippis, N. Pozzi et al., "Formation of methionine sulfoxide by peroxynitrite at position 1606 of von Willebrand factor inhibits its cleavage by ADAMTS-13: a new prothrombotic mechanism in diseases associated with oxidative stress," *Free Radical Biology & Medicine*, vol. 48, no. 3, pp. 446–456, 2010.

[60] M. M. Ciccone, M. Principi, E. Ierardi et al., "Inflammatory bowel disease, liver diseases and endothelial function: is there a linkage?," *Journal of Cardiovascular Medicine*, vol. 16, no. 1, pp. 11–21, 2015.

[61] P. Desreumaux, G. Huet, F. Zerimech et al., "Acute inflammatory intestinal vascular lesions and in situ abnormalities of the plasminogen activation system in Crohn's disease," *European Journal of Gastroenterology & Hepatology*, vol. 11, no. 10, pp. 1113–1120, 1999.

[62] M. Principi, M. Mastrolonardo, P. Scicchitano et al., "Endothelial function and cardiovascular risk in active inflammatory bowel diseases," *Journal of Crohn's and Colitis*, vol. 7, no. 10, pp. e427–e433, 2013.

[63] E. Theocharidou, T. D. Gossios, T. Griva et al., "Is there an association between inflammatory bowel diseases and carotid intima-media thickness? Preliminary data," *Angiology*, vol. 65, no. 6, pp. 543–550, 2013.

[64] S. I. van Leuven, R. Hezemans, J. H. Levels et al., "Enhanced atherogenesis and altered high density lipoprotein in patients with Crohn's disease," *Journal of Lipid Research*, vol. 48, no. 12, pp. 2640–2646, 2007.

[65] A. Papa, A. Santoliquido, S. Danese et al., "Increased carotid intima–media thickness in patients with inflammatory bowel disease," *Alimentary Pharmacology & Therapeutics*, vol. 22, no. 9, pp. 839–846, 2005.

[66] N. Dagli, O. K. Poyrazoglu, A. Ferda Dagli et al., "Is inflammatory bowel disease a risk factor for early atherosclerosis?," *Angiology*, vol. 61, no. 2, pp. 198–204, 2009.

[67] N. Maharshak, Y. Arbel, N. M. Bornstein et al., "Inflammatory bowel disease is not associated with increased intimal media thickening," *The American Journal of Gastroenterology*, vol. 102, no. 5, pp. 1050–1055, 2007.

[68] E. Broide, A. Schopan, M. Zaretsky, N. A. Kimchi, M. Shapiro, and E. Scapa, "Intima media thickness of the common carotid artery is not significantly higher in Crohn's disease patients compared to healthy population," *Digestive Diseases and Sciences*, vol. 56, no. 1, pp. 197–202, 2011.

[69] A. Di Sabatino, R. Ciccocioppo, E. Armellini et al., "Serum bFGF and VEGF correlate respectively with bowel wall thickness and intramural blood flow in Crohn's disease," *Inflammatory Bowel Diseases*, vol. 10, no. 5, pp. 573–577, 2004.

[70] W. B. Song, Y. H. Lv, Z. S. Zhang et al., "Soluble intercellular adhesion molecule-1, D-lactate and diamine oxidase in patients with inflammatory bowel disease," *World Journal of Gastroenterology*, vol. 15, no. 31, pp. 3916–3919, 2009.

[71] F. Magro, F. Araujo, P. Pereira, E. Meireles, M. Diniz-Ribeiro, and F. T. Velosom, "Soluble selectins, sICAM, sVCAM, and angiogenic proteins in different activity groups of patients with inflammatory bowel disease," *Digestive Diseases and Sciences*, vol. 49, no. 7/8, pp. 1265–1274, 2004.

[72] G. Murdaca, B. M. Colombo, P. Cagnati, R. Gulli, F. Spano, and F. Puppo, "Endothelial dysfunction in rheumatic autoimmune diseases," *Atherosclerosis*, vol. 224, no. 2, pp. 309–317, 2012.

[73] C. Prati, C. Demougeot, X. Guillot, M. Godfrin-Valnet, and D. Wendling, "Endothelial dysfunction in joint disease," *Joint, Bone, Spine*, vol. 81, no. 5, pp. 386–391, 2014.

[74] J. Davignon and P. Ganz, "Role of endothelial dysfunction in atherosclerosis," *Circulation*, vol. 109, 23_Supplement_1, pp. III-27–III-32, 2004.

[75] C. Rungoe, S. Basit, M. F. Ranthe, J. Wohlfahrt, E. Langholz, and T. Jess, "Risk of ischaemic heart disease in patients with inflammatory bowel disease: a nationwide Danish cohort study," *Gut*, vol. 62, no. 5, pp. 689–694, 2013.

[76] T. Jess, M. Gamborg, P. Munkholm, and T. I. A. Sørensen, "Overall and causespecific mortality in ulcerative colitis:

meta-analysis of population based inception cohort studies," *The American Journal of Gastroenterology*, vol. 102, no. 3, pp. 609–617, 2007.

[77] M. Bewtra, L. M. Kaiser, T. TenHave, and J. D. Lewis, "Crohn's disease and ulcerative colitis are associated with elevated standardized mortality ratios: a meta-analysis," *Inflammatory Bowel Diseases*, vol. 19, no. 3, pp. 599–613, 2013.

[78] K. Ozturk, A. K. Guler, M. Cakir et al., "Pulse wave velocity, intima media thickness, and flow-mediated dilatation in patients with normotensive normoglycemic inflammatory bowel disease," *Inflammatory Bowel Diseases*, vol. 21, no. 6, pp. 1314–1320, 2015.

[79] M. M. Ciccone, V. Miniello, R. Marchioli et al., "Morphological and functional vascular changes induced by childhood obesity," *European Journal of Cardiovascular Prevention and Rehabilitation*, vol. 18, no. 6, pp. 831–835, 2011.

[80] Z. Caliskan, N. Keles, H. S. Gokturk et al., "Is activation in inflammatory bowel diseases associated with further impairment of coronary microcirculation?," *International Journal of Cardiology*, vol. 223, pp. 176–181, 2016.

[81] O. A. Hatoum and D. G. Binion, "The vasculature and inflammatory bowel disease: contribution to pathogenesis and clinical pathology," *Inflammatory Bowel Diseases*, vol. 11, no. 3, pp. 304–313, 2005.

[82] S. Kaptoge, S. R. K. Seshasai, P. Gao et al., "Inflammatory cytokines and risk of coronary heart disease: new prospective study and updated metaanalysis," *European Heart Journal*, vol. 35, no. 9, pp. 578–589, 2014.

[83] S. Van Doornum, G. McColl, A. Jenkins, D. J. Green, and I. P. Wicks, "Screening for atherosclerosis in patients with rheumatoid arthritis: comparison of two in vivo tests of vascular function," *Arthritis and Rheumatism*, vol. 48, no. 1, pp. 72–80, 2003.

[84] M. M. Ciccone, G. De Pergola, M. T. Porcelli et al., "Increased carotid IMT in overweight and obese women affected by Hashimoto's thyroiditis: an adiposity and autoimmune linkage?," *BMC Cardiovascular Disorders*, vol. 10, no. 1, p. 22, 2010.

[85] S. L. Kristensen, O. Ahlehoff, J. Lindhardsen et al., "Prognosis after first-time myocardial infarction in patients with inflammatory bowel disease according to disease activity: nationwide cohort study," *Circulation Cardiovascular Quality and Outcomes*, vol. 7, no. 6, pp. 857–862, 2014.

[86] M. Principi, L. Montenegro, G. Losurdo et al., "Endothelial function and cardiovascular risk in patients with inflammatory bowel disease in remission phase," *Scandinavian Journal of Gastroenterology*, vol. 51, no. 2, pp. 253–255, 2015.

[87] F. M. Ruemmele, G. Veres, K. L. Kolho et al., "Consensus guidelines of ECCO/ESPGHAN on the medical management of pediatric Crohn's disease," *Journal of Crohn's & Colitis*, vol. 8, no. 10, pp. 1179–1207, 2014.

[88] S. Singh, H. Singh, E. V. Loftus Jr, and D. S. Pardi, "Risk of cerebrovascular accidents and ischemic heart disease in patients with inflammatory bowel disease: a systematic review and meta-analysis," *Clinical Gastroenterology and Hepatology*, vol. 12, no. 3, pp. 382–393.e1, 2014.

[89] M. Fumery, C. Xiaocang, L. Dauchet, C. Gower-Rousseau, L. Peyrin-Biroulet, and J. F. Colombel, "Thromboembolic events and cardiovascular mortality in inflammatory bowel diseases: a meta-analysis of observational studies," *Journal of Crohn's & Colitis*, vol. 8, no. 6, pp. 469–479, 2014.

[90] D. Szpak, A. Grochowalski, R. Chrząszcz, E. Florek, W. Jawień, and A. Undas, "Tobacco smoke exposure and endothelial dysfunction in patients with advanced coronary artery disease," *Polish Archives of Internal Medicine*, vol. 123, no. 9, pp. 474–481, 2013.

[91] M. Ray and M. V. Autieri, "Regulation of pro- and anti-atherogenic cytokines," *Cytokine*, 2017.

[92] P. Wang, Z. F. Ba, and I. H. Chaudry, "Administration of tumor necrosis factor-alpha in vivo depresses endothelium-dependent relaxation," *American Journal of Physiology-Heart and Circulatory Physiology*, vol. 266, no. 6, pp. H2535–H2541, 1994.

[93] K. Kotani, M. Miyamoto, and H. Ando, "The effect of treatments for rheumatoid arthritis on endothelial dysfunction evaluated by flow-mediated vasodilation in patients with rheumatoid arthritis," *Current Vascular Pharmacology*, vol. 15, no. 1, pp. 10–18, 2017.

[94] S. Danese, M. Sans, F. Scaldaferri et al., "TNF-alpha blockade down-regulates the CD40/CD40L pathway in the mucosal microcirculation: a novel anti-inflammatory mechanism of infliximab in Crohn's disease," *Journal of Immunology*, vol. 176, no. 4, pp. 2617–2624, 2006.

[95] J. M. Lü, P. H. Lin, Q. Yao, and C. Chen, "Chemical and molecular mechanisms of antioxidants: experimental approaches and model systems," *Journal of Cellular and Molecular Medicine*, vol. 14, no. 4, pp. 840–860, 2009.

[96] K. Tran and A. C. Chan, "R,R,R-α-tocopherol potentiates prostacyclin release in human endothelial cells. Evidence for structural specificity of the tocopherol molecule," *Biochimica et Biophysica Acta (BBA) - Lipids and Lipid Metabolism*, vol. 1043, no. 2, pp. 189–197, 1990.

[97] R. Brigelius-Flohé and M. G. Traber, "Vitamin E: function and metabolism," *The FASEB Journal*, vol. 13, no. 10, pp. 1145–1155, 1999.

[98] J. Armour, K. Tyml, D. Lidington, and J. X. Wilson, "Ascorbate prevents microvascular dysfunction in the skeletal muscle of the septic rat," *Journal of Applied Physiology*, vol. 90, no. 3, pp. 795–803, 2001.

[99] J. M. May and F. E. Harrison, "Role of vitamin C in the function of the vascular endothelium," *Antioxidants & Redox Signaling*, vol. 19, no. 17, pp. 2068–2083, 2013.

[100] T. Heitzer, H. Just, and T. Münzel, "Antioxidant vitamin C improves endothelial dysfunction in chronic smokers," *Circulation*, vol. 94, no. 1, pp. 6–9, 1996.

[101] H. Amagase, B. Sun, and C. Borek, "Lycium barbarum [goji] juice improves in vivo antioxidant biomarkers in serum of healthy adults," *Nutrition Research*, vol. 29, no. 1, pp. 19–25, 2009.

[102] X. M. Li, Y. L. Ma, and X. J. Liu, "Effect of the Lycium barbarum polysaccharides on age-related oxidative stress in aged mice," *Journal of Ethnopharmacology*, vol. 111, no. 3, pp. 504–511, 2007.

[103] A. Keshavarzian, G. Morgan, S. Sedghi, J. H. Gordon, and M. Doria, "Role of reactive oxygen metabolites in experimental colitis," *Gut*, vol. 31, no. 7, pp. 786–790, 1990.

[104] B. Xia, C. S. Deng, D. J. Chen, Y. Zhou, and J. Q. Xiao, "Role of copper zinc superoxide dismutase in the short-term treatment of acetic acid-induced colitis in rats," *Acta Gastroenterologica Latinoamericana*, vol. 26, no. 4, pp. 227–230, 1996.

[105] J. Seguí, F. Gil, M. Gironella et al., "Down-regulation of endothelial adhesion molecules and leukocyte adhesion by treatment with superoxide dismutase is beneficial in chronic immune experimental colitis," *Inflammatory Bowel Diseases*, vol. 11, no. 10, pp. 872–882, 2005.

[106] J. Seguí, M. Gironella, M. Sans et al., "Superoxide dismutase ameliorates TNBS-induced colitis by reducing oxidative stress, adhesion molecule expression, and leukocyte recruitment into the inflamed intestine," *Journal of Leukocyte Biology*, vol. 76, no. 3, pp. 537–544, 2004.

[107] N. Martins, L. Barros, C. Santos-Buelga, S. Silva, M. Henriques, and I. C. F. R. Ferreira, "Decoction, infusion and hydroalcoholic extract of cultivated thyme: antioxidant and antibacterial activities, and phenolic characterisation," *Food Chemistry*, vol. 167, pp. 131–137, 2015.

[108] B. Nickavar and N. Esbati, "Evaluation of the antioxidant capacity and phenolic content of three thymus species," *Journal of Acupuncture and Meridian Studies*, vol. 5, no. 3, pp. 119–125, 2012.

[109] T. Murase, S. Haramizu, A. Shimotoyodome, I. Tokimitsu, and T. Hase, "Green tea extract improves running endurance in mice by stimulating lipid utilization during exercise," *American Journal of Physiology Regulatory, Integrative and Comparative Physiology*, vol. 290, no. 6, pp. R1550–R1556, 2006.

[110] Q.-Y. Lu, Y. Jin, J. T. Mao et al., "Green tea inhibits cycolooxygenase-2 in non-small cell lung cancer cells through the induction of annexin-1," *Biochemical and Biophysical Research Communications*, vol. 427, no. 4, pp. 725–730, 2012.

[111] K. M. Kim, S. B. Chun, M. S. Koo et al., "Differential regulation of NO availability from macrophages and endothelial cells by the garlic component S-allyl cysteine," *Free Radical Biology & Medicine*, vol. 30, no. 7, pp. 747–756, 2001.

[112] S. D. Rodrigues, K. C. França, F. T. Dallin et al., "N-acetylcysteine as a potential strategy to attenuate the oxidative stress induced by uremic serum in the vascular system," *Life Sciences*, vol. 121, pp. 110–116, 2015.

[113] M. Sasaki, D. Ostanin, J. W. Elrod et al., "TNF-α-induced endothelial cell adhesion molecule expression is cytochromeP-450 monooxygenase dependent," *American Journal of Physiology Cell Physiology*, vol. 284, no. 2, pp. C422–C428, 2003.

[114] G. S. Ribas, C. R. Vargas, and M. Wajner, "L-Carnitine supplementation as a potential antioxidant therapy for inherited neurometabolic disorders," *Gene*, vol. 533, no. 2, pp. 469–476, 2014.

[115] M. A. Stasi, M. G. Scioli, G. Arcuri et al., "Propionyl-L-carnitine improves postischemic blood flow recovery and arteriogenetic revascularization and reduces endothelial NADPH-oxidase 4-mediated superoxide production," *Arteriosclerosis, Thrombosis, and Vascular Biology*, vol. 30, no. 3, pp. 426–435, 2010.

[116] G. D'Argenio, G. Mazzone, C. Tuccillo et al., "Apple polyphenols extract (APE) improves colon damage in a rat model of colitis," *Digestive and Liver Disease*, vol. 44, no. 7, pp. 555–562, 2012.

[117] D. G. Binion, J. Heidemann, M. S. Li, V. M. Nelson, M. F. Otterson, and P. Rafiee, "Vascular cell adhesion molecule-1 expression in human intestinal microvascular endothelial cells is regulated by PI 3-kinase/Akt/MAPK/NF-kappaB: inhibitory role of curcumin," *American Journal of Physiology-Gastrointestinal and Liver Physiology*, vol. 297, no. 2, pp. G259–G268, 2009.

[118] W. J. Zhang and B. Frei, "Alpha-lipoic acid inhibits TNF-alpha-induced NF-kappaB activation and adhesion molecule expression in human aortic endothelial cells," *The FASEB Journal*, vol. 15, no. 13, pp. 2423–2432, 2001.

[119] K. M. Sakthivel and C. Guruvayoorappan, "Amentoflavone inhibits iNOS, COX-2 expression and modulates cytokine profile, NF-κB signal transduction pathways in rats with ulcerative colitis," *International Immunopharmacology*, vol. 17, no. 3, pp. 907–916, 2013.

[120] B. J. Geerling, A. Badart-Smook, R. W. Stockbrügger, and R. J. Brummer, "Comprehensive nutritional status in recently diagnosed patients with inflammatory bowel disease compared with population controls," *European Journal of Clinical Nutrition*, vol. 54, no. 6, pp. 514–521, 2000.

[121] J. Jahnsen, J. A. Falch, P. Mowinckel, and E. Aadland, "Body composition in patients with inflammatory bowel disease: a population-based study," *The American Journal of Gastroenterology*, vol. 98, no. 7, pp. 1556–1562, 2003.

[122] P. Ruisi, J. N. Makaryus, M. Ruisi, and A. N. Makaryus, "Inflammatory bowel disease as a risk factor for premature coronary artery disease," *Journal of Clinical Medicine Research*, vol. 7, no. 4, pp. 257–261, 2015.

Hindawi
Oxidative Medicine and Cellular Longevity
Volume 2018, Article ID 5879281, 9 pages
https://doi.org/10.1155/2018/5879281

Research Article

A Typical Immune T/B Subset Profile Characterizes Bicuspid Aortic Valve: In an Old Status?

Carmela R. Balistreri,[1] **Silvio Buffa**,[1] **Alberto Allegra**,[2] **Calogera Pisano**,[3] **Giovanni Ruvolo**,[3] **Giuseppina Colonna-Romano**,[1] **Domenico Lio**,[1] **Giuseppe Mazzesi**,[4] **Sonia Schiavon**,[5] **Ernesto Greco**,[6] **Silvia Palmerio**,[7] **Sebastiano Sciarretta**,[5,7] **Elena Cavarretta**,[5] **Antonino G. M. Marullo**,[5] **and Giacomo Frati**[5,7]

[1]*Department of Pathobiology and Medical Biotechnologies, University of Palermo, Palermo, Italy*
[2]*Unit of Cardiac Surgery, Department of Surgery and Oncology, University of Palermo, Palermo, Italy*
[3]*Department of Experimental Medicine and Surgery, University of Rome "Tor Vergata", Rome, Italy*
[4]*Department of General and Specialist Surgery, University of Rome "Sapienza", 00161 Rome, Italy*
[5]*Department of Medico-Surgical Sciences and Biotechnologies, Sapienza University of Rome, Latina, Italy*
[6]*Department of Cardiovascular, Respiratory, Nephrological, Anesthesiological, and Geriatric Sciences, Sapienza University of Rome, Rome, Italy*
[7]*IRCCS Neuromed, Pozzilli, Italy*

Correspondence should be addressed to Carmela R. Balistreri; carmelarita.balistreri@unipa.it

Received 1 November 2017; Revised 11 December 2017; Accepted 5 February 2018; Published 5 April 2018

Academic Editor: Sid D. Ray

Bicuspid valve disease is associated with the development of thoracic aortic aneurysm. The molecular mechanisms underlying this association still need to be clarified. Here, we evaluated the circulating levels of T and B lymphocyte subsets associated with the development of vascular diseases in patients with bicuspid aortic valve or tricuspid aortic valve with and without thoracic aortic aneurysm. We unveiled that the circulating levels of the MAIT, CD4+IL−17A+, and NKT T cell subsets were significantly reduced in bicuspid valve disease cases, when compared to tricuspid aortic valve cases in either the presence or the absence of thoracic aortic aneurysm. Among patients with tricuspid aortic valve, these cells were higher in those also affected by thoracic aortic aneurysm. Similar data were obtained by examining CD19+ B cells, naïve B cells (IgD+CD27−), memory unswitched B cells (IgD+CD27+), memory switched B cells (IgD−CD27+), and double-negative B cells (DN) (IgD−CD27−). These cells resulted to be lower in subjects with bicuspid valve disease with respect to patients with tricuspid aortic valve. In whole, our data indicate that patients with bicuspid valve disease show a quantitative reduction of T and B lymphocyte cell subsets. Future studies are encouraged to understand the molecular mechanisms underlying this observation and its pathophysiological significance.

1. Introduction

Bicuspid aortic valve disease (BAV) is a relatively frequent congenital disorder, affecting approximately 1.3% of the population worldwide with a male prevalence of 3 : 1 [1]. BAV is associated with an increased incidence of valvular and vascular diseases [1]. BAV is an important risk factor predisposing to the development of thoracic aortic aneurysm (TAA) [1, 2]. The molecular mechanisms underlying the association between BAV and aortic disease still need to be clarified [2].

In recent years, accumulating lines of evidence indicated that an increased inflammation of the aortic wall contributes to the development and progression of aortic aneurysm [3–5]. Inflammatory cytokines and an infiltrate of CD3+ CD4+CD8+CD68+CD20+ cells have been demonstrated to

significantly increase in human aneurysm specimens from patients with Marfan syndrome and familial and sporadic TAA [3–9]. B lymphocytes were also found to infiltrate the wall of aortic aneurysms significantly contributing to their expansion and progression [10]. Significant amounts of immune/inflammatory cells have been also detected by our group in aorta tissues from 24 BAV patients with TAA than control aortas, but with higher levels in individuals with tricuspid aortic valve (TAV) and affected by TAA [11]. However, their phenotypes and their possible differences were not assessed in our study [11]. Accordingly, some experimental studies in animal models have demonstrated that the attenuation of aortic immune/inflammation prevents or delays the progression of aortic aneurysm [3–6]. Pharmacological or genetic depletion of T helper lymphocytes and $\gamma\delta$ T cells, a subset of T cells, was observed to reduce the progression of aortic aneurysms [12–15]. However, at the moment, no literature data do exist about the types of phenotypes of immune/inflammatory cells and their related number differences between patients with BAV and TAV, with and without concomitant TAA.

Therefore, in this study, we evaluated, for the first time, whether BAV subjects have typical signatures in peripheral blood immune cell levels and phenotypes, and particularly in T and B cell subsets, with respect to TAV subjects in the presence or absence of concomitant TAA. On the other hand, the presence of typical molecular, cellular, and genetic profiles in BAV patients with TAA in comparison to TAV with TAA continues to be evidenced in the literature, as amply stressed and demonstrated in our previous studies [9, 11, 16, 17].

2. Subjects and Methods

2.1. BAV and TAV Subjects. Our study included a total of 25 BAV subjects (19 males and 6 females; mean age: 56.7 ± 13.5 years) and 35 TAV subjects (23 males and 12 females, mean age: 66.4 ± 7.1 years). They were randomly selected from patients undergone to surgery replacement or routine care screening in the Unit of Cardiac Surgery (Department of Surgery and Oncology, University of Palermo), by using apposite exclusion criteria for arteriosclerosis or other cardiovascular diseases, connective tissue disorders, and inflammatory diseases (from infections to hematological, gastrointestinal, urogenital, pulmonary, neurological, and endocrinal inflammatory disorders and neoplasia included). They were enrolled from January 2015 to December 2016. Furthermore, we selected BAV and TAV individuals with or without TAA, as a complication, for evaluating appropriate controls for the same groups. In addition, they belonged to the same ethnic group, since their parents and grandparents were born in Western Sicily.

Elective or urgent surgical treatments (using Bentall-De Bono and Tirone David surgical techniques, whenever possible) with complementary tubular-ascending aorta resection were performed in both BAV and TAV patients with TAA after the evaluation of aortic transverse diameter sizes. The evaluation of aorta diameters was done preoperatively as well as in the operating theatre performed by an experienced physician by transesophageal echocardiography (*Philips Ie. 33*) before the institution of the cardiopulmonary bypass. The dimension of the aortic annulus, sinuses of Valsalva, proximal ascending aorta (above 2.5 cm of the sinotubular junction), and aortic arch are assessed and presented in Table 1.

Table 1: Demographic and clinical characteristics, comorbidity conditions, and complications of 25 BAV and 35 TAV subjects with or without TAA.

Variables	BAV $N = 25$	TAV $N = 35$
Demographic characteristics		
Age, mean (SD)	56.7 (13.5)	66.4 (7.1)
Male sex, number (%)	19 (76)	23 (66)
Female sex, number (%)	6 (24)	12 (34)
Body mass index, mean (SD)	26 (4.8)	26.3 (3.2)
Size and location of TAA		
Subjects affected (%)	12 (48)	17 (48)
Size (mm), mean (SD)	53.3 (7.4)	50.3 (6.9)
Location, number (%):		
Tubular ascending aorta	12 (100)	17 (100)
Comorbidity conditions, number (%)		
CVD family history	7 (28)	5 (7.1)
Smoking	6 (24)	7 (20)
Hypertension	18 (72)	25 (71)
Dyslipidemia	3 (12)	5 (14)
Diabetes mellitus	0 (0)	0 (0)
Renal failure	0 (0)	1 (2)
Dissection	0 (0)	0 (0)
Aortic valve pathology, number (%)		
Normal	0 (0)	27 (77)
Prolapse	3 (12)	1 (2)
Vascular calcium fibrosis	7 (28)	7 (20)
Atherosclerosis coronary syndrome, number (%)	0 (0)	0 (0)

Demographic and clinical data, including comorbidities, were obtained from patients' medical records (Table 1). In all BAV and TAV cases, hypertension was treated by using beta-blockers.

Blood samples were collected into EDTA-coated tubes from all individuals enrolled and at the moment of their admission in the Unit of Cardiac Surgery. They were transported to the laboratory and processed within 1 to 2 hours after the collection.

2.2. Ethical Study Approval. Our study was performed in accordance with ethical standards of the Helsinki Declaration of the World Medical Association; it received approval from local ethics committees (number APUNIP0094517), and all participants gave their informed consent. Data were encrypted in order to ensure the patient's privacy. All measurements were performed by physicians in a blind manner.

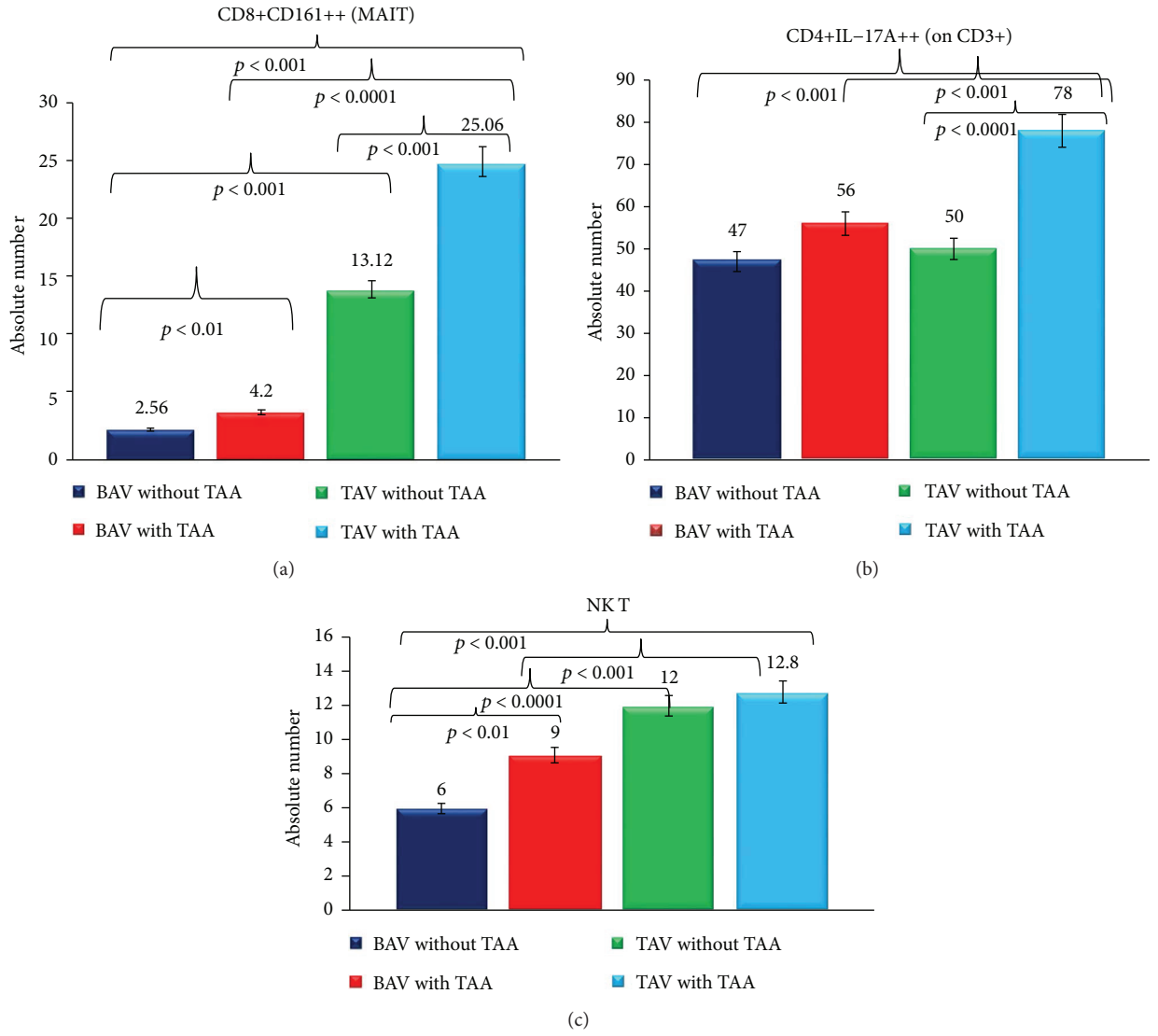

Figure 1: (a–c). Circulating levels of MAIT, CD4+IL−17A+, and NKT cells in the BAV and the TAV groups. Circulating MAIT and CD4+IL −17A+ levels were evaluated in patients with BAV and TAV with or without TAA. They were expressed as the absolute numbers (on CD3+). For the description of data, remand to Results.

2.3. Antibody Panels and Multiparametric Flow Cytometry Analyses for Evaluating Circulating Levels and Phenotypes of T and B Cell Subsets. After separation from the whole blood in EDTA, 100 μl of viable PBMC (*peripheral blood mononuclear cell*) was stained with different combinations of monoclonal antibodies. To characterize the phenotype of T and B cell subsets, extracellular labeling was performed with anti-$CD8_{FITC}$, anti-$CD161_{PE}$, anti-$CD3_{ECD}$, anti-$CD4_{PC5.5}$, anti-$CD16_{FITC}$, anti-$CD56_{PE}$, anti-IgD_{FITC}, anti-$CD27_{PC5.5}$, and anti-$CD19_{ECD}$ (Beckman Coulter, Miami, FL). Living cells were gated within the side/forward scatter (SSC/FSC) lymphocyte gate. For intracellular staining, cells were permeabilized with Cytofix/Citoperm (BD Biosciences). Finally, the cells were stained with anti-IL-$17A_{FITC}$ (MiltenyiBiotec), washed, and analyzed. All measurements were made with a CyAN ADP flow cytometer (Beckman Coulter, Miami, FL, USA) with the same instrument setting. At least 105 lymphocytes were acquired and analyzed using FlowJo (Tree Star) software. Leukocyte count and differential were determined with a routine hematology analyzer. The absolute counts of total lymphocytes were calculated by multiplying the relative size of the T and B cells and the absolute lymphocyte count.

2.4. Statistical Analysis. As reported in Figures 1 and 2, the levels in the absolute number of MAIT, CD4+IL−17A+ and NKT T cells (for T compartment examined), and CD19+ B cells, naïve B cells (IgD+CD27−), memory unswitched B cells (IgD+CD27+), memory switched B cells (IgD−CD27+), and double-negative (DN) B cells (IgD−CD27−) (for B compartment evaluated) were expressed as the mean ± SD. Statistical analyses were performed using SPSS software version 20. Precisely, we used the analysis of variance (ANOVA) test (corrected by Bonferroni), for performing the comparisons among all groups. Unpaired *t*-test (Welch corrected) was utilised to analyze the data between two

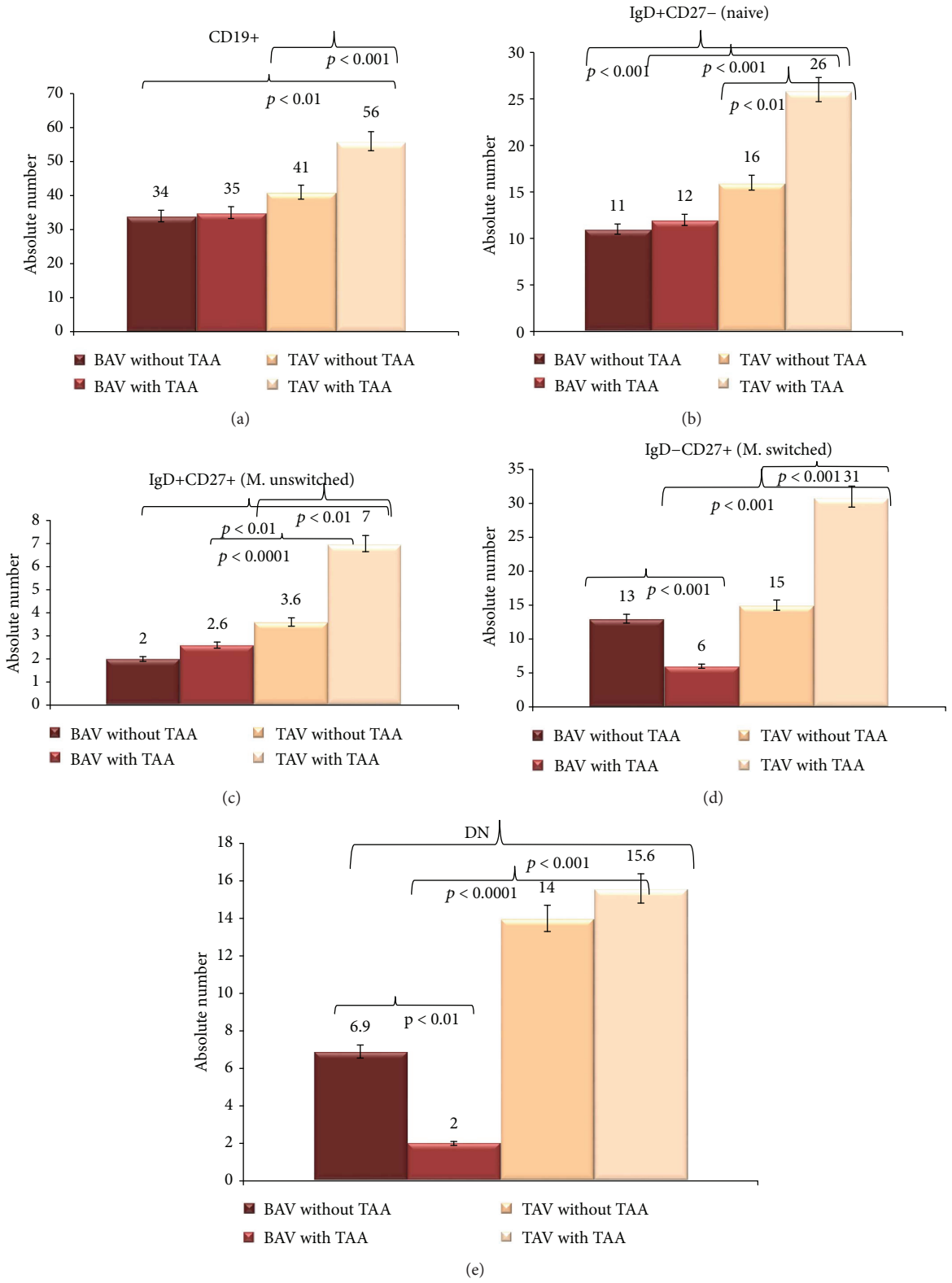

FIGURE 2: Circulating levels of B subsets in the BAV and the TAV groups. Circulating CD19+ B cells (a), naïve B IgD+CD27− cells (b), memory unswitched IgD+CD27+ B cells (c), memory switched B IgD−CD27+ cells (d), and double-negative B cells (e) were evaluated in patients with BAV and TAV with or without TAA. Cells were expressed as the absolute numbers. For the description of data, see Results.

groups. Differences are considered significant when a p value < 0.05 was obtained by a comparison between the different groups.

3. Results

3.1. Patient and Control Characteristics. All BAV and TAV patient features are summarized in Table 1. A significant difference was observed in age between BAV and TAV patients. BAV patients were significantly younger than TAV cases (56.7 ± 13.5 versus 66.4 ± 7.1 years, resp., $p < 0.0001$). No significant differences were evidenced in the number of males and females between the two groups, as well as in the size of aorta dilatation between BAV and TAV cases. Among TAA risk factors, no significant differences were detected. We only observed in BAV cases a not significant prevalence of valvular complications compared to TAV cases.

3.2. Differences in the Circulating Levels of T Subsets in BAV and TAV Cases. We initially compared the circulating levels of Mucosal-associated invariant T (MAIT) cells in BAV versus TAV cases with and without TAA. MAIT cells represent a novel innate-like T cell subsets consisting of 1%–10% of T cells in the peripheral blood [18–20]. They mediate a pivotal role in immune-dysregulated diseases and other pathologies, like infections, inflammatory diseases, and others [18–20]. We observed that the mean blood levels of MAIT cells, expressed in absolute numbers, were significantly different between the BAV and the TAV groups, with and without TAA (see Figure 1(a)). Precisely, the comparisons among the four groups (see Figure 1(a)) demonstrated significant differences ($p < 0.001$, by the ANOVA test corrected by Bonferroni, in all comparisons effectuated), with the lowest blood levels in the BAV groups and more marked in the two TAV groups. A weak, but significant, the difference was assessed between the two BAV groups ($p < 0.01$, by the t-test corrected by Welch). Differently, between the two TAV groups, the mean blood levels of MAIT cells were significantly higher ($p < 0.001$, by the t-test corrected by Welch). Likewise, the comparisons of the mean levels of MAIT cells between BAV and TAV not complicated ($p < 0.001$, by the t-test corrected by Welch) and between BAV and TAV complicated ($p < 0.0001$, by the t-test corrected by Welch) were significantly different (see Figure 1(a)).

Similar results were observed regarding another T cell subset, namely, the CD4+IL−17A+, which has a recognized role in contributing to hypertension, vascular dysfunction, and damage [21–24]. Recent evidence suggests the participation of this T cell subset also in the development of aortic aneurysms [12, 22–24]. Circulating levels of CD4+ IL−17A+, expressed in absolute numbers, were significantly different among the four groups ($p < 0.001$, by the ANOVA test corrected by Bonferroni, in all comparisons effectuated) (see Figure 1(b)). TAA was associated with significantly higher mean CD4+IL−17A+ levels in the TAV group. No difference between BAV and TAV subjects without TAA was assessed. In contrast, mean circulating CD4+IL−17A+ levels resulted to be significantly higher in TAV versus BAV subjects affected by TAA ($p < 0.001$, by the t-test corrected by Welch).

Furthermore, we also examined with regard to the T compartment the circulating levels of NKT cells, since they are involved in the genesis of atherosclerosis, coronary artery diseases, and aneurysms [25]. The comparisons of mean levels expressed in the absolute number of NKT cells among the four groups showed significant differences ($p < 0.001$, by the ANOVA test corrected by Bonferroni, in all comparisons effectuated) (see Figure 1(c)). In addition, the NKT population was markedly represented in TAV cases than BAV cases, in the presence or without TAA ($p < 0.001$ and $p < 0.0001$, by the t-test corrected by Welch, resp.; in particular, they were about the half in BAV versus TAV cases without TAA) (see Figure 1(c)). No differences were detected between the two TAV groups, while significantly higher mean levels of NKT cells were assessed in BAV TAA affected versus BAV subjects not affected ($p < 0.01$, by the t-test corrected by Welch) (see Figure 1(c)).

3.3. Variations in the Circulating Levels of B Cell Populations. As evidenced in Introduction, B cells contribute in the chronic immune/inflammatory pathophysiology of TAA [3–10]. Thus, we also evaluated the mean circulating levels expressed in the absolute number of CD19+ cells, naïve B cells (IgD+CD27−), memory unswitched B cells (IgD+ CD27+), memory switched B cells (IgD−CD27+), and double-negative (DN) B cells (IgD−CD27−; i.e., exhausted memory cells) (see Figures 2(a)–2(e)) in the four groups. Regarding the CD19+ cells, significant differences were observed among the four groups ($p < 0.01$, by the ANOVA test corrected by Bonferroni, in all comparisons effectuated) (see Figure 2(a)). Furthermore, the comparisons detected significantly higher mean levels of the CD19+ cells in the TAV group with TAA versus the TAV group without TAA ($p < 0.001$, by the t-test corrected by Welch). No other differences were observed (see Figure 2(a)). Likewise, the mean blood levels expressed in the absolute number of the IgD+CD27− (naive) B subset were significantly different among the four groups ($p < 0.001$, by the ANOVA test corrected by Bonferroni, in all comparisons effectuated) (see Figure 2(b)). They resulted to be more marked in the BAV and the TAV groups with TAA, with higher mean values in TAV ($p < 0.001$, by the t-test corrected by Welch). Between the two BAV groups, no differences were detected, while higher mean values were assessed in TAV with TAA versus TAV without TAA ($p < 0.01$, by the ANOVA test corrected by Bonferroni, in all comparisons effectuated) (see Figure 2(b)).

Similarly, mean levels expressed in the absolute number of IgD+CD27+ (M. unswitched) B cells (see Figure 2(c)) were moderately different among the four groups ($p < 0.01$, by the ANOVA test corrected by Bonferroni, in all comparisons effectuated). The highest mean values were detected in TAV with TAA, which significantly differed from those in BAV affected by TAA (they were about 3 times in TAA) ($p < 0.0001$, by the t-test corrected by Welch) (see Figure 2(c)).

Interestingly, an opposite trend was observed in the BAV and the TAV groups with respect to IgD−CD27+ (M. switched) B subset levels in patients with and without TAA (see Figure 2(d)). The mean circulating levels of the IgD−CD27+ (M. switched) B subset expressed in the absolute number were more marked in BAV without TAA versus BAV with TAA ($p < 0.001$, by the *t*-test corrected by Welch; in BAV with TAA, the values were about the half of those of BAV with TAA). Significant differences were also detected between the two TAV groups (without versus with TAA, $p < 0.001$, by the *t*-test corrected by Welch) and between BAV and TAV affected by TAA ($p < 0.001$, by the *t*-test corrected by Welch) (see Figure 2(d)).

Finally, the mean circulating levels of DN B cells expressed in the absolute number (see Figure 2(e)) were significantly different among the four groups ($p < 0.001$, by the ANOVA test corrected by Bonferroni, in all comparisons effectuated). However, the lowest values were detected in BAV with TAA, which significantly differed with those of BAV without TAA with $p < 0.01$ (by the *t*-test corrected by Welch) and with those of TAV with TAA ($p < 0.0001$, by the *t*-test corrected by Welch). No differences were observed between the two TAA groups (see Figure 2(e)).

4. Discussion

Our study demonstrates that BAV is associated with a reduction in the circulating levels of some T and B lymphocyte subsets. BAV patients show a significant reduction in a number of all T and B subsets examined, with respect to TAV individuals, with a little trend in the increase (but not significant) in those with TAA (see Figures 1 and 2). Precisely, they have the lowest levels in MAIT and NKT cell subsets. The mean levels of the CD4+IL−17A+ cell subset were similar in the two BAV groups. But they also reflect the pattern of TAV patients without TAA, with the difference that likely in BAV patients they are not able to clonically expand and result as poorly functional, given the trend not in the increase with the TAA complication (see Figure 1(b)). The same results have been also obtained (see Figures 2(a)–2(d)) in all B subsets evaluated, with the exception of the DN B cell subset. These last showed an inverse trend with more pronounced levels in BAV individuals without TAA versus BAV individuals with TAA, but are like those in TAV without TAA (see Figure 2(e)). Differently, TAV individuals with or without TAA showed significant levels of all T and B subsets analyzed, with a significant trend in the increase in those affected by TAA (see Figures 1 and 2). Thus, the data obtained agree upon the results detected from our previous studies on BAV and TAA conditions [9, 11, 16, 17, 26]. Furthermore, they additionally confirm our previous suggestions about the presence in BAV individuals of unique cellular, molecular, and genetic mechanisms associated with TAA onset [11].

Previous studies' evidence indicated that lymphocytes play a significant role in the development and progression of aortic aneurysms. T lymphocyte infiltration is abundant in the aortic aneurysm wall in patients [3–9]. B lymphocytes were also found to infiltrate the wall of aortic aneurysms significantly contributing to their expansion and progression [10]. Significant amounts of T and B immune/inflammatory cells have been also detected by our group in aorta tissues from 24 BAV patients with TAA than control aortas, but with higher levels in individuals with tricuspid aortic valve (TAV) affected by TAA [11]. Animal studies showed that depletion of both T and B lymphocytes delays the progression of the disease [3–6]. Pharmacological or genetic depletion of T helper lymphocytes and $\gamma\delta$ T cells, a subset of T cells, was, indeed, observed to reduce the progression of aortic aneurysms [12–15].

Surprisingly, even though the presence of BAV is associated with a higher incidence of TAA with respect to TAV, our data firstly indicate that this valvular defect is associated with a reduction in the circulating levels of some T and B lymphocyte subsets that usually take part to the chronic immune/inflammatory processes involved in the development of common cardiovascular diseases, such as TAA [6, 10, 18–25]. This data may suggest that the T and B lymphocyte activation is not likely the unique factor, which can contribute to the increased rate of the development of TAA in subjects with BAV. Probably, it might be hypothesized that the potential cause might be a close relationship between BAV itself condition and the compromised T and B compartment. Future studies are encouraged to test this hypothesis and to understand the molecular mechanisms underlying the reduced circulating lymphocyte levels in subjects with BAV. Previous studies have indicated that BAV patients more frequently carry mutations in the *NOTCH1 gene* [27–33]. Moreover, BAV condition presenting together with ascending aortic dilation has been also demonstrated to be significantly associated with other rare variants in the *NOTCH1 gene* [32, 33]. Notch signaling is an important regulator of inflammatory cell maturation and mobilization [27]. Therefore, it is possible that a defect of Notch signaling leads to a deregulation of inflammatory cells in patients with BAV.

5. Conclusions: Our Suggestions and Recommendations

The data obtained indicate that BAV subjects have significantly reduced levels in all T and B subsets examined. They lead us to propose some crucial suggestions, which might lead to new ways to research. They are summarized in Table 2. Firstly, this typical profile in T and B lymphocyte subsets would seem to suggest that BAV individuals may have an appropriate response to chronic tissue damage, and earlier than TAV individuals, that generally develop TAA disease in older ages [17]. Accordingly, this clinical situation seems to reflect what has been observed in older people, as demonstrated in previous studies from our and other groups [34–36]. In other words, the immune system in BAV cases would seem likely to appear as an "*old immune system*" with an altered specific clonotypic component and an increased innate/inflammatory compartment, which is consequently more easily vulnerable to internal and external stressors, frailty, disability, and disease [34–36]. In agreement with this suggestion, very marked levels of

Table 2: Our findings and suggestions.

Findings	Suggestions
BAV subjects showed the lowest levels in MAIT and NKT cell subsets for T compartment examined (see all Figures 1(a)–1(c). Despite this, they surprisingly had mean levels of CD4+IL−17A+ cell subset, which were like those of TAV without TAA. While for the B compartment, the BAV individuals, independent to TAA disease, showed low and similar levels in the two groups (see Figures 2(a)–2(d)) in all B subsets evaluated, with the exception of the DN B cell subset. These last showed an inverse trend with more pronounced levels in BAV without TAA versus BAV individuals with TAA, but are like those in TAV without TAA (see Figure 2(e)).	(1) They would suggest that BAV individuals may have unaltered response to chronic tissue damage and, earlier than TAV individuals, that generally develop TAA disease in older ages [17]. (2) Although, they show a CD4+IL−17A+ cell subset that would seem to be not compromised, but not able probably to clonically expand, or poorly functional. Accordingly, the significantly reduced numbers of T and B lymphocyte subsets from BAV individuals would be likely similar to those observed in older people, as demonstrated in previous studies by our and other groups [33–35]. (3) The immune system in BAV cases would seem likely to appear as an "*old immune system*" with an altered specific clonotypic component and an increased innate/inflammatory compartment, which is consequently more easily vulnerable to internal and external stressors, frailty, disability, and disease [27–29]. In agreement with this suggestion, very marked levels of CD68+ monocyte cells have been observed by our and other groups in aorta specimens from BAV cases with TAA [3–9, 11]. (4) This might likely justify their higher incidence of chronic immune/inflammatory vascular and aortic complications, such as TAA, at younger ages than TAV subjects. (5) A close relationship between BAV itself condition and the compromised T and B lymphocyte compartments would seem to be the cause of this altered T and B profile. Here, we hypothesize that defects in the Notch signaling pathway may be the close link between the deregulated T and B response and the BAV itself condition.
TAV individuals with or without TAA showed very significant levels of all T and B subsets analyzed, with a significant trend in augment in those affected by TAA (see Figures 1 and 2). The data obtained agree the results detected from our previous studies on BAV and TAA conditions.	(1) In BAV individuals, unique cellular, molecular, and genetic mechanisms are associated with TAA onset [11].

CD68+ monocyte cells have been observed by our and other groups in aorta specimens from BAV cases with TAA [3–9, 11]. This might likely justify their higher incidence of chronic immune/inflammatory vascular and aortic complications, such as TAA, at younger ages than TAV subjects.

Furthermore, this altered T and B immune profile in BAV patients, although evaluated only from a quantitative view point, may lead us likely to hypothesize the existence of a close relationship between BAV itself condition and the compromised T and B lymphocyte compartments. Indeed, it might speculate the existence in BAV individuals of alterations in pathways physiologically involved in two processes or in targets that were not exhaustively investigated in our study. In fact, aneurysm formation and progression are the outcomes of a complex process, in which more pathways, like Notch, Toll-like receptor-4, TGF-β, and so on, and their downstream components might play relevant roles, as elegantly stressed in a model proposed in our recent review published in a renowned journal [26]. This could also be the case of some proteases, whose function has been reported to be either protective or worsening depending on the aneurysm's location or with TGF-β signaling, recently demonstrated to be able to activate an autocrine IL-1β pathway acting as a signal recruiting innate immune cells in the adventitia through CCL2IL-1β [37].

In our case, a pathway that mediates these functions is the Notch pathway, characterized by 4 type transmembrane receptors (Notch1–Notch4) in human. In our specific case, our attention is focused on Notch 1. It has been shown to have pleiotropic effects: stem/progenitor cell fate; regulation of the life cycle of adult cells and regulation of multiple steps of T and B cell development in both central and peripheral lymphoid organs; and the development of cardiovascular system and so on, as amply described in our recent review [27]. Furthermore, BAV has been significantly associated with rare but highly penetrant exonal mutations in the *NOTCH1* gene [27–33], and BAV presenting together with ascending aortic dilation has been also demonstrated to be significantly associated with other rare variants in the *NOTCH1 gene* [32, 33]. Accordingly, an impairment of Notch signaling has been also shown to be involved in the development and progression of aortic aneurysm, as elegantly summarized in 2017 by Yassine and co-workers [38] and recently demonstrated by our group in a recent study (data not shown).

Certainly, additional and larger studies are mandatory to confirm these promising findings as well as our suppositions.

The replication of our results from a very large sample size might give the possibility of detecting potential molecular, cellular, and genetic biomarkers to be translated in the daily clinical practice. In turn, they might consent to identify BAV subjects at high risk to develop TAA and to provide an appropriate guidance about their treatments, which might be different from those for TAV subjects with TAA. This could consent us to suggest specific clinical recommendations on the surgical approaches to apply in the case of BAV patients with TAA. The selection of drug therapies and more suitable surgical procedures with or without composite aortic root replacement represents the major object of current cardiovascular studies. Based on our previous and current data, we suggest to go beyond the values of the aorta's diameter and growth rate as the only parameters for the surgical recommendation [39]. The surgical strategy would also consider not only the clinical features but also the molecular, cellular, and genetic profiles of everyone and particularly in the case of BAV condition. It would be interesting to initiate discussion about personalized therapeutic and surgical recommendations, particularly in the case of BAV condition.

Conflicts of Interest

The authors declare to have no conflict interests.

Authors' Contributions

Dr. Carmela R. Balistreri was involved in the conception and design of the study. Drs. Calogera Pisano, Antonino G. M. Marullo, and Giovanni Ruvolo were involved in the enrolment of the study population. Drs. Carmela R. Balistreri, Sonia Schiavon, Silvia Palmerio, and Silvio Buffa conducted the experiments and acquired the data. Drs. Carmela R. Balistreri and Silvio Buffa acquired the results obtained and performed their analyses. Drs. Carmela R. Balistreri, Giuseppina Colonna-Romano, Giacomo Frati, Giuseppe Mazzesi, Giovanni Ruvolo, Elena Cavarretta, and Sebastiano Sciarretta were involved in data interpretation. Drs. Carmela R. Balistreri, Giacomo Frati, Elena Cavarretta, and Sebastiano Sciarretta were also involved in drafting the paper. Dr. Carmela R. Balistreri was involved its critical revision and supervision. All authors participated in the study, and they reviewed and approved the final version of the paper. Drs. Carmela R. Balistreri, Sebastiano Sciarretta, Elena Cavarretta, Antonino G. M. Marullo, and Giacomo Frati equally contributed to this work.

Acknowledgments

The authors gratefully acknowledge Dr. Matteo Bulati, who was involved in acquiring the data. This work was supported by grants from the Italian Ministry of Education, University and Research, to Dr. Carmela R. Balistreri, and Prof. Giovanni Ruvolo, and Giuseppe Mazzesi (000134_RDB_2014 "Focus on cellular and molecular mechanisms of both, protection and repair in BAV vs. TAV patients as novel tools for personalized treatments").

References

[1] S. C. Siu and C. K. Silversides, "Bicuspid aortic valve disease," *Journal of the American College of Cardiology*, vol. 55, no. 25, pp. 2789–2800, 2010.

[2] K. L. Losenno, R. L. Goodman, and M. W. A. Chu, "Bicuspid aortic valve disease and ascending aortic aneurysms: gaps in knowledge," *Cardiology Research and Practice*, vol. 2012, Article ID 145202, 16 pages, 2012.

[3] N. Abdulkareem, J. Smelt, and M. Jahangiri, "Bicuspid aortic valve aortopathy: genetics, pathophysiology and medical therapy," *Interactive Cardiovascular and Thoracic Surgery*, vol. 17, no. 3, pp. 554–559, 2013.

[4] M. A. Dale, M. K. Ruhlman, and B. T. Baxter, "Inflammatory cell phenotypes in AAAs: their role and potential as targets for therapy," *Arteriosclerosis, Thrombosis, and Vascular Biology*, vol. 35, no. 8, pp. 1746–1755, 2015.

[5] H. Lu and A. Daugherty, "Aortic aneurysms," *Arteriosclerosis, Thrombosis, and Vascular Biology*, vol. 37, no. 6, pp. e59–e65, 2017.

[6] C. Pisano, C. R. Balistreri, A. Ricasoli, and G. Ruvolo, "Cardiovascular disease in ageing: an overview on thoracic aortic aneurysm as an emerging inflammatory disease," *Mediators of Inflammation*, vol. 2017, Article ID 1274034, 8 pages, 2017.

[7] R. He, D. C. Guo, A. L. Estrera et al., "Characterization of the inflammatory and apoptotic cells in the aortas of patients with ascending thoracic aortic aneurysms and dissections," *The Journal of Thoracic and Cardiovascular Surgery*, vol. 131, no. 3, pp. 671–678.e2, 2006.

[8] R. He, D. C. Guo, W. Sun et al., "Characterization of the inflammatory cells in ascending thoracic aortic aneurysms in patients with Marfan syndrome, familial thoracic aortic aneurysms, and sporadic aneurysms," *The Journal of Thoracic and Cardiovascular Surgery*, vol. 136, no. 4, pp. 922–929.e1, 2008.

[9] G. Ruvolo, C. Pisano, G. Candore et al., "Can the TLR-4-mediated signaling pathway be "a key inflammatory promoter for sporadic TAA"?," *Mediators of Inflammation*, vol. 2014, Article ID 349476, 14 pages, 2014.

[10] L. Zhang and Y. Wang, "B lymphocytes in abdominal aortic aneurysms," *Atherosclerosis*, vol. 242, no. 1, pp. 311–317, 2015.

[11] C. R. Balistreri, C. Pisano, G. Candore, E. Maresi, M. Codispoti, and G. Ruvolo, "Focus on the unique mechanisms involved in thoracic aortic aneurysm formation in bicuspid aortic valve versus tricuspid aortic valve patients: clinical implications of a pilot study," *European Journal of Cardiothoracic Surgery*, vol. 43, no. 6, pp. e180–e186, 2013.

[12] X. Ju, T. Ijaz, H. Sun et al., "Interleukin-6-signal transducer and activator of transcription-3 signaling mediates aortic dissections induced by angiotensin II via the T-helper lymphocyte 17-interleukin 17 axis in C57BL/6 mice," *Arteriosclerosis, Thrombosis, and Vascular Biology*, vol. 33, no. 7, pp. 1612–1621, 2013.

[13] H. F. Zhou, H. Yan, J. L. Cannon, L. E. Springer, J. M. Green, and C. T. N. Pham, "CD43-mediated IFN-γ production by $CD8^+$ T cells promotes abdominal aortic aneurysm in mice," *The Journal of Immunology*, vol. 190, no. 10, pp. 5078–5085, 2013.

[14] J. Wang, J. S. Lindholt, G. K. Sukhova et al., "IgE actions on $CD4^+$ T cells, mast cells, and macrophages participate in the pathogenesis of experimental abdominal aortic aneurysms," *EMBO Molecular Medicine*, vol. 6, no. 7, pp. 952–969, 2014.

[15] E. Vorkapic, E. Dugic, S. Vikingsson et al., "Imatinib treatment attenuates growth and inflammation of angiotensin II induced abdominal aortic aneurysm," *Atherosclerosis*, vol. 249, pp. 101–109, 2016.

[16] C. Pisano, E. Maresi, C. R. Balistreri et al., "Histological and genetic studies in patients with bicuspid aortic valve and ascending aorta complications," *Interactive CardioVascular and Thoracic Surgery*, vol. 14, no. 3, pp. 300–306, 2012.

[17] C. R. Balistreri, "Genetic contribution in sporadic thoracic aortic aneurysm? Emerging evidence of genetic variants related to TLR-4-mediated signaling pathway as risk determinants," *Vascular Pharmacology*, vol. 74, pp. 1–10, 2015.

[18] M. Dusseaux, E. Martin, N. Serriari et al., "Human MAIT cells are xenobiotic-resistant, tissue-targeted, $CD161^{hi}$ IL-17-secreting T cells," *Blood*, vol. 117, no. 4, pp. 1250–1259, 2011.

[19] L. Le Bourhis, L. Guerri, M. Dusseaux, E. Martin, C. Soudais, and O. Lantz, "Mucosal-associated invariant T cells: unconventional development and function," *Trends in Immunology*, vol. 32, no. 5, pp. 212–218, 2011.

[20] C. Sugimoto, H. Fujita, and H. Wakao, "Mucosal-associated invariant T cells from induced pluripotent stem cells: a novel approach for modeling human diseases," *World Journal of Stem Cells*, vol. 8, no. 4, pp. 158–169, 2016.

[21] W. G. McMaster, A. Kirabo, M. S. Madhur, and D. G. Harrison, "Inflammation, immunity, and hypertensive end-organ damage," *Circulation Research*, vol. 116, no. 6, pp. 1022–1033, 2015.

[22] T. Honjo, K. Y. Chyu, P. C. Dimayuga et al., "ApoB-100-related peptide vaccine protects against angiotensin II-induced aortic aneurysm formation and rupture," *Journal of the American College of Cardiology*, vol. 65, no. 6, pp. 546–556, 2015.

[23] Z. Wei, Y. Wang, K. Zhang et al., "Inhibiting the Th17/IL-17A-related inflammatory responses with digoxin confers protection against experimental abdominal aortic aneurysm," *Arteriosclerosis, Thrombosis, and Vascular Biology*, vol. 34, no. 11, pp. 2429–2438, 2014.

[24] M. Romain, S. Taleb, M. Dalloz et al., "Overexpression of SOCS3 in T lymphocytes leads to impaired interleukin-17 production and severe aortic aneurysm formation in mice–brief report," *Arteriosclerosis, Thrombosis, and Vascular Biology*, vol. 33, no. 3, pp. 581–584, 2013.

[25] G. H. M. van Puijvelde and J. Kuiper, "NKT cells in cardiovascular diseases," *European Journal of Pharmacology*, vol. 816, pp. 47–57, 2017.

[26] C. R. Balistreri, G. Ruvolo, D. Lio, and R. Madonna, "Toll-like receptor-4 signaling pathway in aorta aging and diseases: "*its double nature*"," *Journal of Molecular and Cellular Cardiology*, vol. 110, pp. 38–53, 2017.

[27] C. R. Balistreri, R. Madonna, G. Melino, and C. Caruso, "The emerging role of Notch pathway in ageing: focus on the related mechanisms in age-related diseases," *Ageing Research Reviews*, vol. 29, pp. 50–65, 2016.

[28] V. Garg, A. N. Muth, J. F. Ransom et al., "Mutations in *NOTCH1* cause aortic valve disease," *Nature*, vol. 437, no. 7056, pp. 270–274, 2005.

[29] S. A. Mohamed, Z. Aherrahrou, H. Liptau et al., "Novel missense mutations (p.T596M and p.P1797H) in NOTCH1 in patients with bicuspid aortic valve," *Biochemical and Biophysical Research Communications*, vol. 345, no. 4, pp. 1460–1465, 2006.

[30] I. Foffa, L. Ait Alì, P. Panesi et al., "Sequencing of *NOTCH1, GATA5, TGFBR1* and *TGFBR2* genes in familial cases of bicuspid aortic valve," *BMC Medical Genetics*, vol. 14, no. 1, p. 44, 2013.

[31] N. Dargis, M. Lamontagne, N. Gaudreault et al., "Identification of gender-specific genetic variants in patients with bicuspid aortic valve," *The American Journal of Cardiology*, vol. 117, no. 3, pp. 420–426, 2016.

[32] S. H. McKellar, D. J. Tester, M. Yagubyan, R. Majumdar, M. J. Ackerman, and T. M. Sundt III, "Novel *NOTCH1* mutations in patients with bicuspid aortic valve disease and thoracic aortic aneurysms," *The Journal of Thoracic and Cardiovascular Surgery*, vol. 134, no. 2, pp. 290–296, 2007.

[33] E. Girdauskas, L. Geist, K. Disha et al., "Genetic abnormalities in bicuspid aortic valve root phenotype: preliminary results," *European Journal of Cardio-thoracic Surgery*, vol. 52, no. 1, pp. 156–162, 2017.

[34] T. Ogawa, M. Kitagawa, and K. Hirokawa, "Age-related changes of human bone marrow: a histometric estimation of proliferative cells, apoptotic cells, T cells, B cells and macrophages," *Mechanisms of Ageing and Development*, vol. 117, no. 1–3, pp. 57–68, 2000.

[35] L. Lazuardi, B. Jenewein, A. M. Wolf, G. Pfister, A. Tzankov, and B. Grubeck-Loebenstein, "Age-related loss of naïve T cells and dysregulation of T-cell/B-cell interactions in human lymph nodes," *Immunology*, vol. 114, no. 1, pp. 37–43, 2005.

[36] G. Colonna-Romano, S. Buffa, M. Bulati et al., "B cells compartment in centenarian offspring and old people," *Current Pharmaceutical Design*, vol. 16, no. 6, pp. 604–608, 2010.

[37] F. Da Ros, R. Carnevale, G. Cifelli et al., "Targeting interleukin-1β protects from aortic aneurysms induced by disrupted transforming growth factor β signaling," *Immunity*, vol. 47, no. 5, pp. 959–973.e9, 2017.

[38] N. M. Yassine, J. T. Shahram, and S. C. Body, "Pathogenic mechanisms of bicuspid aortic valve aortopathy," *Frontiers in Physiology*, vol. 8, p. 687, 2017.

[39] C. Pisano, C. Rita Balistreri, O. Fabio Triolo, V. Argano, and G. Ruvolo, "Acute type a aortic dissection: beyond the diameter," *Journal of Heart Valve Disease*, vol. 25, no. 6, pp. 764–768, 2016.

Hindawi
Oxidative Medicine and Cellular Longevity
Volume 2018, Article ID 2609847, 12 pages
https://doi.org/10.1155/2018/2609847

Research Article

Formyl Peptide Receptor 1 Modulates Endothelial Cell Functions by NADPH Oxidase-Dependent VEGFR2 Transactivation

Fabio Cattaneo, Martina Castaldo, Melania Parisi, Raffaella Faraonio, Gabriella Esposito, and Rosario Ammendola

Department of Molecular Medicine and Medical Biotechnology, School of Medicine, University of Naples Federico II, Naples, Italy

Correspondence should be addressed to Rosario Ammendola; rosario.ammendola@unina.it

Received 19 December 2017; Accepted 29 January 2018; Published 18 March 2018

Academic Editor: Valeria Conti

In the vasculature, NADPH oxidase is the main contributor of reactive oxygen species (ROS) which play a key role in endothelial signalling and functions. We demonstrate that ECV304 cells express $p47^{phox}$, $p67^{phox}$, and $p22^{phox}$ subunits of NADPH oxidase, as well as formyl peptide receptors 1 and 3 (FPR1/3), which are members of the GPCR family. By RT-PCR, we also detected Flt-1 and Flk-1/KDR in these cells. Stimulation of FPR1 by N-fMLP induces $p47^{phox}$ phosphorylation, which is the crucial event for NADPH oxidase-dependent superoxide production. Transphosphorylation of RTKs by GPCRs is a biological mechanism through which the information exchange is amplified throughout the cell. ROS act as signalling intermediates in the transactivation mechanism. We show that N-fMLP stimulation induces the phosphorylation of cytosolic Y951, Y996, and Y1175 residues of VEGFR2, which constitute the anchoring sites for signalling molecules. These, in turn, activate PI3K/Akt and PLC-γ1/PKC intracellular pathways. FPR1-induced ROS production plays a critical role in this cross-talk mechanism. In fact, inhibition of FPR1 and/or NADPH oxidase functions prevents VEGFR2 transactivation and the triggering of the downstream signalling cascades. N-fMLP stimulation also ameliorates cellular migration and capillary-like network formation ability of ECV304 cells.

1. Introduction

Vascular endothelial growth factor receptor 2 (VEGFR2)/Flk-1/KDR and VEGFR1/Flt1 are members of the receptor tyrosine kinase (RTK) family and bind to vascular endothelial growth factor (VEGF) promoting organization, migration, proliferation, and formation of vascular structures of endothelial cells (ECs) [1]. In the human VEGFR2, Y951, Y1054, Y1059, Y1175, and Y1214 residues have been detected as phosphorylation sites [2, 3] and Y801, Y996, and Y1008 residues have been involved in VEGFR2 signalling [4, 5]. The phosphorylated Y1175 residue binds to phospholipase Cγ (PLC-γ) [3], as well as with the adaptor molecules Shb [6] and Sck [7], whereas the phosphorylated Y951 residue mediates binding for VEGF receptor-associated protein (VRAP), which is also known as a T cell-specific adapter (TSAd), which is crucial for EC migration in vitro and cell actin reorganization [2]. The phosphorylated Y1214 residue of VEGFR2 represents an anchoring site for the adaptor protein Nck [8], whereas the role of the phosphorylation of Y1224, Y1305, Y1309, and Y1319 residues in the C-terminal tail still remains to be determined.

The G protein-coupled receptors (GPCRs) are a superfamily of plasma membrane proteins activated by several ligands. Their agonist-specific stimulation induces G protein dissociation and, in turn, the activation of membrane-associated enzymes, intracellular second messengers, or ion channels. The human formyl peptide receptors 1, 2, and 3 (FPR1, FPR2, and FPR3) are members of the GPCR family and are all associated with pertussis toxin- (PTX-) sensitive Gi proteins [9–11]. FPR1 binds to efficiently N-formyl-methionyl-leucyl-phenylalanine (N-fMLP), whereas FPR2 is effectively activated by low concentrations of WKYMVm peptide [12]. The significant biological functions of FPR1 and FPR2 are supported by the discovery of high-affinity host-derived ligands. These two receptors are expressed in

several cell types [13, 14], whereas FPR3, which does not bind to N-fMLP or WKYMVm, is expressed in monocytes, dendritic cells [9–11], and human umbilical vein endothelial cell (HUVEC) primary cultures [15]. FPR2 is also expressed on nuclear membranes of human lung carcinoma CaLu-6 and human gastric adenocarcinoma AGS cell lines [16, 17].

The most important source of ROS in ECs is NADPH oxidase, which consists of cytosolic subunits $p47^{phox}$, $p40^{phox}$, $p67^{phox}$, and the small GTPase Rac1 and of membrane-associated proteins $p22^{phox}$ and $gp91^{phox}$. In several cell types, FPR stimulation by N-fMLP or WKYMVm induces superoxide generation as a consequence of MEK- and PKC-dependent phosphorylation of the regulatory subunit $p47^{phox}$, which is in large part prevented by preincubation with PTX [13, 18–20]. NADPH oxidase-derived ROS act as intracellular second messengers by activating several redox signalling cascades implicated in VEGFR2 autophosphorylation, EC migration, angiogenesis, proliferation [21], and postnatal angiogenesis *in vivo* [22]. Nevertheless, molecular mechanisms responsible for NADPH oxidase activation and the function of ROS in redox signalling linked to angiogenesis remain unclear.

Even though GPCRs are deficient of an intrinsic tyrosine kinase activity, binding of specific ligands may induce tyrosine phosphorylation of RTKs. The agonist-dependent stimulation of GPCRs can enhance the signalling activity of RTKs, linking the ample heterogeneity of GPCRs with the effective signalling abilities of RTKs. Transactivation of RTKs by GPCRs may occur by diverse molecular mechanisms, which include the activation of metalloexopeptidases and metalloendopeptidases, the involvement of nonreceptor tyrosine kinases associated with the membrane, or NADPH oxidase-dependent ROS generation [23]. In different cell types, FPR2 stimulation prompts phosphorylation of tyrosine residues of EGFR, which provide anchoring sites for the recruitment and activation of intracellular signalling pathways [24], and HGF receptor transphosphorylation, thereby inducing part of the molecular responses triggered by c-Met/HGF binding [19]. ROS play a crucial role in these cross-talk mechanisms since the inhibition of NADPH oxidase functions prevents EGFR and c-Met transactivation [19, 24].

Herein, we show that ECV304 cells express FPR1, Flk-1/KDR, and $p47^{phox}$ and that FPR1 stimulation by N-fMLP induces NADPH oxidase-dependent ROS generation as well as the transphosphorylation of cytosolic Y951, Y996, and Y1175 residues of VEGFR2. These phosphotyrosines represent anchoring sites for signalling molecules that, in turn, activate PI3K/Akt and PLC-γ1/PKC intracellular pathways involved in cell attachment and cell migration of ECs. Furthermore, FPR1 activation also ameliorates cellular migration and capillary-like network formation of ECV304 cells.

2. Materials and Methods

2.1. Antibodies and Chemicals. The N-fMLP peptide was synthesized and HPLC-purified by PRIMM (Milan, Italy). SDS-PAGE reagents were purchased from Bio-Rad (Hercules, CA, USA). Protein A/G Plus, anti-Flk1, anti-p-Flk1 (Tyr951), anti-p-Flk1 (Tyr996), anti-p-Flk1 (Tyr1175), anti-p-Flk1 (Tyr1214), anti-p-Tyr, anti-$p47^{phox}$, anti-$p22^{phox}$, anti-p-PLCγ1 (Y783), anti-PLCγ1, anti-PKCα, anti-PKCβII, anti-PKCζ, anti-PKCδ, anti-tubulin, anti-mouse, and anti-rabbit were from Santa Cruz Biotechnology (Santa Cruz, CA, USA). Anti-p-PI3K (p85) and anti-p-Akt (Ser473) were from Cell Signaling Technology (Danvers, MA, USA). Anti-p-Ser, $p22^{phox}$ siRNA (SI03078523), and scramble control siRNA (SI03650318) were from Qiagen (Hiden, Germany). FPR1 siRNA (L-005140-00) and scramble control (D-001810-10) were purchased from Dharmacon (Lafayette, CO, USA). Protein A-horseradish peroxidase was from Amersham Pharmacia Biotech (Little Chalfont, Buckinghamshire, UK). Pertussis toxin (PTX), apocynin, wortmannin, and LY294002 were from Sigma (St. Louis, MO, USA).

2.2. RNA Purification and RT-PCR Analysis. Total RNA was purified from ECV304 cells by TRIzol reagents (Thermo Fisher Scientific) according to the manufacturer's instruction, and 0.1 μg of RNA was used as a template for reverse transcription experiments, as previously described [25]. Primer sequences designed to amplify human coding regions and relative product sizes are reported in Table 1.

2.3. Cell Culture. ECV304 cells (ATCC®CRL-1998) were obtained from ATCC (Rockville, MD, USA) and were grown in Dulbecco's modified Eagle's medium (DMEM) containing 10% fetal bovine serum (FBS), 100 U/ml penicillin, and 100 μg/ml streptomycin. Cells were serum-starved for 24 hours, once they reached 80% of confluence, and then stimulated with 0.1 μM N-fMLP peptide for various times, as reported in the figures. In other experiments, serum-starved cells were preincubated with 100 ng/ml PTX for 16 hours, 50 μM LY294002 for 1 hour, 0.5 μM wortmannin for 1 hour, or 100 μM apocynin for 2 hours, before stimulation with 0.1 μM N-fMLP for 5 minutes. Short interfering RNA experiments were performed incubating 4×10^5 cells with 5 nM siRNAs for 12 hours, in DMEM containing 10% FBS and 20 μl of HiPerFect (Qiagen, Hiden, Germany). Cells were then serum-starved for 24 hours and stimulated with 0.1 μM N-fMLP for 5 minutes. ECV304 cells were also incubated with 20 ng/ml VEGF, as a control.

2.4. Western Blotting and Immunoprecipitation Assays. ECV304 cells were incubated with N-fMLP with or without specific inhibitors as described above. Whole lysates were purified in buffer containing 150 mmol/l NaCl, 50 mmol/l Tris-HCl (pH 8.5), 2 mmol/l EDTA, 1% *v*/*v* NP-40, 0.5% *w*/*v* deoxycholate, 10 mmol/l NaF, 10 mM sodium pyrophosphate, 2 mmol/l PMSF, 2 μg/ml leupeptin, and 2 μg/ml aprotinin (pH 7.4), as previously described [26]. Lysates were incubated at 0°C for 15 min and then centrifuged at 38000 ×g for 15 min at 4°C. Purification of membrane proteins was performed as previously described [19]. Bio-Rad protein assay (Bio-Rad, Hercules, CA, USA) was used to determine protein concentration. Proteins were resolved on a 10% SDS-PAGE, and immunoblot experiments were

Table 1: Forward and reverse PCR primer sequences.

Primers	Primer sequence	Product size
β-Actin	5′-TGATCACCATTGGGAATGAG-3′ 5′-CAGTGTGTTGGCGTAGAGGT-3′	154 bp
Flk-1/KDR	5′-GAGGGCCACTCATGGTGATTG-3′ 5′-TGCCAGCAGTCCAGCATGGTCTG-3′	709 bp
Flt-1	5′-GAGAATTCACTATGGAAGATCTGATTTCTTACAGT-3′ 5′-GAGCATGCGGATAAATACACATGTGCTTCTAG-3′	498 bp
Flt-4	5′-CCCACGCAGACATCAAGACG-3′ 5′-TGCAGAACTCCACGATCACC-3′	380 bp
FPR1	5′-GACCACAGCTGGTGAACAGT-3′ 5′-GATGCAGGACGCAAACACAG-3′	474 bp
FPR2	5′-GGATTTGCACCCACTGCATTT-3′ 5′-ATCCAAGGTCCGACGATCAC-3′	528 bp
FPR3	5′-GAGTTGCTCCACAGGAATCCA-3′ 5′-ATAGGCACGCTGAAGCCAAT-3′	760 bp
$p47^{phox}$	5′-GGTGGGTCATCAGGAAAGAC-3′ 5′-GCAGAAAACGGACGCTGTTG-3′	210 bp
$p22^{phox}$	5′-TGTGCCTGCTGGAGTACCCC-3′ 5′-ACACGACCTCGTCGGTCACC-3′	441 bp
$p67^{phox}$	5′-GCCAGGTGAAAAACTACTGC-3′ 5′-CTTCCAGCCATTCTTCATTC-3′	246 bp

performed as previously described [24]. Immunoprecipitation experiments were performed by incubating equal amounts of proteins with 3 μg of anti-$p47^{phox}$ or anti-Flk1 antibodies. Protein expression or phosphorylation was detected by the ECL chemiluminescence reagent kit (Amersham Pharmacia Biotech) and visualized by autoradiography. Densitometry analysis was used to quantify protein or phosphorylation levels by using a Discover Pharmacia scanner.

2.5. Superoxide Production Assay. Membranes and cytosol fractions were purified from serum-starved ECV304 cells stimulated with 0.1 μM N-fMLP for the times reported in the figure. The reduction of cytochrome c was measured to determine NADPH-dependent superoxide generation, as previously described [24]. Briefly, 10 μg of membrane proteins and 200 μg of cytosolic proteins were incubated in PBS in the presence of 15 μM GTP-γ-S, 100 μM cytochrome c, and 10 μM FAD in a final volume of 1 ml. Superoxide production was monitored at 550 nm, after the addition of 100 μM NADPH. Cells were also incubated with 200 U/ml superoxide dismutase (SOD), as the control of the specificity of cytochrome c reduction. Superoxide anion generation was measured as the SOD-inhibitable reduction of ferricytochrome c. Individual treatments were compared with the values obtained from growth-arrested ECV304 cells by Student's *t*-test.

2.6. Cell Migration Assay. ECV304 cells were grown as described above until they reached 100% confluence, and a wound was induced in the monolayer by scratching it with a sterile 80 μm diameter tip. Cells were incubated in serum-deprived medium at 37°C at 5% CO_2, and time-lapse images were taken every 12 hours up to 36 hours after wound generation by using the Leica AF6000 Modular System and processed by using the Leica LAS AF light software. The covered surface was quantified with the ImageJ software.

2.7. Capillary-Like Network Formation. 48-multiwell plates were coated with 150 μL of Matrigel (BD Bioscience) per well and then allowed to polymerize for 30 minutes at 37°C, according to the manufacturer's instructions. 1×10^5 ECV304 cells, pretreated or not with 100 ng/ml PTX, were plated in the precoated wells with serum-free DMEM in the presence or absence of 0.1 μM N-fMLP or 20 ng/ml VEGF (Gold Biotechnology, Olivette, USA) for 16 hours at 37°C. Network formation was acquired with the Leica AF6000 Modular System, and the total tube length was measured by using the ImageJ software.

2.8. Statistical Analysis. All the reported data are expressed as means ± SD and represent at least three unrelated experiments. Statistical analyses were evaluated by Student's *t*-test, and their significance was considered with a minimum value

of $p < 0.05$. All statistical analyses were performed with the Prism statistical software.

3. Results and Discussion

3.1. ECV304 Cells Express Flt-1, Flk-1/KDR, NADPH Oxidase, and a Functional FPR1 Receptor. ECV304 cells were initially described as a HUVEC-derived transformed cell line [27], but they were later characterized, by genetic relationship, as a cell line derived from human urinary bladder carcinoma T24 cells [28]. Nevertheless, although not of HUVEC origin, ECV304 cells show many characteristics of ECs [29, 30] and present both epithelial and endothelial features [31], a number of which are solely endothelial markers and consequently not detected in T24 cells [30]. Therefore, ECV304 cells seem to be a relevant model for the study of molecular mechanisms in the endothelium, such as signal transduction, cell migration, and capillary-like network formation.

In these cells, we detected, by RT-PCR, the expression of Flt-1 and Flk-1/KDR (Figure 1(a)), but not of Flt-4, which is expressed only in lymphatic endothelial cells. The two VEGF receptors were also detected by immunostaining in ECV304 cells [32]. We also analyzed the expression of FPRs, and we provided the first evidence that FPR1 and FPR3 but not FPR2 (Figure 1(b)) are expressed in ECV304 cells. This cell line also expresses $p47^{phox}$, $p67^{phox}$, and $p22^{phox}$ subunits of the NADPH oxidase enzymatic complex (Figure 1(c)). In human fibroblasts, stimulation of FPRs with N-fMLP induces $p47^{phox}$ phosphorylation, which is the crucial event required for NADPH oxidase activation [13]. In ECV304 cells, FPR1 is a functional receptor; in fact, stimulation with 0.1 μM N-fMLP triggers time-dependent phosphorylation of $p47^{phox}$ (Figure 1(d)) which is entirely inhibited by preincubation with PTX (Figure 1(e)). Furthermore, incubation with N-fMLP for different times stimulates NADPH oxidase-dependent superoxide production, with a maximum of ROS generation occurring at 6 min (Figure 1(f)).

3.2. FPR1 Stimulation by N-fMLP Promotes Flk-1/KDR Transactivation. Cellular effects of VEGF-A on ECs, such as permeability, migration, survival, and proliferation, are mediated by Flk-1/KDR, which binds VEGF-A to the second and third extracellular Ig-like domains. This allows the correct placement of the intracellular kinase domains, which results in the Flk-1/KDR autophosphorylation [33].

Cross-talk between GPCRs and RTKs modulates downstream signalling pathways involved in many biological functions of mammalian cells [19, 23, 24, 34]. Therefore, we analyzed Flk-1/KDR transactivation by FPR1 in ECV304 cells, and in Western blot experiments, we noticed that the incubation with 0.1 μM N-fMLP increases Flk-1/KDR tyrosine phosphorylation in a time-dependent manner (Figure 2(a)). VEGFR2 is the main signal transducer in ECs, and in the human Flk-1/KDR intracellular domain, multiple tyrosine residues have been detected as phosphorylation sites, including Y801, Y951, Y996, Y1008, Y1054, Y1059, Y1175, and Y1214 [2–4]. The FPR1 agonist triggers the phosphorylation of Y951, Y996, and Y1175 residues of Flk-1/KDR within the first 5 min (Figure 2(b)), which is completely inhibited by preincubating ECV304 cells with PTX before N-fMLP exposure (Figure 2(c)). A significant reduction in the phosphorylation levels of Y951, Y996, and Y1175 residues is observed when cells are preincubated with siRNAs against FPR1 before N-fMLP treatment (Figure 2(d)), indicating that VEGFR2 transphosphorylation is mediated by FPR1.

3.3. Flk-1/KDR Transactivation Depends on NADPH Oxidase-Dependent ROS Generation. The main source of ROS in the arterial wall and ECs is NADPH oxidase [35], which can be activated by several stimuli including GPCR agonists [23, 36]. In nonphagocytic cells, NADPH oxidase expression depends on the cellular types and surrounding conditions and produces ROS at low levels [21, 23], which can act as signalling molecules by reversible oxidation/reduction of cysteines located in the catalytic site of protein tyrosine phosphatases (PTPs) [19, 21, 37, 38]. ROS can play a role in RTK transphosphorylation by preventing the PTPase action and, in turn, changing the RTK from a nonphosphorylated to a phosphorylated state. A number of PTPs, such as LMW-PTP (HCPTPA), SHP-1, and SHP-2, are associated with Flk-1/KDR upon VEGF stimulation [39, 40]. We preincubated ECV304 cells with apocynin (Figure 3(a)), which specifically inhibits NADPH oxidase, or with a siRNA against $p22^{phox}$ (Figure 3(b)), an essential component of the membrane-associated NADPH oxidase, and we noticed that the FPR1-induced transphosphorylation of Y951, Y996, and Y1175 residues of Flk-1/KDR is prevented by the arrest of NADPH oxidase functions (Figures 3(a) and 3(b)). These results demonstrate that FPR1-mediated superoxide generation feeds the cross-talk between FPR1 and Flk-1/KDR.

3.4. FPR1-Induced Flk-1/KDR Transactivation Triggers the PI3K/Akt Pathway. Phosphorylated tyrosine residues of Flk-1/KDR represent anchoring sites for signalling molecules that trigger intracellular pathways, which, in turn, activate biological responses such as cell proliferation and migration [41]. In the human VEGFR2, several phospho-tyrosines have been identified [1–4] and so far Y951, Y996, Y1054, Y1059, Y1175, and Y1214, in the kinase insert domain, in the kinase domain, and in the C-terminal tail of VEGFR2, have been defined as the main autophosphorylation sites [42]. Phosphorylation of Y1175, within the pYIVL sequence, provides a docking site for several signalling molecules, including PLC-γ [3] and the adaptor proteins Sck [7] and Shb [6]. Shb contains an SH2 and a PTB domain, four presumed tyrosine phosphorylation sites, and a proline-rich N-terminus motif [6]. Shb binds to phospho-tyrosine Y1175 of VEGFR2, resulting in its Src-dependent phosphorylation [6]. Shb-dependent binding to the Y1175 residue is important for the PI3K response, but it is unclear how this effect is pursued. The SH3 domain of PI3K (p85) could interact with Shb at the level of the proline-rich motif; otherwise, the effect could be mediated by focal adhesion kinase (FAK), which is involved in cellular attachment and migration [43]. Silencing of Shb by small interfering RNA (siRNA) results in the arrest of PI3K activation.

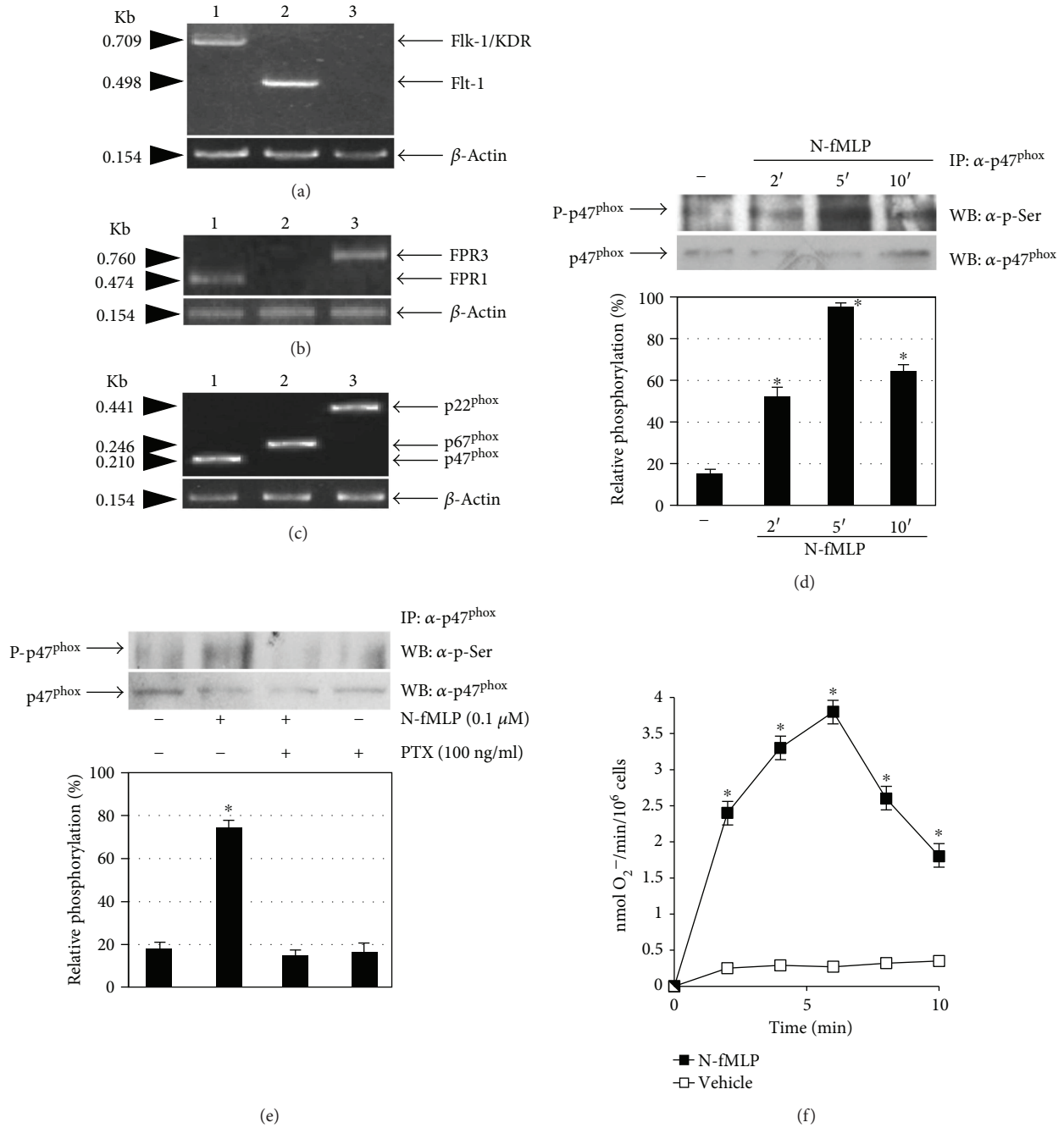

Figure 1: ECV304 cells express Flk-1/KDR, FPR1, and NADPH oxidase. Total RNA was purified from ECV304 cells. cDNA was coamplified by using (a) Flk-1/KDR (lane 1), Flt-1 (lane 2), or Flt-4 (lane 3); (b) FPR1 (lane 1), FPR2 (lane 2), or FPR3 (lane 3); and (c) $p47^{phox}$ (lane 1), $p67^{phox}$ (lane 2), $p22^{phox}$ (lane 3), or β-actin primers. PCR products were separated on a 1.5% agarose gel and stained with ethidium bromide. (d) Serum-starved ECV304 cells were stimulated with 0.1 μM N-fMLP for the indicated times or (e) preincubated with PTX before N-fMLP stimulation for 5 minutes. Whole lysates (1 mg) were immunoprecipitated with an α-$p47^{phox}$ antibody and resolved on 10% SDS-PAGE. $p47^{phox}$ phosphorylation was determined by using an α-p-Ser antibody. An α-$p47^{phox}$ antibody served as a control for protein loading. (f) Superoxide production was determined as a SOD-sensitive rate reduction of cytochrome c in serum-starved ECV304 cells stimulated or not with 0.1 μM N-fMLP for the indicated times. All the experiments are representative of at least three independent experiments. $^*p < 0.05$ compared with unstimulated cells.

The phosphorylated Y951 residue in the VEGFR2 kinase insert domain binds to TSAd which is equivalent to Rlk- and Itk-binding protein (RIBP), Lck adaptor (LAD), and VRAP [44]. Y951-mediated binding between VEGFR2 and TSAd plays a critical role in cell migration of ECs and VEGF-induced actin reorganization. In fact, site-directed mutagenesis of Y951 to F951 in Flk1/KDR, or silencing by siRNA of VRAP/TSAd expression, prevents VEGFA-mediated migration [2]. Stimulated RTKs typically activate PI3K by inducing phosphorylation of a tyrosine residue within an YXXM

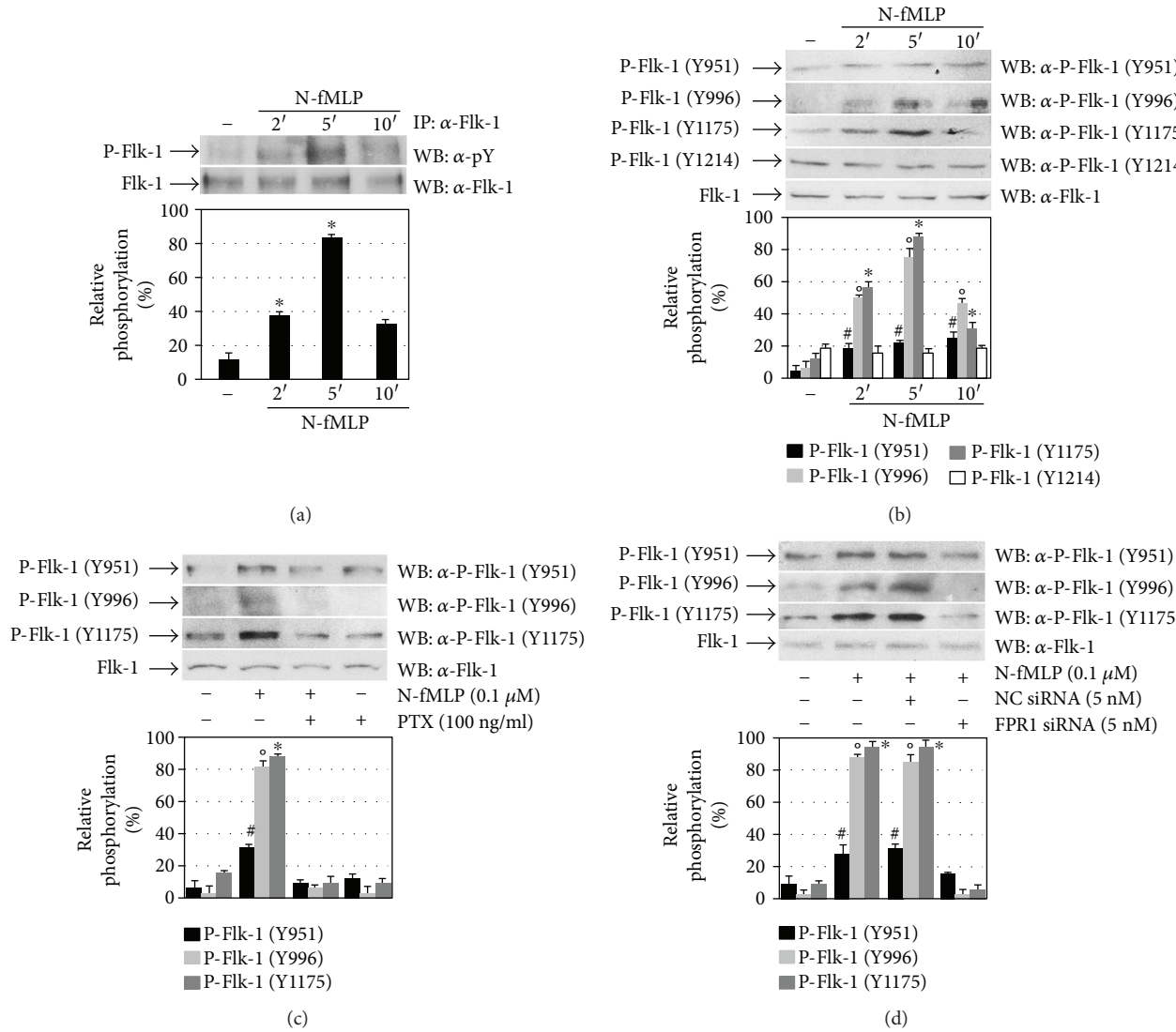

Figure 2: FPR1 activation promotes Flk-1/KDR transphosphorylation. (a) Whole lysates (900 μg) purified from serum-starved ECV304 cells stimulated with 0.1 μM N-fMLP for the indicated times were immunoprecipitated with an α-Flk-1 antibody, and Flk-1 tyrosine phosphorylation was detected with an α-pY antibody. An α-Flk1 antibody served as a control for protein loading. (b, c, d) Fifty micrograms of whole lysates, purified from ECV304 cells, was resolved on 10% SDS-PAGE. The cells were (b) stimulated with N-fMLP for the indicated times, (c) stimulated with N-fMLP for 5 minutes in the presence or absence of PTX, or (d) incubated for 12 hours with 5 nM siRNA against FPR1 (FPR1 siRNA) or negative control siRNA (NC siRNA) in DMEM containing 10% FBS in the presence of 20 μl of HiPerfect. The filters were immunoblotted with α-pFlk-1 (Y951), α-pFlk-1 (Y996), α-pFlk-1 (Y1175), or α-pFlk-1 (Y1214) antibodies. An α-Flk-1 antibody served as a control for protein loading. $^{*}p < 0.05$ compared with unstimulated cells. $^{\circ}p < 0.05$ compared with unstimulated cells. $^{\#}p < 0.05$ compared with unstimulated cells.

motif, which represents an anchoring site for SH2 domains of the p85 regulatory subunit of PI3K. Binding of PI3K to the YXXM motif mediates Akt activation. Phosphorylation of the tyrosine residue is mediated by TSAd, which activates members of Src family kinases [45, 46]. Flk-1/KDR does not have a pYXXM motif detected by the SH2 domain of the p85 subunit [47]; nevertheless, a binding site for the p85 subunit of PI3K is localized in the Gab1 adaptor protein, which also binds to VEGFR2, although the exact binding site in the receptor is unknown [48, 49].

In ECs, VEGFA-induced cell survival depends on Flk-1/KDR and on the consequent activation of PI3K and Akt, which induces A1 and Bcl-2 expression [50]. We analyzed PI3K activation in N-fMLP-stimulated ECV3014 cells, and in Western blot experiments, we detected that N-fMLP stimulates PI3K (p85) phosphorylation in a time-dependent manner (Figure 4(a)). This is prevented by pretreating EVC304 cells with PTX or apocynin (Figure 4(b)), suggesting that PI3K (p85) phosphorylation depends on PTX-sensible GPCR and NADPH oxidase-dependent superoxide generation.

Activation of PI3K and production of phosphatidylinositol (3,4,5)-trisphosphate (PIP3) result in the consequent activation of Akt by PDK1 and PDK2, which phosphorylate Akt at T308 and S473 residues, respectively.

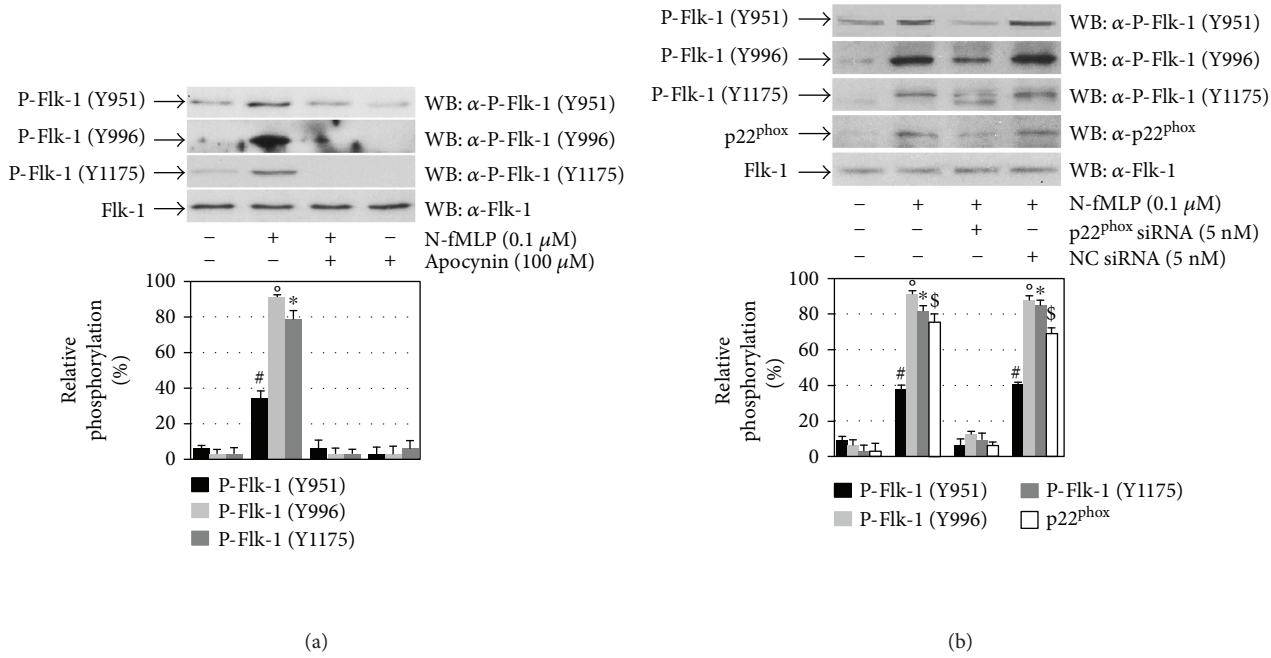

(a) (b)

Figure 3: Flk-1/KDR transactivation depends on NADPH oxidase activation. (a) Serum-starved ECV304 cells were stimulated with 0.1 μM N-fMLP for 5 minutes in the presence or absence of 100 μM apocynin, or (b) ECV304 cells serum-deprived for 24 hours were incubated for 12 hours with 5 nM siRNA against p22^{phox} (p22^{phox} siRNA) or negative control siRNA (NC siRNA) in DMEM containing 10% FBS in the presence of 20 μl of HiPerfect and stimulated with 0.1 μM N-fMLP for 5 minutes. Fifty micrograms of whole lysates were resolved on 10% SDS-PAGE and immunoblotted with α-pFlk-1 (Y951), α-pFlk-1 (Y996), α-pFlk-1 (Y1175), α-pFlk-1 (Y1214), or α-p22phox antibodies. An α-Flk-1 antibody served as a control for protein loading. All the experiments are representative of at least three independent experiments. $^{*}p < 0.05$ compared with unstimulated cells. $^{\circ}p < 0.05$ compared with unstimulated cells. $^{\#}p < 0.05$ compared with unstimulated cells. $^{\$}p < 0.05$ compared with unstimulated cells.

We analyzed Akt phosphorylation in FPR1-stimulated ECV304 cells, and we observed that N-fMLP induces Akt (S473) phosphorylation in the same time interval of PI3K (p85) phosphorylation (Figure 4(c)). Akt (S473) phosphorylation is prevented by preincubation of ECV304 cells with selective PI3K inhibitors (Figure 4(d)), as well as with PTX, which blocks FPR1-bound G_i proteins in their inactive form, or with apocynin (Figure 4(e)). The critical role of FPR1 and NADPH oxidase in the Akt (Ser473) phosphorylation is supported by the finding that preincubation with siRNAs against FPR1 (Figure 4(f)) or against p22^{phox} (Figure 4(g)) before N-fMLP treatment results in a substantial decrease in the phosphorylation levels of Akt.

3.5. FPR1-Mediated Phosphorylation of the Y1175 Residue Provides a Docking Site for PLC-γ1 Activation. The phosphorylated Y1175 residue of Flk-1/KDR represents a binding site for PLC-γ1 [3] and other adaptor proteins [6, 7]. PLC-γ1 is phosphorylated and its catalytic activity is enhanced as a consequence of binding to pY1175. PLC-γ plays a crucial role in angiogenesis, as demonstrated by the observation that PLC-γ1-deficient mouse embryos die at nearly E9.0 with substantially reduced erythropoiesis and vasculogenesis [51, 52] and that the mutation of Y1173 in mice (Y1175 in human) is responsible for the embryonic mortality at E8.5–9.5, as a consequence of anomalies of haematopoietic and endothelial cells [53]. Furthermore, in zebrafish, PLC-γ1 is required for arterial development, as demonstrated by the observation that zebrafish embryos lacking in PLC-γ1 do not respond to VEGF [54]. These results support the idea that signalling from pY1175 of VEGFR2 to the PLC-γ/PKC pathway is essential for vasculogenesis in embryogenesis.

Four activation-induced tyrosine phosphorylation sites (Y472, Y771, Y783, and Y1254) have been described in PLC-γ1 [55]. In time-course experiments, we observed that N-fMLP induces PLC-γ1 activation with the highest level of Y783 residue phosphorylation occurring at 2 min (Figure 5(a)). Preincubation of ECV304 cells with PTX or apocynin prevents PLC-γ1 (Y783) phosphorylation (Figure 5(b)), suggesting that PLC-γ1 activation depends on FPR1 stimulation and NADPH oxidase-dependent ROS generation.

PLC-γ1 catalyzes the hydrolysis of the phosphatidylinositol (4,5)-bisphosphate (PIP2), which results in the production of diacylglycerol (DAG) and inositol 1,4,5-trisphosphate (IP3). IP3 triggers the release of calcium from endoplasmic reticulum and, therefore, an increase in its intracellular concentration, whereas DAG activates protein kinase C (PKC). The PKC isoenzymes PKCα, PKCβ, and PKCζ are implicated in VEGF-mediated signalling [41, 56]. In N-fMLP-stimulated ECV304 cells, we investigated the activation of PKC isoenzymes by analyzing their membrane translocation. We observed that in response to the FPR1 agonist, PKCα, PKCβII, and PKCζ translocate to the membrane and a substantial increment in their amount was found within 2 min of N-fMLP treatment. On the other hand, we did not observe PKCδ translocation (Figure 5(c)).

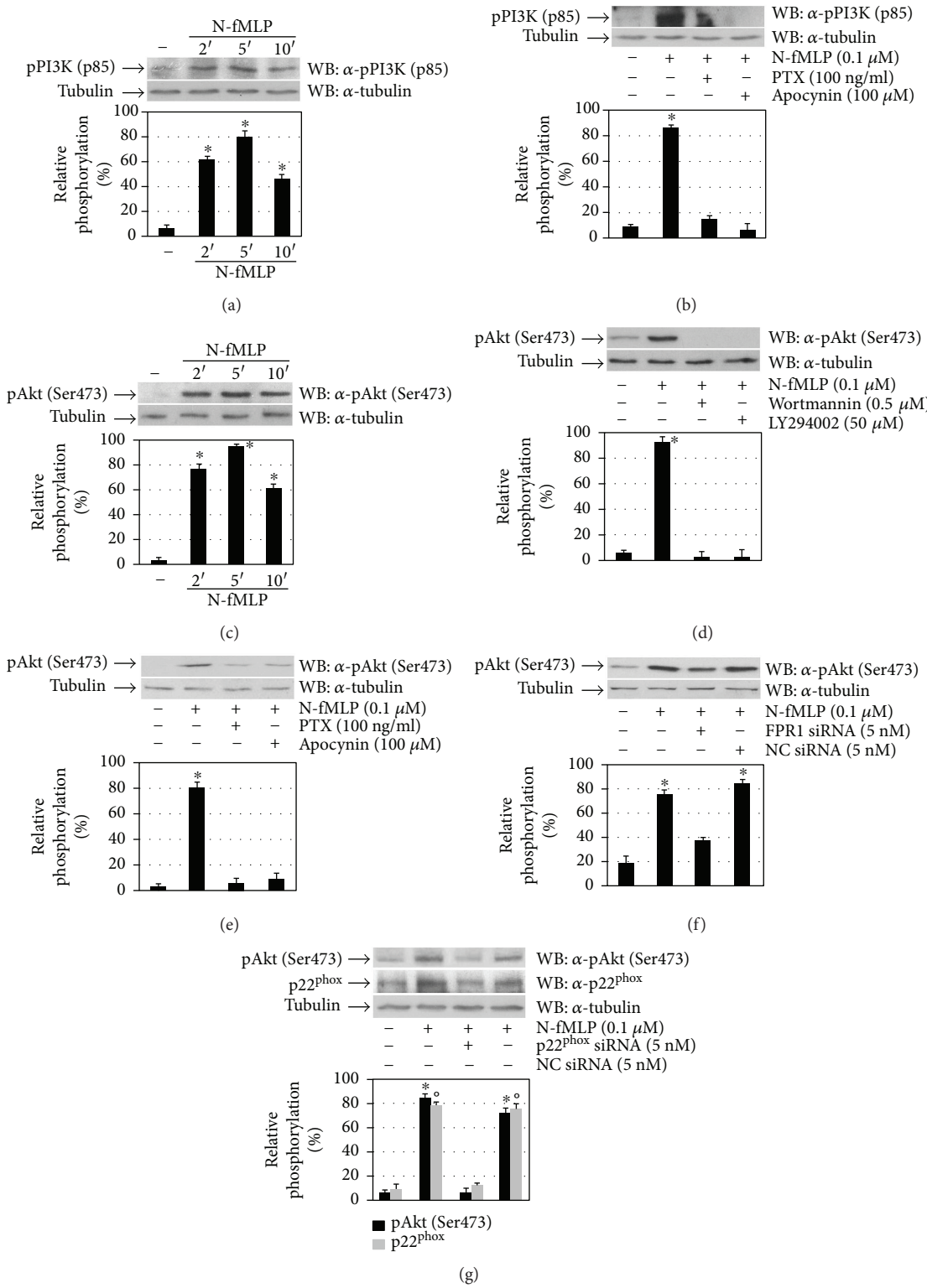

Figure 4: FPR1-mediated Flk-1/KDR transactivation triggers the PI3K-Akt pathway. (a, c) Cell lysates were purified from serum-starved ECV304 cells exposed to 0.1 μM N-fMLP for the indicated times. (b, e) ECV304 cells were serum-deprived for 24 hours before the stimulation for 5 minutes with N-fMLP in the absence or presence of PTX, apocynin, (d) wortmannin, or LY294002. (f) ECV304 cells were serum-deprived for 24 hours, incubated for 12 hours with 5 nM siRNA against FPR1 (FPR1 siRNA) or (g) against $p22^{phox}$ ($p22^{phox}$ siRNA) or negative control siRNA (NC siRNA), in DMEM containing 10% FBS in the presence of 20 μl of HiPerfect, and stimulated with 0.1 μM N-fMLP for 5 minutes. Fifty micrograms of whole lysates was resolved on 10% SDS-PAGE and immunoblotted with (a, b) an α-pPI3K (p85) or (c–g) an α-pAkt (S473) antibody. An α-tubulin antibody served as a control for protein loading. All the experiments are representative of at least three independent experiments. $^{*}p < 0.05$ compared with unstimulated cells. $^{\circ}p < 0.05$ compared with unstimulated cells.

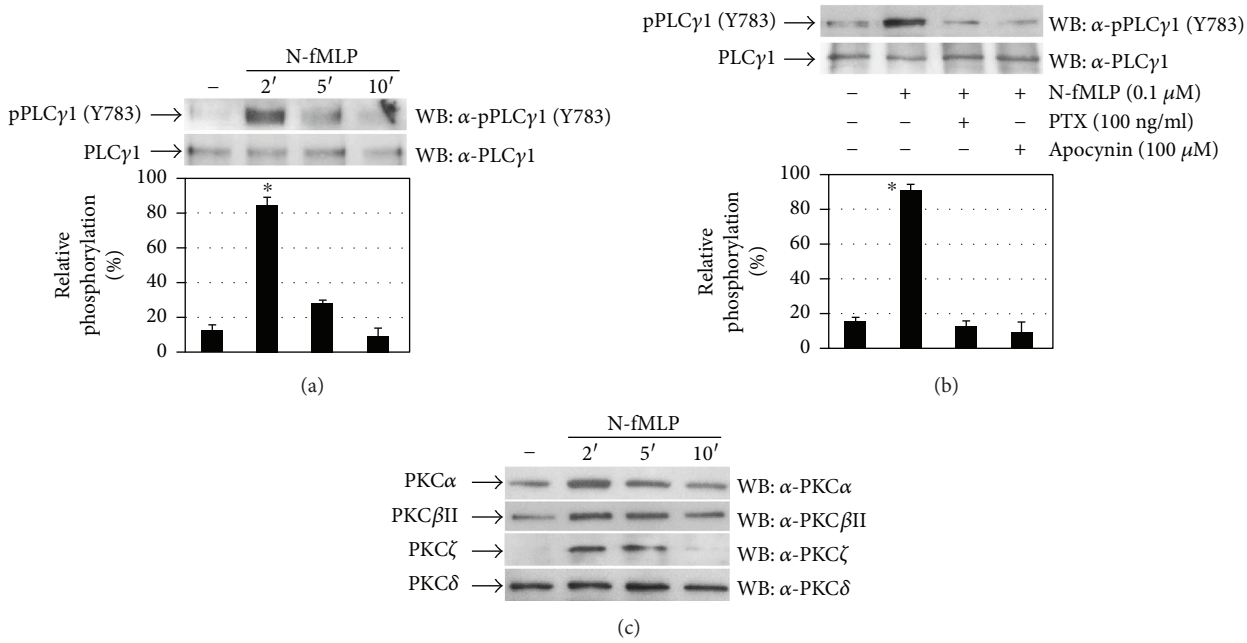

Figure 5: Tyrosine phosphorylation of 1175 residues of Flk-1/KDR triggers the PLC-γ1/PKC pathway. (a, c) Serum-deprived ECV304 cells were stimulated with 0.1 μM N-fMLP for the indicated times or (b) for 5 minutes in the presence or absence of PTX or apocynin. (a, b) Fifty micrograms of whole lysates was resolved on 10% SDS-PAGE, and PLCγ1 phosphorylation on the Y783 residue was detected by using an α-pPLCγ1 (Y783) antibody. An α-PLCγ1 antibody was used as a control for protein loading. (c) Membrane proteins (50 μg) were resolved on 10% SDS-PAGE, and PKC isoforms were detected by using the specific antibodies α-PKCα, α-PKCβII, α-PKCζ, or α-PKCδ as indicated. All the experiments are representative of at least three independent experiments. $^*p < 0.05$ compared with unstimulated cells.

3.6. FPR1 Stimulation by N-fMLP Promotes Wound Healing and Capillary-Like Network Formation. Endothelial cell migration is a very critical event during the angiogenesis process. In tumor angiogenesis, endothelial cells invade the surrounding basement membrane and migrate into the stroma. Finally, they organize themselves in the formation of new blood capillaries, which are crucial for tumor growth.

Several signalling cascades are implicated in Flk-1/KDR-mediated migration. These involve Y1175 residue phosphorylation and, in turn, the activation of PI3K, as well as the phosphorylation of the Y951 residue, which is a binding site for TSAd [41]. To assess whether FPR1 stimulation by N-fMLP induces cell migration, thus promoting wound closure, we tested ECV304 cells in an *in vitro* wound healing assay. Our results show that N-fMLP induces a more rapid cell migration with respect to unstimulated cells, after both 24 and 36 hours (Figure 6(a)). The preincubation with PTX, before stimulation, prevents N-fMLP-induced wound closure (Figure 6(a)), suggesting that it depends on FPR1 activation.

We also assessed the effects of N-fMLP on capillary-like network formation in a Matrigel assay, which is considered an *in vitro* correlate of angiogenesis. The level of capillary-like network formation was analyzed by measuring the tube length after 1 day of culture. Cells incubated with 20 ng/ml VEGF were used as a control. As shown in Figure 6(b), FPR1 stimulation by N-fMLP results in a significant increase in capillary-like network formation, which is prevented by preincubation with PTX. The tube lengths were substantially increased also in control ECV304 cells exposed to VEGF, compared to untreated cells (Figure 6(b)).

4. Conclusions

We demonstrate that, in ECV304 cells, FPR1 stimulation by N-fMLP results in NADPH oxidase-dependent ROS production and VEGFR2 transphosphorylation. Moreover, we demonstrate that ROS bridge the signals from FPR1 to Flk-1/KDR, as evidenced by the results obtained with apocynin and with $p22^{phox}$ silencing on VEGFR2 transactivation and on the intracellular signalling cascades elicited by this receptor. We also show that, as a result of the transactivation mechanism, phosphotyrosines Y951, Y996, and Y1175 of VEGFR2 create anchoring sites for the enrollment and activation of the PI3K/Akt and PLC-γ/PKC pathways, fostering some of the molecular responses elicited by VEGFA. Finally, we prove that the FPR1-induced signalling promotes cellular migration and capillary-like network formation of ECV304 cells.

GPCRs represent the largest family of drug targets, which can bind to receptors with high selectivity and regulate several functions in a predictable manner. The observation that each GPCR can engage multiple signalling partners, driving multiple cellular responses, leads to the concept that different ligands can have distinct efficacies toward these different pathways.

GPCRs can trigger signalling cascades in a ligand-specific manner and can cross-talk with RTKs by amplifying intracellular signalling pathways. NADPH oxidase-derived ROS

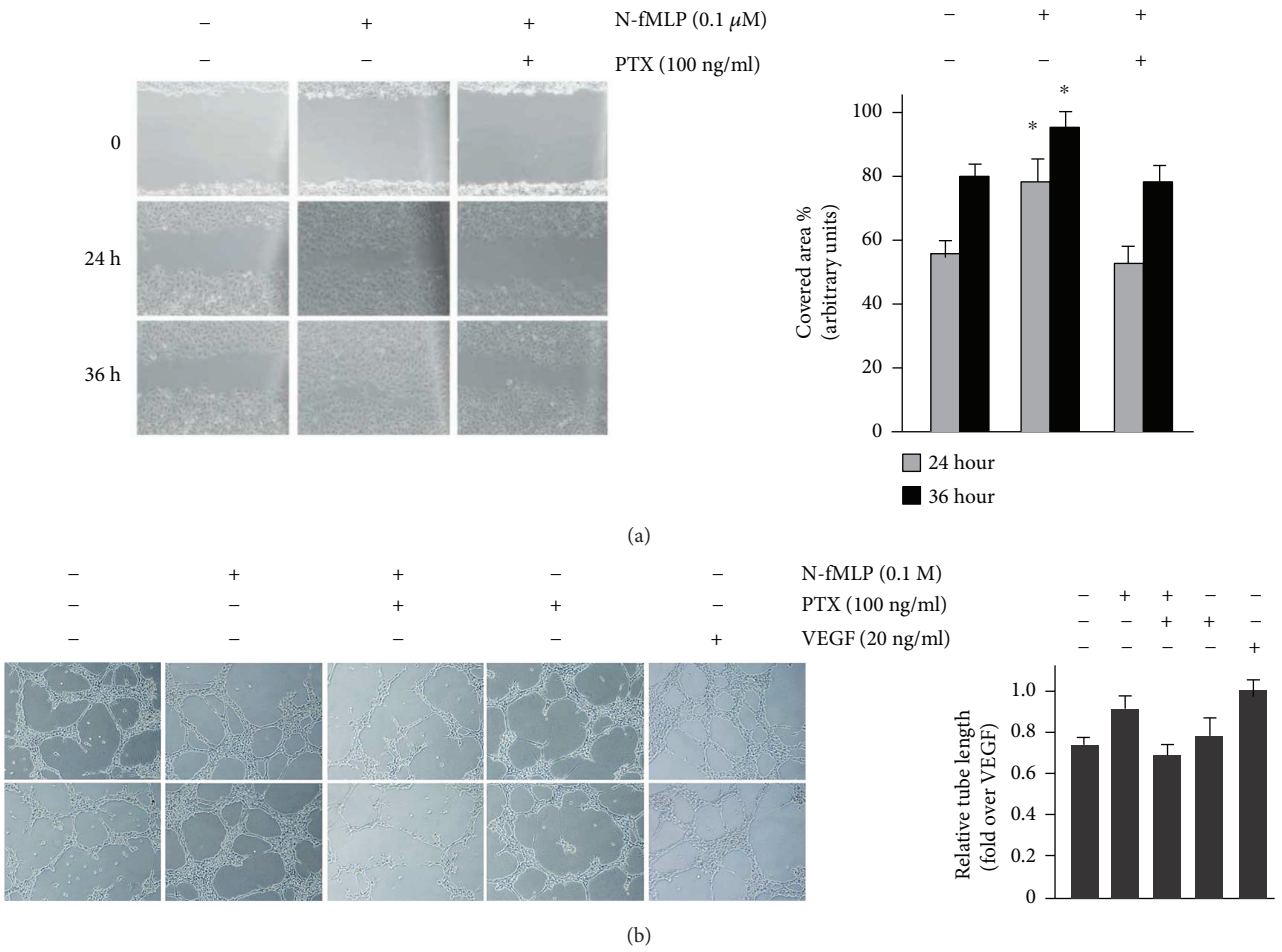

Figure 6: Wound healing and capillary-like network formation induced by FPR1. (a) Representative images (left) and bar graph quantification (right) of ECV304 cell migration from 5 independent experiments. Cells were incubated with 0.1 μM N-fMLP or vehicle in the presence or absence of PTX. Images were acquired at different times (0, 24, and 36 hours) after wound injury (scale bar: 20 μm). (b) Capillary-like network formation (left) was performed in Matrigel-coated plates. ECV304 cells were incubated with N-fMLP in the presence or absence of PTX, and bar graphs (right) show the quantification of relative tube length from four independent experiments. Cells incubated with VEGF (20 μg/ml) were used as a positive control (scale bar: 50 μm). $^*p < 0.05$ compared with unstimulated cells.

act as signalling molecules by reversible oxidative inactivation of cysteine sulfhydryl groups of PTPs, which can, in turn, control the activity of RTKs and their transactivation [19, 20, 24]. Phosphorylation of cytosolic subunits $p47^{phox}$ and $p67^{phox}$ is required for NADPH oxidase activation. Our results show that ROS generation by NADPH oxidase is tightly regulated and depends on FPR1 stimulation by N-fMLP, which triggers $p47^{phox}$ phosphorylation and, in turn, superoxide generation. The finding that ROS mediate Flk-1/KDR transactivation, playing a crucial role in VEGFR2 signalling related to angiogenesis, provides new insights into NADPH oxidase and/or FPR1 as possible targets for therapies against angiogenesis-dependent diseases. The identified antiangiogenic drugs targeting the VEGFR2 signalling pathways are shared by several RTKs that do not evoke angiogenesis, and the actual antiangiogenic therapies, which target either VEGFA action or Flk-1/KDR activity, may induce the upregulation of other RTKs to overcome the VEGFR blockade. Cross-talk between FPR1 and Flk-1/KDR provides further opportunities for drug discovery strategies for angiogenesis driven by an increase in VEGFR2 activity, disputing actual thinking in the notion of pharmacological targets. Elucidation of the signalling cascades responsible for VEGFR2 transactivation can contribute to the identification of new therapeutic targets able to interfere with the FPR1 pathway. Furthermore, our results suggest that targeting both FPR1 and VEGFR2 might provide improved therapeutic effects, compared to targeting either receptor distinctively.

Conflicts of Interest

The authors declare that they have no conflicts of interest.

Acknowledgments

This work was supported by POR Campania FSE 2007–2013 (Project CREME) and Italian Ministry of Health (RF-2011-02349269).

References

[1] Z. Sun, X. Li, S. Massena et al., "VEGFR2 induces c-Src signaling and vascular permeability in vivo via the adaptor protein TSAd," *The Journal of Experimental Medicine*, vol. 209, no. 7, pp. 1363–1377, 2012.

[2] T. Matsumoto, S. Bohman, J. Dixelius et al., "VEGF receptor-2 Y951 signaling and a role for the adapter molecule TSAd in tumor angiogenesis," *The EMBO Journal*, vol. 24, no. 13, pp. 2342–2353, 2005.

[3] T. Takahashi, S. Yamaguchi, K. Chida, and M. Shibuya, "A single autophosphorylation site on KDR/Flk-1 is essential for VEGF-A-dependent activation of PLC-γ and DNA synthesis in vascular endothelial cells," *The EMBO Journal*, vol. 20, no. 11, pp. 2768–2778, 2001.

[4] J. Solowiej, S. Bergqvist, M. A. McTigue et al., "Characterizing the effects of the juxtamembrane domain on vascular endothelial growth factor receptor-2 enzymatic activity, autophosphorylation, and inhibition by axitinib," *Biochemistry*, vol. 48, no. 29, pp. 7019–7031, 2009.

[5] R. D. Meyer, C. Latz, and N. Rahimi, "Recruitment and activation of phospholipase Cγ1 by vascular endothelial growth factor receptor-2 are required for tubulogenesis and differentiation of endothelial cells," *The Journal of Biological Chemistry*, vol. 278, no. 18, pp. 16347–16355, 2003.

[6] K. Holmqvist, M. J. Cross, C. Rolny et al., "The adaptor protein shb binds to tyrosine 1175 in vascular endothelial growth factor (VEGF) receptor-2 and regulates VEGF-dependent cellular migration," *The Journal of Biological Chemistry*, vol. 279, no. 21, pp. 22267–22275, 2004.

[7] A. J. Warner, J. Lopez-Dee, E. L. Knight, J. R. Feramisco, and S. A. Prigent, "The Shc-related adaptor protein, Sck, forms a complex with the vascular-endothelial-growth-factor receptor KDR in transfected cells," *Biochemical Journal*, vol. 347, no. 2, pp. 501–509, 2000.

[8] L. Lamalice, F. Houle, and J. Huot, "Phosphorylation of Tyr^{1214} within VEGFR-2 triggers the recruitment of Nck and activation of Fyn leading to SAPK2/p38 activation and endothelial cell migration in response to VEGF," *The Journal of Biological Chemistry*, vol. 281, no. 45, pp. 34009–34020, 2006.

[9] F. Cattaneo, G. Guerra, and R. Ammendola, "Expression and signaling of formyl-peptide receptors in the brain," *Neurochemical Research*, vol. 35, no. 12, pp. 2018–2026, 2010.

[10] A. Iaccio, A. Angiolillo, and R. Ammendola, "Intracellular signaling triggered by formyl-peptide receptors in nonphagocytic cells," *Current Signal Transduction Therapy*, vol. 3, no. 2, pp. 88–96, 2008.

[11] A. Iaccio, F. Cattaneo, M. Mauro, and R. Ammendola, "FPRL1-mediated induction of superoxide in LL-37-stimulated IMR90 human fibroblast," *Archives of Biochemistry and Biophysics*, vol. 481, no. 1, pp. 94–100, 2009.

[12] Y. Le, W. Gong, B. Li et al., "Utilization of two seven-transmembrane, G protein-coupled receptors, formyl peptide receptor-like 1 and formyl peptide receptor, by the synthetic hexapeptide WKYMVm for human phagocyte activation," *The Journal of Immunology*, vol. 163, no. 12, pp. 6777–6784, 1999.

[13] R. Ammendola, L. Russo, C. De Felice, F. Esposito, T. Russo, and F. Cimino, "Low-affinity receptor-mediated induction of superoxide by N-formyl-methionyl-leucyl-phenylalanine and WKYMVm in IMR90 human fibroblasts," *Free Radical Biology & Medicine*, vol. 36, no. 2, pp. 189–200, 2004.

[14] Y. Le, P. M. Murphy, and J. M. Wang, "Formyl-peptide receptors revisited," *Trends in Immunology*, vol. 23, no. 11, pp. 541–548, 2002.

[15] S. Rezzola, M. Corsini, P. Chiodelli et al., "Inflammation and *N-formyl* peptide receptors mediate the angiogenic activity of human vitreous humour in proliferative diabetic retinopathy," *Diabetologia*, vol. 60, no. 4, pp. 719–728, 2017.

[16] F. Cattaneo, M. Parisi, T. Fioretti, D. Sarnataro, G. Esposito, and R. Ammendola, "Nuclear localization of formyl-peptide receptor 2 in human cancer cells," *Archives of Biochemistry and Biophysic*, vol. 603, pp. 10–19, 2016.

[17] F. Cattaneo, M. Parisi, T. Fioretti, G. Esposito, and R. Ammendola, "Intranuclear signaling cascades triggered by nuclear GPCRs," *Journal of Cell Signaling*, vol. 01, no. 04, p. 128, 2016.

[18] A. Iaccio, C. Collinet, N. Montesano Gesualdi, and R. Ammendola, "Protein kinase C-α and-δ are required for NADPH oxidase activation in WKYMVm-stimulated IMR90 human fibroblasts," *Archives of Biochemistry and Biophysics*, vol. 459, no. 2, pp. 288–294, 2007.

[19] F. Cattaneo, M. Parisi, and R. Ammendola, "WKYMVm-induced cross-talk between FPR2 and HGF receptor in human prostate epithelial cell line PNT1A," *FEBS Letters*, vol. 587, no. 10, pp. 1536–1542, 2013.

[20] F. Cattaneo, M. Parisi, and R. Ammendola, "Distinct signaling cascades elicited by different formyl peptide receptor 2 (FPR2) agonists," *International Journal of Molecular Sciences*, vol. 14, no. 4, pp. 7193–7230, 2013.

[21] M. Ushio–Fukai, "VEGF signaling through NADPH oxidase-derived ROS," *Antioxidants & Redox Signaling*, vol. 9, no. 6, pp. 731–739, 2007.

[22] T. Tojo, M. Ushio–Fukai, M. Yamaoka–Tojo, S. Ikeda, N. A. Patrushev, and R. W. Alexander, "Role of $gp91^{phox}$ (Nox2)-containing NAD(P)H oxidase in angiogenesis in response to hindlimb ischemia," *Circulation*, vol. 111, no. 18, pp. 2347–2355, 2005.

[23] F. Cattaneo, G. Guerra, M. Parisi et al., "Cell-surface receptors transactivation mediated by G protein-coupled receptors," *International Journal of Molecular Sciences*, vol. 15, no. 12, pp. 19700–19728, 2014.

[24] F. Cattaneo, A. Iaccio, G. Guerra, S. Montagnani, and R. Ammendola, "NADPH-oxidase-dependent reactive oxygen species mediate EGFR transactivation by FPRL1 in WKYMVm-stimulated human lung cancer cells," *Free Radical Biology and Medicine*, vol. 51, no. 6, pp. 1126–1136, 2011.

[25] R. Caggiano, F. Cattaneo, O. Moltedo et al., "miR-128 is implicated in stress responses by targeting MAFG in skeletal muscle cells," *Oxidative Medicine and Cellular Longevity*, vol. 2017, Article ID 9308310, 13 pages, 2017.

[26] S. De Marino, F. Cattaneo, C. Festa et al., "Imbricatolic acid from *Juniperus communis* L. prevents cell cycle progression in CaLu-6 cells," *Planta Medica*, vol. 77, no. 16, pp. 1822–1828, 2011.

[27] S. E. Hughes, "Functional characterization of the spontaneously transformed human umbilical vein endothelial cell line ECV304: use in an *in vitro* model of angiogenesis," *Experimental Cell Research*, vol. 225, no. 1, pp. 171–185, 1996.

[28] W. G. Dirks, R. A. MacLeod, and H. G. Drexler, "ECV304 (endothelial) is really T24 (bladder carcinoma): cell line cross-contamination at source," *In Vitro Cellular & Developmental Biology - Animal*, vol. 35, no. 10, pp. 558-559, 1999.

[29] K. Suda, B. Rothen-Rutishauser, M. Gunthert, and H. Wunderli-Allenspach, "Phenotypic characterization of human umbilical vein endothelial (ECV304) and urinary carcinoma (T24) cells: endothelial versus epithelial features," *In Vitro Cellular & Developmental Biology - Animal*, vol. 37, no. 8, pp. 505–514, 2001.

[30] M. B. Andozia, C. S. Vieira, S. A. Franceschini, M. R. Torqueti Tolloi, M. F. Silva de Sa, and R. A. Ferriani, "Ethinylestradiol and estradiol have different effects on oxidative stress and nitric oxide synthesis in human endothelial cell cultures," *Fertility and Sterility*, vol. 94, no. 5, pp. 1578–1582, 2010.

[31] F. Kiessling, J. Kartenbeck, and C. Haller, "Cell-cell contacts in the human cell line ECV304 exhibit both endothelial and epithelial characteristics," *Cell and Tissue Research*, vol. 297, no. 1, pp. 131–140, 1999.

[32] X. W. Bian, X. F. Jiang, J. H. Chen et al., "Increased angiogenic capabilities of endothelial cells from microvessels of malignant human gliomas," *International Immunopharmacology*, vol. 6, no. 1, pp. 90–99, 2006.

[33] I. Zachary and G. Gliki, "Signaling transduction mechanisms mediating biological actions of the vascular endothelial growth factor family," *Cardiovascular Research*, vol. 49, no. 3, pp. 568–581, 2001.

[34] H. M. El-Shewy, K. R. Johnson, M. H. Lee, A. A. Jaffa, L. M. Obeid, and L. M. Luttrell, "Insulin-like growth factors mediate heterotrimeric G protein-dependent ERK1/2 activation by transactivating sphingosine 1-phosphate receptors," *The Journal of Biological Chemistry*, vol. 281, no. 42, pp. 31399–31407, 2006.

[35] A. Gorlach, R. P. Brandes, K. Nguyen, M. Amidi, F. Dehghani, and R. Busse, "A gp91phox containing NADPH oxidase selectively expressed in endothelial cells is a major source of oxygen radical generation in the arterial wall," *Circulation Research*, vol. 87, no. 1, pp. 26–32, 2000.

[36] K. K. Griendling, D. Sorescu, and M. Ushio-Fukai, "NAD(P)H oxidase: role in cardiovascular biology and disease," *Circulation Research*, vol. 86, no. 5, pp. 494–501, 2000.

[37] P. Chiarugi and P. Cirri, "Redox regulation of protein tyrosine phosphatases during receptor tyrosine kinase signal transduction," *Trends in Biochemical Sciences*, vol. 28, no. 9, pp. 509–514, 2003.

[38] T. Finkel, "Signal transduction by reactive oxygen species in non-phagocytic cells," *Journal of Leukocyte Biology*, vol. 65, no. 3, pp. 337–340, 1999.

[39] D. Q. Guo, L. W. Wu, J. D. Dunbar et al., "Tumor necrosis factor employs a protein-tyrosine phosphatase to inhibit activation of KDR and vascular endothelial cell growth factor-induced endothelial cell proliferation," *The Journal of Biological Chemistry*, vol. 275, no. 15, pp. 11216–11221, 2000.

[40] L. Huang, S. Sankar, C. Lin et al., "HCPTPA, a protein tyrosine phosphatase that regulates vascular endothelial growth factor receptor-mediated signal transduction and biological activity," *The Journal of Biological Chemistry*, vol. 274, no. 53, pp. 38183–38188, 1999.

[41] K. Holmes, O. Ll Roberts, A. M. Thomas, and M. J. Cross, "Vascular endothelial growth factor receptor-2: structure, function, intracellular signalling and therapeutic inhibition," *Cellular Signalling*, vol. 19, no. 10, pp. 2003–2012, 2007.

[42] T. Matsumoto and H. Mugishima, "Signal transduction via vascular endothelial growth factor (VEGF) receptors and their roles in atherogenesis," *Journal of Atherosclerosis and Thrombosis*, vol. 13, no. 3, pp. 130–135, 2006.

[43] J. H. Qi and L. Claesson-Welsh, "VEGF-induced activation of phosphoinositide 3-kinase is dependent on focal adhesion kinase," *Experimental Cell Research*, vol. 263, no. 1, pp. 173–182, 2001.

[44] L. W. Wu, L. D. Mayo, J. D. Dunbar et al., "VRAP is an adaptor protein that binds KDR, a receptor for vascular endothelial cell growth factor," *The Journal of Biological Chemistry*, vol. 275, no. 9, pp. 6059–6062, 2000.

[45] M. Cully, H. You, A. J. Levine, and T. W. Mak, "Beyond PTEN mutations: the PI3K pathway as an integrator of multiple inputs during tumorigenesis," *Nature Reviews Cancer*, vol. 6, no. 3, pp. 184–192, 2006.

[46] G. X. Ruan and A. Kazlauskas, "Axl is essential for VEGF-A-dependent activation of PI3K/Akt," *The EMBO Journal*, vol. 31, no. 7, pp. 1692–1703, 2012.

[47] Z. Songyang, S. E. Shoelson, M. Chaudhuri et al., "SH2 domains recognize specific phosphopeptide sequences," *Cell*, vol. 72, no. 5, pp. 767–778, 1993.

[48] M. Dance, A. Montagner, A. Yart et al., "The adaptor protein Gab1 couples the stimulation of vascular endothelial growth factor receptor-2 to the activation of phosphoinositide 3-kinase," *The Journal of Biological Chemistry*, vol. 281, no. 32, pp. 23285–23295, 2006.

[49] M. Laramee, C. Chabot, M. Cloutier et al., "The scaffolding adapter Gab1 mediates vascular endothelial growth factor signaling and is required for endothelial cell migration and capillary formation," *The Journal of Biological Chemistry*, vol. 282, no. 11, pp. 7758–7769, 2007.

[50] H. P. Gerber, V. Dixit, and N. Ferrara, "Vascular endothelial growth factor induces expression of the antiapoptotic proteins Bcl-2 and A1 in vascular endothelial cells," *The Journal of Biological Chemistry*, vol. 273, no. 21, pp. 13313–13316, 1998.

[51] Q. S. Ji, G. E. Winnier, K. D. Niswender et al., "Essential role of the tyrosine kinase substrate phospholipase C-γ1 in mammalian growth and development," *Proceedings of the National Academy of Sciences of the United States of America*, vol. 94, no. 7, pp. 2999–3003, 1997.

[52] H. J. Liao, T. Kume, C. McKay, M. J. Xu, J. N. Ihle, and G. Carpenter, "Absence of erythrogenesis and vasculogenesis in *Plcg*1-deficient mice," *The Journal of Biological Chemistry*, vol. 277, no. 11, pp. 9335–9341, 2002.

[53] Y. Sakurai, K. Ohgimoto, Y. Kataoka, N. Yoshida, and M. Shibuya, "Essential role of Flk-1 (VEGF receptor 2) tyrosine residue 1173 in vasculogenesis in mice," *Proceedings of the National Academy of Sciences of the United States of America*, vol. 102, no. 4, pp. 1076–1081, 2005.

[54] N. D. Lawson, J. W. Mugford, B. A. Diamond, and B. M. Weinstein, "*Phospholipase C gamma-1* is required downstream of *vascular endothelial growth factor* during arterial development," *Genes & Development*, vol. 17, no. 11, pp. 1346–1351, 2003.

[55] C. J. Serrano, L. Graham, K. DeBell et al., "A new tyrosine phosphorylation site in PLCγ1: the role of tyrosine 775 in immune receptor signaling," *The Journal of Immunology*, vol. 174, no. 10, pp. 6233–6237, 2005.

[56] S. Koch, S. Tugues, X. Li, L. Gualandi, and L. Claesson-Welshi, "Signal transduction by vascular endothelial growth factor receptors," *Biochemical Journal*, vol. 437, no. 2, pp. 169–183, 2011.

Hindawi
Oxidative Medicine and Cellular Longevity
Volume 2018, Article ID 4946289, 13 pages
https://doi.org/10.1155/2018/4946289

Review Article

Targeting the Endoplasmic Reticulum Unfolded Protein Response to Counteract the Oxidative Stress-Induced Endothelial Dysfunction

Giuseppina Amodio,[1] **Ornella Moltedo**,[2] **Raffaella Faraonio**,[3] **and Paolo Remondelli**[1]

[1]*Dipartimento di Medicina, Chirurgia e Odontoiatria "Scuola Medica Salernitana", Università degli Studi di Salerno, 84081 Baronissi, Italy*
[2]*Dipartimento di Farmacia, Università degli Studi di Salerno, 84084 Fisciano, Italy*
[3]*Dipartimento di Medicina Molecolare e Biotecnologie Mediche, Università degli studi di Napoli "Federico II", 80131 Naples, Italy*

Correspondence should be addressed to Paolo Remondelli; premondelli@unisa.it

Received 21 December 2017; Accepted 18 February 2018; Published 14 March 2018

Academic Editor: Javier Egea

In endothelial cells, the tight control of the redox environment is essential for the maintenance of vascular homeostasis. The imbalance between ROS production and antioxidant response can induce endothelial dysfunction, the initial event of many cardiovascular diseases. Recent studies have revealed that the endoplasmic reticulum could be a new player in the promotion of the pro- or antioxidative pathways and that in such a modulation, the unfolded protein response (UPR) pathways play an essential role. The UPR consists of a set of conserved signalling pathways evolved to restore the proteostasis during protein misfolding within the endoplasmic reticulum. Although the first outcome of the UPR pathways is the promotion of an adaptive response, the persistent activation of UPR leads to increased oxidative stress and cell death. This molecular switch has been correlated to the onset or to the exacerbation of the endothelial dysfunction in cardiovascular diseases. In this review, we highlight the multiple chances of the UPR to induce or ameliorate oxidative disturbances and propose the UPR pathways as a new therapeutic target for the clinical management of endothelial dysfunction.

1. Introduction

Endothelial cells produce different vasoactive substances that control vascular homeostasis in concert with pro- and antioxidant or pro- and anti-inflammatory factors [1–3]. Among them, nitric oxide (NO) which is produced by nitric oxide synthases (NOS) and targets guanylyl cyclase of the underlying smooth muscle cells to activate the signalling of vasodilatation plays a key function in blood vessel homeostasis [4, 5]. Endothelial dysfunction (ED) occurs when vascular homeostasis is altered in favour of vasoconstriction, inflammation, and prooxidation, all factors that produce a proatherogenic and prothrombotic phenotype [3, 6]. ED is the early pathogenic event of several cardiovascular and metabolic diseases and therefore is predictive of cardiovascular events with fatal outcome [7, 8]. Reduced endothelium-dependent dilatation (EDD) is the initial signal of ED. EDD is the consequence of reduced NO bioavailability resulting from impaired NO production or increased NO degradation. In this state, endothelial NOS (eNOS) begins to generate reactive oxygen species (ROS), such as superoxide, a phenomenon known as "uncoupling" [3–5]. Furthermore, peroxynitrite ($ONOO^-$) promotes nitration of the eNOS cofactor BH4 and critical antioxidants, leading to propagation of ED and endothelial cell death [9]. Similar to eNOS uncoupling, other enzymes may function as ROS sources, such as NADPH oxidase, xanthine oxidase, and the mitochondrial respiratory chain complex, giving rise to OS-induced ED, an event that occurs in several different cardiovascular diseases (CVDs) [10–14]. Increasing evidence identifies endoplasmic reticulum stress (ER stress) as another source of ROS [15, 16]. As a consequence, a growing number of studies are focused on defining

the role of ER stress in OS induction aiming at understanding whether ER stress could have a role as a promoter of ED or merely worsen ED in human pathologies [14, 17–19]. In this review, we will analyse the basic mechanisms of ER production of ROS and discuss novel targets for the pharmacological therapy of CVDs derived from ED.

2. Endoplasmic Reticulum Function and the Control of the Redox State of the Cell

Redox homeostasis inside the cell is controlled by specialized mechanisms located in the cytosol, as well as within the peroxisomes, mitochondria, and the ER. The ER is intensely engaged in the control of folding and trafficking of secretory proteins [20]. Within the ER lumen, a quality control system (ERQC) selects properly folded from misfolded proteins that are addressed to degradation rather than to access downstream cell compartments of the secretory pathway. In this way, the ER ensures the functions of post ER compartments and controls the proteostasis and the trafficking of secretory proteins [21–24]. Under normal conditions, the ER has restricted antioxidant activity and the ER proteostasis is highly sensitive to the redox state of the cell. Several pathophysiological conditions could disturb the ER proteostasis by inducing the accumulation of misfolded or unfolded proteins within the ER [25, 26]. This condition is called ER stress and activates the signalling pathways of the unfolded protein response (UPR) [27, 28]. The UPR pathways aim to reestablish ER proteostasis throughout different outcomes: reducing ER protein load, potentiating the ER quality control, activating the ER-associated protein degradation machinery (ERAD), and, eventually, activating autophagy [29]. However, when all the adaptive responses fail, the UPR can activate the apoptotic programme [30, 31]. Since protein folding is coupled to ROS formation, the increment of folding load during ER stress strongly induces ROS production and exacerbates OS [16, 32–34]. The formation of disulfide bonds within the ER requires a stable redox environment. In order to maintain redox homeostasis during protein folding, the ER is provided with several buffering factors, such as glutathione (GSH), ascorbic acid, and flavin nucleotides. Specifically, GSH reacts with and reduces nonnative disulfide bonds, thus allowing misfolded proteins to fold again [35]. In the meantime, specific oxidoreductases such as protein disulfide isomerases (PDIs), in conjunction with the ER oxidoreductase 1 (Ero1), catalyse disulfide bond formation [36–38], but this event generates the formation of hydrogen peroxide (H_2O_2), the most abundant ROS produced in the ER. During ER stress, the accumulation of misfolded proteins, which requires more cycles of disulfide bond formation and isomerization, produces a higher amount of H_2O_2, depletes the ER GSH level, and, as a consequence, devastates the redox state of the ER [39].

3. The Unfolded Protein Response Pathways: Oxidative and Antioxidative Control

The ER stress activates the UPR pathways by means of three transmembrane transducers: the inositol-requiring kinase 1 (IRE1), the pancreatic ER kinase (PERK), and the activating transcription factor 6 (ATF6) [28]. In normal conditions, the three transducers are maintained inactive by the chaperone binding immunoglobulin protein/78 kDa glucose-regulated protein (Bip/GRP78). In stressed conditions, Bip/GRP78 dissociates from IRE1, PERK, and ATF6 and allows UPR activation (Figure 1). The adaptive response induced by the UPR, if successful, can moderate ROS production within the ER, not only by simply reducing the folding demand but also by performing another compensative response consisting in the activation of genes encoding antioxidant factors (Figure 2). In particular, antioxidant control has been linked to the PERK and IRE1 pathways as shown by the work of Harding et al. [40]. They demonstrated that ATF4 is essential for GSH synthesis and, as a consequence, for the maintenance of redox balance in the ER. Moreover, the IRE1/XBP1 branch of the UPR stimulates the hexosamine biosynthetic pathway (HBP), which is essential for the production of UDP-N-acetylglucosamine (UDP-GlcNAc). This compound is crucial for the stress-induced O-GlcNAc modifications, which favour cell survival and increase the defence against ROS [41]. Besides the ATF4/GSH and the XBP1/HBP antioxidant pathways, the UPR controls the activation of a potent transcription factor involved in the antioxidant response: the nuclear factor erythroid 2-related factor 2 (NRF2) [42, 43]. Under basal conditions, NRF2 is inactivated by the Kelch-like ECH-associated protein 1 (KEAP1), which induces its degradation through the cullin3/ring box 1-depedent ubiquitin ligase complex. During OS, ROS react with specific KEAP1 cysteines inducing conformational changes that prevent the binding of de novo-produced NRF2. As a consequence, newly translated NRF2 can migrate into the nucleus to activate antioxidant gene transcription [44]. In addition to that, it is well established that OS-activated PERK could induce NRF2 phosphorylation and dissociation from KEAP1 [45] enhancing the antioxidant activity of NRF2. Since ER protein misfolding highly increases ROS, we would expect that UPR activation could preferentially reduce abnormal production of ROS. On the contrary, evidence shows that UPR pathways can even activate ROS production during ER stress and therefore aggravate the OS (Figure 2). This is the case of the PERK pathway of the UPR that activates the transcription factor C/EBP homologous protein (CHOP), which induces the expression of Ero1 that accounts for the peroxide production during the oxidative protein folding [37, 38, 46]. Additionally, CHOP expression can be enhanced by the ROS-induced activation of the NADPH oxidase (NOX) members 2 or 4, which induce the double-stranded RNA-dependent protein kinase (PKR), another activator of CHOP [47]. The PERK/CHOP axis is not the only pathway of the UPR that initiates ROS formation. In fact, the IRE1 pathway of the UPR activates the apoptosis signal-regulating kinase 1 (ASK1) [48] and ASK1 activation is also sustained by the mitochondrial ROS production deriving from c-Jun N-terminal kinase- (JNK-) mediated inhibition of the mitochondrial electron transport chain (ETC) [49]. This event leads to the persistent activation of ASK1 thus linking the activation of UPR to OS-induced apoptosis. The

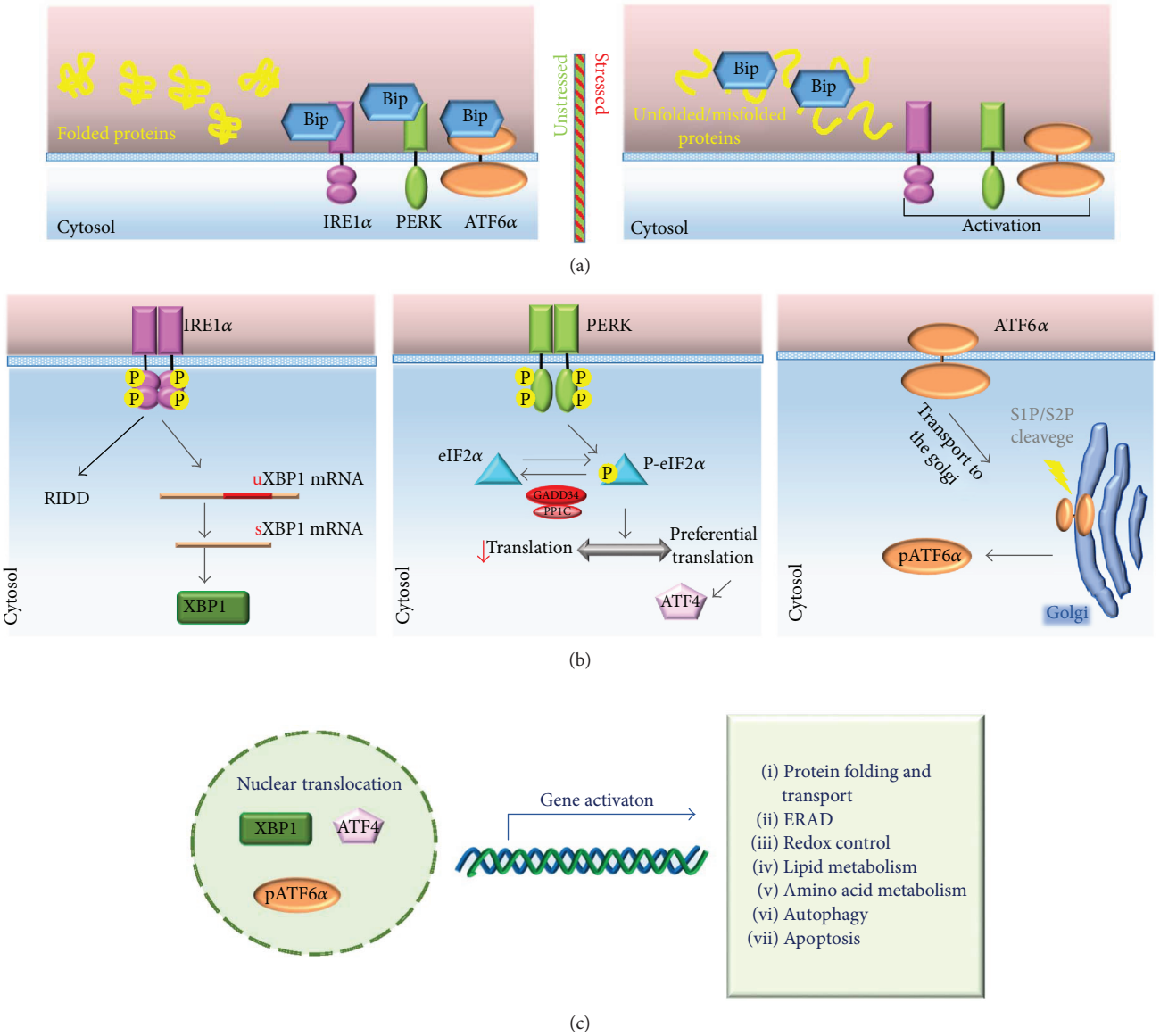

Figure 1: The signalling pathways of UPR. (a) During normal conditions, Bip/GRP78 binding to IRE1α, PERK, and ATF6α maintains the three transducers in an inactive state. In stressed conditions, Bip/GRP78 dissociates from IRE1α, PERK, and ATF6α to help the folding of secretory proteins and allows the activation of the transducers [28]. (b) After the release from Bip/GRP78, IRE1α dimerizes and autophosphorylates to activate its kinase and endoribonuclease domains [15]. Activated IRE1α cleaves 26 nucleotides from the mRNA encoding the X-box-binding protein 1 (XBP1) allowing the translation of XBP1 [140]. Bip/GRP78 dissociation enables also PERK activation through dimerization and *trans*-autophosphorylation. Activated PERK phosphorylates eIF2α at Ser51 leading to attenuation of protein synthesis, thereby reducing ER protein load. During this condition, some mRNA, such as the activating transcription factor 4 (ATF4) mRNA, are preferentially translated [141]. During severe ER stress, ATF4 strongly induces CHOP that triggers the apoptotic programme in different ways [31]. The eIF2α-ATF4 axis can also be activated by other cytosolic kinases allowing the regulation of global protein synthesis and the preferential translation of specific mRNA in response to different stimuli in a convergent signalling pathway known as integrated stress response (ISR) [20, 30]. ATF6α is the third ER stress sensor located in the ER membrane. Upon ER stress and release by Bip/GRP78, ATF6α is packaged into COPII vesicles and transferred to the *cis*-Golgi where it undergoes intramembrane proteolysis-specific cleavage by site 1 protease (S1P) and S2P to produce a transcriptionally active fragment (pATF6α). (c) XBP1, ATF4, and pATF6α migrate into the nucleus to activate the transcription of specific UPR genes involved in protein folding and trafficking, ERAD, cellular metabolism, autophagy, and apoptosis [20, 142]. Bip: Bip/GRP78; uXBP1: unspliced XBP1; sXBP1: spliced XBP1.

IRE1 pathway of the UPR also contributes to OS by increasing thioredoxin-interacting protein (TXNIP) mRNA levels throughout the reduction of the TXNIP inhibitory microRNA-17 [50], and such event makes cells more susceptible to OS, since TXNIP inhibits the antioxidant thioredoxin (TRX) enzyme. Several studies have demonstrated the fine tuning of the UPR by the OS [51, 52]. OS control of the UPR is mediated by the protein disulfide isomerases PDIA5, which reduces disulfide bonds in the luminal domain of ATF6, and PDIA6, which reduces specific cysteines of the

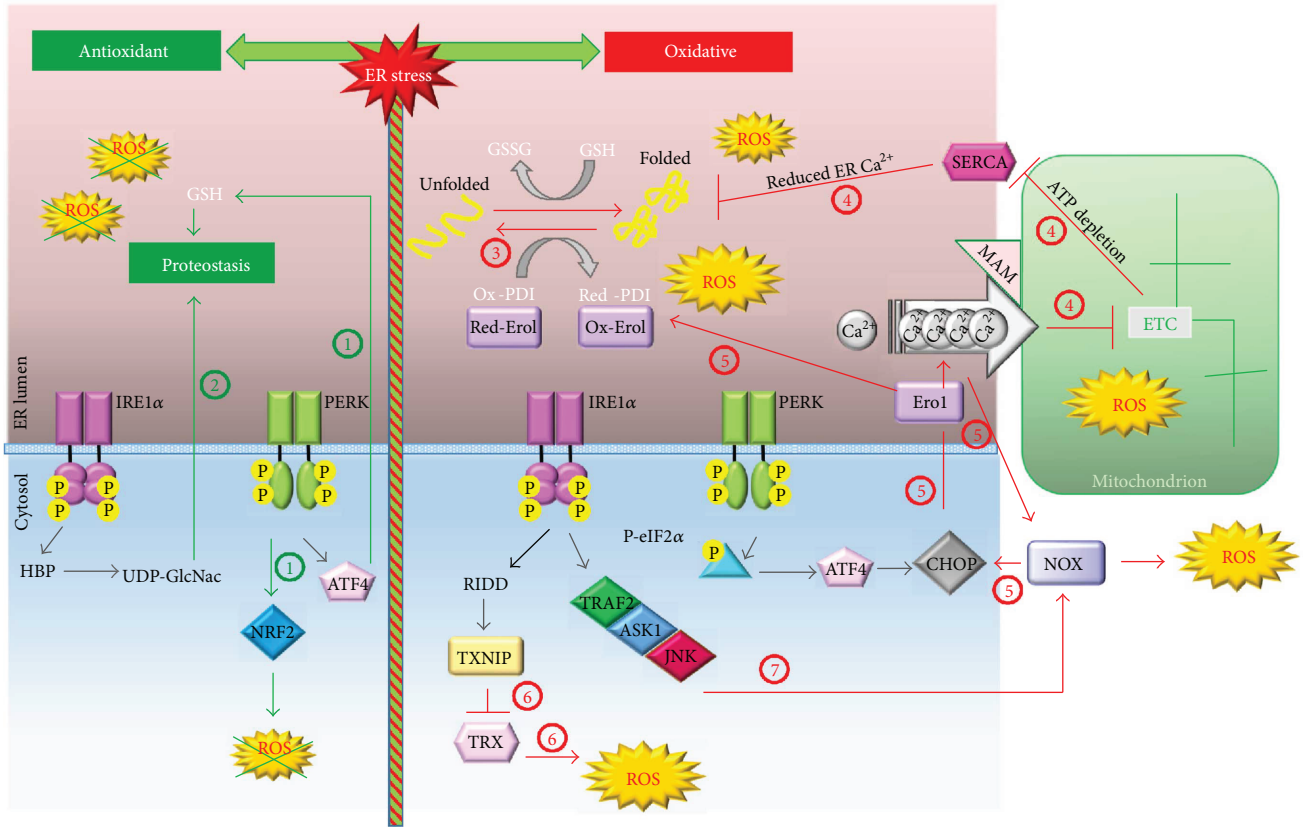

Figure 2: The oxidative and antioxidant programmes of UPR. The antioxidant (green lines) and oxidative (red lines) pathways of UPR are depicted on the left or on the right, respectively. The PERK and IRE1α/XBP1 pathways promote the maintenance of ER proteostasis as follows. (1) There is PERK-mediated activation of the antioxidant transcription factor NRF2 and the promotion of GSH synthesis [45]. (2) There is IRE1α/XBP1-mediated induction of the hexosamine biosynthetic pathway (HBP), which is important for the production of UDP-GlcNAc [41]. On the right, the ER stress-dependent amplification of ROS production (red lines) is depicted. (3) Following ER stress, the increased folding activity of ER augments ROS production. (4) The ER stress increases the MAM-mediated calcium flux to mitochondria that inhibits ETC and increases mitochondrial ROS production; moreover, reduced ATP synthesis from the impaired ETC affects SERCA activity and the consequent ER calcium content which in turn boosts up unfolding [143]. (5) CHOP, through the induction of Ero1, potentiates calcium efflux from the ER. The higher cytosolic calcium activates the Ca^{2+}/calmodulin-dependent protein kinase II- (CaMKII-) JNK-NOX-protein kinase R (PKR) pathway, which in turn positively feedbacks on CHOP expression [47, 57]. In addition, Ero1-increased expression potentiates the oxidative protein folding and ROS production. (6) Through microRNA inhibition, the RIDD activity of IRE1 relieves the expression of TXNIP protein that blocks the antioxidant enzyme TRX [50]. (7) IRE1α activates the tumor necrosis factor α-associated receptor 2 (TRAF2)/ASK1/JNK pathway that further upregulates the NOX-dependent ROS production [48, 144]. For detailed discussion and references, see the text. Red: reduced; Ox: oxidized; TRX: thioredoxin.

luminal domain of PERK and IRE1. In this way, by promoting oxidation of the three UPR sensors, ROS could modulate the UPR by inhibiting the ATF6 pathway and, simultaneously, potentiating the IRE1 and PERK pathways.

4. The Endoplasmic Reticulum/Mitochondria Axis for Reactive Oxygen Species Production

OS activated at the ER level can be transmitted in a Ca^{2+}-dependent manner to mitochondria with a consequent production of ROS. Mitochondria are connected to the ER through mitochondrial-associated ER membranes (MAMs) [53]. Across MAMs, ATP, Ca^{2+}, metabolites, and ROS are rapidly transmitted from the ER to mitochondria [54]. As a consequence, the sustained calcium influx from the ER into mitochondria triggers the opening of the permeability transition pore and the release of cytochrome C. Loss of cytochrome C impairs complex III of the mitochondrial ETC with the consequent increase of ROS production [55, 56]. Moreover, Ero1 that is transcriptionally induced by CHOP during the UPR potentiates the inositol-1,4,5-trisphosphate receptor (IP3R)-mediated Ca^{2+} leakage from the ER [57, 58]. Under these circumstances, ROS production could even be enhanced by other mechanisms. Firstly, the UPR induces the expression of a truncated isoform of SERCA pumps that increase Ca^{2+} transfer to mitochondria [59]. Then, impaired ETC affects ATP production inhibiting SERCA pumps [60]. Furthermore, the ER protein sigma-1 receptor dissociates from Bip/GRP78 following calcium depletion from ER and stabilizes IP3R at MAM leading

to a prolonged calcium signalling to mitochondria [61]. Next, PERK is uniquely enriched in MAMs and helps the tightening of ER-mitochondria contact sites during chronic ER stress facilitating calcium influx and ROS-mediated mitochondrial apoptosis [62, 63]. Nevertheless, ER Ca^{2+} pumps and IP3R or ryanodine receptor (RyR) channels are themselves influenced by the redox state of ER [64] together with the IP3 agonist of IP3R channels [65]. Thus, Ca^{2+}-mediated mitochondrial ROS production further enhances calcium release from ER, which in turn impairs Ca^{2+}-dependent chaperone activity and ER homeostasis, resulting in ER stress. Moreover, ROS themselves impair the ER oxidative protein folding. Indeed, the futile cycles of disulfide bond formation produce more ROS and, by depleting ATP, stimulate mitochondrial ROS production and so on. Taken together, these mechanisms create a vicious cycle of ER stress and mitochondrial dysfunction that boost each other and decide for apoptosis commitment.

5. Endoplasmic Reticulum Stress and the Unfolded Protein Response Pathways as Therapeutic Targets in the Oxidative Stress-Induced Endothelial Dysfunction

The role of the UPR pathways in the beginning of ED is a relatively recent area of investigation. Just over ten years ago Gargalovic et al. [66] were among the first to demonstrate the activation of UPR in human aortic endothelial cells exposed to oxidized phospholipids. In this work, it was demonstrated that the UPR factors ATF4 and XBP1 were both required for the activation of proinflammatory proteins and that the silencing of their expression abolished these effects. Although the authors did not demonstrate the mechanisms of the UPR induction by oxidised phospholipids, they hypothesised that an increase in OS could at least in part explain UPR activation and, in this way, they provided the first proof of the contribution of the ER stress in ED. Since then, several studies have shown the correlation of ER stress and UPR to ED in both animal and cellular models [67–70]. The failure of antioxidant therapy in decreasing cardiovascular risk in human clinical trials [71, 72] points up the importance to find new therapeutic approaches to counteract OS induced ED. Since ER stress is closely linked to OS, as discussed in depth in this review, targeting the UPR pathways or the ER stress could be a successful approach in the attempt to neutralise OS. Two possible approaches can be used to counteract OS-induced UPR. One is to modulate directly the activity of individual UPR mediators. Another consists of the activation of auxiliary pathways potentiating the adaptive response to ER stress to relieve unfolding. With reference to the last option, novel pharmacological inhibitors of ER stress-induced ED have been identified. One example is hyperhomocysteinemia. Hyperomocysteinemia is a cardiovascular risk factor associated with ED, atherosclerotic vascular diseases, and ischemic heart attacks [73]. It is well established that homocysteine (HC) induces ER stress by disrupting disulfide bond formation and that ER stress activates apoptosis in vascular cells through the upregulation of CHOP [74]. Instead, the activation of the PERK pathway of the UPR can induce endothelial detachment-mediated apoptosis through the overexpression of the T cell death-associated gene 51 (TDAG51) [75]. Recently, it has been reported that HC also impairs EDD following ER stress-mediated inhibition of the Ca^{2+}-activated potassium channel [76] and that the resveratrol analogue piceatannol displays a protective effect on HC-induced ED through the NRF2-mediated upregulation of heme oxygenase 1 (HO-1) [77]. In particular, pretreatment with piceatannol significantly reduced ER stress, homocysteine-induced apoptosis, and ROS production in endothelial cells [77]. Interestingly, many natural compounds can ameliorate ED through the reduction of ER stress-induced OS. As an example, black tea extracts improved endothelial-dependent relaxation and attenuated ROS production in HC-treated rat aortae and in cultured rat aortae cells through the suppression of ER stress both in HC- and angiotensin II-induced hypertension [78]. Another compound extracted from the Chinese herb barberine showed the ability to reduce endothelial-dependent contraction in carotid arteries from spontaneous hypertensive rats through the alleviation of ER stress, the reduction of ER stress-dependent ROS production, and the downregulation of the ROS-dependent expression of cyclooxygenase-2 (COX-2) [79]. This effect depended on the activation of AMP activated protein kinase (AMPK). AMPK is a protein involved in the control of energy status, whose induction has been correlated with the mitigation of ER stress in several studies [79–82]. The upregulation of AMPK is another putative way to induce an auxiliary pathway reducing ER stress. An example of the therapeutic effect of AMPK activation is the work by Li et al. [83], in which the natural triterpenoid ilexgenin A was found to be therapeutic in high-fat diet- (HFD-) fed mice and in endothelial cells stimulated with palmitate. In these models, ilexgenin A reduced ER stress and ER stress-dependent ROS generation through the inhibition of the NOD-like receptor family pyrin domain containing 3 (NLRP3) inflammasome and this effect depended on enhanced AMPK activity. Moreover, in HFD-fed mice the oral administration of ilexgenin A improved significantly endothelial function with the recovery of EDD and NO production [83]. These results strongly suggested that AMPK activation is helpful to reduce ER stress and ED and have triggered the study of new pharmacological inducers of AMPK. Among them, aminoimidazole carboxamide riboside (AICAR), salicylate, cycloastragenol, and astragaloside-IV inhibit ER stress-dependent ROS generation and the induction of NLRP3 inflammasome in various models of palmitate-induced ED [84, 85].

Although the molecular mechanism involved in AMPK-dependent mitigation of ER stress was not fully addressed, it could be possible that the key target of the AMPK action is the inhibition of the OS-generated upstream or downstream of the ER stress, so that this event is responsible for the TXNIP induction and NLRP3 inflammasome formation. In this regard, Li et al. [84] demonstrated that salicylate and AICAR, through the activation of AMPK, inhibited ROS production and the subsequent recruitment of the dynamin-related protein 1 (Drp1) on the mitochondrial membrane

preventing mitochondrial fission and ER stress, thus, linking mitochondrial dysfunction to ER stress and OS in the generation of endothelial disturbances. Previously, Dong et al. [80] demonstrated that the AMPK activation by AICAR, metformin, and simvastatin suppresses ER stress through the inhibition of NOX-derived ROS and SERCA oxidation in glycated and oxidized-LDL- (HOG-LDL-) induced ED. Metformin, in particular, is widely used in diabetic patients and has been shown to be a strong activator of AMPK in vasculature [86–89]. AMPK activation following metformin administration had a therapeutic effect on HFD-fed mice with the inhibition of ER stress and OS and the restoration of EDD and NO production [67]. These effects were mediated by the interaction with the proliferator-activated receptor δ (PPARδ) that is responsible for the upregulation of important pathways involved in lipid metabolism [67, 90]. Similarly, a recent work Choy et al. demonstrated that paeonol exerted a protective effect against tunicamycin-induced ER stress and the subsequent ED via activation of the AMPK/PPARδ signalling pathway [91]. AMPK activation and its beneficial effects on endothelium functions are also involved in the molecular activity of mangiferin. The xanthonoid mangiferin was shown to be effective in high-glucose-induced ED by inhibiting ER stress and ER stress-dependent OS, and as for other AMPK activators, the inhibition of NLRP3 inflammasome allowed restoration of NO production and endothelial homeostasis [92]. Still concerning high-glucose-induced ED, cobalt (III) protoporphyrin IX chloride (CoPP) prevented ER stress, reduced inflammation and apoptosis, and improved endothelium functions and angiogenesis through the induction of NO release and vascular endothelial growth factor A (VEGFA) expression [93]. All these effects were mediated by CoPP-mediated induction of HO-1 [93]. A variety of other novel inhibitors of ER stress including fenofibrate, salidroside, and sodium hydrogen sulfide also have shown to be effective in the restoration of ER stress-dependent ED [94–96].

Another promising approach to reduce ER stress is represented by the upregulation of the ER folding capacity of ER chaperones or by the use of chemical chaperones. Tauroursodeoxycholate (TUDCA) and sodium phenylbutyrate (PBA) are two chemical chaperones previously approved by the Food and Drug Administration (FDA) for the treatment of, respectively, primary biliary cirrhosis and urea-cycle disorders and several diseases associated to ER stress and OS [97–100]. Interestingly, TUDCA and PBA have also displayed cardioprotection effects and therapeutic function on some CVDs such as ischemia/reperfusion and atherosclerosis [101–103]. Regarding the potential use of TUDCA and PBA for the treatment of ED, Walsh et al. demonstrated that oral administration of TUDCA reduced hyperglycemia-induced ED in humans [104]. In addition, the extensive use of TUDCA and PBA as chemical inhibitors of ER stress revealed their ability to inhibit ER stress-dependent features of ED such as EDD reduction, reduced eNOS phosphorylation, inflammatory response, and ROS production in experimental models of ED including hypertension [70, 78, 105], hyperglycemia [106–108], hyperhomocysteinemia [77], and hyperlipidemia [83, 84].

Another therapeutic strategy to neutralise ER stress-induced ED is the modulation of Bip/GRP78, PDI or Ero1 activity. In particular, a screening study, aimed at the discovery of Bip/GRP78 inducers, identified the compound BIX (Bip inducer X). BIX was found to induce Bip/GRP78 expression via the ATF6 pathway and to have protective effects towards ER stress-dependent apoptosis of neuroblastoma cells [109]. More interestingly, BIX intracerebral administration in ischemic mice reduced the area of infarction suggesting its potential use also in an ischemic heart [109].

Another promising, therapeutic approach is the targeting of Ero1. With this regard, Blais et al. identified the small Ero1α inhibitor EN460, reporting that this molecule interacted specifically with the active form of Ero1α and prevented its reoxidation [110]. In the same work, the authors found that the continuous exposure to a low concentration of EN460 protected the ER stress-sensitive PERK^{-}/$^{-}$ mouse embryonic fibroblasts from the exposure to tunicamycin, suggesting the potential use of Ero1α inhibitors in the protection against the consequences of severe ER stress in mammalian cells.

Similarly, in the same year, Pal et al. demonstrated that curcumin and masoprocol preserved PDI from S-nitrosylation during cycles of OS, protecting its functional integrity [111]. In particular, curcumin is a recognised anti-inflammatory and antioxidant drug, whose beneficial effect is well known for several diseases including cancer, diabetes, neurological, and CVDs thanks to its capacity to augment the activity of different antioxidant enzymes other than PDI [112, 113]. Only recently, curcumin was found to inhibit ER stress, to reduce insulin resistance through the inhibition of the JNK/insulin receptor substrate-1 (IRS-1) signalling, and to promote autophagy in endothelial cells exposed to palmitate, thus emphasizing its possible therapeutic outcome in ED [114].

An alternative strategy for mitigating ER stress is the modulation of individual UPR pathways such as PERK/eukaryotic initiation factor 2α (eIF2α) and IRE1/XBP1. These compounds revealed potential therapeutic features in several diseases related to ER stress including neurodegenerative and metabolic disorders, cancer, inflammatory disorders, and finally CVDs [115, 116].

With regard to the modulators of the PERK/eIF2α axis, several small molecules have been identified. This class includes salubrinal, a small compound that prevents the dephosphorylation of eIF2α through the inhibition of GADD34 and CReP, the two enzymes that direct the activity of the eIF2α protein phosphatase PP1 [117]. Salubrinal showed powerful protection from ER stress in several conditions [117–119] including myocardial infarction [120, 121] and oxidized-LDL-mediated ED [122]. On the contrary, recent studies found that salubrinal could potentiate lipid-induced ER stress with cytotoxic outcome [123, 124] suggesting that salubrinal employment in CVDs has to be accurately evaluated in clinical conditions.

Similarly to salubrinal, guanabenz, which is FDA-approved for the treatment of hypertension, increases eIF2α phosphorylation during ER stress condition through the inhibition of the CReP/PP1 complex [125].

Among the molecules that act directly on the PERK protein, GSK2606414 and GSK2656157 inhibit PERK phosphorylation showing promising anticancer activity [126, 127] and reduced development of prion disease in prion-infected mice [128]. Recently, ex vivo treatment of mouse mesenteric arteries with GSK2606414 was found to counteract the positive effect on vascular function and eNOS phosphorylation deriving from the overexpression of a longevity-associated genetic variant of the bactericidal/permeability increasing fold-containing-family-B-member-4 (LAV-BPIFB4) [129]. This work suggests that the potential therapeutic use of GSK2606414 in CVD could be negated in patients carrying the LAV-BPIFB4 genetic variant. In addition, or as an alternative, to the modulation of PERK/eIF2α signalling, the inhibition of the IRE1/XBP1 pathway can also be achieved to impair UPR in ER stress-dependent diseases. IRE1/XBP1 signalling can be impaired by inhibiting either IRE1 kinase activity or IRE1 RNAse activity. STF-083010, 4μ8C, MKC-3946, toyocamycin, and salicylaldehydes are small molecules targeting IRE1α RNAse activity and blocking XBP1 mRNA splicing and regulated IRE1-dependent decay of mRNA (RIDD) [130–134]. In contrast, APY29 or sunitinib inhibited IRE1α kinase activity without affecting oligomerization and RNAse activity while both activities were impaired by compound 3 [135, 136].

Overall, the efficacy of these molecules has been tested in vitro and in few in vivo models of various diseases, and no data are available from models of CVD. However, given their therapeutic potential, it will be interesting to investigate their clinical and biological effects on animal and cellular models of ER stress-dependent ED and CVD.

6. Conclusive Remarks

CVDs represent the most common cause of death worldwide, and although the clinical management and the prevention strategies have improved remarkably, they are still a public health issue in developed countries. Therefore, the discovery of new targets for the development of innovative therapeutic approaches for CVDs remains a fundamental mission of medical science, also considering that in the future this matter will be even more critical in view of the rise in life-expectancy levels in the population.

In this review, we extensively discussed the connections between ER stress, UPR, and OS in the pathogenesis of CVDs derived from ED. Although many aspects are only in part clear, for example, the contribution of each of the three branches of UPR and how it changes in acute and chronic ED, the ER stress and its signalling response certainly represent a promising system to design new molecules and elaborate new therapeutic methodologies for the management of ED. In this context, we examined how the signalling pathways of the UPR could be modulated to establish therapeutic strategies to alleviate ED. Such a result has been achieved either by enhancing the antioxidative mechanisms or by inhibiting prooxidative properties of the UPR pathways. The choice between the two strategies depends on the different temporal outcomes of the adaptive response with regard to the prooxidative and proapoptotic response, the first being activated earlier and the second upon prolonged stress induction.

Another factor that should be taken into account might be the effect of UPR inhibition on other tissues not experiencing ER stress. For example, PERK expression is essential for pancreatic β cells, while IRE1α RIDD activity is expressed in basal conditions and is essential to maintain ER homeostasis [20, 137]. Moreover, unexpected effects could come by the inhibition of UPR transducers also in the targeted tissue. For example, the RIDD activity of IRE1 is crucial for the regulation of microRNA expression during UPR activation [138, 139]; therefore, inhibition of IRE1 RIDD activity could have deleterious effects on the expression of the microRNA targets. The conflicting data regarding UPR inhibition (such as those concerning salubrinal, as reported previously) reveal the complexity of UPR response and indicate that its modulation may exert both protective and toxic effects depending on the nature of the insult. These considerations highlight that future efforts are necessary to solve this puzzle in order to develop new clinical protocols for the management of ED.

Therefore, further studies are needed in order to define the optimal targets for each specific clinical condition, develop novel drugs, and prevent possible side effects deriving from the UPR perturbations.

Abbreviations

AICAR: Aminoimidazole carboxamide riboside
AMPK: AMP-activated protein kinase
ASK1: Apoptosis signal-regulating kinase 1
ATF4: Activating transcription factor 4
ATF6: Activating transcription factor 6
Bip/GRP78: Binding immunoglobulin protein/78 kDa glucose-regulated protein
BIX: Bip inducer X
BPIFB4: Bactericidal/permeability increasing fold-containing-family-B-member-4
CaMKII: Ca^{2+}/calmodulin-dependent protein kinase II
CHOP: C/EBP homologous protein
CoPP: Cobalt (III) protoporphyrin IX chloride
COX-2: Cyclooxygenase-2
CReP: Constitutive reverter of eIF2α phosphorylation
CVDs: Cardiovascular diseases
Drp1: Dynamin-related protein 1
ED: Endothelial dysfunction
EDD: Endothelium-dependent dilatation
eIF2α: Eukaryotic initiation factor 2α
eNOS: Endothelial NOS
ER: Endoplasmic reticulum
ERAD: ER-associated degradation
Ero1: ER oxidoreductase 1
ERQC: ER quality control
ETC: Electron transport chain
FDA: Food and drug administration
GADD34: Growth arrest and DNA damage-inducible protein

GSH: Glutathione
HBP: Hexosamine biosynthetic pathway
HC: Homocysteine
HFD: High-fat diet
HO-1: Heme oxygenase 1
HOG-LDL: Glycated and oxidized-LDL
IP3R: Inositol-1,4,5-trisphosphate receptor
IRE1: Inositol-requiring kinase 1
IRS-1: Insulin receptor substrate-1
ISR: Integrated stress response
JNK: c-Jun N-terminal kinase
KEAP1: Kelch-like ECH-associated protein 1
LAV-BPIFB4: Longevity-associated variant of BPIFB4
MAM: Mitochondrial-associated ER membranes
NLRP3: NOD-like receptor family pyrin domain containing 3
NO: Nitric oxide
NOS: Nitric oxide synthase
NOX: NADPH oxidase
NRF2: Nuclear factor erythroid 2-related factor 2
OS: Oxidative stress
PBA: Sodium phenylbutyrate
PDI: Protein disulfide isomerase
PDIA5: Protein disulfide isomerase A5
PDIA6: Protein disulfide isomerase A6
PERK: Pancreatic ER kinase
PKR: Protein kinase R
PP1: Protein phosphatase 1
PPARδ: Proliferator-activated receptor δ
RIDD: Regulated IRE1-dependent decay of mRNA
ROS: Reactive oxygen species
RyR: Ryanodine receptor
S1P: Site 1 protease
S2P: Site 2 protease
SERCA: Sarcoplasmic reticulum calcium transport ATPase
TDAG51: T cell death-associated gene 51
TRAF2: Tumor necrosis factor α-associated receptor 2
TRX: Thioredoxin
TUDCA: Tauroursodeoxycholate
TXNIP: Thioredoxin-interacting protein
UDP-GlcNAc: UDP-N-acetylglucosamine
UPR: Unfolded protein response
VEGFA: Vascular endothelial growth factor A
XBP1: X-box-binding protein 1.

Conflicts of Interest

The authors declare that there is no conflict of interest regarding the publication of this paper.

References

[1] W. L. Henrich, "Southwestern internal medicine conference: the endothelium—a key regulator of vascular tone," *The American Journal of the Medical Sciences*, vol. 302, no. 5, pp. 319–328, 1991.

[2] G. Jia, W. Durante, and J. R. Sowers, "Endothelium-derived hyperpolarizing factors: a potential therapeutic target for vascular dysfunction in obesity and insulin resistance," *Diabetes*, vol. 65, no. 8, pp. 2118–2120, 2016.

[3] M. Feletou and P. M. Vanhoutte, "Endothelial dysfunction: a multifaceted disorder (The Wiggers Award Lecture)," *American Journal of Physiology-Heart and Circulatory Physiology*, vol. 291, no. 3, pp. H985–H1002, 2006.

[4] M. Félétou, R. Köhler, and P. M. Vanhoutte, "Nitric oxide: orchestrator of endothelium-dependent responses," *Annals of Medicine*, vol. 44, no. 7, pp. 694–716, 2012.

[5] N. J. Alp and K. M. Channon, "Regulation of endothelial nitric oxide synthase by tetrahydrobiopterin in vascular disease," *Arteriosclerosis, Thrombosis, and Vascular Biology*, vol. 24, no. 3, pp. 413–420, 2004.

[6] S. Verma and T. J. Anderson, "Fundamentals of endothelial function for the clinical cardiologist," *Circulation*, vol. 105, no. 5, pp. 546–549, 2002.

[7] J. K. Liao, "Linking endothelial dysfunction with endothelial cell activation," *Journal of Clinical Investigation*, vol. 123, no. 2, pp. 540-541, 2013.

[8] M. E. Widlansky, N. Gokce, J. F. Keaney Jr., and J. A. Vita, "The clinical implications of endothelial dysfunction," *Journal of the American College of Cardiology*, vol. 42, no. 7, pp. 1149–1160, 2003.

[9] L. Liaudet, G. Vassalli, and P. Pacher, "Role of peroxynitrite in the redox regulation of cell signal transduction pathways," *Frontiers in Bioscience*, vol. 14, pp. 4809–4814, 2009.

[10] X. Tang, Y.-X. Luo, H.-Z. Chen, and D.-P. Liu, "Mitochondria, endothelial cell function, and vascular diseases," *Frontiers in Physiology*, vol. 5, p. 175, 2014.

[11] F. Chen, S. Haigh, S. Barman, and D. J. R. Fulton, "From form to function: the role of Nox4 in the cardiovascular system," *Frontiers in Physiology*, vol. 3, p. 412, 2012.

[12] A. F. Chen, D. D. Chen, A. Daiber et al., "Free radical biology of the cardiovascular system," *Clinical Science*, vol. 123, no. 2, pp. 73–91, 2012.

[13] M. G. Battelli, A. Bolognesi, and L. Polito, "Pathophysiology of circulating xanthine oxidoreductase: new emerging roles for a multi-tasking enzyme," *Biochimica et Biophysica Acta (BBA) - Molecular Basis of Disease*, vol. 1842, no. 9, pp. 1502–1517, 2014.

[14] M. A. Incalza, R. D'Oria, A. Natalicchio, S. Perrini, L. Laviola, and F. Giorgino, "Oxidative stress and reactive oxygen species in endothelial dysfunction associated with cardiovascular and metabolic diseases," *Vascular Pharmacology*, vol. 100, pp. 1–19, 2018.

[15] S. S. Cao and R. J. Kaufman, "Endoplasmic reticulum stress and oxidative stress in cell fate decision and human disease," *Antioxidants & Redox Signaling*, vol. 21, no. 3, pp. 396–413, 2014.

[16] J. D. Malhotra and R. J. Kaufman, "Endoplasmic reticulum stress and oxidative stress: a vicious cycle or a double-edged sword?," *Antioxidants & Redox Signaling*, vol. 9, no. 12, pp. 2277–2294, 2007.

[17] J. Hong, K. Kim, J.-H. Kim, and Y. Park, "The role of endoplasmic reticulum stress in cardiovascular disease and exercise," *International Journal of Vascular Medicine*, vol. 2017, Article ID 2049217, 9 pages, 2017.

[18] L. Cominacini, C. Mozzini, U. Garbin et al., "Endoplasmic reticulum stress and Nrf2 signaling in cardiovascular

diseases," *Free Radical Biology & Medicine*, vol. 88, Part B, pp. 233–242, 2015.

[19] F. Luchetti, R. Crinelli, E. Cesarini et al., "Endothelial cells, endoplasmic reticulum stress and oxysterols," *Redox Biology*, vol. 13, pp. 581–587, 2017.

[20] D. Ron and P. Walter, "Signal integration in the endoplasmic reticulum unfolded protein response," *Nature Reviews Molecular Cell Biology*, vol. 8, no. 7, pp. 519–529, 2007.

[21] L. Ellgaard and A. Helenius, "Quality control in the endoplasmic reticulum," *Nature Reviews Molecular Cell Biology*, vol. 4, no. 3, pp. 181–191, 2003.

[22] L. Plate and R. L. Wiseman, "Regulating secretory proteostasis through the unfolded protein response: from function to therapy," *Trends in Cell Biology*, vol. 27, no. 10, pp. 722–737, 2017.

[23] G. Amodio, R. Venditti, M. A. de Matteis, O. Moltedo, P. Pignataro, and P. Remondelli, "Endoplasmic reticulum stress reduces COPII vesicle formation and modifies Sec23a cycling at ERESs," *FEBS Letters*, vol. 587, no. 19, pp. 3261–3266, 2013.

[24] G. Amodio, L. Margarucci, O. Moltedo, A. Casapullo, and P. Remondelli, "Identification of cysteine ubiquitylation sites on the Sec23A protein of the COPII complex required for vesicle formation from the ER," *The Open Biochemistry Journal*, vol. 11, no. 1, pp. 36–46, 2017.

[25] J. Han and R. J. Kaufman, "Physiological/pathological ramifications of transcription factors in the unfolded protein response," *Genes & Development*, vol. 31, no. 14, pp. 1417–1438, 2017.

[26] M. Wang and R. J. Kaufman, "Protein misfolding in the endoplasmic reticulum as a conduit to human disease," *Nature*, vol. 529, no. 7586, pp. 326–335, 2016.

[27] M. Schröder and R. J. Kaufman, "ER stress and the unfolded protein response," *Mutation Research/Fundamental and Molecular Mechanisms of Mutagenesis*, vol. 569, no. 1-2, pp. 29–63, 2005.

[28] M. Schröder and R. J. Kaufman, "The mammalian unfolded protein response," *Annual Review of Biochemistry*, vol. 74, no. 1, pp. 739–789, 2005.

[29] P. Walter and D. Ron, "The unfolded protein response: from stress pathway to homeostatic regulation," *Science*, vol. 334, no. 6059, pp. 1081–1086, 2011.

[30] C. Hetz, "The unfolded protein response: controlling cell fate decisions under ER stress and beyond," *Nature Reviews Molecular Cell Biology*, vol. 13, no. 2, pp. 89–102, 2012.

[31] I. Tabas and D. Ron, "Integrating the mechanisms of apoptosis induced by endoplasmic reticulum stress," *Nature Cell Biology*, vol. 13, no. 3, pp. 184–190, 2011.

[32] D. Eletto, E. Chevet, Y. Argon, and C. Appenzeller-Herzog, "Redox controls UPR to control redox," *Journal of Cell Science*, vol. 127, no. 17, pp. 3649–3658, 2014.

[33] C. X. C. Santos, L. Y. Tanaka, J. Wosniak, and F. R. M. Laurindo, "Mechanisms and implications of reactive oxygen species generation during the unfolded protein response: roles of endoplasmic reticulum oxidoreductases, mitochondrial electron transport, and NADPH oxidase," *Antioxidants & Redox Signaling*, vol. 11, no. 10, pp. 2409–2427, 2009.

[34] B. P. Tu and J. S. Weissman, "Oxidative protein folding in eukaryotes," *The Journal of Cell Biology*, vol. 164, no. 3, pp. 341–346, 2004.

[35] S. Chakravarthi and N. J. Bulleid, "Glutathione is required to regulate the formation of native disulfide bonds within proteins entering the secretory pathway," *Journal of Biological Chemistry*, vol. 279, no. 38, pp. 39872–39879, 2004.

[36] D. M. Ferrari and H. D. Söling, "The protein disulphide-isomerase family: unravelling a string of folds," *Biochemical Journal*, vol. 339, no. 1, pp. 1–10, 1999.

[37] A. R. Frand and C. A. Kaiser, "The *ERO1* gene of yeast is required for oxidation of protein dithiols in the endoplasmic reticulum," *Molecular Cell*, vol. 1, no. 2, pp. 161–170, 1998.

[38] M. G. Pollard, K. J. Travers, and J. S. Weissman, "Ero1p: a novel and ubiquitous protein with an essential role in oxidative protein folding in the endoplasmic reticulum," *Molecular Cell*, vol. 1, no. 2, pp. 171–182, 1998.

[39] R. Ushioda, J. Hoseki, K. Araki, G. Jansen, D. Y. Thomas, and K. Nagata, "ERdj5 is required as a disulfide reductase for degradation of misfolded proteins in the ER," *Science*, vol. 321, no. 5888, pp. 569–572, 2008.

[40] H. P. Harding, Y. Zhang, H. Zeng et al., "An integrated stress response regulates amino acid metabolism and resistance to oxidative stress," *Molecular Cell*, vol. 11, no. 3, pp. 619–633, 2003.

[41] L. Vincenz and F. U. Hartl, "Sugarcoating ER stress," *Cell*, vol. 156, no. 6, pp. 1125–1127, 2014.

[42] Q. Ma, "Role of Nrf2 in oxidative stress and toxicity," *Annual Review of Pharmacology and Toxicology*, vol. 53, no. 1, pp. 401–426, 2013.

[43] H. Digaleh, M. Kiaei, and F. Khodagholi, "Nrf2 and Nrf1 signaling and ER stress crosstalk: implication for proteasomal degradation and autophagy," *Cellular and Molecular Life Sciences*, vol. 70, no. 24, pp. 4681–4694, 2013.

[44] K. Itoh, N. Wakabayashi, Y. Katoh, T. Ishii, T. O'Connor, and M. Yamamoto, "Keap1 regulates both cytoplasmic-nuclear shuttling and degradation of Nrf2 in response to electrophiles," *Genes to Cells*, vol. 8, no. 4, pp. 379–391, 2003.

[45] S. B. Cullinan, D. Zhang, M. Hannink, E. Arvisais, R. J. Kaufman, and J. A. Diehl, "Nrf2 is a direct PERK substrate and effector of PERK-dependent cell survival," *Molecular and Cellular Biology*, vol. 23, no. 20, pp. 7198–7209, 2003.

[46] S. J. Marciniak, C. Y. Yun, S. Oyadomari et al., "CHOP induces death by promoting protein synthesis and oxidation in the stressed endoplasmic reticulum," *Genes & Development*, vol. 18, no. 24, pp. 3066–3077, 2004.

[47] G. Li, C. Scull, L. Ozcan, and I. Tabas, "NADPH oxidase links endoplasmic reticulum stress, oxidative stress, and PKR activation to induce apoptosis," *The Journal of Cell Biology*, vol. 191, no. 6, pp. 1113–1125, 2010.

[48] F. Urano, X. Wang, A. Bertolotti et al., "Coupling of stress in the ER to activation of JNK protein kinases by transmembrane protein kinase IRE1," *Science*, vol. 287, no. 5453, pp. 664–666, 2000.

[49] S. Win, T. A. Than, J. C. Fernandez-Checa, and N. Kaplowitz, "JNK interaction with Sab mediates ER stress induced inhibition of mitochondrial respiration and cell death," *Cell Death & Disease*, vol. 5, no. 1, article e989, 2014.

[50] A. G. Lerner, J.-P. Upton, P. V. K. Praveen et al., "IRE1α induces thioredoxin-interacting protein to activate the NLRP3 inflammasome and promote programmed cell death under irremediable ER stress," *Cell Metabolism*, vol. 16, no. 2, pp. 250–264, 2012.

[51] D. Eletto, D. Eletto, D. Dersh, T. Gidalevitz, and Y. Argon, "Protein disulfide isomerase A6 controls the decay of IRE1α signaling via disulfide-dependent association," *Molecular Cell*, vol. 53, no. 4, pp. 562–576, 2014.

[52] A. Higa, S. Taouji, S. Lhomond et al., "Endoplasmic reticulum stress-activated transcription factor ATF6α requires the disulfide isomerase PDIA5 to modulate chemoresistance," *Molecular and Cellular Biology*, vol. 34, no. 10, pp. 1839–1849, 2014.

[53] A. R. van Vliet, T. Verfaillie, and P. Agostinis, "New functions of mitochondria associated membranes in cellular signaling," *Biochimica et Biophysica Acta (BBA) - Molecular Cell Research*, vol. 1843, no. 10, pp. 2253–2262, 2014.

[54] T. K. Rainbolt, J. M. Saunders, and R. L. Wiseman, "Stress-responsive regulation of mitochondria through the ER unfolded protein response," *Trends in Endocrinology & Metabolism*, vol. 25, no. 10, pp. 528–537, 2014.

[55] M. D. Brand, "The sites and topology of mitochondrial superoxide production," *Experimental Gerontology*, vol. 45, no. 7-8, pp. 466–472, 2010.

[56] J. St-Pierre, J. A. Buckingham, S. J. Roebuck, and M. D. Brand, "Topology of superoxide production from different sites in the mitochondrial electron transport chain," *Journal of Biological Chemistry*, vol. 277, no. 47, pp. 44784–44790, 2002.

[57] T. Anelli, L. Bergamelli, E. Margittai et al., "Ero1α regulates Ca^{2+} fluxes at the endoplasmic reticulum-mitochondria interface (MAM)," *Antioxidants & Redox Signaling*, vol. 16, no. 10, pp. 1077–1087, 2012.

[58] S. Kiviluoto, T. Vervliet, H. Ivanova et al., "Regulation of inositol 1,4,5-trisphosphate receptors during endoplasmic reticulum stress," *Biochimica et Biophysica Acta (BBA) - Molecular Cell Research*, vol. 1833, no. 7, pp. 1612–1624, 2013.

[59] M. Chami, B. Oulès, G. Szabadkai, R. Tacine, R. Rizzuto, and P. Paterlini-Bréchot, "Role of SERCA1 truncated isoform in the proapoptotic calcium transfer from ER to mitochondria during ER stress," *Molecular Cell*, vol. 32, no. 5, pp. 641–651, 2008.

[60] C. E. Moore, O. Omikorede, E. Gomez, G. B. Willars, and T. P. Herbert, "PERK activation at low glucose concentration is mediated by SERCA pump inhibition and confers preemptive cytoprotection to pancreatic β-cells," *Molecular Endocrinology*, vol. 25, no. 2, pp. 315–326, 2011.

[61] T. Hayashi and T. P. Su, "Sigma-1 receptor chaperones at the ER-mitochondrion interface regulate Ca^{2+} signaling and cell survival," *Cell*, vol. 131, no. 3, pp. 596–610, 2007.

[62] G. Csordás, C. Renken, P. Várnai et al., "Structural and functional features and significance of the physical linkage between ER and mitochondria," *The Journal of Cell Biology*, vol. 174, no. 7, pp. 915–921, 2006.

[63] T. Verfaillie, N. Rubio, A. D. Garg et al., "PERK is required at the ER-mitochondrial contact sites to convey apoptosis after ROS-based ER stress," *Cell Death & Differentiation*, vol. 19, no. 11, pp. 1880–1891, 2012.

[64] A. L. Chernorudskiy and E. Zito, "Regulation of calcium homeostasis by ER redox: a close-up of the ER/mitochondria connection," *Journal of Molecular Biology*, vol. 429, no. 5, pp. 620–632, 2017.

[65] S. Bánsághi, T. Golenár, M. Madesh et al., "Isoform- and species-specific control of inositol 1,4,5-trisphosphate (IP_3) receptors by reactive oxygen species," *Journal of Biological Chemistry*, vol. 289, no. 12, pp. 8170–8181, 2014.

[66] P. S. Gargalovic, N. M. Gharavi, M. J. Clark et al., "The unfolded protein response is an important regulator of inflammatory genes in endothelial cells," *Arteriosclerosis, Thrombosis, and Vascular Biology*, vol. 26, no. 11, pp. 2490–2496, 2006.

[67] W. S. Cheang, X. Y. Tian, W. T. Wong et al., "Metformin protects endothelial function in diet-induced obese mice by inhibition of endoplasmic reticulum stress through 5′ adenosine monophosphate-activated protein kinase-peroxisome proliferator-activated receptor δ pathway," *Arteriosclerosis, Thrombosis, and Vascular Biology*, vol. 34, no. 4, pp. 830–836, 2014.

[68] S. K. Choi, M. Lim, S. H. Byeon, and Y. H. Lee, "Inhibition of endoplasmic reticulum stress improves coronary artery function in the spontaneously hypertensive rats," *Scientific Reports*, vol. 6, no. 1, article 31925, 2016.

[69] S. K. Choi, M. Lim, S. I. Yeon, and Y. H. Lee, "Inhibition of endoplasmic reticulum stress improves coronary artery function in type 2 diabetic mice," *Experimental Physiology*, vol. 101, no. 6, pp. 768–777, 2016.

[70] M. Kassan, M. Galan, M. Partyka et al., "Endoplasmic reticulum stress is involved in cardiac damage and vascular endothelial dysfunction in hypertensive mice," *Arteriosclerosis, Thrombosis, and Vascular Biology*, vol. 32, no. 7, pp. 1652–1661, 2012.

[71] P. M. Kris-Etherton, A. H. Lichtenstein, B. V. Howard, D. Steinberg, J. L. Witztum, and Nutrition Committee of the American Heart Association Council on Nutrition, Physical Activity, and Metabolism, "Antioxidant vitamin supplements and cardiovascular disease," *Circulation*, vol. 110, no. 5, pp. 637–641, 2004.

[72] K. J. Williams and E. A. Fisher, "Oxidation, lipoproteins, and atherosclerosis: which is wrong, the antioxidants or the theory?," *Current Opinion in Clinical Nutrition and Metabolic Care*, vol. 8, no. 2, pp. 139–146, 2005.

[73] W. K. C. Lai and M. Y. Kan, "Homocysteine-induced endothelial dysfunction," *Annals of Nutrition and Metabolism*, vol. 67, no. 1, pp. 1–12, 2015.

[74] C. Zhang, Y. Cai, M. T. Adachi et al., "Homocysteine induces programmed cell death in human vascular endothelial cells through activation of the unfolded protein response," *Journal of Biological Chemistry*, vol. 276, no. 38, pp. 35867–35874, 2001.

[75] G. S. Hossain, J. V. van Thienen, G. H. Werstuck et al., "TDAG51 is induced by homocysteine, promotes detachment-mediated programmed cell death, and contributes to the development of atherosclerosis in hyperhomocysteinemia," *Journal of Biological Chemistry*, vol. 278, no. 32, pp. 30317–30327, 2003.

[76] X. C. Wang, W. T. Sun, C. M. Yu et al., "ER stress mediates homocysteine-induced endothelial dysfunction: modulation of IK_{Ca} and SK_{Ca} channels," *Atherosclerosis*, vol. 242, no. 1, pp. 191–198, 2015.

[77] J. S. Kil, S. O. Jeong, H. T. Chung, and H. O. Pae, "Piceatannol attenuates homocysteine-induced endoplasmic reticulum stress and endothelial cell damage via heme oxygenase-1 expression," *Amino Acids*, vol. 49, no. 4, pp. 735–745, 2017.

[78] W. San Cheang, C. Yuen Ngai, Y. Yen Tam et al., "Black tea protects against hypertension-associated endothelial

dysfunction through alleviation of endoplasmic reticulum stress," *Scientific Reports*, vol. 5, no. 1, article 10340, 2015.

[79] L. Liu, J. Liu, Z. Huang et al., "Berberine improves endothelial function by inhibiting endoplasmic reticulum stress in the carotid arteries of spontaneously hypertensive rats," *Biochemical and Biophysical Research Communications*, vol. 458, no. 4, pp. 796–801, 2015.

[80] Y. Dong, M. Zhang, S. Wang et al., "Activation of AMP-activated protein kinase inhibits oxidized LDL-triggered endoplasmic reticulum stress in vivo," *Diabetes*, vol. 59, no. 6, pp. 1386–1396, 2010.

[81] B. Liang, S. Wang, Q. Wang et al., "Aberrant endoplasmic reticulum stress in vascular smooth muscle increases vascular contractility and blood pressure in mice deficient of AMP-activated protein kinase-α2 in vivo," *Arteriosclerosis, Thrombosis, and Vascular Biology*, vol. 33, no. 3, pp. 595–604, 2013.

[82] K. Terai, Y. Hiramoto, M. Masaki et al., "AMP-activated protein kinase protects cardiomyocytes against hypoxic injury through attenuation of endoplasmic reticulum stress," *Molecular and Cellular Biology*, vol. 25, no. 21, pp. 9554–9575, 2005.

[83] Y. Li, J. Yang, M. H. Chen et al., "Ilexgenin A inhibits endoplasmic reticulum stress and ameliorates endothelial dysfunction via suppression of TXNIP/NLRP3 inflammasome activation in an AMPK dependent manner," *Pharmacological Research*, vol. 99, pp. 101–115, 2015.

[84] J. Li, Y. Wang, Y. Wang et al., "Pharmacological activation of AMPK prevents Drp1-mediated mitochondrial fission and alleviates endoplasmic reticulum stress-associated endothelial dysfunction," *Journal of Molecular and Cellular Cardiology*, vol. 86, pp. 62–74, 2015.

[85] Y. Zhao, Q. Li, W. Zhao et al., "Astragaloside IV and cycloastragenol are equally effective in inhibition of endoplasmic reticulum stress-associated TXNIP/NLRP3 inflammasome activation in the endothelium," *Journal of Ethnopharmacology*, vol. 169, pp. 210–218, 2015.

[86] J. W. Calvert, S. Gundewar, S. Jha et al., "Acute metformin therapy confers cardioprotection against myocardial infarction via AMPK-eNOS-mediated signaling," *Diabetes*, vol. 57, no. 3, pp. 696–705, 2008.

[87] H. Sasaki, H. Asanuma, M. Fujita et al., "Metformin prevents progression of heart failure in dogs: role of AMP-activated protein kinase," *Circulation*, vol. 119, no. 19, pp. 2568–2577, 2009.

[88] R. S. Hundal, M. Krssak, S. Dufour et al., "Mechanism by which metformin reduces glucose production in type 2 diabetes," *Diabetes*, vol. 49, no. 12, pp. 2063–2069, 2000.

[89] A. Gorrasi, A. Li Santi, G. Amodio et al., "The urokinase receptor takes control of cell migration by recruiting integrins and FPR1 on the cell surface," *PLoS One*, vol. 9, no. 1, article e86352, 2014.

[90] Y. X. Wang, C. H. Lee, S. Tiep et al., "Peroxisome-proliferator-activated receptor δ activates fat metabolism to prevent obesity," *Cell*, vol. 113, no. 2, pp. 159–170, 2003.

[91] K.-W. Choy, M. R. Mustafa, Y. S. Lau et al., "Paeonol protects against endoplasmic reticulum stress-induced endothelial dysfunction via AMPK/PPARδ signaling pathway," *Biochemical Pharmacology*, vol. 116, pp. 51–62, 2016.

[92] J. Song, J. Li, F. Hou, X. Wang, and B. Liu, "Mangiferin inhibits endoplasmic reticulum stress-associated thioredoxin-interacting protein/NLRP3 inflammasome activation with regulation of AMPK in endothelial cells," *Metabolism*, vol. 64, no. 3, pp. 428–437, 2015.

[93] T. Mori, T. Hayashi, E. Hayashi, and T. P. Su, "Sigma-1 receptor chaperone at the ER-mitochondrion interface mediates the mitochondrion-ER-nucleus signaling for cellular survival," *PLoS One*, vol. 8, no. 10, article e76941, 2013.

[94] Y. Lu, J. Cheng, L. Chen et al., "Endoplasmic reticulum stress involved in high-fat diet and palmitic acid-induced vascular damages and fenofibrate intervention," *Biochemical and Biophysical Research Communications*, vol. 458, no. 1, pp. 1–7, 2015.

[95] H. J. Hu, Z. S. Jiang, J. Qiu, S. H. Zhou, and Q. M. Liu, "Protective effects of hydrogen sulfide against angiotensin II-induced endoplasmic reticulum stress in HUVECs," *Molecular Medicine Reports*, vol. 15, no. 4, pp. 2213–2222, 2017.

[96] L. Zhu, F. Jia, J. Wei et al., "Salidroside protects against homocysteine-induced injury in human umbilical vein endothelial cells via the regulation of endoplasmic reticulum stress," *Cardiovascular Therapeutics*, vol. 35, no. 1, pp. 33–39, 2017.

[97] C. Ji, N. Kaplowitz, M. Y. Lau, E. Kao, L. M. Petrovic, and A. S. Lee, "Liver-specific loss of glucose-regulated protein 78 perturbs the unfolded protein response and exacerbates a spectrum of liver diseases in mice," *Hepatology*, vol. 54, no. 1, pp. 229–239, 2011.

[98] A. Ricobaraza, M. Cuadrado-Tejedor, S. Marco, I. Pérez-Otaño, and A. García-Osta, "Phenylbutyrate rescues dendritic spine loss associated with memory deficits in a mouse model of Alzheimer disease," *Hippocampus*, vol. 22, no. 5, pp. 1040–1050, 2012.

[99] U. Özcan, E. Yilmaz, L. Ozcan et al., "Chemical chaperones reduce ER stress and restore glucose homeostasis in a mouse model of type 2 diabetes," *Science*, vol. 313, no. 5790, pp. 1137–1140, 2006.

[100] P. Remondelli and M. Renna, "The endoplasmic reticulum unfolded protein response in neurodegenerative disorders and its potential therapeutic significance," *Frontiers in Molecular Neuroscience*, vol. 10, p. 187, 2017.

[101] C. Daosukho, Y. Chen, T. Noel et al., "Phenylbutyrate, a histone deacetylase inhibitor, protects against adriamycin-induced cardiac injury," *Free Radical Biology & Medicine*, vol. 42, no. 12, pp. 1818–1825, 2007.

[102] E. Erbay, V. R. Babaev, J. R. Mayers et al., "Reducing endoplasmic reticulum stress through a macrophage lipid chaperone alleviates atherosclerosis," *Nature Medicine*, vol. 15, no. 12, pp. 1383–1391, 2009.

[103] W. P. Cheng, B. W. Wang, and K. G. Shyu, "Regulation of GADD153 induced by mechanical stress in cardiomyocytes," *European Journal of Clinical Investigation*, vol. 39, no. 11, pp. 960–971, 2009.

[104] L. K. Walsh, R. M. Restaino, M. Neuringer, C. Manrique, and J. Padilla, "Administration of tauroursodeoxycholic acid prevents endothelial dysfunction caused by an oral glucose load," *Clinical Science*, vol. 130, no. 21, pp. 1881–1888, 2016.

[105] K. M. Spitler, T. Matsumoto, and R. C. Webb, "Suppression of endoplasmic reticulum stress improves endothelium-dependent contractile responses in aorta of the spontaneously hypertensive rat," *American Journal of Physiology-Heart and Circulatory Physiology*, vol. 305, no. 3, pp. H344–H353, 2013.

[106] H. Maamoun, M. Zachariah, J. H. McVey, F. R. Green, and A. Agouni, "Heme oxygenase (HO)-1 induction prevents endoplasmic reticulum stress-mediated endothelial cell death and impaired angiogenic capacity," *Biochemical Pharmacology*, vol. 127, pp. 46–59, 2017.

[107] M. Galán, M. Kassan, P. J. Kadowitz, M. Trebak, S. Belmadani, and K. Matrougui, "Mechanism of endoplasmic reticulum stress-induced vascular endothelial dysfunction," *Biochimica et Biophysica Acta (BBA) - Molecular Cell Research*, vol. 1843, no. 6, pp. 1063–1075, 2014.

[108] M. Galan, M. Kassan, S. K. Choi et al., "A novel role for epidermal growth factor receptor tyrosine kinase and its downstream endoplasmic reticulum stress in cardiac damage and microvascular dysfunction in type 1 diabetes mellitus," *Hypertension*, vol. 60, no. 1, pp. 71–80, 2012.

[109] T. Kudo, S. Kanemoto, H. Hara et al., "A molecular chaperone inducer protects neurons from ER stress," *Cell Death & Differentiation*, vol. 15, no. 2, pp. 364–375, 2008.

[110] J. D. Blais, K. T. Chin, E. Zito et al., "A small molecule inhibitor of endoplasmic reticulum oxidation 1 (ERO1) with selectively reversible thiol reactivity," *Journal of Biological Chemistry*, vol. 285, no. 27, pp. 20993–21003, 2010.

[111] R. Pal, E. A. Cristan, K. Schnittker, and M. Narayan, "Rescue of ER oxidoreductase function through polyphenolic phytochemical intervention: implications for subcellular traffic and neurodegenerative disorders," *Biochemical and Biophysical Research Communications*, vol. 392, no. 4, pp. 567–571, 2010.

[112] Y. He, Y. Yue, X. Zheng, K. Zhang, S. Chen, and Z. Du, "Curcumin, inflammation, and chronic diseases: how are they linked?," *Molecules*, vol. 20, no. 12, pp. 9183–9213, 2015.

[113] S. J. Hewlings and D. S. Kalman, "Curcumin: a review of its' effects on human health," *Food*, vol. 6, no. 10, p. 92, 2017.

[114] M. Ye, H. Qiu, Y. Cao et al., "Curcumin improves palmitate-induced insulin resistance in human umbilical vein endothelial cells by maintaining proteostasis in endoplasmic reticulum," *Frontiers in Pharmacology*, vol. 8, p. 148, 2017.

[115] S. S. Cao and R. J. Kaufman, "Targeting endoplasmic reticulum stress in metabolic disease," *Expert Opinion on Therapeutic Targets*, vol. 17, no. 4, pp. 437–448, 2013.

[116] C. Hetz, E. Chevet, and H. P. Harding, "Targeting the unfolded protein response in disease," *Nature Reviews Drug Discovery*, vol. 12, no. 9, pp. 703–719, 2013.

[117] M. Boyce, K. F. Bryant, C. Jousse et al., "A selective inhibitor of eIF2α dephosphorylation protects cells from ER stress," *Science*, vol. 307, no. 5711, pp. 935–939, 2005.

[118] D. Y. Lee, K. S. Lee, H. J. Lee et al., "Activation of PERK signaling attenuates Aβ-mediated ER stress," *PLoS One*, vol. 5, no. 5, article e10489, 2010.

[119] A. L. Sokka, N. Putkonen, G. Mudo et al., "Endoplasmic reticulum stress inhibition protects against excitotoxic neuronal injury in the rat brain," *Journal of Neuroscience*, vol. 27, no. 4, pp. 901–908, 2007.

[120] R.-J. Li, K.-L. He, X. Li, L.-L. Wang, C.-L. Liu, and Y.-Y. He, "Salubrinal protects cardiomyocytes against apoptosis in a rat myocardial infarction model via suppressing the dephosphorylation of eukaryotic translation initiation factor 2α," *Molecular Medicine Reports*, vol. 12, no. 1, pp. 1043–1049, 2015.

[121] Y. Liu, J. Wang, S. Y. Qi et al., "Reduced endoplasmic reticulum stress might alter the course of heart failure via caspase-12 and JNK pathways," *Canadian Journal of Cardiology*, vol. 30, no. 3, pp. 368–375, 2014.

[122] D. Hong, Y. P. Bai, H. C. Gao et al., "Ox-LDL induces endothelial cell apoptosis via the LOX-1-dependent endoplasmic reticulum stress pathway," *Atherosclerosis*, vol. 235, no. 2, pp. 310–317, 2014.

[123] M. Cnop, L. Ladriere, P. Hekerman et al., "Selective inhibition of eukaryotic translation initiation factor 2α dephosphorylation potentiates fatty acid-induced endoplasmic reticulum stress and causes pancreatic β-cell dysfunction and apoptosis," *Journal of Biological Chemistry*, vol. 282, no. 6, pp. 3989–3997, 2007.

[124] L. Ladrière, M. Igoillo-Esteve, D. A. Cunha et al., "Enhanced signaling downstream of ribonucleic acid-activated protein kinase-like endoplasmic reticulum kinase potentiates lipotoxic endoplasmic reticulum stress in human islets," *The Journal of Clinical Endocrinology & Metabolism*, vol. 95, no. 3, pp. 1442–1449, 2010.

[125] P. Tsaytler, H. P. Harding, D. Ron, and A. Bertolotti, "Selective inhibition of a regulatory subunit of protein phosphatase 1 restores proteostasis," *Science*, vol. 332, no. 6025, pp. 91–94, 2011.

[126] J. M. Axten, J. R. Medina, Y. Feng et al., "Discovery of 7-methyl-5-(1-{[3-(trifluoromethyl)phenyl]acetyl}-2,3-dihydro-1*H*-indol-5-yl)-7*H*-pyrrolo[2,3-*d*]pyrimidin-4-amine (GSK2606414), a potent and selective first-in-class inhibitor of protein kinase R (PKR)-like endoplasmic reticulum kinase (PERK)," *Journal of Medicinal Chemistry*, vol. 55, no. 16, pp. 7193–7207, 2012.

[127] C. Atkins, Q. Liu, E. Minthorn et al., "Characterization of a novel PERK kinase inhibitor with antitumor and antiangiogenic activity," *Cancer Research*, vol. 73, no. 6, pp. 1993–2002, 2013.

[128] J. A. Moreno, M. Halliday, C. Molloy et al., "Oral treatment targeting the unfolded protein response prevents neurodegeneration and clinical disease in prion-infected mice," *Science Translational Medicine*, vol. 5, no. 206, article 206ra138, 2013.

[129] F. Villa, A. Carrizzo, C. C. Spinelli et al., "Genetic analysis reveals a longevity-associated protein modulating endothelial function and angiogenesis," *Circulation Research*, vol. 117, no. 4, pp. 333–345, 2015.

[130] I. Papandreou, N. C. Denko, M. Olson et al., "Identification of an Ire1alpha endonuclease specific inhibitor with cytotoxic activity against human multiple myeloma," *Blood*, vol. 117, no. 4, pp. 1311–1314, 2011.

[131] K. Volkmann, J. L. Lucas, D. Vuga et al., "Potent and selective inhibitors of the inositol-requiring enzyme 1 endoribonuclease," *Journal of Biological Chemistry*, vol. 286, no. 14, pp. 12743–12755, 2011.

[132] B. C. S. Cross, P. J. Bond, P. G. Sadowski et al., "The molecular basis for selective inhibition of unconventional mRNA splicing by an IRE1-binding small molecule," *Proceedings of the National Academy of Sciences of the United States of America*, vol. 109, no. 15, pp. E869–E878, 2012.

[133] N. Mimura, M. Fulciniti, G. Gorgun et al., "Blockade of XBP1 splicing by inhibition of IRE1α is a promising therapeutic option in multiple myeloma," *Blood*, vol. 119, no. 24, pp. 5772–5781, 2012.

[134] M. Ri, E. Tashiro, D. Oikawa et al., "Identification of toyocamycin, an agent cytotoxic for multiple myeloma cells, as a

potent inhibitor of ER stress-induced XBP1 mRNA splicing," *Blood Cancer Journal*, vol. 2, no. 7, article e79, 2012.

[135] M. M. U. Ali, T. Bagratuni, E. L. Davenport et al., "Structure of the Ire1 autophosphorylation complex and implications for the unfolded protein response," *The EMBO Journal*, vol. 30, no. 5, pp. 894–905, 2011.

[136] L. Wang, B. G. K. Perera, S. B. Hari et al., "Divergent allosteric control of the IRE1α endoribonuclease using kinase inhibitors," *Nature Chemical Biology*, vol. 8, no. 12, pp. 982–989, 2012.

[137] M. Maurel, E. Chevet, J. Tavernier, and S. Gerlo, "Getting RIDD of RNA: IRE1 in cell fate regulation," *Trends in Biochemical Sciences*, vol. 39, no. 5, pp. 245–254, 2014.

[138] G. Amodio, E. Sasso, C. D'Ambrosio et al., "Identification of a microRNA (miR-663a) induced by ER stress and its target gene PLOD3 by a combined microRNome and proteome approach," *Cell Biology and Toxicology*, vol. 32, no. 4, pp. 285–303, 2016.

[139] S. Bartoszewska, K. Kochan, P. Madanecki et al., "Regulation of the unfolded protein response by microRNAs," *Cellular and Molecular Biology Letters*, vol. 18, no. 4, pp. 555–578, 2013.

[140] M. Calfon, H. Zeng, F. Urano et al., "IRE1 couples endoplasmic reticulum load to secretory capacity by processing the XBP-1 mRNA," *Nature*, vol. 415, no. 6867, pp. 92–96, 2002.

[141] K. M. Vattem and R. C. Wek, "Reinitiation involving upstream ORFs regulates *ATF4* m*RNA* translation in mammalian cells," *Proceedings of the National Academy of Sciences of the United States of America*, vol. 101, no. 31, pp. 11269–11274, 2004.

[142] K. Haze, H. Yoshida, H. Yanagi, T. Yura, and K. Mori, "Mammalian transcription factor ATF6 is synthesized as a transmembrane protein and activated by proteolysis in response to endoplasmic reticulum stress," *Molecular Biology of the Cell*, vol. 10, no. 11, pp. 3787–3799, 1999.

[143] A. Raturi, C. Ortiz-Sandoval, and T. Simmen, "Redox dependence of endoplasmic reticulum (ER) Ca^{2+} signaling," *Histology and Histopathology*, vol. 29, no. 5, pp. 543–552, 2014.

[144] H. Nishitoh, A. Matsuzawa, K. Tobiume et al., "ASK1 is essential for endoplasmic reticulum stress-induced neuronal cell death triggered by expanded polyglutamine repeats," *Genes & Development*, vol. 16, no. 11, pp. 1345–1355, 2002.

Hindawi
Oxidative Medicine and Cellular Longevity
Volume 2018, Article ID 5942916, 13 pages
https://doi.org/10.1155/2018/5942916

Research Article

Transplantation of Bone Marrow Mesenchymal Stem Cells Prevents Radiation-Induced Artery Injury by Suppressing Oxidative Stress and Inflammation

Yanjun Shen,[1,2] **Xin Jiang**,[3] **Lingbin Meng**,[4] **Chengcheng Xia**,[3] **Lihong Zhang**,[1] **and Ying Xin**[1]

[1]*Key Laboratory of Pathobiology, Ministry of Education, Jilin University, Changchun, China*
[2]*Department of Pathology, Shanxi Medical University, Taiyuan, China*
[3]*Department of Radiation Oncology, The First Hospital of Jilin University, Changchun, China*
[4]*Department of Internal Medicine, Florida Hospital, Orlando, USA*

Correspondence should be addressed to Ying Xin; xiny@jlu.edu.cn

Received 8 August 2017; Revised 16 October 2017; Accepted 16 December 2017; Published 28 February 2018

Academic Editor: Albino Carrizzo

The present study aims to explore the protective effect of human bone marrow mesenchymal stem cells (hBMSCs) on radiation-induced aortic injury (RIAI). hBMSCs were isolated and cultured from human bone marrow. Male C57/BL mice were irradiated with a dose of 18-Gy 6MV X-ray and randomly treated with either vehicle or hBMSCs through tail vein injection with a dose of 10^3 or 10^4 cells/g of body weight (low or high dose of hBMSCs) within 24 h. Aortic inflammation, oxidative stress, and vascular remodeling were assessed by immunohistochemical staining at 3, 7, 14, 28, and 84 days after irradiation. The results revealed irradiation caused aortic cell apoptosis and fibrotic remodeling indicated by aortic thickening, collagen accumulation, and increased expression of profibrotic cytokines (CTGF and TGF-β). Further investigation showed that irradiation resulted in elevated expression of inflammation-related molecules (TNF-α and ICAM-1) and oxidative stress indicators (4-HNE and 3-NT). Both of the low and high doses of hBMSCs alleviated the above irradiation-induced pathological changes and elevated the antioxidant enzyme expression of HO-1 and catalase in the aorta. The high dose even showed a better protective effect. In conclusion, hBMSCs provide significant protection against RIAI possibly through inhibition of aortic oxidative stress and inflammation. Therefore, hBMSCs can be used as a potential therapy to treat RIAI.

1. Introduction

Radiotherapy is an important treatment for malignant tumors. During the process, normal tissues surrounding the tumor would be irradiated and damaged. Therefore, when thoracic malignancies undergo radiotherapy, the thoracic aorta and other surrounding blood vessels are inevitably subject to radiation damage. Radiation-induced arterial injury (RIAI) was first reported in 1959 and considered as a chronic damage due to its insidious development for decades before the appearance of clinical symptoms [1]. Radiation exposure causes excessive production of eicosanoids, which are endogenous mediators of inflammatory reactions, such as vasodilation and vasoconstriction, increased vascular permeability and extravasation of leukocytes, microthrombus formation, and vascular endothelial apoptosis [2]. In large vessels, the main clinical manifestations of RIAI are atherosclerosis, stenosis, and obstruction [1]. It could occur in a variety of locations, including carotid artery [3], arteries of the upper limbs, axillary artery [4], and subclavian artery [5]. Previous studies have proved that the severity of large vessel injury was directly proportional to the dose and length of irradiation [6]. High-dose radiotherapy is a significant risk factor of accelerated carotid atherosclerotic disease [7].

Numerous clinical observations found that patients with RIAI suffered a lot and even died. For example, stroke cases were reported after radiotherapy to head and neck cancers [8]. Patients also suffered from angioplasty and

stenting due to the radiotherapy-related artery stenosis and thrombosis [4]. However, the clinical drugs of glucocorticoid, antibiotics, and anticoagulant are only effective for symptomatic relief of RIAI but invalid for prevention. Therefore, it is urgent to find effective methods to prevent or alleviate RIAI-induced symptoms.

Mesenchymal stem cells (MSCs) are considered as important seed cells in regenerative medicine due to its powerful capacities of cytokines secretion, immune regulation, and multiple differentiation potential [9]. MSCs can be derived from many tissues, such as umbilical cord blood, placenta, muscle, adipose tissue, and bone marrow. Among these, MSCs from bone marrow have the highest proliferative capacity and keep their pluripotency even after 50 passages [10]. More and more studies indicated that MSCs had the beneficial effects on vascular injury [11, 12]. MSCs orchestrate the repair process of injured vessels by various mechanisms such as transdifferentiation, microvesicles or exosomes, and secreting cytokines [13, 14]. MSCs can directly differentiate into endothelial cells to participate in angiogenesis [15] or migrate and home to the injured large blood vessel for vascular repair by regulating various cell cytokines, such as transforming growth factor beta (TGF-β), vascular endothelial growth factor (VEGF), and intercellular cell adhesion molecules (ICAM) [16, 17].

Radiation exposure causes vascular endothelial dysfunction, which leads to vascular inflammatory and oxidative stress [18]. MSCs have been revealed to have the anti-inflammatory function in the repairing process of vascular injuries [19]. Recently, studies also proved that MSCs provide protection against radiation-induced liver injury and radiation-induced proctitis by antioxidative and anti-inflammatory process to maintain the vascular endothelial function [20, 21]. MSC treatment also protected lungs from radiation-induced endothelial cell loss and vascular damage by restoring antioxidant enzyme superoxide dismutase 1 expression [22]. Most importantly, clinical trials have reported that intravenous administration of allogeneic human bone marrow MSCs (hBMSCs) is safe for patients [23]. Based on these, cellular therapy of hBMSCs will be a potential approach to treat RIAI. However, there is no publication to observe the therapeutic effect of hBMSCs on RIAI.

Therefore, the present study is designed to apply intravenous administration of hBMSCs to an established RIAI mouse model so as to evaluate hBMSCs' potential protective role against RIAI. This study will provide evidence to use the human MSCs as a treatment for RIAI.

2. Materials and Methods

2.1. Isolation and culture of hBMSCs. The protocol used in this experiment was approved by the Ethics Committee of the College of Basic Medical Sciences of Jilin University (Changchun, China). Written informed consent was obtained from healthy volunteers with age from 18 to 45. Samples of human bone marrow were collected from healthy volunteers by lumbar puncture in The First Hospital of Jilin University (Changchun, China). The hBMSCs were isolated and cultured as described in previous studies [10]. Briefly, bone mononuclear cells were isolated from human bone marrow by density gradient centrifugation in a Percoll solution (1.073 g/ml, Pharmacia, USA). The isolated cells (P0) were cultured in Dulbecco's Modified Eagle's Medium containing 5.6 mmol/L glucose (DMEM) with 10% fetal bovine serum (FBS, Invitrogen, Carlsbad, CA). 48 h later, the medium was changed to wash off the nonadherent cells. 8–12 days later, individual colonies were selected, trypsinized, and replated as the first passage culture (P1). Cells were passaged every 3-4 days, and hBMSCs at the 5th passage (P5) were harvested for identification and transplantation *in vivo*.

2.2. Flow Cytometry Analysis. P5 hBMSCs were incubated for 1 h at 4°C with the following mouse anti-human antibodies (diluted at 1 : 100): CD105, CD73 (BD Biosciences, Bedford, MA), CD166, CD44, CD34, CD45, and CD31(Neo Marker, Fremont, CA) then incubated with secondary antibodies of CY3 or FITC (Abcam, Cambridge, MA) for 30 min at 4°C. hBMSCs were then analyzed using a FACS Calibur flow cytometer (BD Biosciences, San Jose, CA, USA).

For cell cycle analysis, 1×10^7 hBMSCs at P5 were harvested, fixed in 70% ethanol for 20 min at 4°C, washed twice with PBS, and stained with 50 μg/ml propidium iodide (PI, BD Biosciences) at 4°C for 30 min in the dark. Samples were analyzed by FACS Calibur using Cell Quest software in 24 h.

2.3. Immunofluorescent Staining. The P5 hBMSCs were fixed with 4% formaldehyde, treated with 3% H_2O_2, blocked in 1%BSA, then incubated with monoclonal antibodies against CD44, CD73, CD166, and CD105 (BD Biosciences, Franklin Lakes, NJ, USA, 1 : 1000 dilution) at 4°C overnight, and then incubated with IgG conjugated with fluorescence CY3 or FITC (1 : 200). Fluorescence signals were observed by laser scanning confocal microscopy (Olympus FV500, Japan).

2.4. Adipogenic, Osteogenic, and Chondrogenic Differentiation of hBMSCs. To evaluate the multilineage differentiation potential, the cells were induced to differentiation in adipogenic, osteogenic, or chrondrogenic medium for 2–4 weeks according to the manufacturer's protocol [24]. Lipid droplets in the cells were stained with Oil Red O solution. Calcium deposition was assessed by von Kossa, and chondrogenic differentiation was identified by Alcian blue staining.

2.5. Establishment of RIAI Mouse Models and Cell Transplantation. One hundred and forty male C57BL/6 mice, at 8 weeks of age, were purchased from Beijing Experimental Animal Technical Co. LTD. (Beijing, China). Mice were housed in the Animal Center of Jilin University (Changchun, China). All animal procedures were approved by the Animal Care and Use Committee of the Chinese Academy of Medical Sciences (Beijing, China). To establish RIAI model, mice were fixed in supine position after anesthesia with sodium pentobarbital and irradiated by 6MV X-ray of 18Gy once when mice lungs were shielded with lead sheaths. For hBMSC treatment, mice were given a tail vein injection of hBMSCs with a low dose of 10^3 cells/g or a high dose of 10^4 cells/g of body weight within 24 h after radiation. Mice serving as vehicle controls were given the same volume of PBS. Therefore, the mice were evenly divided into four

groups ($n = 7$): the control group (control), the radiation group (IR), the radiation with low dose of the hBMSC group (IR + LD hBMSCs), and the radiation with high dose of the hBMSC group (IR + HD hBMSCs). At 3, 7, 14, 28, and 84 days after irradiation, mice were sacrificed with the heart perfusion of 4% phosphate-buffered formalin under anesthesia. Then the aortas were separated and fixed in 10% formalin. Each aorta of mice was average cut into 3 segments and embedded in one paraffin block and sectioned at 5 μm thickness for histological studies.

2.6. Histopathological Examination. Hematoxylin and eosin (HE) staining was performed to examine the morphological changes and the thickness of the aortic wall. The thickness of aorta presented as width from intima to adventitia was measured by the Digimizer software in 30 randomly selected fields from 3 segments per aorta with total 7 mice in each group.

For immunohistochemical staining, the aortic paraffin sections were dewaxed, rehydrated, and incubated with citric acid buffer at 98°C for antigen retrieval, then with 3% hydrogen peroxide and 5% animal serum treatments. Those sections were incubated with primary antibodies against TGF-β, connective tissue growth factor (CTGF), ICAM-1, and tumor necrosis factor-α (TNF-α) at 1 : 300 dilution, heme oxygenase 1 (HO-1) and catalase at 1 : 200 dilution, 4- hydroxynonenal (4-HNE) at 1 : 400 dilution (all from Santa Cruz Biotechnology, Santa Cruz, CA), and 3-Nitrotyosine (3-NT) at 1 : 400 dilution (Millipore, Billerica, CA), overnight at 4°C. After being washed, sections were incubated with horseradish peroxidase-conjugated secondary antibodies (1 : 300–400 dilutions with PBS) and then treated with peroxidase substrate DAB kit (Vector Laboratories, Inc., Burlingame, CA) for the development of color and counterstained with hematoxylin.

The quantitative analyses of these immunohistochemical staining were achieved from 7 mice of each group. Three sections at an interval of 10 sections from each aorta (per mouse) were selected and at least five high-power fields were randomly captured in each section. Image Pro Plus 6.0 software was used to transfer the staining density in the area of interest to an integrated optical density (IOD), and the ratio of IOD/area in the experimental group was presented as a fold relative to that of control.

2.7. Apoptosis Assay. Apoptosis in the aorta was assessed by TUNEL assay using Peroxidase In Situ Apoptosis Detection Kit S7100 (Millipore, Billerica, MA), according to the manufacturer's instructions. Under the microscope, the cells with dark-brown nuclei were positive and counted in 30 random microscopic fields from 3 segments per aorta with total 7 mice per group. The results were presented as TUNEL positive cells relative to 100 cells.

2.8. Sirius Red Staining for Collagen. Sirius red staining for collagen accumulation was performed to examine aortic fibrosis. Sections were stained with 0.1% Sirius red F3BA and Mayer's Hematoxylin and then assessed for the presence of collagen using a Nikon Eclipse E600 microscopy system.

2.9. Statistical Analysis. Data are presented as the means ± standard deviation (SD, $n = 7$). Statistical evaluation was analyzed with SPSS 17.0 software. One-way ANOVA was performed to compare differences between groups, followed by pairwise repetitive comparisons using Tukey's test. Statistical significance was considered as $P < 0.05$.

3. Results

3.1. Morphology and Features of hBMSCs. 2 weeks after isolation and culture by density gradient centrifugation combined with individual colonies screening, P1 hBMSCs reached 80% confluence and then were passaged every 4-5 days for 9–12th passages without morphologic alteration. hBMSCs displayed fibroblast-like shape and homogenous and vortex-like growth in monolayers (Figure 1(a)). Cell cycle analysis revealed that P5 hBMSCs in quiescent phase of G_0/G_1 was 86.65 ± 2.8%, and in active proliferative phase of $S + G_2/M$ was 14.35 ± 2.8% (Figure 1(b)), with typical stem cell proliferation characteristics. Flow cytometry analysis of surface antigens on P5 hBMSCs showed that more than 90% of cells expressed CD44, CD73, CD166, and CD105, but less than 2% expressed CD34, CD31, and CD45 (Figure 1(c)). Immunofluorescence staining also confirmed these results (Figure 1(d)). Cultured in adipogenic medium for 2 weeks, P5 hBMSCs differentiated into adipogenic cells as shown by positive Oil Red O staining (Figure 1(e), upper). hBMSCs cultured in osteogenic medium for 3 weeks formed mineral deposits as demonstrated by positive von Kossa staining (Figure 1(e), down left). After induction for 3 weeks in chondrogenic medium, Alcian blue staining showed that hBMSCs expressed proteoglycan, an indicative of chondrogenic differentiation (Figure 1(e), down right). These results indicated that the cultured cells with relative homogeneity exhibited the characteristics of hBMSCs.

3.2. hBMSCs Alleviated Radiation-Induced Aortic Remodeling. Aortic pathological changes were firstly examined by H&E staining (Figure 2(a)), which displayed significantly increased tunica media thickness in the IR group mice at 7, 14, and 28 days after irradiation and slight-increased thickness at 84 days without significant difference, as compared with the controls. Meanwhile, low or high dose of hBMSC treatment could largely prevent those increased aortic thickening induced by radiation (Figure 2(a)) at each time point. Sirius red staining also revealed an increased collagen accumulation in aortic tunica media at 14, 28, and 84 days after exposure to 6MV X-ray (Figure 2(b)). High dose of hBMSC treatment significantly inhibited radiation-induced collagen accumulation in aortas on day 14, 28, and 84, while the inhibitory effect in low dose of the hBMSC treatment group was only observed on day 84. To further detect the effect of hBMSCs on radiation-induced aortic fibrosis, immunohistochemical staining for protein levels of profibrotic mediators, CTGF (Figure 3(a)) and TGF-β (Figure 3(b)) were measured. Compared with control mice, aortic CTGF and TGF-β levels in the IR group mice were all significantly increased on day 3, 7, 14, 28, and 84. Low dose of hBMSCs could prevent the increased CTGF expression in the aortas induced by

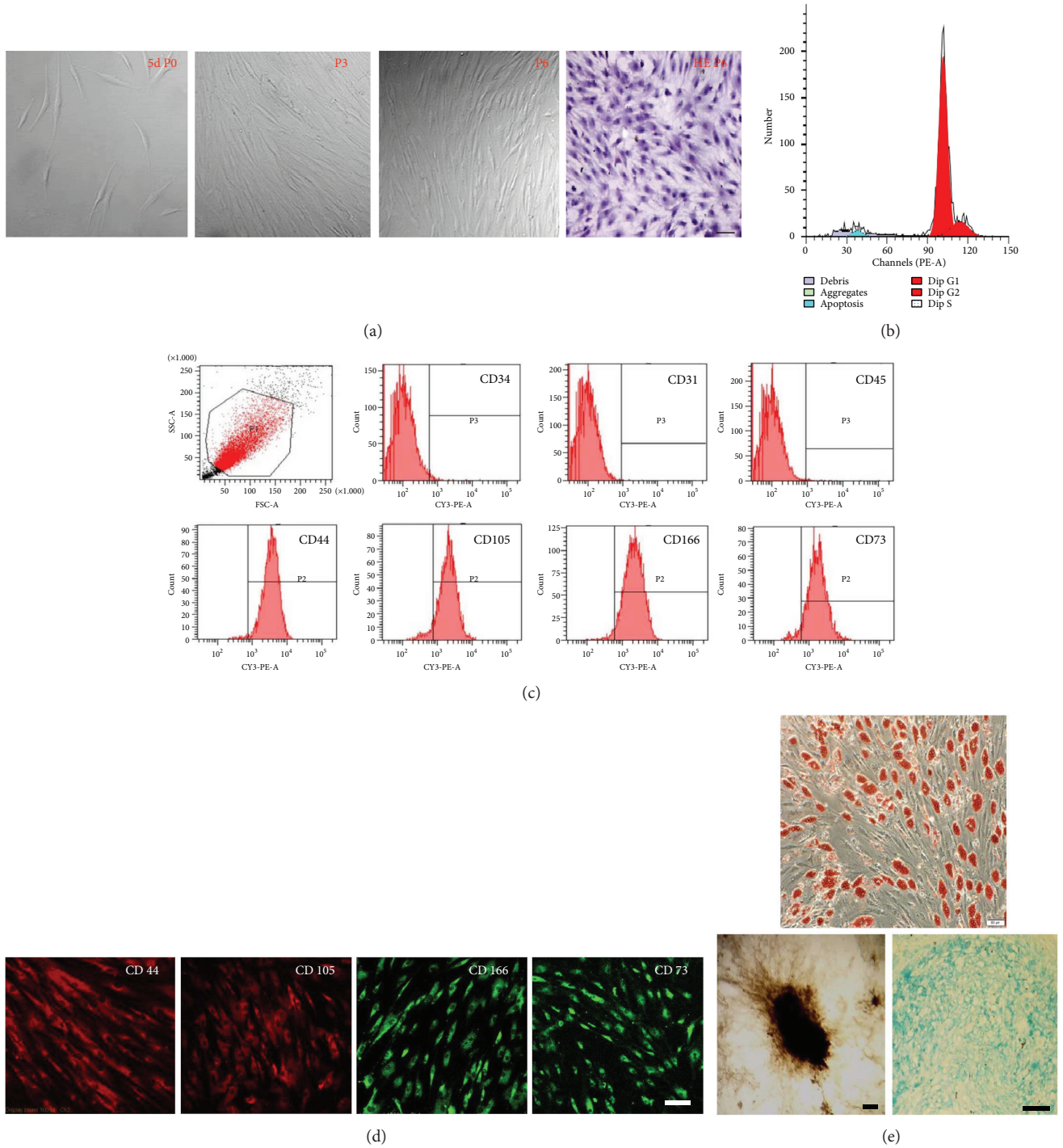

Figure 1: Morphology and features of human bone marrow mesenchymal stem cells (hBMSCs). (a) The morphological features of cultured hBMSCs at the 5th day; the 3rd and 6th passages (P3 and P6) were evaluated by the light microscope or HE staining. (b) Cell cycle analysis by FACS showed that (86.65% ± 2.8%) of P5 hBMSCs was in the G_0/G_1 phase and (14.35% ± 2.8%) was in the S + G_2/M phase. (c) Flow cytometry analysis disclosed that more than 90% of P5 hBMSCs were positive for CD44, CD105, CD166, and CD73; however, they were negative for CD34, CD31, and CD45. (d) Immunofluorescence staining revealed that P5 hBMSCs expressed the antigens of CD73, CD44, CD105, and CD166. (e) hBMSCs differentiated into adipose cells that formed lipid droplets in the cytoplasm, indicated by positive Oil Red staining (upper). The differentiation of hBMSCs to bone was demonstrated by positive von Kossa staining (bottom left). The differentiation to cartilage was reflected by positive Alcian blue staining (bottom right). Scale bar, 50 μm.

radiation on day 14, 28, and 84, while the inhibitory effect of high dose of hBMSCs was observed as early as day 7 (Figure 3(a)). Increased aortic TGF-β expression induced by radiation was obviously suppressed by both low and high dose of hBMSC treatment at each time point (Figure 3(b)). Moreover, high dose of hBMSCs showed the stronger

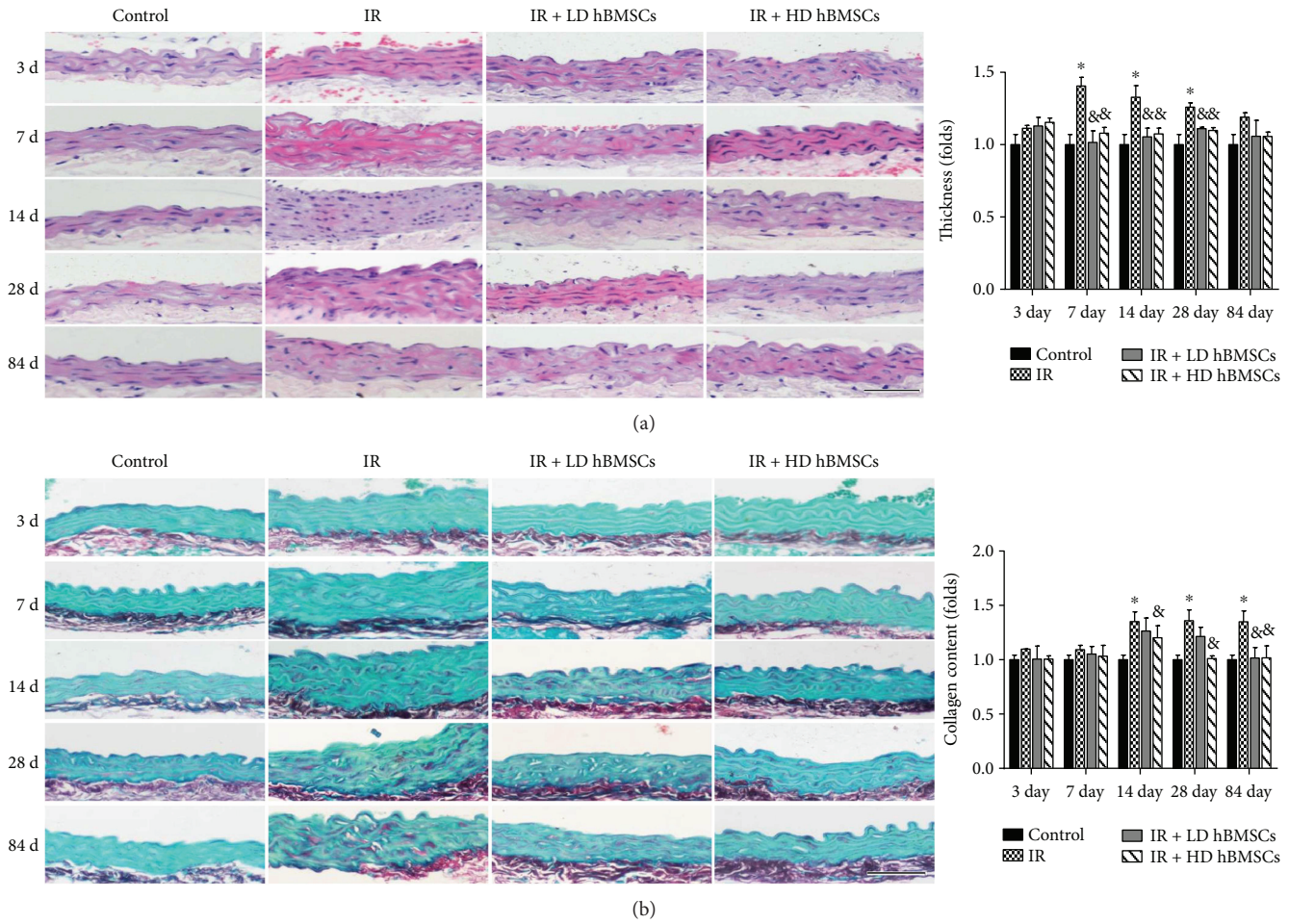

FIGURE 2: hBMSCs alleviated radiation-induced aortic pathological changes. Male C57BL/6 mice were irradiated by 6MV X-ray of 18Gy once with their lungs were shielded to establish the RIAI model. hBMSCs were injected by tail vein in a dose of 10^3 or 10^4 cells/g of body weight within 24 h after radiation. Therefore, the mice were evenly divided into four groups: the control group (control), the radiation group (IR), the radiation with low or high dose of the hBMSC group (IR + LD hBMSCs and IR + HD hBMSCs). At 3, 7, 14, 28, and 84 days after radiation, the aortas were isolated for histological studies. The pathological changes of aortas were examined by HE staining (a) and the accumulation of collagen was detected by Sirius red staining (b), followed by semiquantitative analysis. Data were presented as means ± SD ($n = 7$). $^*P < 0.05$ versus control group; $^{\&}P < 0.05$ versus IR group; $^{\#}P < 0.05$ versus IR + LD hBMSC group. Scale bar, 50 μm.

inhibitory effect on those two profibrotic mediators than low dose of hBMSCs (Figures 3(a) and 3(b)).

3.3. hBMSCs Reduced Radiation-Induced Aortic Inflammation. Previous studies have suggested sustained inflammatory response occurs in irradiated human arteries [25]. Regarding inflammation as the primary risk factor for vascular endothelium remodeling, the protein levels of TNF-α (Figure 4(a)) and ICAM-1 (Figure 4(b)) were examined by immunohistochemical staining. Compared to the control group, aortic TNF-α expression in the IR group mice was significantly increased on day 7 and then progressively decreased. The difference between the two groups was still remarkable until day 28. Low or high dose of hBMSC treatment prevented increased TNF-α expression in IR groups (Figure 4(a)). It was also noticed that ICAM-1 expression in aortas was significantly increased at 3, 7, 14, 28, and 84 days after exposure to X-ray. This increase was significantly reduced by high dose of hBMSC treatment. The inhibitory effect of low dose of hBMSCs on ICAM-1 expression was only observed on day 7 and 28 (Figure 4(b)).

3.4. hBMSCs Attenuated Radiation-Induced Aortic Oxidative Damage. Oxidative damage was detected by examining the accumulation of 4-HNE (Figure 5(a)) and 3-NT (Figure 5(b)) as indices of lipid peroxidation and protein nitration, respectively. Results of immunohistochemical staining showed a significant accumulation of 3-NT and 4-HNE in the aortas of irradiated mice on day 3, 7, 14, 28, and 84. High dose of hBMSC treatment significantly inhibited the radiation-induced expression of 3-NT and 4-HNE from 7 days to 84 days, while low dose of hBMSCs showed the inhibitory effect on 4-HNE only at day 14, as well as on 3-NT at day 7. On day 14 and 28, high dose of hBMSCs shows a stronger inhibitory effect on 3-NT (Figure 5(b)) than low dose of hBMSCs, while no difference was observed on 4-HNE expression between those two groups.

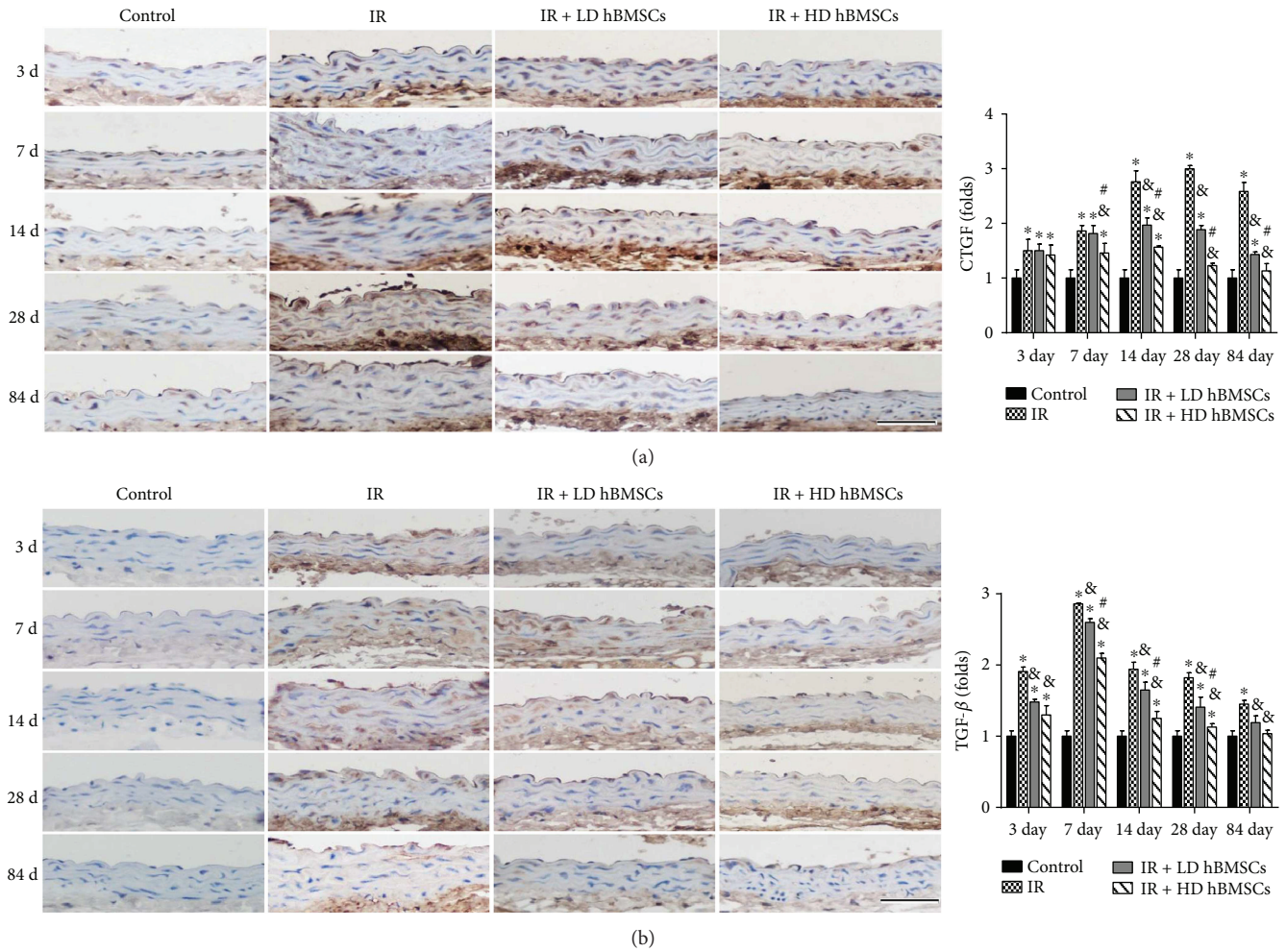

Figure 3: hBMSCs alleviated radiation-induced aortic fibrosis. Aortic fibrosis was examined by immunohistochemical staining for the expression of CTGF (a) and TGF-β (b), followed by semiquantitative analysis. Data were presented as means ± SD ($n = 7$). $^{*}P < 0.05$ versus control group; $^{\&}P < 0.05$ versus IR group; $^{\#}P < 0.05$ versus IR + LD hBMSC group. Scale bar, 50 μm.

3.5. hBMSCs Reduced Radiation-Induced Aortic Cell Apoptosis. Effect of radiation and hBMSCs on aortic cell apoptosis was evaluated by TUNEL staining (Figure 6). The results showed that cell apoptosis in aortas of irradiated mice was significantly increased compared with that in control mice on day 3, 7, 14, 28, and 84 but was reduced by low or high dose of hBMSC treatment. Moreover, compared with the LD hBMSC group, HD hBMSCs revealed a stronger inhibitory effect on radiation-induced aortic cell apoptosis, indicated by a lower TUNEL positive ratio on day 7, 14, 28, and 84 (Figure 6).

3.6. hBMSC Upregulated Antioxidant Enzymes Expression of HO-1 and Catalase in Aortas. Since hBMSCs attenuated radiation-induced aortic oxidative damage (Figure 5), whether this protective effect of hBMSCs on the aorta is associated with upregulation of antioxidant enzymes was examined first by measuring HO-1 and catalase expression with immunohistochemical staining (Figure 7). The results showed that compared with the control group, HO-1 expression was significantly increased in the aorta of the IR group and hBMSC group mice at each time point (Figure 7(a)). There was a further increase of the HO-1 expression in the aorta of low and high dose of hBMSC treatment mice compared with the IR group (Figure 7(a)). Moreover, it was shown that catalase expression in the aorta of irradiated mice was significantly decreased compared with that in control mice on day 3, 7, 14, 28, and 84 but was significantly elevated by low or high dose of hBMSC treatment (Figure 7(b)).

4. Discussion

In the present study, we have explored for the first time the protective effects of bone marrow mesenchymal stem cells on radiation-induced pathological changes and damage in the aorta. We demonstrated the establishment of RIAI mouse model by evaluating the aortic thickening, fibrotic remodeling, inflammation, oxidative stress and cell apoptosis. We showed low or high dose of hBMSC treatment can partially reverse radiation-induced pathologic changes in aortas and the high dose of hBMSCs has even a better protective effect.

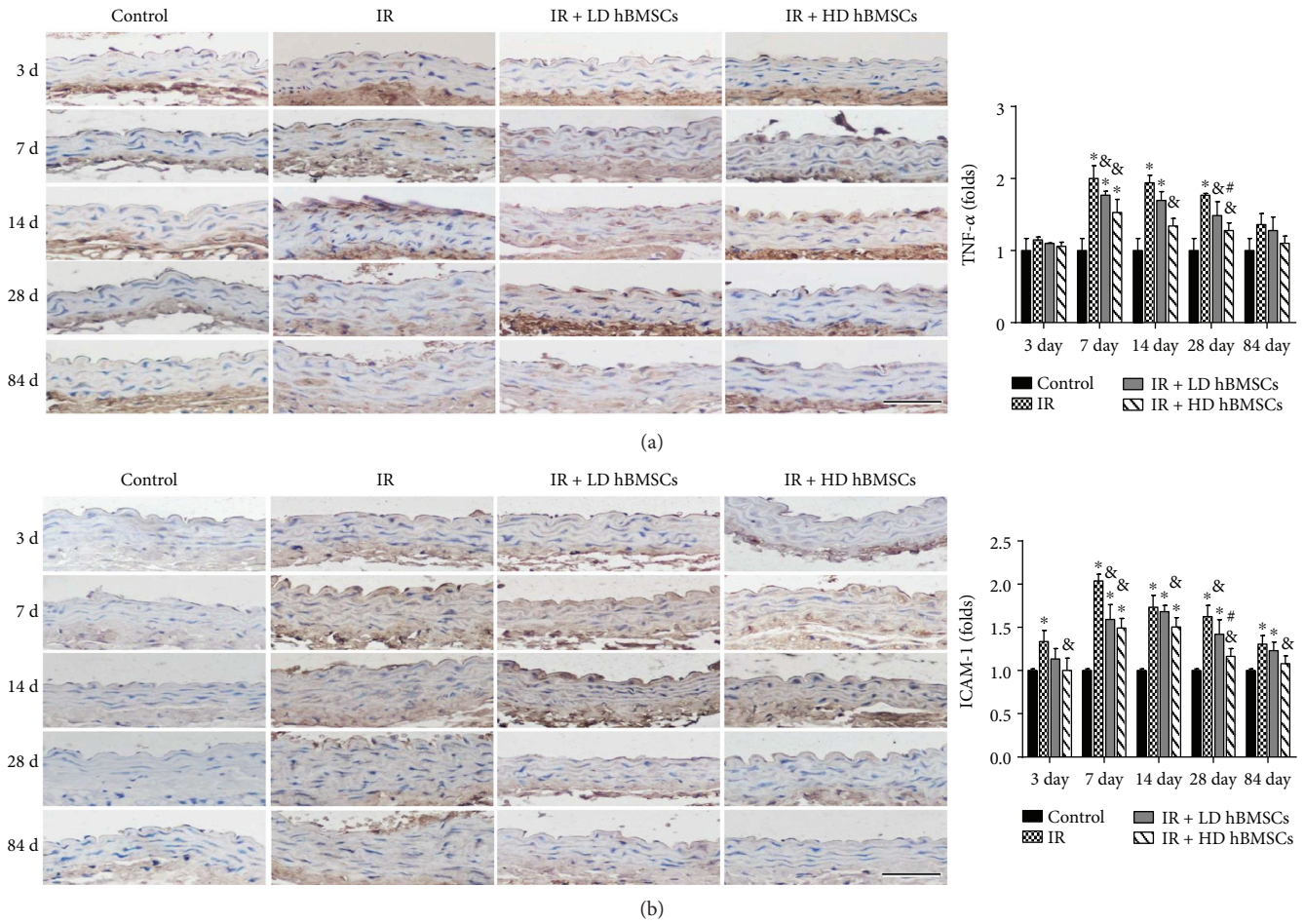

Figure 4: hBMSCs reduced radiation-induced aortic inflammation. Aortic inflammation was examined by immunohistochemical staining for the expression of TNF-α (a) and ICAM-1 (b), followed by semiquantitative analysis. Data were presented as means ± SD ($n = 7$). $^{*}P < 0.05$ versus control group; $^{\&}P < 0.05$ versus IR group; $^{\#}P < 0.05$ versus IR + LD hBMSC group. Scale bar, 50 μm.

Based on the ability to adhere to plastic culture dishes, MSCs derived from human adult bone marrow of healthy donors were selected [24]. In our study, to get more uniform hBMSCs, individual colonies were selected and expanded after the original seeding for 8–12 days. The flow cytometry analysis showed that the cultured P5 cells expressed mesenchymal stem cell markers of CD73, CD105, CD44, and CD166 but were negative for hematopoietic stem/progenitor cell marker of CD34, endothelial cell marker of CD31, and leukocyte cell marker of CD45. The cell cycle analysis demonstrated that more than 86% of P5 cells were in quiescent phase (G_0/G_1phase). Meanwhile, the isolated cells exhibited their capacity to undergo adipogenic, chondrogenic, and osteogenic differentiation (Figure 1). These results fully confirmed the obtained hBMSCs were highly homogenous and pluripotent and therefore could be used as seed cells for the following experiments.

Previous studies have investigated irradiation to carotid arteries of ApoE^{-}/$^{-}$mice induced inflammatory and thrombotic responses *in vivo* with various radiation doses [26]. Based on those references, C57/BL mice were radiated with a single dose of 18Gy X-ray to establish RIAI mice models in our study. RIAI in our mice model was successfully developed, indicated by significant increases of aortic remodeling and cell apoptosis, as well as aortic, inflammation, and oxidative stress.

MSCs have been reported to repair the injured vascular wall [12] and play a local immunomodulation on injured rat carotids [11]. Yang et al. also confirmed that BMSC transplantation through tail vein injection promotes angiogenesis and VEGF expression in rats [27]. However, previous studies also revealed that different doses of MSCs could exert different effects *in vivo*. Appropriate dose of MSCs was required for successful transplantation and improvement of functional properties [28]. In addition, a higher incidence of adverse events may occur in a high-dose MSC treatment. For example, intravenous administration of a high-dose MSC (5.0×10^5 and 1.0–3.0×10^6 cells/mice) induced a lethal portal vein or pulmonary embolism [29, 30]. Therefore, the doses of 1×10^3 and 1×10^4 cells/g of mice body weight (approximate to 2.0×10^4 and 2.0×10^5 cells/g) were chosen in the present study, which were also supported by a previous study [31]. Similarly, no embolism and related death were observed in the present study. Our data demonstrated that both doses of hBMSCs had partially prevented the radiation-induced aortic injury, including the aortic cell

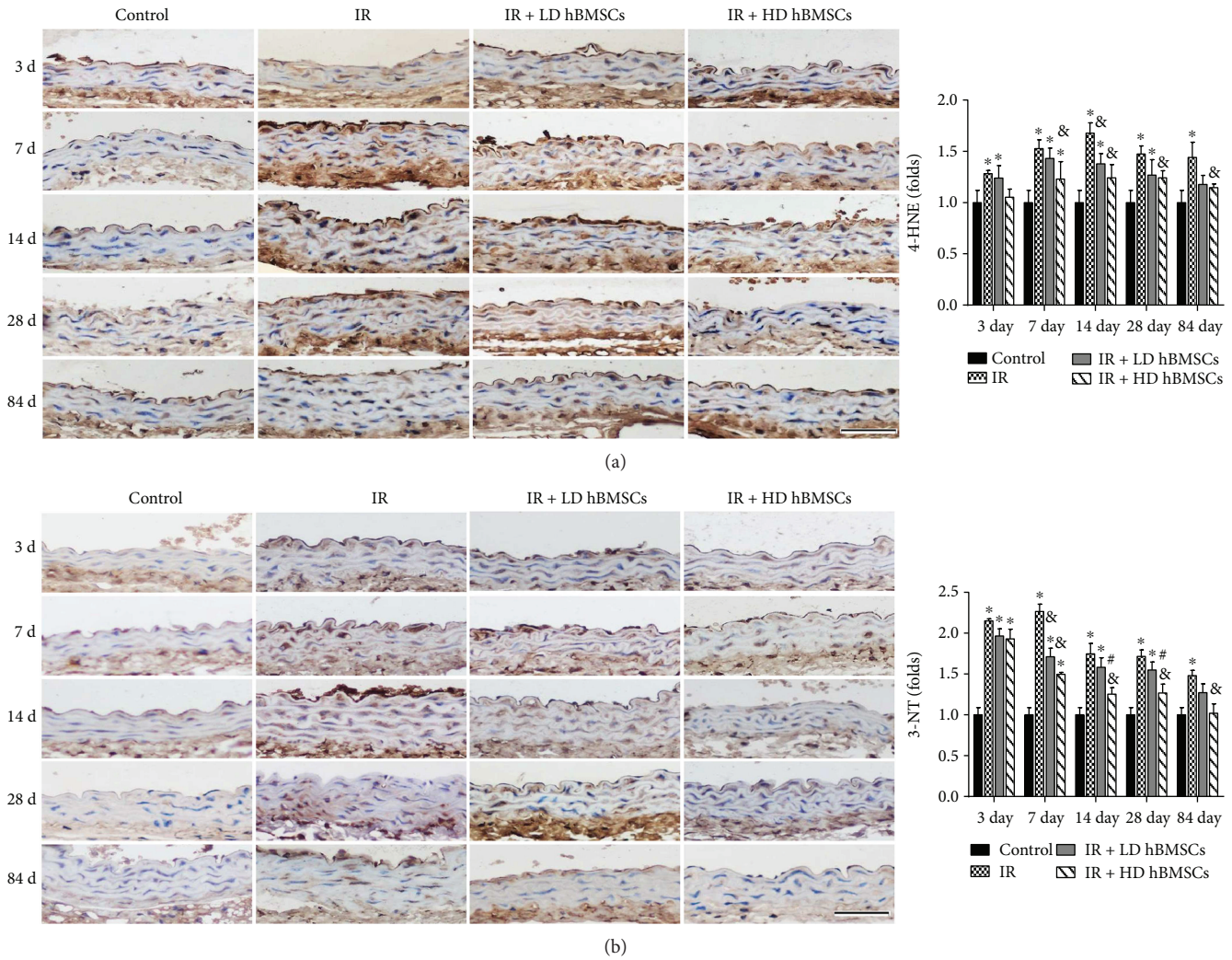

Figure 5: hBMSCs attenuated radiation-induced aortic oxidative damage. Aortic oxidative damage was examined by immunohistochemical staining for the expressions of 4-HNE (a) and 3-NT (b), followed by semiquantitative analysis. Data were presented as means ± SD ($n = 7$). $^{*}P < 0.05$ versus control group; $^{\&}P < 0.05$ versus IR group; $^{\#}P < 0.05$ versus IR + LD hBMSC group. Scale bar, 50 μm.

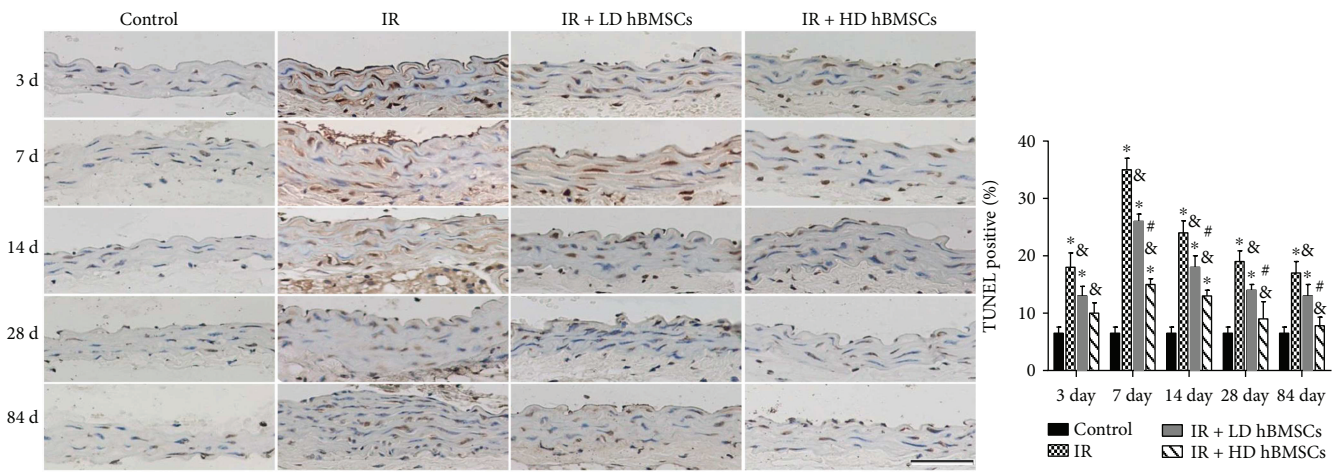

Figure 6: hBMSCs reduced radiation-induced aortic apoptosis. The apoptotic cell was examined by TUNEL staining followed with semiquantitative analysis. Data were presented as means ± SD ($n = 7$). $^{*}P < 0.05$ versus control group; $^{\&}P < 0.05$ versus IR group; $^{\#}P < 0.05$ versus IR + LD hBMSC group. Scale bar, 50 μm.

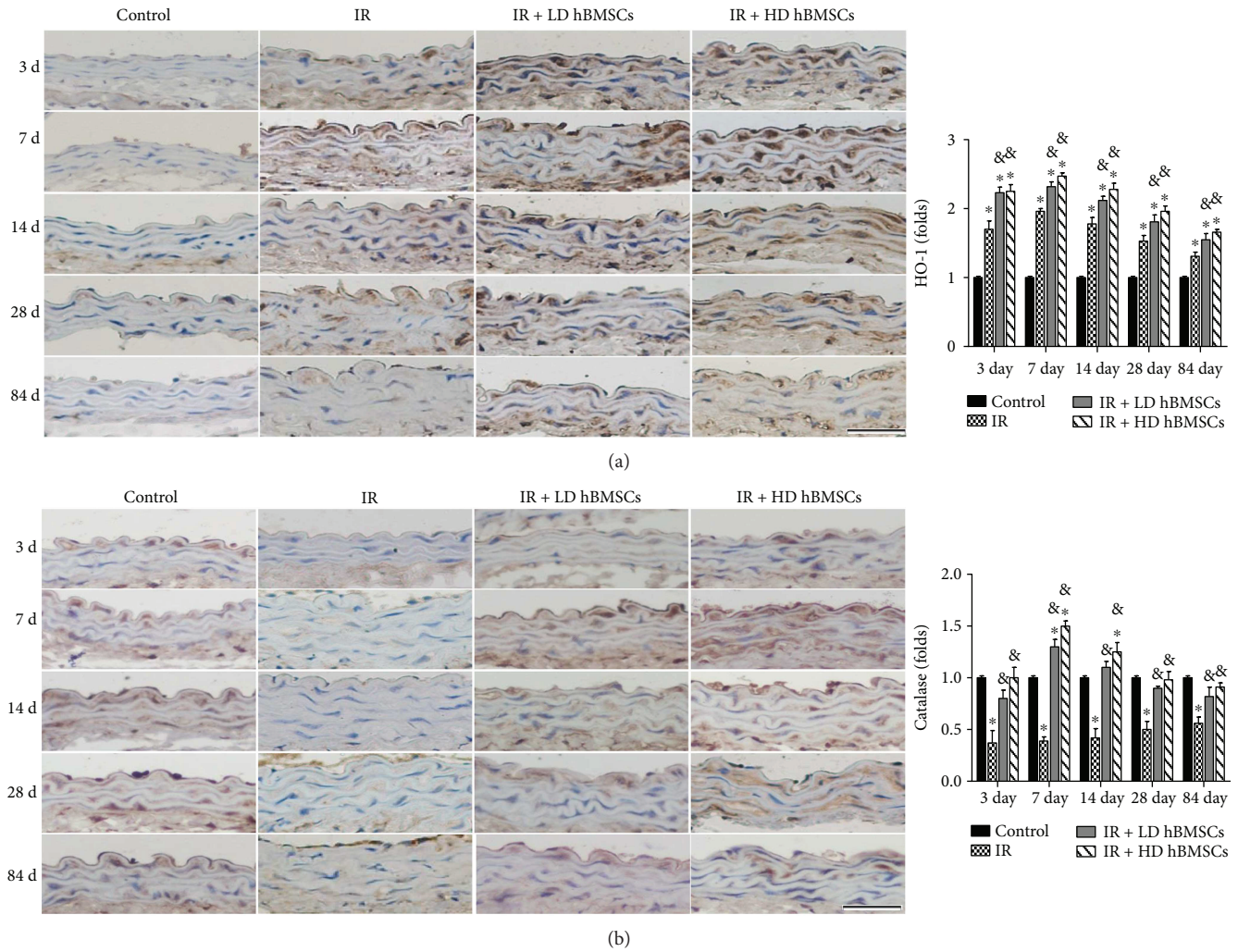

Figure 7: hBMSC upregulated antioxidant enzymes expression of HO-1 and catalase in aortas. The antioxidant enzyme expression of HO-1 (a) and catalase (b) was examined by immunohistochemical staining followed with semiquantitative analysis. Data were presented as means ± SD ($n = 7$). $^{*}P < 0.05$ versus control group; $^{\&}P < 0.05$ versus IR group; $^{\#}P < 0.05$ versus IR + LD hBMSC group. Scale bar, 50 μm.

apoptosis, fibrotic remodeling, inflammation, and oxidative stress. Moreover, the higher dose of hBMSCs showed more remarkable protective effects, implied by the less aortic cell apoptosis (Figure 6) and lower expression of CTGF and TGF-β (Figure 3).

Vascular inflammation is one of the prominent features of radiation-induced tissue injury [32]. The effects of inflammation include induction of oxidative stress, cell apoptosis, and endothelial dysfunction, all of which could contribute to the structural and functional abnormalities of the blood vessel [33]. Recent studies have revealed that endothelial cells were injured shortly after radiotherapy [34]. It is widely believed that radiation upregulates proinflammatory cytokines and adhesion molecules in endothelial cells of injured blood vessels [25, 35]. Consistent with those findings, we observed that the expression of ICAM-1, an adhesion molecule, as well as TNF-α, a proinflammatory cytokine, was significantly increased in aortas as early as 3 days and 7 days after irradiation, respectively, and kept at the high levels until 84 days or 28 days (Figure 4). These results indicated that both ICAM-1 and TNF-α were involved in the radiation-induced aortic inflammatory injuries. It is reported that inflammation was observed in early stage of irradiated arteries [26]. TNF-α was shown to enhance ICAM-1 on activated endothelial cells in the artery inflammation disease [36]. Therefore, at 84 days of later postirradiation, the expression of TNF-α in irradiated aortas was no difference with the control, while the expression of ICAM-1was still kept higher than the control (Figure 4). It has also been reported that rat MSCs play an immunomodulatory role via diminishing secretion of inflammation-related molecules CXCL1 and ICAM-1 to accelerate reparation of abnormal arteries [37]. BMSC inhibits TNF-α production of anti-inflammatory and antifibrosis in lung injury [38]. In addition, the study by Forte et al. also disclosed that MSCs inhibited inflammatory response to facilitate endothelial reparation [11]. Consistent with this, our present study found that hBMSCs diminished radiation-induced increase of TNF-α and ICAM-1 expressions in aortas, which illustrated that

hBMSCs had an effect on diminishing radiation-induced aortic inflammation.

Inflammation and oxidative stress are reciprocal causes and outcomes, both of which are main pathogenic factors for the development of various cardiovascular diseases [39]. It has been well established that irradiation causes radiolysis of intracellular water molecules, leading to increased production of ROS. In addition, inflammatory cytokines can induce reactive oxygen species (ROS)/reactive nitrogen species (RNS) production in the vascular system [40]. Extra generation of those species or insufficient endogenous antioxidant defenses results in oxidative stress in the organs. The vascular endothelium is a major target of oxidant stress [41]. Endothelial dysfunction is described as the initial pathogenic event of radiation-injured vascular injury. Vascular oxidative stress contributes to vascular dysfunction [42]. This study showed that accompanied with increased expressions of inflammation-related molecules TNF-α and ICAM-1, the markers of oxidative stress (4-HNE and 3-NT) were significantly upregulated in aortas of RIAI mice. Meanwhile, hBMSC administration, especially the high dose of hBMSCs, significantly inhibited the accumulation of 3-NT and 4-HNE in aortas from 7 days to 84 days after radiation (Figure 5). These results implied the antioxidant effect of hBMSCs, which was in accord with a previous report that BMSC administration attenuated hepatic ischemia-reperfusion injury by suppressing oxidative stress and apoptosis in rats [43].

To further detect the potential mechanism of antioxidant effect of hBMSCs, the antioxidant enzyme expression of HO-1 and catalase was observed in the aorta. It was found that radiation significantly induced the HO-1 expression (Figure 7(a)) and attenuated the catalase expression (Figure 7(b)) in the aortas, in agreement with those observations on radiation-induced lung and hematopoietic system injury [44–46]. Based on vascular disease studies, HO-1 has shown the beneficial effects on the endothelium [47] and plays an antioxidant effect on vascular injury [48]. Catalase, as an H_2O_2 scavenging enzyme, has been found to be protective against vascular endothelial oxidative damage [49]. Prior studies showed that MSCs could resort the radiation-induced low activity of antioxidant enzymes, including catalase [50]. Consistent with those observations, our study found that the low or high dose of hBMSC treatment further enhanced the upregulation of HO-1 and reversed the decrease of catalase induced by the radiation in the aorta (Figure 7). These findings indicated that hBMSCs possibly suppresses ROS generation by upregulating expression of related antioxidant enzymes. However, there may be a concern that hBMSCs further increased the expression of HO-1 compared with the IR group (Figure 7(a)). We speculate that irradiation as a stress stimulating antioxidant reaction including the increase of HO-1 expression is an adaptive response. This adaptive response tries to provide certain protections but is not sufficient to completely prevent the progression of aortic pathological changes. However, upregulated levels of HO-1 in hBMSC-treated RIAI mice are high enough to efficiently reduce radiation-induced oxidative damage, as we observed here. This speculation was also supported by the observations of astaxanthin's protection on irradiation-induced hematopoietic system injury [44] and antioxidant MG132 on diabetes-induced aortic oxidative damage [51].

Radiation-induced vascular fibrosis is a complex and dynamic process, which is initiated and aggravated by proinflammatory and profibrotic cytokines and oxidative stress. Arteries injured by radiation could easily develop spontaneous atherosclerosis [52], which was associated with the increased inflammation and fibrinogen [53]. Studies have proved that high dose of radiation can induce vascular fibrosis [54] and TGF-β, a profibrotic cytokine, which plays a critical role in the process of radiation-induced vascular smooth muscle cells fibrosis [55]. Connective tissue growth factor (CTGF) is induced by TGF-β and also contributes to collagen synthesis and fibroblast proliferation [56]. Therefore, suppression of TGF-β and CTGF may be sufficient to prevent radiation-induced aorta remodeling. Expectedly, our study found the expressions of TGF-β and CTGF in aortas were all significantly increased from day 3 to 84 after radiation (Figure 3), accompanied with increased collagen accumulation in aortic tunica media (Figure 2) from day 14 to 84. hBMSC administration partially prevented the aortic fibrosis and remodeling, reflected by the complete suppression of increased TGF-β expression and partial inhibition of CTGF expression, as well as aortic collagen accumulation (Figures 2 and 3).

The acute phase of vascular injury occurs within hours to weeks after irradiation is characterized by endothelial swelling, apoptosis, and vascular permeability and edema [57]. This phase is often accompanied by an inflammatory reaction, leading to tissue edema [58]. As time goes on, secretion of inflammatory factors and inflammatory response was gradually decreased. Later vascular injury appears weeks to months postirradiation and includes thickening of basement membranes, collagen deposition, fibrosis, and scar [59]. According to this, we observed that inflammation-related cytokines of ICAM-1 and TNF-α, as well as aortic cell apoptosis, were increased in aortas as early as 3 days and reached their peaks at 7 days after irradiation. While the radiation-induced vascular fibrosis reflected by the collagen accumulation appeared at 14 days, later than aortic inflammation and cell apoptosis. Meanwhile, the tunica media thickness in the IR group mice after irradiation was significantly increased at 7, 14, 28, days and without a significant difference at 84 days, as compared with the controls. Therefore, it is suspected that the increased thickness of aortas at 7 days of postirradiation was mainly caused by inflammatory exudation and tissue edema, and at 14 and 28 days, it was by inflammation combined with collagen accumulation. At a later stage of 84 days, slight increased aortic thickness without significant difference in the IR group was probably due to less inflammation. However, aortic thickness in hBMSC treatment groups was always kept at the normal level.

More and more evidences show that BMSCs could directly differentiate into vascular endothelial cells and smooth muscle cells, even forming functional vessels [15, 60]. However, reports suggest that differentiation either by transdifferentiation or cell fusion appears too low to explain the significant improvement of vascular repair [61]. Based on this, we had not focused on the transdifferentiation of

hBMSCs to vascular cells in this study but observed the expression of vascular damage-related cytokines. Recent studies have shown the key mechanism by which MSCs enhance tissue function is through its paracrine functions. For example, Ortiz et al. report that BMSC inhibits TNF-α production by the secretion of the IL-1 receptor agonist [38]. MSCs induced an increase in antioxidant gene expression of Nrf2, which reduce ROS production decreasing oxidative stress induced by irradiation in the injured liver [20]. Extracellular vesicles derived from MSCs protect against acute kidney injury through antioxidation by enhancing Nrf2 activation [62] and against experimental colitis by suppressing the apoptosis via reducing the apoptotic genes of caspase-3, 8, and 9 in rats [63]. Considering the facts that hBMSCs significantly diminished the expressions of proinflammatory molecules (TNF-α and ICAM-1) and profibrotic cytokines (TGF-β and CTGF) in the present study, as well as the report of its paracrine activity on attenuating inflammation, oxidative stress, and apoptosis [63], we speculate that hBMSCs facilitated aortic repair mainly through paracrine actions, without largely depending on direct differentiation.

There may be also a couple of limitations of the present study. Although publications have demonstrated that MSCs could migrate and home to the injured large blood vessel for vascular repair [16, 17], the location, transdifferentiation, and protective mechanism of MSCs in the irradiated aortas have not been directly observed. Parameters, strictly correlated with the endothelial function, such as vasorelaxation and nitric oxide production, as well as vascular permeability, have not been assessed in the present study. And it is uncertain whether the aortic injury caused by a prolonged radiotherapy can be prevented by hBMSCs. Thus, further experiments are needed to clarify the unknown.

In conclusion, hBMSC administration alleviated radiation-induced aortic injuries indicated by attenuated aortic thickening, fibrotic remodeling, and cell apoptosis. We considered the protective effect of hBMSCs is mainly through the suppression of radiation-induced oxidative stress and inflammation, including downregulation of TNF-α, ICAM-1, TGF-β, and CTGF as well as upregulation of antioxidant enzymes HO-1 and catalase. Therefore, hBMSCs may be a promising therapeutic approach to treat RIAI.

Conflicts of Interest

The authors have no conflicts of interest to report.

Authors' Contributions

Yanjun Shen and Xin Jiang contributed equally to this work.

Acknowledgments

This work was supported by projects in part from the National Science Foundation of China (81570344 to Ying Xin), the Norman Bethune Program of Jilin University (2015225 to Ying Xin and 2015203 to Xin Jiang), the Jilin Provincial Science & Technology Foundations (20150204093SF to Xin Jiang), the Education Department of Jilin Province Foundations (2016-448 to Xin Jiang), and the Health and Family Planning Commission of Jilin Province Foundations (2016Q034 to Ying Xin and 2015Q010 to Xin Jiang).

References

[1] E. Thomas and W. D. Forbus, "Irradiation injury to the aorta and the lung," *A.M.A. Archives of Pathology*, vol. 67, no. 3, pp. 256–263, 1959.

[2] F. A. Stewart, S. Hoving, and N. S. Russell, "Vascular damage as an underlying mechanism of cardiac and cerebral toxicity in irradiated cancer patients," *Radiation Research*, vol. 174, no. 6b, pp. 865–869, 2010.

[3] J. Xu and Y. Cao, "Radiation-induced carotid artery stenosis: a comprehensive review of the literature," *Interventional Neurology*, vol. 2, no. 4, pp. 183–192, 2014.

[4] F. Bucci, F. Robert, L. Fiengo, and P. Plagnol, "Radiotherapy-related axillary arteriopathy," *Interactive Cardiovascular and Thoracic Surgery*, vol. 15, no. 1, pp. 176-177, 2012.

[5] T. Etgen, M. Hochreiter, and V. Kiechle, "Subclavian-axillary graft plus graft-carotid interposition in symptomatic radiation-induced occlusion of bilateral subclavian and common carotid arteries," *Vasa*, vol. 42, no. 3, pp. 223–226, 2013.

[6] S. Lindasay, C. Entenman, E. E. Ellis, and C. L. Geraci, "Aortic arteriosclerosis in the dog after localized aortic irradiation with electrons," *Circulation Research*, vol. 10, no. 1, pp. 61–67, 1962.

[7] C. Thalhammer, M. Husmann, C. Glanzmann, G. Studer, and B. R. Amann-Vesti, "Carotid artery disease after head and neck radiotherapy," *Vasa*, vol. 44, no. 1, pp. 23–30, 2015.

[8] E. Arthurs, T. P. Hanna, K. Zaza, Y. Peng, and S. F. Hall, "Stroke after radiation therapy for head and neck cancer: what is the risk?," *International Journal of Radiation Oncology, Biology, Physics*, vol. 96, no. 3, pp. 589–596, 2016.

[9] A. Klimczak and U. Kozlowska, "Mesenchymal stromal cells and tissue-specific progenitor cells: their role in tissue homeostasis," *Stem Cells International*, vol. 2016, Article ID 4285215, 11 pages, 2016.

[10] X. He, Y. L. Li, X. R. Wang, X. Guo, and Y. Niu, "Mesenchymal stem cells transduced by PLEGFP-N1 retroviral vector maintain their biological features and differentiation," *Chinese Medical Journal*, vol. 118, no. 20, pp. 1728–1734, 2005.

[11] A. Forte, M. Finicelli, M. Mattia et al., "Mesenchymal stem cells effectively reduce surgically induced stenosis in rat carotids," *Journal of Cellular Physiology*, vol. 217, no. 3, pp. 789–799, 2008.

[12] A. Forte, U. Galderisi, M. Cipollaro, and A. Cascino, "Mesenchymal stem cells: a good candidate for restenosis therapy?," *Current Vascular Pharmacology*, vol. 7, no. 3, pp. 381–393, 2009.

[13] X. D. Tang, L. Shi, A. Monsel et al., "Mesenchymal stem cell microvesicles attenuate acute lung injury in mice partly mediated by Ang-1 mRNA," *Stem Cells*, vol. 35, no. 7, pp. 1849–1859, 2017.

[14] D. Pankajakshan and D. K. Agrawal, "Mesenchymal stem cell paracrine factors in vascular repair and regeneration," *Journal of Biomedical Technology and Research*, vol. 1, no. 1, p. 1, 2014.

[15] Q. Li, S. Xia, H. Fang, J. Pan, Y. Jia, and G. Deng, "VEGF treatment promotes bone marrow-derived CXCR4$^+$ mesenchymal stromal stem cell differentiation into vessel endothelial cells," *Experimental and Therapeutic Medicine*, vol. 13, no. 2, pp. 449–454, 2017.

[16] A. Yamawaki-Ogata, X. Fu, R. Hashizume et al., "Therapeutic potential of bone marrow-derived mesenchymal stem cells in formed aortic aneurysms of a mouse model," *European Journal of Cardio-Thoracic Surgery*, vol. 45, no. 5, pp. e156–e165, 2014.

[17] H. J. Dong, C. Z. Shang, G. Li et al., "The distribution of transplanted umbilical cord mesenchymal stem cells in large blood vessel of experimental design with traumatic brain injury," *Journal of Craniofacial Surgery*, vol. 28, no. 6, pp. 1615–1619, 2017.

[18] J. R. Cuomo, G. K. Sharma, P. D. Conger, and N. L. Weintraub, "Novel concepts in radiation-induced cardiovascular disease," *World Journal of Cardiology*, vol. 8, no. 9, pp. 504–519, 2016.

[19] M. Shoji, A. Oskowitz, C. D. Malone, D. J. Prockop, and R. Pochampally, "Human mesenchymal stromal cells (MSCs) reduce neointimal hyperplasia in a mouse model of flow-restriction by transient suppression of anti-inflammatory cytokines," *Journal of Atherosclerosis and Thrombosis*, vol. 18, no. 6, pp. 464–474, 2011.

[20] S. Francois, M. Mouiseddine, B. Allenet-Lepage et al., "Human mesenchymal stem cells provide protection against radiation-induced liver injury by antioxidative process, vasculature protection, hepatocyte differentiation, and trophic effects," *Biomed Research International*, vol. 2013, Article ID 151679, 14 pages, 2013.

[21] C. Linard, E. Busson, V. Holler et al., "Repeated autologous bone marrow-derived mesenchymal stem cell injections improve radiation-induced proctitis in pigs," *Stem Cells Translational Medicine*, vol. 2, no. 11, pp. 916–927, 2013.

[22] D. Klein, J. Steens, A. Wiesemann et al., "Mesenchymal stem cell therapy protects lungs from radiation-induced endothelial cell loss by restoring superoxide dismutase 1 expression," *Antioxidants & Redox Signaling*, vol. 26, no. 11, pp. 563–582, 2017.

[23] J. M. Hare, J. H. Traverse, T. D. Henry et al., "A randomized, double-blind, placebo-controlled, dose-escalation study of intravenous adult human mesenchymal stem cells (prochymal) after acute myocardial infarction," *Journal of the American College of Cardiology*, vol. 54, no. 24, pp. 2277–2286, 2009.

[24] Y. Xin, X. Jiang, Y. Wang et al., "Insulin-producing cells differentiated from human bone marrow mesenchymal stem cells *in vitro* ameliorate streptozotocin-induced diabetic hyperglycemia," *PLoS One*, vol. 11, no. 1, article e0145838, 2016.

[25] M. Halle, A. Gabrielsen, G. Paulsson-Berne et al., "Sustained inflammation due to nuclear factor-kappa B activation in irradiated human arteries," *Journal of the American College of Cardiology*, vol. 55, no. 12, pp. 1227–1236, 2010.

[26] S. Hoving, S. Heeneman, M. J. Gijbels et al., "Irradiation induces different inflammatory and thrombotic responses in carotid arteries of wildtype C57BL/6J and atherosclerosis-prone ApoE(−/−) mice," *Radiotherapy and Oncology*, vol. 105, no. 3, pp. 365–370, 2012.

[27] Z. Yang, X. Cai, A. Xu, F. Xu, and Q. Liang, "Bone marrow stromal cell transplantation through tail vein injection promotes angiogenesis and vascular endothelial growth factor expression in cerebral infarct area in rats," *Cytotherapy*, vol. 17, no. 9, pp. 1200–1212, 2015.

[28] T. J. Kean, P. Lin, A. I. Caplan, and J. E. Dennis, "MSCs: delivery routes and engraftment, cell-targeting strategies, and immune modulation," *Stem Cells International*, vol. 2013, Article ID 732742, 13 pages, 2013.

[29] Z. Li, X. Hu, J. Mao et al., "Optimization of mesenchymal stem cells (MSCs) delivery dose and route in mice with acute liver injury by bioluminescence imaging," *Molecular Imaging and Biology*, vol. 17, no. 2, pp. 185–194, 2015.

[30] H. Yukawa, H. Noguchi, K. Oishi et al., "Cell transplantation of adipose tissue-derived stem cells in combination with heparin attenuated acute liver failure in mice," *Cell Transplantation*, vol. 18, no. 5-6, pp. 611–618, 2009.

[31] C. Xia, P. Chang, Y. Zhang et al., "Therapeutic effects of bone marrow-derived mesenchymal stem cells on radiation-induced lung injury," *Oncology Reports*, vol. 35, no. 2, pp. 731–738, 2016.

[32] L. F. Fajardo and M. Berthrong, "Vascular lesions following radiation," *Pathology Annual*, vol. 23, Part 1, pp. 297–330, 1988.

[33] M. W. Hung, G. M. Kravtsov, C. F. Lau, A. M. Poon, G. L. Tipoe, and M. L. Fung, "Melatonin ameliorates endothelial dysfunction, vascular inflammation, and systemic hypertension in rats with chronic intermittent hypoxia," *Journal of Pineal Research*, vol. 55, no. 3, pp. 247–256, 2013.

[34] N. L. Weintraub, W. K. Jones, and D. Manka, "Understanding radiation-induced vascular disease," *Journal of the American College of Cardiology*, vol. 55, no. 12, pp. 1237–1239, 2010.

[35] O. Azimzadeh, W. Sievert, H. Sarioglu et al., "Integrative proteomics and targeted transcriptomics analyses in cardiac endothelial cells unravel mechanisms of long-term radiation-induced vascular dysfunction," *Journal of Proteome Research*, vol. 14, no. 2, pp. 1203–1219, 2015.

[36] F. Carbone and F. Montecucco, "Inflammation in arterial diseases," *IUBMB Life*, vol. 67, no. 1, pp. 18–28, 2015.

[37] A. Forte, B. Rinaldi, L. Sodano et al., "Stem cell therapy for arterial restenosis: potential parameters contributing to the success of bone marrow-derived mesenchymal stromal cells," *Cardiovascular Drugs and Therapy*, vol. 26, no. 1, pp. 9–21, 2012.

[38] L. A. Ortiz, M. Dutreil, C. Fattman et al., "Interleukin 1 receptor antagonist mediates the antiinflammatory and antifibrotic effect of mesenchymal stem cells during lung injury," *Proceedings of the National Academy of Sciences of the United States of America*, vol. 104, no. 26, pp. 11002–11007, 2007.

[39] S. Gupta, J. K. Gambhir, O. Kalra et al., "Association of biomarkers of inflammation and oxidative stress with the risk of chronic kidney disease in type 2 diabetes mellitus in North Indian population," *Journal of Diabetes and its Complications*, vol. 27, no. 6, pp. 548–552, 2013.

[40] K. K. Koh, P. C. Oh, and M. J. Quon, "Does reversal of oxidative stress and inflammation provide vascular protection?," *Cardiovascular Research*, vol. 81, no. 4, pp. 649–659, 2009.

[41] H. Lum and K. A. Roebuck, "Oxidant stress and endothelial cell dysfunction," *American Journal of Physiology. Cell Physiology*, vol. 280, no. 4, pp. C719–C741, 2001.

[42] U. Forstermann, "Oxidative stress in vascular disease: causes, defense mechanisms and potential therapies," *Nature Clinical Practice. Cardiovascular Medicine*, vol. 5, no. 6, pp. 338–349, 2008.

[43] G. Jin, G. Qiu, D. Wu et al., "Allogeneic bone marrow-derived mesenchymal stem cells attenuate hepatic ischemia-reperfusion injury by suppressing oxidative stress and inhibiting apoptosis in rats," *International Journal of Molecular Medicine*, vol. 31, no. 6, pp. 1395–1401, 2013.

[44] X. L. Xue, X. D. Han, Y. Li et al., "Astaxanthin attenuates total body irradiation-induced hematopoietic system injury in mice

via inhibition of oxidative stress and apoptosis," *Stem Cell Research & Therapy*, vol. 8, no. 1, p. 7, 2017.

[45] S. J. Lee, C. O. Yi, R. W. Heo et al., "Clarithromycin attenuates radiation-induced lung injury in mice," *PLoS One*, vol. 10, no. 6, article e131671, 2015.

[46] R. Malaviya, A. J. Gow, M. Francis, E. V. Abramova, J. D. Laskin, and D. L. Laskin, "Radiation-induced lung injury and inflammation in mice: role of inducible nitric oxide synthase and surfactant protein D," *Toxicological Sciences*, vol. 144, no. 1, pp. 27–38, 2015.

[47] D. Calay and J. C. Mason, "The multifunctional role and therapeutic potential of HO-1 in the vascular endothelium," *Antioxidants & Redox Signaling*, vol. 20, no. 11, pp. 1789–1809, 2014.

[48] S. Turkseven, A. Kruger, C. J. Mingone et al., "Antioxidant mechanism of heme oxygenase-1 involves an increase in superoxide dismutase and catalase in experimental diabetes," *American Journal of Physiology. Heart and Circulatory Physiology*, vol. 289, no. 2, pp. H701–H707, 2005.

[49] J. Han, V. V. Shuvaev, and V. R. Muzykantov, "Catalase and superoxide dismutase conjugated with platelet-endothelial cell adhesion molecule antibody distinctly alleviate abnormal endothelial permeability caused by exogenous reactive oxygen species and vascular endothelial growth factor," *Journal of Pharmacology and Experimental Therapeutics*, vol. 338, no. 1, pp. 82–91, 2011.

[50] L. Wei, J. Zhang, Z. L. Yang, and H. You, "Extracellular superoxide dismutase increased the therapeutic potential of human mesenchymal stromal cells in radiation pulmonary fibrosis," *Cytotherapy*, vol. 19, no. 5, pp. 586–602, 2017.

[51] X. Miao, W. Cui, W. Sun et al., "Therapeutic effect of MG132 on the aortic oxidative damage and inflammatory response in OVE26 type 1 diabetic mice," *Oxidative Medicine and Cellular Longevity*, vol. 2013, Article ID 879516, 12 pages, 2013.

[52] N. Zidar, D. Ferluga, A. Hvala, M. Popovic, and E. Soba, "Contribution to the pathogenesis of radiation-induced injury to large arteries," *The Journal of Laryngology and Otology*, vol. 111, no. 10, pp. 988–990, 1997.

[53] S. Sabeti, M. Exner, W. Mlekusch et al., "Prognostic impact of fibrinogen in carotid atherosclerosis: nonspecific indicator of inflammation or independent predictor of disease progression?," *Stroke*, vol. 36, no. 7, pp. 1400–1404, 2005.

[54] O. Blanck, F. Bode, M. Gebhard et al., "Dose-escalation study for cardiac radiosurgery in a porcine model," *International Journal of Radiation Oncology, Biology, Physics*, vol. 89, no. 3, pp. 590–598, 2014.

[55] F. Milliat, A. Francois, M. Isoir et al., "Influence of endothelial cells on vascular smooth muscle cells phenotype after irradiation: implication in radiation-induced vascular damages," *The American Journal of Pathology*, vol. 169, no. 4, pp. 1484–1495, 2006.

[56] V. Haydont, D. Mathe, C. Bourgier et al., "Induction of CTGF by TGF-β1 in normal and radiation enteritis human smooth muscle cells: Smad/Rho balance and therapeutic perspectives," *Radiotherapy and Oncology*, vol. 76, no. 2, pp. 219–225, 2005.

[57] F. Paris, Z. Fuks, A. Kang et al., "Endothelial apoptosis as the primary lesion initiating intestinal radiation damage in mice," *Science*, vol. 293, no. 5528, pp. 293–297, 2001.

[58] M. M. Satyamitra, A. L. DiCarlo, and L. Taliaferro, "Understanding the pathophysiology and challenges of development of medical countermeasures for radiation-induced vascular/endothelial cell injuries: report of a NIAID workshop, August 20, 2015," *Radiation Research*, vol. 186, no. 2, pp. 99–111, 2016.

[59] F. Milliat, J. C. Sabourin, G. Tarlet et al., "Essential role of plasminogen activator inhibitor type-1 in radiation enteropathy," *American Journal of Pathology*, vol. 172, no. 3, pp. 691–701, 2008.

[60] M. Choi, H. S. Lee, P. Naidansaren et al., "Proangiogenic features of Wharton's jelly-derived mesenchymal stromal/stem cells and their ability to form functional vessels," *The International Journal of Biochemistry & Cell Biology*, vol. 45, no. 3, pp. 560–570, 2013.

[61] M. Gnecchi, Z. Zhang, A. Ni, and V. J. Dzau, "Paracrine mechanisms in adult stem cell signaling and therapy," *Circulation Research*, vol. 103, no. 11, pp. 1204–1219, 2008.

[62] G. Zhang, X. Zou, Y. Huang et al., "Mesenchymal stromal cell-derived extracellular vesicles protect against acute kidney injury through anti-oxidation by enhancing Nrf2/ARE activation in rats," *Kidney & Blood Pressure Research*, vol. 41, no. 2, pp. 119–128, 2016.

[63] J. Yang, X. X. Liu, H. Fan et al., "Extracellular vesicles derived from bone marrow mesenchymal stem cells protect against experimental colitis via attenuating colon inflammation, oxidative stress and apoptosis," *PLoS One*, vol. 10, no. 10, article e140551, 2015.